

**THE UNIVERSITY OF HULL**

**The Impact of Erythropoietin on Uraemic Cardiomyopathy**

being a Thesis submitted for the Degree of Doctor of Philosophy

in the University of Hull

by

Katie Smith BSc (Hons)

December 2009

## Abstract

Cardiovascular complications are the leading cause of death in patients with chronic kidney disease (CKD). The uraemic heart is characterised by cellular and structural remodelling, including left ventricular hypertrophy (LVH), which contribute to heart failure. Erythropoietin (EPO) has revolutionised the treatment of the anaemia associated with CKD. The discovery that the EPO receptor is also expressed on cardiomyocytes highlights a role of EPO beyond haematopoiesis. However, little is known on the cellular impact of EPO on the uraemic heart. The aim of this study was to determine the effect of EPO administration on uraemic cardiomyopathy.

Uraemia was induced surgically in male Sprague-Dawley rats *via* a subtotal nephrectomy and animals retained for 3, 6, 9 or 12 weeks post-surgery. EPO was administered subcutaneously twice a week for 2 weeks prior to sacrifice at a dose of 30 µg/Kg. Cardiac function was assessed *in vitro* in the perfused heart and *in vivo* using an arterial pressure catheter. Cardiac metabolism was analysed using <sup>13</sup>C NMR along with the activity and protein expression of key metabolic enzymes. In a separate set of experiments, mitochondrial function was determined *in vitro* using an oxygen electrode. To determine the extent of cardiac fibrosis, collagen was stained using picro-sirius red in frozen sections.

Kidney dysfunction was observed from 3 weeks post-surgery as evident by significantly raised serum creatinine and urea, and development of anaemia. LVH was present at 6 and 12 weeks post-induction of uraemia, however *in vitro* and *in*

*vivo* cardiac function was preserved, highlighting a compensatory phase. EPO did not impact on renal function, however, EPO significantly improved haematocrit and induced regression of LVH in uraemic animals at 12 weeks. In addition to preserved cardiac function, myocardial mitochondrial respiration was not modified by uraemia and unaffected by EPO administration. There was a decrease in palmitate utilisation in uraemic hearts compared to controls at 6 weeks post-surgery despite the unchanged activities of key metabolic enzymes including citrate synthase, medium chain acyl-CoA dehydrogenase and pyruvate dehydrogenase activity. Furthermore, the protein expression of CD36 and PPAR $\alpha$  was the same in uraemic and control hearts. At 12 weeks post-surgery, uraemic animals exhibited significantly increased collagen within the heart compared to controls, highlighting cardiac fibrosis.

In summary, by 12 weeks post-induction of uraemia, animals exhibited impaired kidney dysfunction, LVH, metabolic remodelling and cardiac fibrosis with preserved cardiac and mitochondrial function. Further work is required to determine whether the structural and metabolic remodelling which accompany uraemic cardiomyopathy would lead to a deterioration in cardiac function with prolonged uraemia.

## Acknowledgments

I am extremely grateful to my supervisor, Dr Anne-Marie Seymour, for her guidance, encouragement and patience throughout my PhD. In particular, I would like to thank Dr Seymour for her time and supervision when writing the thesis. I am also thankful to my second supervisor, Dr Sunil Bhandari for the support he has provided throughout my PhD and guidance writing the thesis.

I would like to thank Mrs Jenny Foster and Mrs Kathleen Bulmer for their invaluable technical support. In particular, I am grateful to Kath for her assistance with the western blotting and Dr Yong Wang for his help with the *in vivo* pressure measurements. I also wish to thank Mrs Ann Lowry for her guidance on the histological techniques and Dr Chee-Kay Cheung for the kidney images.

I would like to dedicate this thesis in memory of my dad, who supported and encouraged me throughout my education. I am also indebted to my mum and sister; without their strength and support over the last three years, this thesis would not have been possible.

My sincere gratitude also goes to my partner Mark, friends and family for their encouragement during my PhD. I should also like to thank my colleagues and friends at the University, David Semple, Dunja Aksentijevic and Thomas Butler.

Finally, I am grateful for to the British Heart Foundation for funding this PhD. This work has funded by a BHF studentship, grant number FS/06/047.

## Contents

	Page
Abstract	i-ii
Acknowledgments	iii
Contents	iv-vii
Figure List	viii-ix
Table List	x
Abbreviations	xi-xii
Chapter 1: Introduction	1
1.1 Chronic Kidney Disease (CKD)	2
1.2 Myocardial Calcium Handling	4
1.3 Left Ventricular Hypertrophy (LVH)	7
1.3.1 Metabolic Remodelling in LVH	9
1.4 Capillary Abnormalities	12
1.5 Cardiac Fibrosis	15
1.5.1 Extracellular Matrix (ECM)	15
1.6 Erythropoietin (EPO)	18
1.6.1 Biochemistry of EPO and EPO Receptor	19
1.6.2 Cardiovascular Effects of EPO	21
1.6.2.1 Acute Cardioprotective Effects	23
1.6.2.2 Chronic Cardioprotective Effects	27
1.7 Objectives	29
Chapter 2: Materials and Methods	31
2.1 Materials	32
2.2 Methods	35
2.2.1 Induction of Uraemia	35
2.2.2 Preparation of Krebs-Hensleit (K-H) Buffer	36
2.2.3 Preparation of Bovine Serum Albumin (BSA)	37
2.2.4 Heart Perfusion	38
2.2.4.1 Pacing	40
2.2.4.2 <i>In Vitro</i> Cardiac Function	41
2.2.4.3 Oxygen Consumption (MVO <sub>2</sub> )	43
2.2.4.4 Indices of Hypertrophy	45
2.2.4.5 Haematocrit and Serum Analysis	45
2.2.5 <sup>13</sup> C NMR Spectroscopy	45
2.2.5.1 Perchloric Acid (PCA) Tissue Extraction	45
2.2.5.2 Preparation of NMR samples	46

2.2.5.3	Acquisition of <sup>13</sup> C Spectra	46
2.2.5.4	<sup>13</sup> C Labelling Profiles	47
2.2.6	Biochemical Assays	53
2.2.6.1	Pyruvate Dehydrogenase (PDH) Assay	53
2.2.6.2	Citrate Synthase (CS) Assay	56
2.2.6.3	Medium chain Acyl Co-A dehydrogenase (MCAD) Assay	56
2.2.6.3.1	Preparation of Ferricene Salt	56
2.2.6.3.2	MCAD Assay	57
2.2.7	<i>In Vitro</i> Mitochondrial Function	57
2.2.7.1	Isolation of Mitochondria	57
2.2.7.2	Mitochondrial Respiration	58
2.2.8	Western Blotting	60
2.2.8.1	Preparation of Samples	60
2.2.8.2	SDS- Page and Western Blotting	61
2.2.8.3	Visualisation and Quantification	61
2.3	Statistical Analysis	63
Chapter 3: Characterisation of the Experimental Model		64
3.1	Introduction	65
3.1.1	Experimental Models of CKD	65
3.1.2	Erythropoietin Treatment	68
3.1.3	Objectives	70
3.2	Materials and Methods	71
3.2.1	Induction of Uraemia	71
3.2.2	Erythropoietin Treatment	71
3.2.3	Biochemical Analysis and Determination of LVH	72
3.2.4	<i>In Vivo</i> Haemodynamic Analysis	73
3.3	Results	75
3.3.1	Degree of Uraemia	75
3.3.2	<i>In Vivo</i> Blood Pressure	84
3.3.3	Indices of LVH	87
3.4	Discussion	94
3.4.1	Experimental Model of CKD	94
3.4.2	Blood Pressure	96
3.4.3	LVH	98
3.4.4	EPO Treatment	100
3.4.5	Conclusions	101
Chapter 4: <i>In Vitro</i> Cardiac Function and Metabolism		102
4.1	Introduction	103

4.1.1	Determination of <i>In Vitro</i> Cardiac Function	103
4.1.2	Metabolic Remodelling	104
4.1.3	Objectives	106
4.2	Materials and Methods	108
4.2.1	Effects of Acute EPO Administration	108
4.2.2	Effects of Uraemia and Chronic EPO Administration	108
4.2.3	Mitochondrial Enzyme Activities	109
4.3	Results	111
4.3.1	Effects of Acute EPO Administration	111
4.3.2	Effects of Uraemia and Chronic EPO Administration	112
4.3.3	Cardiac Metabolism	121
4.3.4	Mitochondrial Enzyme Activities	124
4.4	Discussion	127
4.4.1	Effects of Acute EPO Administration	127
4.4.2	Effects of Uraemia and Chronic EPO Administration	128
4.4.3	Myocardial Metabolism	130
4.4.4	Conclusion	133
Chapter 5: <i>In Vivo</i> Cardiac Function and Fibrosis		135
5.1	Introduction	136
5.1.1	Cardiac Fibrosis	136
5.1.2	<i>In Vivo</i> Cardiac Function	139
5.1.3	Objectives	140
5.2	Methods	141
5.2.1	Induction of Uraemia and EPO treatment	141
5.2.2	Determination of <i>In Vivo</i> Cardiac Function	141
5.2.3	Histology of Uraemic Hearts	142
5.3	Results	146
5.3.1	<i>In Vivo</i> Cardiac Function	146
5.3.2	Cardiac Fibrosis	149
5.4	Discussion	154
5.4.1	<i>In Vivo</i> Cardiac Function	154
5.4.2	Cardiac Fibrosis	156
5.4.2.1	The Impact of EPO on Cardiac Fibrosis	160
5.4.3	Conclusions	161
Chapter 6: Mitochondrial Function and Protein Expression		163
6.1	Introduction	164
6.1.1	Electron Transport Chain (ETC)	164

6.1.2	Reactive Oxygen Species (ROS) Production	166
6.1.3	Mitochondrial Function in Uraemia	168
6.1.4	Objectives	169
6.2	Methods	170
6.2.1	Mitochondrial Respiration	170
6.2.2	Protein Expression	172
6.3	Results	173
6.3.1	Mitochondrial Respiration	173
6.3.2	Metabolic Protein Expression	181
6.4	Discussion	183
6.4.1	Mitochondrial Respiration	183
6.4.2	Metabolic Protein Expression	188
6.4.2.1	Impact of EPO on Protein Expression	189
6.4.3	Conclusions	190
Chapter 7: Discussion and Future Work		191
7.1	Discussion	192
7.1.1	Extent of Kidney Dysfunction	192
7.1.2	EPO Treatment	194
7.2	Future Work	196
Publications		201
References		202-226

## Figure List

Chapter 1: Introduction		
1.1	Myocardial calcium handling	5
1.2	Schematic diagram of eccentric and concentric LVH	8
1.3	Myocardial substrate metabolism	9
1.4	PPAR $\alpha$ activation	11
1.5	Diagram showing the sequence of events leading to heart failure in uraemia	14
1.6	Diagram of extracellular matrix distribution in muscle	16
1.7	Schematic diagram of EPO signalling	20
1.8	Apoptosis pathway	54
Chapter 2: Materials and Methods		
2.1	Isovolumic Langendorff perfusion apparatus	39
2.2	Isolated perfused rat heart	40
2.3	Recording of cardiac function	42
2.4	Recording of cardiac contractility	43
2.5	a) Profile following 1- <sup>13</sup> C glucose	49
	b) Profile following U- <sup>13</sup> C palmitate	50
2.6	<sup>13</sup> C NMR spectra showing expansion of resonances of glutamate	51
2.7	Recording showing oxygen consumption of isolated mitochondria	59
Chapter 3: Characterisation of the Experimental Model		
3.1	Experimental protocol	72
3.2	Diagram of positioning of catheter	73
3.3	Serum biochemistry	76
3.4	Haematocrit 12 weeks post-induction of uraemia	78
3.5	Spleen weight at 3, 6, 9 and 12 weeks uraemia	80
3.6	Water content of lungs	83
3.7	Systolic and diastolic blood pressures at 12 weeks post-induction of uraemia	85
3.8	Indices of LVH at 12 weeks post-induction of uraemia	91
3.9	Correlation between haematocrit and extent of LVH	92
3.10	Correlation between serum creatinine and extent of LVH	92
3.11	Correlation between systolic blood pressure and extent of LVH	93

Chapter 4: <i>In Vitro</i> Cardiac Function and Metabolism		
4.1	Perfusion protocols	110
4.2	Rate pressure product at 3 weeks post-induction of uraemia	113
4.3	MVO <sub>2</sub> at 3 weeks post-induction of uraemia	113
4.4	Cardiac efficiency in uraemia	114
4.5	Rate pressure product at 6 weeks post-induction of uraemia	117
4.6	MVO <sub>2</sub> at 6 weeks post-induction of uraemia	117
4.7	Rate pressure product at 12 weeks post-induction of uraemia	120
4.8	MVO <sub>2</sub> at 12 weeks post-induction of uraemia	120
4.9	Contribution of <sup>13</sup> C substrates to oxidative metabolism in uraemia	122-123
4.10	MCAD activity at 3 weeks post-induction of uraemia	125
4.11	MCAD activity at 12 weeks post-induction of uraemia	125
4.12	PDH activity at 12 weeks post-induction of uraemia	126
Chapter 5: <i>In Vivo</i> Cardiac Function and Fibrosis		
5.1	Recording of <i>in vivo</i> function	142
5.2	Sequence of collagen quantification (using ImageJ software)	145
5.3	<i>In vivo</i> cardiac contractility at 12 weeks post-induction of uraemia	148
5.4	Cardiac tissue stained using picro-sirius red	150
5.5	Quantification of cardiac fibrosis at 12 weeks uraemia	151
5.6	Sections from uraemic hearts showing types of fibrosis	152
5.7	Cardiac tissue stained using Haematoxylin and Eosin	153
Chapter 6: Mitochondrial Function and Protein Expression		
6.1	Schematic representation of the electron transport chain (ETC)	165
6.2	Mitochondrial ROS generation and induction of apoptosis	167
6.3	Clark- type Electrode	171
6.4	Myocardial mitochondrial respiration using complex I substrates	174
6.5	State 3 respiration in the presence of rotenone	175
6.6	Myocardial respiration rates using complex I substrates at 12 weeks uraemia	180
6.7	Cardiac PPAR $\alpha$ protein expression at 12 weeks uraemia	182
6.8	Cardiac CD36 protein expression at 12 weeks uraemia	182
Chapter 7: Discussion and Future Work		
7.1	Kidney section stained with Masson's trichrome stain	194
7.2	Recovery of rate pressure product (RPP) during reperfusion	198

## Table List

Chapter 1: Introduction	
1.1 Classification of the cardio-renal syndrome	3
1.2 Factors involved in the pathophysiological cardiac phenotype in CKD	4
Chapter 2: Materials and Methods	
2.1 Materials and Suppliers	32
2.2 Components of PDHt and PDHa homogenisation buffers	54
2.3 Antibody dilutions and suppliers	62
Chapter 3: Characterisation of the Experimental Model	
3.1 Haematocrit	78
3.2 Left kidney weights	81
3.3 <i>In vivo</i> blood pressure at 12 weeks post-induction of uraemia	86
3.4 Measurement of LVH during progression of uraemia	89-90
Chapter 4: <i>In Vitro</i> Cardiac Function and Metabolism	
4.1 Effects of acute EPO administration	111
4.2 <i>In Vitro</i> cardiac function at 3 weeks uraemia	112
4.3 <i>In Vitro</i> cardiac function at 6 weeks uraemia	116
4.4 <i>In Vitro</i> cardiac function at 12 weeks uraemia	119
4.5 Citrate Synthase (CS) activity at 6 and 12 week post-induction of uraemia	124
Chapter 5: <i>In Vivo</i> Cardiac Function and Fibrosis	
5.1 <i>In vivo</i> cardiac function at 12 weeks post-induction of uraemia	147
Chapter 6: Mitochondrial Function and Protein Expression	
6.1 Myocardial mitochondrial yields at 12 weeks uraemia	174
6.2 Mitochondrial respiration at 9 weeks post-induction of uraemia using complex I and complex II substrates	177
6.3 Mitochondrial respiration at 12 weeks post-induction of uraemia using complex I and complex II substrates	178-179

## Abbreviations

ACE.....	Angiotensin Converting Enzyme
ACEi.....	Angiotensin Converting Enzyme Inhibitor
ATP.....	Adenosine Triphosphate
bpm.....	beats per minute
CEPO.....	Carbamylated Erythropoietin
CHF.....	Chronic Heart Failure
CKD.....	Chronic Kidney Disease
CPT.....	Carnitine Palmitoyltransferase
CRS.....	Cardio-renal Syndrome
CS.....	Citrate Synthase
DCA.....	Dichloroacetic acid
DP.....	Diastolic Pressure
DTT.....	Dithiothreitol
ECC.....	Excitation-Contraction Coupling
EDP.....	End Diastolic Pressure
EDTA.....	Ethylenediaminetetraacetic acid
EPC.....	Erythroid Progenitor Cell
EPO.....	Erythropoietin
EPOR.....	Erythropoietin Receptor
ER.....	Endoplasmic Reticulum
ESRD.....	End Stage Renal Disease
ETC.....	Electron Transport Chain
FA.....	Fatty Acid
FAD.....	flavin-adenine dinucleotide
FAO.....	Fatty Acid Oxidation
FAT.....	Fatty Acid Translocase
FATP.....	Fatty Acid Transport Protein
G-6-P.....	Glucose-6-Phospahte
GFR.....	Glomerular Filtration Rate
GSK3- $\beta$ .....	Glycogen Synthase Kinase 3- $\beta$
HCM.....	Hypertrophic Cardiomyopathy
HF.....	Heart Failure
HIF-1 $\alpha$ .....	Hypoxia Inducible Factor 1 $\alpha$
HR.....	Heart Rate
ip.....	Intra- Peritoneal
KH.....	Krebs Hensleit (Buffer)
LV.....	Left Ventricle

LVDP.....	Left Ventricular Developed Pressure
LVH.....	Left Ventricular Hypertrophy
MAP.....	Mean arterial pressure
MAPK.....	Mitogen Activated Protein Kinase
MCAD.....	Medium- Chain Acyl Co-A Dehydrogenase
MI.....	Myocardial Infarction
MMP.....	Matrix Metalloproteinase
MPTP.....	Mitochondrial Permeability Transition Pore
NMR.....	Nuclear Magnetic Resonance
NAD.....	Nicotinamide Adenine dinucleotide
NADPH.....	Nicotinamide Adenine dinucleotide phosphate oxidase
NCX.....	Sodium-Calcium Exchanger
NO.....	Nitric Oxide
NOS.....	Nitric Oxide Synthase
PCA.....	Perchloric acid
PCr.....	Phosphocreatine
PDH.....	Pyruvate Dehydrogenase
PGC1 $\alpha$ .....	PPAR $\gamma$ coactivator-1 $\alpha$
PI3K.....	Phosphatidylinositol 3-kinase
PKC.....	Protein Kinase C
PLB.....	Phospholamban
PPAR $\alpha$ .....	Peroxisome Proliferator-Activated Receptor $\alpha$
PPRE.....	Peroxisome Proliferator Response Element
RAAS.....	Renin-Angiotensin-Aldosterone System
RBC.....	Red Blood Cell
rhEPO.....	Recombinant (Human) Erythropoietin
ROS.....	Reactive Oxygen Species
RPP.....	Rate Pressure Product
RXR.....	Retinoid X Receptor
RyR.....	Ryanodine Receptor
s/c.....	Subcutaneous
SNS.....	Sympathetic Nervous System
SERCA.....	Sarco(endo)plasmic reticulum Ca <sup>2+</sup> -ATPase
SHR.....	Spontaneously Hypertensive Rat
SP.....	Systolic Pressure
SR.....	Sarcoplasmic Reticulum
TCA cycle.....	Tricarboxylic acid cycle
TNF $\alpha$ .....	Tumour Necrosis Factor $\alpha$
UCP.....	Uncoupling Protein
VEGF.....	Vascular Endothelial Growth Factor

## **Chapter 1: Introduction**

## 1.1 Chronic Kidney Disease

Cardiovascular complications remain the leading cause of mortality in patients with chronic kidney disease (CKD), accounting for approximately 50% of all deaths (USRDS 1998). Cardiac risk is increased 10-20 times in uraemic patients compared with the aged matched general population (Raine et al., 1992, Foley et al., 1998). In contrast to the general population, the relative importance of arteriosclerotic disease is diminished and those of left ventricular hypertrophy (LVH), heart failure and sudden cardiac death, increased in patients with CKD (Foley et al., 2003).

The coexistence of CKD and cardiac complications, known as the cardio-renal syndrome (CRS), creates a cardiac phenotype unique to the uraemic heart, described as uraemic cardiomyopathy. Recently, a new system for the classification of the cardio-renal syndrome has been proposed, based on the duration and sequence of organ dysfunction (Ronco et al., 2008) (table 1.1).

Table 1.1: Classification of the cardio-renal syndrome (Ronco et al., 2008)

<p style="text-align: center;"><b>CRS Type I (Acute Cardio-renal Syndrome)</b></p> <p>Abrupt worsening of cardiac function (e.g. acute cardiogenic shock or acutely decompensated congestive heart failure) leading to acute kidney injury</p>
<p style="text-align: center;"><b>CRS Type II (Chronic Cardio-renal Syndrome)</b></p> <p>Chronic abnormalities in cardiac function (e.g. chronic congestive heart failure) causing progressive and potentially permanent chronic kidney disease</p>
<p style="text-align: center;"><b>CRS Type III (Acute Reno-cardiac Syndrome)</b></p> <p>Abrupt worsening of renal function (e.g. acute kidney ischaemia or glomerulonephritis) causing acute cardiac disorder (e.g. heart failure, arrhythmia, ischemia)</p>
<p style="text-align: center;"><b>CRS Type IV (Chronic Reno-cardiac Syndrome)</b></p> <p>Chronic kidney disease (e.g. chronic glomerular or interstitial disease) contributing to decreased cardiac function, cardiac hypertrophy and/or increased risk of adverse cardiovascular events</p>
<p style="text-align: center;"><b>CRS Type V (Secondary Cardio-renal Syndrome)</b></p> <p>Systemic condition (e.g. diabetes mellitus, sepsis) causing both cardiac and renal dysfunction</p>

The pathogenesis of uraemic cardiomyopathy is complex and incompletely understood. However, the association and persistence of haemodynamic factors, including anaemia and hypertension, in addition to metabolic and endocrine abnormalities, contribute to the pathophysiological cardiac phenotype observed in patients with CKD (table 1.2).

Table 1.2: Factors involved in the pathophysiological cardiac phenotype in CKD

Cardiac Risk Factors in Uraemia	
• Anaemia	• Chronic inflammation
• LV hypertrophy	• Secondary and tertiary hyperparathyroidism
• Volume overload	• Uraemic toxins
• Hypertension	• Hypoalbuminaemia
• Insulin resistance	• Hyperhomocysteinaemia
• Diabetes	
• Oxidative stress	

The uraemic heart is characterised by complex cellular and structural remodelling, including altered calcium handling, LVH, reduced capillary density and cardiac fibrosis, which contribute to the development of heart failure (HF) and reduced survival in CKD patients (Amann et al., 1998a, Gross and Ritz, 2008).

## 1.2 Myocardial Calcium Handling

Altered calcium homeostasis is central to the progression of cardiac dysfunction and failure (Bers et al., 2006). Indeed, experimental studies show that abnormal calcium handling causes depressed contractility and cardiac dysfunction in LVH (Houser and Margulies 2003).

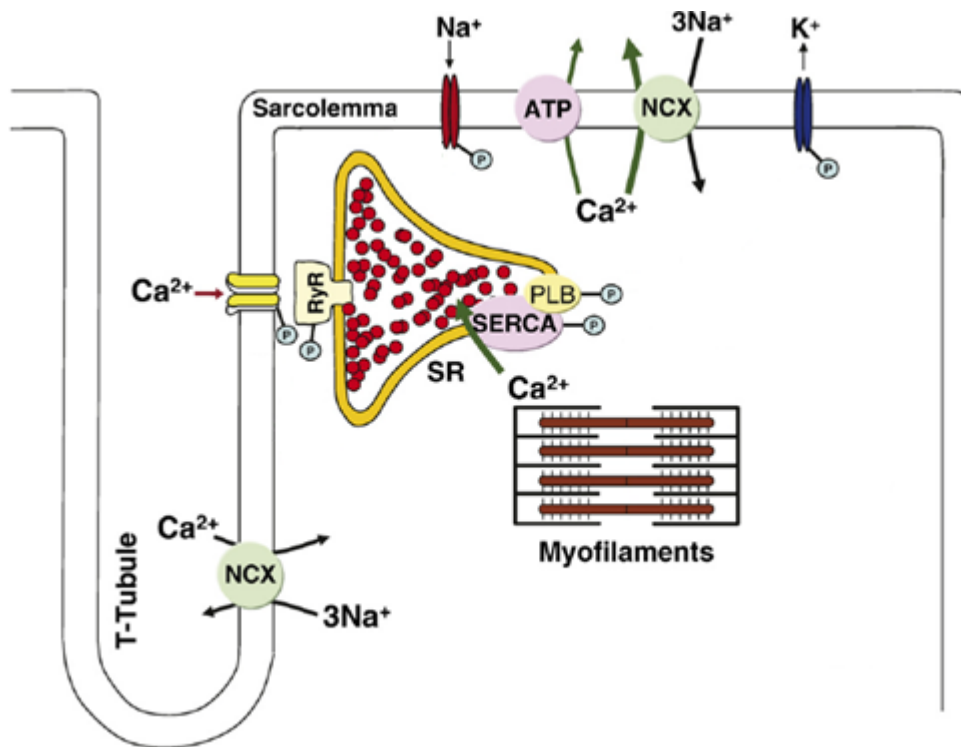


Figure 1.1: Myocardial calcium handling

(adapted from Maier and Bers 2007)

NCX sodium calcium exchanger; RyR ryanodine receptor; SERCA sarco(endoplasmic reticulum Ca<sup>2+</sup>-ATPase; PLB phospholamban; SR sarcoplasmic reticulum

In the normal heart, Ca<sup>2+</sup> transients stimulate muscle contraction in a process known as excitation-contraction coupling (ECC) (Figure 1.1). During membrane depolarisation, Ca<sup>2+</sup> enters the cell *via* the T-tubules using voltage dependent L-type Ca<sup>2+</sup> channels. This triggers an amplification response through Ca<sup>2+</sup> release from the sarcoplasmic reticulum (SR) *via* the ryanodine receptor (RyR), known as calcium-induced calcium release (Fabiato and Fabiato, 1979). In turn, Ca<sup>2+</sup> binds to troponin

C on the thin filaments, causing a conformational change and liberating the actin site to interact with myosin (Bers, 2002). This process leads to cross bridge cycling and muscle contraction. Dissociation of  $\text{Ca}^{2+}$  from troponin C initiates relaxation.  $\text{Ca}^{2+}$  is predominantly removed from the cytosol by the phospholamban-regulated sarco(endo)plasmic reticulum  $\text{Ca}^{2+}$ -ATPase (SERCA), and to a lesser extent the  $\text{Na}^+/\text{Ca}^{2+}$  exchanger (NCX) (Hasenfuss and Pieske, 2002, Yano et al., 2005) (Figure 1.1).

Altered expression of the key regulatory proteins involved in calcium homeostasis contributes to LV dysfunction and failure (Hasenfuss, 1998). In the failing heart, intracellular  $\text{Ca}^{2+}$  transients are decreased, in part due to a reduction in L-type  $\text{Ca}^{2+}$  channel density (Litwin et al., 2000). A decrease in SR  $\text{Ca}^{2+}$  content could also contribute to the diminished calcium transient, possibly as a result of the hyperphosphorylation of RyR causing an increased diastolic SR  $\text{Ca}^{2+}$  leak (Marx et al., 2000). Removal of  $\text{Ca}^{2+}$  from the cytosol may also be impaired during heart failure. Indeed, reductions in SERCA expression have been observed in both experimental (Feldman et al., 1993) and clinical heart failure studies (Hasenfuss, 1998). Furthermore, prolonged calcium transients, highlighting delayed relaxation, have also been observed in the uraemic rat heart (McMahon et al., 2002). SERCA is regulated by phospholamban (PLB). In the dephosphorylated state, PLB exerts an inhibitory effect on SERCA activity.  $\text{Ca}^{2+}$ -calmodulin-dependent or c-AMP dependent protein kinases phosphorylate PLB, thereby relieving SERCA inhibition (Ji et al., 2003, Schwinger et al., 1999). Although PLB expression remains unchanged in HF, phosphorylation is reduced, resulting in a greater inhibitory effect on SERCA (Schwinger et al., 1999). Abnormalities in  $\text{Ca}^{2+}$  regulatory proteins may contribute

to dyssynchronous  $\text{Ca}^{2+}$  release and alterations in myocyte contractility. Thus, correcting these abnormalities may provide an attractive therapeutic target for reversing LV dysfunction in the uraemic heart.

### **1.3 Left Ventricular Hypertrophy (LVH)**

LVH is the most common cardiac adaptation in CKD, present in up to 75% of haemodialysis patients, primarily due to salt and water retention, anaemia and hypertension although metabolic and endocrine abnormalities play a role (Foley et al., 1995). LVH is also observed in patients with modest renal insufficiency and is a powerful independent predictor of survival in these patients (Silberberg et al., 1989, Levin et al., 1999, Ritz and McClellan, 2004).

Cardiomyocytes are terminally differentiated at birth and therefore hypertrophy is the primary adaptive response to a variety of physiological and pathological stresses rather than hyperplasia (Meerson, 1971). Indeed, the enlargement of individual cardiomyocytes helps to normalise wall tension and maintain systolic function (Grossman, 1980). However, clinical studies have shown that hypertrophied hearts are more susceptible to injury and ventricular dysfunction (Maron et al., 2000). Furthermore, epidemiological studies show that LVH may initiate a cascade of detrimental changes, ultimately resulting in heart failure (Levy et al., 1990). This would suggest that the initial hypertrophic response is beneficial but its progression leads to many of the adaptations becoming limiting and thus

maladaptive, contributing to deterioration of cardiac function and onset of heart failure (Meerson, 1971)

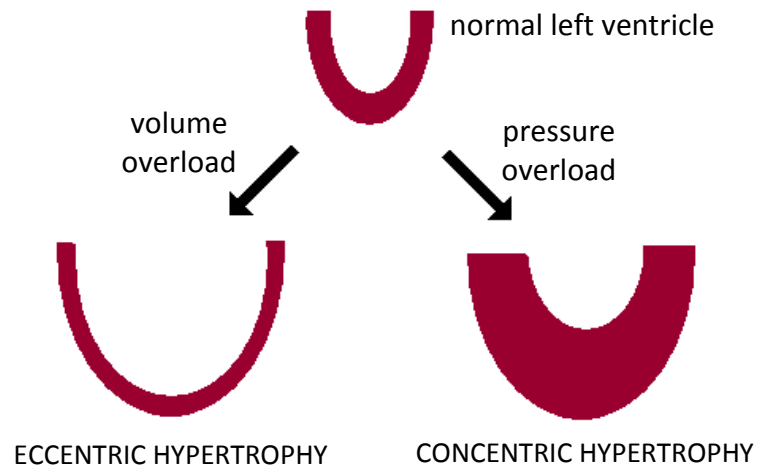


Figure 1.2: Schematic diagram of eccentric and concentric LVH

LVH can be classified into two distinct phenotypes, eccentric and concentric hypertrophy (Figure 1.2). Eccentric hypertrophy is caused by volume overload. In this scenario, new sarcomeres are added in series, which results in ventricular dilation. In contrast, pressure overload leads to thickening of the ventricular wall, known as concentric hypertrophy, and occurs due to the addition of new sarcomeres in parallel to existing sarcomeres.

In a prospective study, Parfrey *et al* (1996) found that eccentric LVH was present in 28%, and concentric LVH in 40% of patients commencing haemodialysis therapy, arising from increased preload (e.g. anaemia and hypervolaemia) and increased afterload (e.g. hypertension and aortic stiffening) respectively (Parfrey *et al.*, 1996, Foley *et al.*, 1995).

### 1.3.1 Metabolic Remodelling in LVH

Hypertrophy per se is associated with cellular remodelling, with strong evidence of altered energy provision (Ingwall, 2009). The heart is reliant upon a continuous supply of oxygen and nutrients to meet the high demands of myocardial tissue and maintain contractile function. Figure 1.3 summarises the pathways involved in myocardial substrate metabolism. Under normal conditions, the heart derives 60%-90% of its energy from fatty acid oxidation (FAO), with the remaining contribution predominantly from glucose and lactate oxidation (Salem et al., 2002, Stanley et al., 2005).

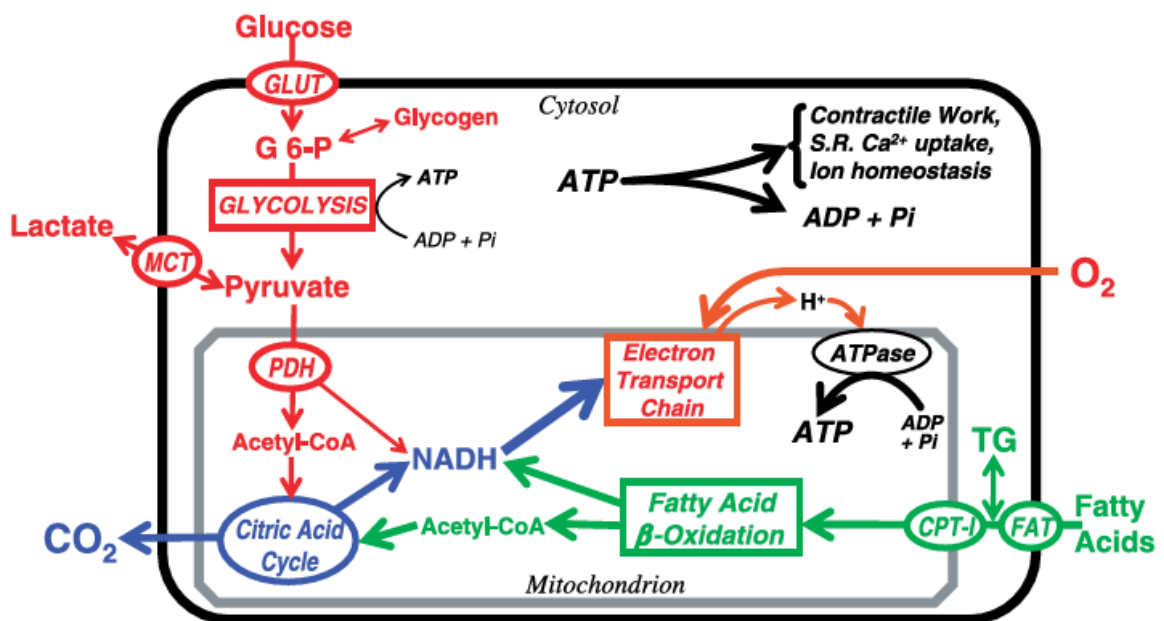


Figure 1.3: Myocardial substrate metabolism

(taken from Stanley et al., 2005)

Fatty acids enter the cell using the FATP and FAT/CD36 transporters and are activated to acyl-CoA *via* esterification by ATP and acyl-CoA synthetase. Subsequently, the carnitine shuttle, (consisting of carnitine palmitoyl transferase-1 (CPT-1), carnitine acyl transferase and carnitine palmitoyl transferase-2 (CPT-2)), transports acyl-CoA into the mitochondrial matrix (Figure 1.3). Oxidation of fatty acids produces acetyl-CoA, which can then enter the tri-carboxylic acid (TCA) cycle.  $\beta$ -oxidation also generates NADH and FADH<sub>2</sub>, which drive the electron transport chain and consequently ATP production (Finck and Kelly, 2002, Stanley and Chandler, 2002).

In contrast, glucose enters the cell using the glucose transporters, GLUT1 and GLUT4, the insulin-dependent transporter. In the cytosol, glucose undergoes glycolysis to form pyruvate. Pyruvate is either converted to lactate, or transported into the mitochondria and converted into acetyl-CoA *via* pyruvate dehydrogenase (PDH) (Sambandam et al., 2002) (Figure 1.3). Under normal conditions, glycolysis accounts for 5-10% of the total ATP production in the heart (Allard et al., 1994, Lopaschuk, 2002).

Experimental models of LVH have shown a decrease in FAO and an enhanced reliance on carbohydrate utilisation, in particular glucose, consistent with a re-expression of the foetal gene programme (Allard et al., 1994, Nascimben et al., 2004, Akki et al., 2008, Seymour, 2003b). The foetus relies on glucose for ATP production; after birth, the up-regulation of FAO parallels mitochondrial development and an increased expression of the regulatory transcription factor,

peroxisome proliferator-activated receptor  $\alpha$  (PPAR $\alpha$ ) (Barger and Kelly, 2000). PPAR $\alpha$  interacts with the heterodimeric receptor, RXR (retinoid X receptor), which together, bind to the consensus DNA sequence known as the peroxisome proliferator response element (PPRE) (Figure 1.4). Gene transcription is initiated upon activation of the complex by the co-factor PGC-1 (PPAR $\gamma$  coactivator-1  $\alpha$ ).

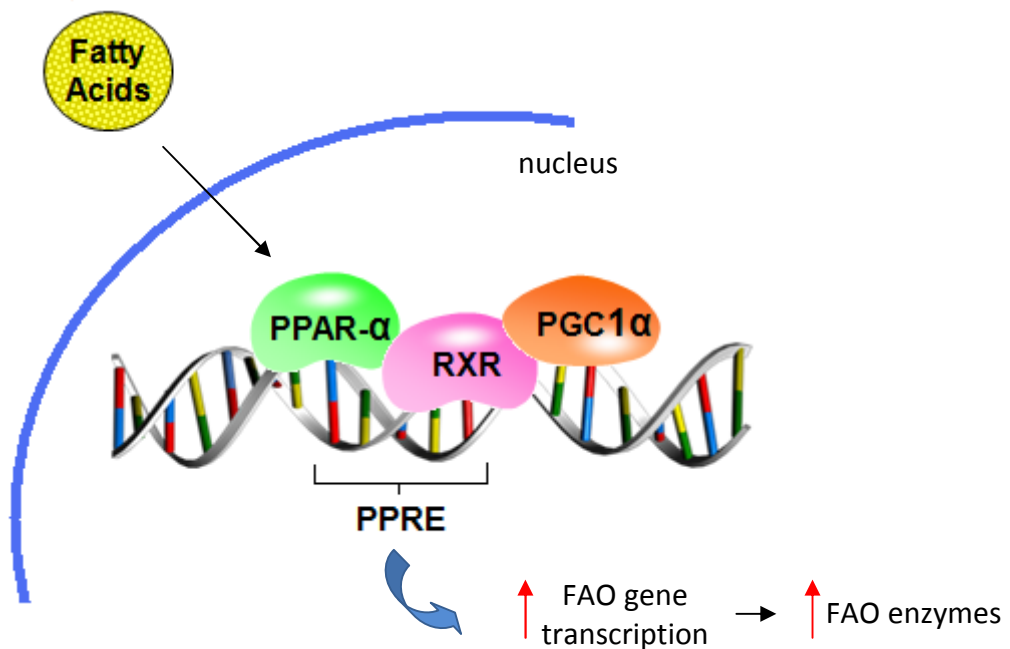


Figure 1.4: PPAR $\alpha$  activation

During hypertrophy, expression of PPAR $\alpha$  is reduced, coinciding with a lowering of the expression of FAO enzymes, including CPT1 and medium chain acyl CoA dehydrogenase (MCAD) (Barger et al., 2000). Although the shift towards glucose utilisation may be initially beneficial in terms of oxygen efficiency (Taegtmeyer, 1986), the change in metabolic profile may, in the longer term, result in complications, including accumulation of lipids and energy depletion (Lehman and Kelly, 2002, Leone et al., 1999, Neubauer, 2007). Specifically, the build up of fatty acyl components, due to reduced oxidation of lipids, results in sequestration of CoA and therefore a reduction in the CoA to acetyl-CoA ratio. This may subsequently cause an inhibition of pyruvate dehydrogenase, the rate limiting step in the entry of glucose in to the TCA cycle, thus resulting in a limited capacity to utilise both fatty acids and glucose (Russell and Taegtmeyer, 1992, Seymour and Chatham, 1997, Seymour, 2003b).

#### **1.4 Capillary Abnormalities**

In experimental models of CKD, and in the clinical setting, it has been shown that capillary growth does not keep pace with cardiomyocyte hypertrophy (Amann et al., 1998a, Amann et al., 1992). Interestingly, the decrease in capillary to myocyte ratio was not observed in an experimental model of essential hypertension, suggesting that this characteristic is specific to uraemic cardiomyopathy, a feature specifically of cardiac rather than muscle in general (Amann et al., 1997).

A reduction in capillary density leads to a greater diffusion distance from the capillary to the myocyte, thus rendering the myocardium oxygen deprived and more susceptible to ischaemic damage. This concept has been supported by experimental studies, showing a larger infarct size following ischaemia in the subtotally nephrectomised rat heart (Dikow et al., 2004). Moreover, a decreased oxygen supply to the cardiomyocyte may compromise mitochondrial function, resulting in a loss of mitochondrial membrane potential and consequently reduced ATP synthesis, which may contribute to the inability of the uraemic heart to adapt to haemodynamic alterations (Seymour, 2003a). Additionally, loss of mitochondrial integrity initiates the apoptotic cascade (Borutaite and Brown, 2003), ultimately leading towards the deterioration of ventricular function and, in turn, progression to heart failure (Figure 1.5).

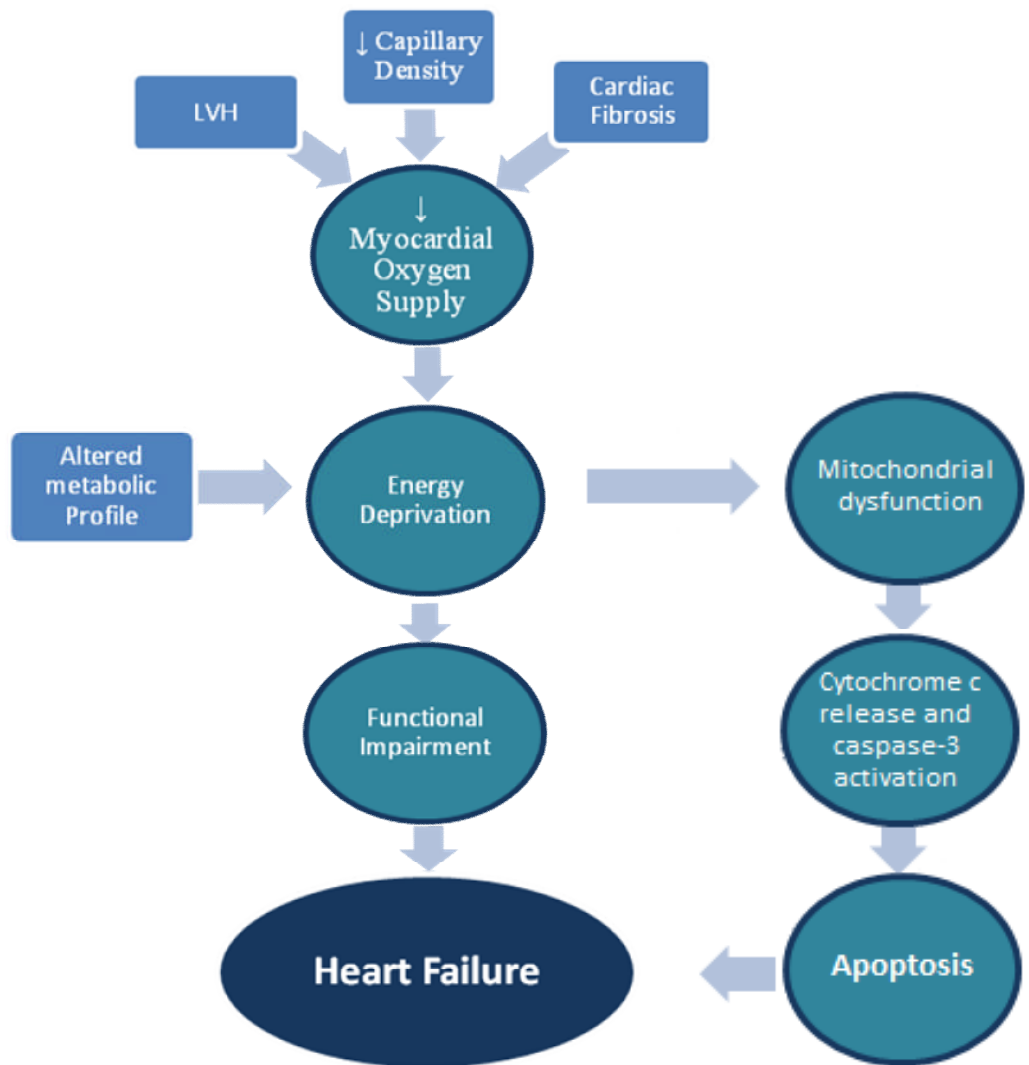


Figure 1.5: Diagram showing the sequence of events leading to heart failure in uraemia

## **1.5 Cardiac Fibrosis**

A further detrimental characteristic of CKD is myocardial fibrosis. During LVH, coupled with the enlargement of cardiomyocytes is the expansion of extracellular matrix (ECM) to preserve myocardial structural integrity. When the heart is subjected to a chronic increase in demand (such as prolonged pressure or volume overload), collagen, the principle component of ECM, accumulates disproportionately, leading to cardiac dysfunction (Weber, 1989).

### **1.5.1 Extracellular Matrix (ECM)**

The ECM can be organised into three distinct forms. The endomysium, which surrounds individual cardiomyocytes, the perimysium, which envelopes bundles of myocytes, and the epimysium, which is the ECM surrounding the whole heart (Weber, 1989, Weber et al., 1994) (Figure 1.6).

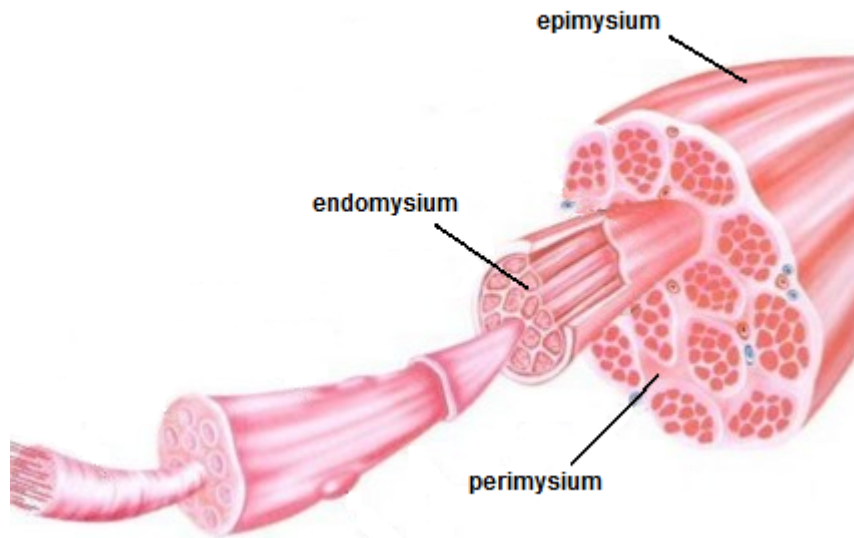


Figure 1.6: Diagram of ECM distribution in muscle  
(Adapted from Hunter and Harris, 2008)

ECM is comprised primarily of collagen, with lesser amounts of fibronectin, laminin and elastin. Over 20 types of collagen fibres exist, which vary depending on their polypeptide chain sequence. The primary collagen fibres within the normal heart are type I, III and V accounting for 85%, 11% and 3% of the total collagen respectively (Weber et al., 1988).

Type I collagen fibres consist of two  $\alpha 1$  polypeptide chains and one  $\alpha 2$  chain, with repeating glycine units, which are tightly wound to form a triple helical structure (van der Rest and Garrone, 1991). Collagen synthesis takes places within cardiac

fibroblasts, which are also responsible for the production of other ECM components including glycosaminoglycans and glycoproteins. Pro- $\alpha$  chains are synthesised on ribosomes of the rough endoplasmic reticulum (ER). They are then secreted into the ER lumen where they combine with 2 other pro- $\alpha$  chains to form a hydrogen-bonded helix, known as procollagen (Ricard-Blum and Ruggiero, 2005). Procollagen contains extra amino acids, or propeptides, at the C- and N- terminals, which are cleaved once the procollagen has been secreted into the extracellular space, forming tropocollagen. Tropocollagens aggregate to form collagen fibrils, which can then be assembled into larger collagen fibres, which are visible under a light microscope (Church et al., 1971).

Experimental models (Amann and Ritz, 1996, Kalk et al., 2007, Mall et al., 1988) and post-mortem studies (Mall et al., 1990) have both revealed extensive interstitial fibrosis in the uraemic heart. Experimental studies using the 5/6<sup>th</sup> nephrectomy model have shown that uraemia enhances the activation and proliferation of cardiac interstitial fibroblasts (Mall et al., 1988, Amann and Ritz, 1997, Amann et al., 1994). Interestingly, the fibrosis observed in hearts from uraemic patients was significantly more pronounced than in non-renal hypertensive controls (Mall et al., 1990). Furthermore, Amann *et al* (1998b) showed that myocardial fibrosis, during experimental CKD, occurs independent of hypertension and LVH.

The presence of myocardial fibrosis contributes toward the development of heart failure and has functional consequences, including arrhythmias and reduced ventricular compliance, leading to impaired relaxation and diastolic dysfunction

(Saito et al., 2007, Varnava et al., 2001). Importantly, diastolic dysfunction is frequently observed in patients with CKD (Otsuka et al., 2009). The deposition of collagen fibres between capillaries and myocytes may also contribute to oxygen depletion (Figure 1.5). Indeed, a mismatch between oxygen supply and demand decreases the tolerance of the uraemic heart to ischaemic insults (Dikow et al., 2004). In support of this, clinical studies have demonstrated that patients with renal insufficiency have an increased risk of death following acute myocardial infarction (Shlipak et al., 2002).

### **1.6 Erythropoietin (EPO)**

Hypoerythropoietinaemia is an established consequence of uraemia (Caro et al., 1979, Eschbach et al., 2002). In addition to decreased EPO production, EPO resistance may also occur in CKD patients due to the production of inflammatory cytokines, including IL-6 and TNF $\alpha$  (Goicoechea et al., 1998). Since the cloning of the gene in 1985, EPO has been widely used as a treatment for anaemia and its use has revolutionised the treatment of CKD (Lin et al., 1985). The haemopoietic effects of EPO are well known, although the effects of EPO extend well beyond the bone marrow.

### 1.6.1 Biochemistry of EPO and EPO Receptor

EPO is a 165 amino acid glycoprotein hormone (30.4kDa) belonging to the type 1 cytokine family (Maiese et al., 2005). Its primary role is to regulate erythropoiesis (production of red blood cells) by controlling the proliferation, differentiation and survival of erythrocytes (Fisher, 2003). During development, the source of EPO production switches from the foetal liver to the peritubular fibroblast cells in the inner cortex and outer medulla of the adult kidney (Lacombe et al., 1988). When the cellular demand for oxygen exceeds supply, cells express hypoxia inducible factor 1 (HIF1), which controls oxygen homeostasis (Wang et al. 1995). HIF-1 comprises two subunits, HIF1 $\alpha$  and HIF1 $\beta$ . Under normoxic conditions, HIF1 $\alpha$  undergoes prolyl hydroxylation, which provides a binding site for E3 ubiquitin ligase containing von Hippel-Lindau tumour-suppressor protein (VHL), resulting in proteasomal degradation. During hypoxia, HIF prolyl-hydroxylation is inhibited leading to HIF-1 activation and increased transcription of a number of proteins, including EPO and vascular endothelial growth factor (VEGF) (Semenza, 1994).

The effects of EPO are mediated through its specific cellular receptor EPOR. EPOR is a type I transmembrane receptor belonging to the cytokine receptor superfamily (Smith et al., 2003). Upon binding, EPO causes homodimerisation of EPOR, causing the phosphorylation and subsequent activation of the receptor-associated Janus Kinase2 (Jak2) (Witthuhn et al., 1993). This results in the phosphorylation of tyrosine residues in EPOR and successive activation of signalling molecules with Src homology domains, including signal transducer and activator of transcription 5

(STAT5) and phosphatidylinositol 3-kinase (PI3K) (Figure 1.7) (Sawyer and Penta, 1996, Um and Lodish, 2006).

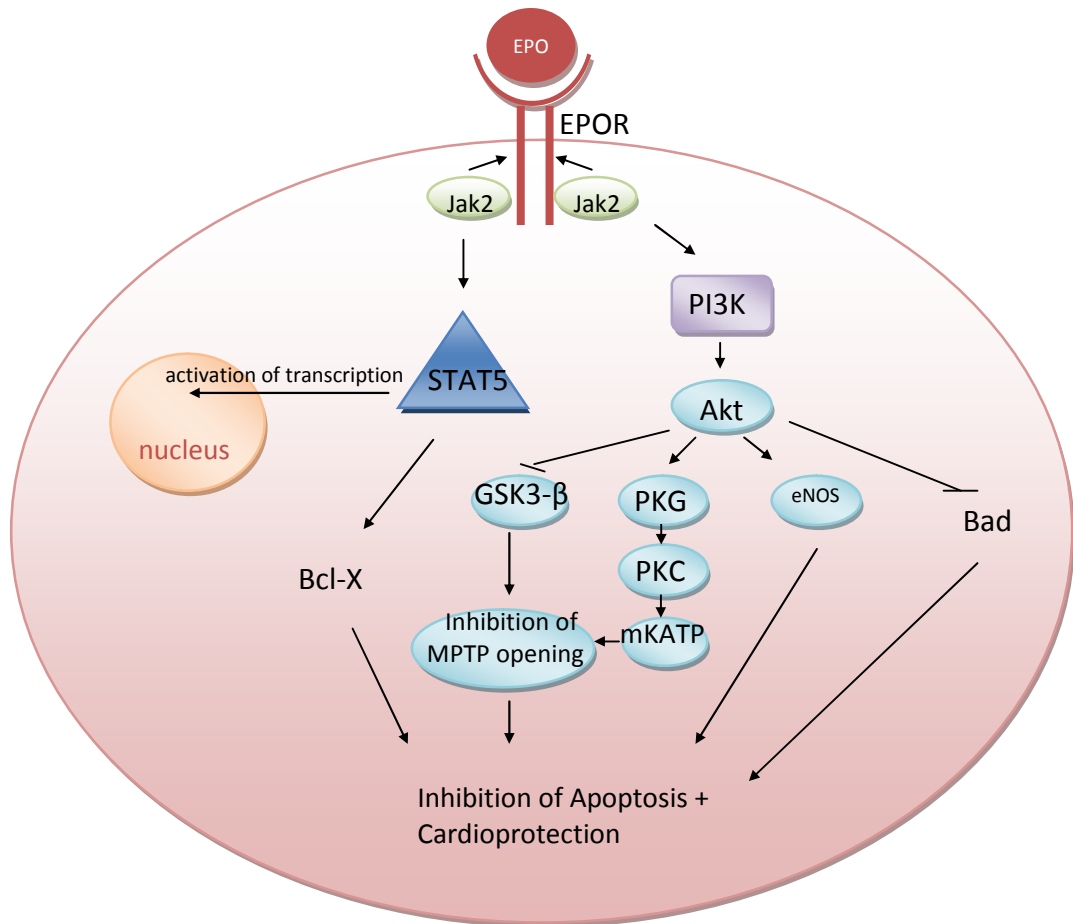


Figure 1.7: Schematic diagram of EPO signalling

eNOS Endothelial Nitric Oxide Synthase; GSK3-β Glycogen Synthase Kinase 3-β; Jak2 Janus Kinase 2; PI3K phosphatidylinositol 3-kinase; MPTP Mitochondrial Permeability Transition Pore; mKATP mitochondrial ATP-dependent potassium channels; PKG/C Protein Kinase G/C; Stat5 signal transducer and activator of transcription 5.

Activation of Stat5 promotes transcription of anti-apoptotic genes, including Bcl-X (Silva et al., 1999, Socolovsky et al., 1999). Indeed, STAT5a<sup>-/-</sup> and STAT5b<sup>-/-</sup> mice show severe anaemia and increased apoptosis, thus suggesting a direct role for STAT5 in the development and survival of erythrocytes (Socolovsky et al., 1999). Stimulation of the PI3K pathway and downstream activation of Akt also reduces erythroblast apoptosis through modulation of pro- and anti-apoptotic proteins including Bad and caspase 9 (Hanlon et al., 2005, Parsa et al., 2003, Smith et al., 2003, Wojchowski et al., 1999).

### **1.6.2 Cardiovascular effects of EPO**

The recent discovery that EPOR is also expressed on non-haematopoietic tissue including neurons (Digicaylioglu and Lipton, 2001, Brines et al., 2000) retinal cells (Junk et al., 2002), smooth muscle cells (Ammarguella et al., 1996), endothelial cells (Anagnostou et al., 1994) and cardiomyocytes (Brines et al., 2004, Depping et al., 2005, van der Meer et al., 2004, Wright et al., 2004) highlights a role of EPO beyond erythropoiesis.

The protective effect of EPO was first demonstrated in ischaemic brain injury. Bernaudin *et al.* (2000) showed a rapid increase in EPOR expression in the presence of ischaemia, correlating with a decrease in caspase-3 cleavage and apoptotic cell death (Bernaudin et al., 2000). In a rat stroke model, EPO reduced the area of neural damage, even when administered 6 h after cerebral artery occlusion (Brines et al., 2000). Furthermore, clinical studies have shown that EPO is safe and well

tolerated, when administered after an acute ischaemic stroke and is associated with a reduction in infarct size (Ehrenreich et al., 2002).

The role of EPO as a cardioprotectant has since been reiterated (Moon et al., 2003a, Shi et al., 2004, Wright et al., 2004). There is little experimental data on the direct effects of EPO in the uraemic heart, however, parallels can be drawn based on animal models of heart failure.

The mechanisms underlying the cardioprotective effect of EPO have not yet been fully elucidated. Improved cardiac function may be partly explained *via* the up-regulation of erythropoiesis. Indeed, stimulating red blood cell production increases the delivery of oxygen to the myocardium and improves function (Fisher, 2003). However, EPO can exert beneficial effects on *ex-vivo* hearts (Wright et al., 2004) and isolated cardiomyocytes (Calvillo et al., 2003). Furthermore, chronic administration of low-dose EPO improved function in an experimental model of post-MI heart failure, without modifying haematocrit (Ben-Dor et al., 2007, Lipsic et al., 2008). Carbamylated erythropoietin (CEPO) is an analogue of EPO that does not bind to the dimeric EPOR and therefore lacks the ability to stimulate erythropoiesis. Administration of CEPO resulted in improved left ventricular function, in addition to a 50% reduction in apoptosis, in an experimental model of post-MI heart failure (Fiordaliso et al., 2005, Moon et al., 2006). These data therefore indicate that the cardioprotective effects of EPO are independent from its haematopoietic effects.

### 1.6.2.1 Acute Cardioprotective Effects

The prevention of cardiomyocyte apoptosis is pivotal in the acute cardioprotective effects of EPO. During LVH, the myocardium has a limited adaptive response to the activation of stress pathways, which predisposes some cells to damage and loss through apoptosis (programmed cell death) (Foo et al., 2005). The gradual loss of irreplaceable cardiomyocytes *via* apoptosis can impair function and may play a central role in the gradual progression to heart failure (Anversa et al., 1996, Gupta et al., 2007, Sharma et al., 2007). Indeed, both experimental (Cheng et al., 1996) and clinical studies (Olivetti et al., 1997) show myocyte apoptosis to be a major characteristic of the failing heart. Apoptosis is an energy requiring, tightly controlled process, characterised by nuclear condensation, membrane blebbing and cell shrinkage (Kunapuli et al., 2006). In response to a variety of stimuli, including mechanical stretch and hypoxia, apoptosis can be triggered *via* two main routes, the extrinsic and intrinsic (mitochondrial) pathway (Figure 1.8).

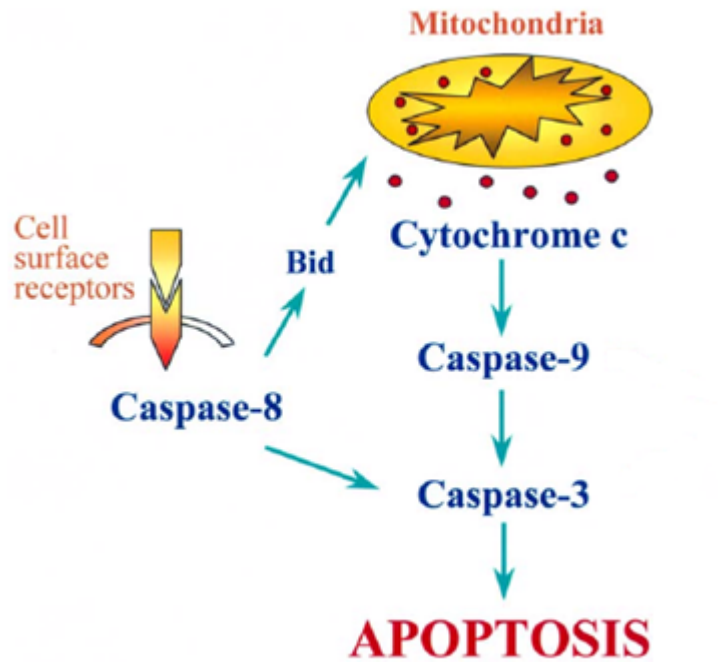


Figure 1.8: Apoptosis pathway  
(adapted from Borutaite and Brown 2003)

The extrinsic pathway is activated upon the binding of extracellular ligands (e.g. Fas ligand or  $TNF\alpha$ ) to their specific cellular receptors, known as death receptors. This results in activation of caspase 8 and downstream activation of caspase 3, triggering apoptosis (Nagata, 1997). Activation of caspase 8 also leads to the cleavage and activation of Bid, a pro-apoptotic member of the Bcl-2 family of proteins. Bid interacts with another Bcl-2 protein, Bax, which may be inserted into the outer mitochondrial membrane, causing a change in the mitochondrial membrane potential and release of cytochrome *c*. Bid links the intrinsic and extrinsic apoptotic pathways (Crow et al., 2004). Mitochondria are central to the intrinsic pathway.

Pro-apoptotic compounds (such as Bax) and damage to mitochondria *via* oxidative stress (including reactive oxygen species; ROS) or other agents, can trigger the release of cytochrome *c*, which stimulates apoptosis *via* activation of caspase 9, and subsequent activation of caspase 3 (Borutaite and Brown, 2003) (Figure 1.8). Cytochrome *c* release occurs from the opening of the mitochondrial permeability transition pore (MPTP) (Zoratti and Szabo, 1995). In response to stress, the inner mitochondrial membrane becomes permeabilised by the opening of MPTP, resulting in loss of ion homeostasis (Halestrap, 2009). The free movement of ions causes mitochondria to swell, resulting in rupture of the outer membrane, thereby releasing cytochrome *c* from the inter membrane space. Interestingly, several experimental studies have shown that inhibiting MPTP opening improves function and protects the heart during ischaemia/ reperfusion (Nazareth et al., 1991, Xu et al., 2001).

A number of experimental studies have shown that EPO reduces apoptosis in cultured neonatal myocytes (Calvillo et al., 2003, Tramontano et al., 2003). Moreover, administration of EPO reduced ventricular dysfunction, improved ejection fraction and ameliorated apoptosis after induction of MI in rats (Bullard and Yellon, 2005).

The mechanisms underlying EPO-mediated cardioprotection remain incompletely understood. Associated with EPO-EPOR interaction is the reperfusion injury salvage kinase (RISK) pathway, involving activation of extracellular signal-related kinase-1

(ERK-1) and PI3K/Akt, which are central to anti-apoptotic signalling (Tramontano et al., 2003, Cai and Semenza, 2004). The role of the PI3K/Akt pathway in the cardioprotective effect of erythropoietin has been substantiated using specific inhibitors of PI3K. Several studies report that the protective effects (improved cardiac function and reduced apoptosis), following EPO treatment, are diminished in the presence of the PI3K inhibitors, LY294002 and wortmannin (Parsa et al., 2003, Sivertsen et al., 2006). More recently it has been shown that the EPO-mediated reduction in cardiomyocyte apoptosis is *via* downstream effects of Akt activation, through deactivation of glycogen synthase kinase (GSK)-3 $\beta$  and, *via* protein kinase G (PKG) phosphorylation, protein kinase C (PKC) activation (Ohori et al., 2008). Both of these effects, either directly or indirectly, inhibit the opening of MPTP (Figure 1.7) (Ohori et al., 2008, Kim et al., 2006). Further support for this comes from findings combining treatment with EPO and the PKC inhibitor, chelerythrine, which reduced functional recovery of hearts when compared with EPO treatment alone (Rafiee et al., 2005). Shi *et al.* (2004) showed that the improved functional recovery observed in EPO treated hearts was also abolished in the presence of the mitochondrial ATP-sensitive potassium (mK<sub>ATP</sub>) channel blocker, glibenclamide (Shi et al., 2004) (Figure 1.7).

Although the prevention of myocyte apoptosis is central to the cardioprotective actions of EPO, several studies report other cellular effects. EPO treatment caused a reduction in oxidative stress and a decreased production of the pro-inflammatory cytokines, IL-1 $\beta$ , IL-6 and TNF $\alpha$ , in an animal model of post-MI heart failure (Li et al., 2006). Furthermore, studies show that EPO is involved in the mobilisation of

endothelial progenitor cells (EPC's), thus promoting vascular repair (Urao et al., 2006, d'Uscio et al., 2007).

EPO has also been shown to modulate nitric oxide (NO) production, *via* up-regulation of eNOS. The anti-apoptotic effects of NO are well documented and include inhibition of NADPH oxidase, thus limiting oxidative stress and cellular damage (Razavi et al., 2005, Smith et al., 2005). Indeed, the protective effect of EPO was abolished in eNOS-deficient mice (Burger et al., 2006). Furthermore, several studies have demonstrated that the anti-apoptotic effect of EPO was abrogated in cultured myocytes, when incubated in the presence of the NOS inhibitor, L-NAME (Bullard and Yellon, 2005, Burger et al., 2006, Joyeux-Faure et al., 2006). EPO is thought to increase eNOS expression *via* activation of the PI3K/Akt pathway (Rui et al., 2005). In contrast, Shi *et al.* (2004) found that L-NAME did not abolish the cardioprotective effect of EPO during ischaemia-reperfusion in isolated rabbit hearts (Shi et al., 2004).

#### **1.6.2.2 Chronic Cardioprotective Effects**

Chronic EPO treatment has beneficial effects, however, the mechanisms underlying these have not yet been fully elucidated. Experimental models of ischaemic heart disease and heart failure have shown that chronic EPO administration stimulates angiogenesis and vascular sprouting (Nishiya et al., 2006, van der Meer et al., 2005, Westenbrink et al., 2007). Interestingly, Jaquet *et al* (2002) demonstrated that EPO

stimulated angiogenesis (*in vitro*) to the same degree as VEGF in myocardial tissue (Jaquet et al., 2002). Furthermore, the administration of EPO to heart failure patients resulted in increased endothelial progenitor cell (EPC) proliferation (George et al., 2005). Westernbrink *et al.* (2007) showed that EPO induced EPC mobilisation and incorporation of these bone-marrow derived EPCs into the endothelium of newly formed vessels.

Chronic EPO administration can ameliorate cardiac fibrosis, potentially, *via* inhibition of transforming growth factor (TGF) $\beta$  (Shushakova et al., 2009). In the post-MI rat heart, Nishiya *et al.* (2006) observed a reduction in cardiac fibrosis in non-infarcted regions, when EPO was given once a day for 4 days (5000U/Kg) and when administered 3 times a week for 4 weeks (1000U/Kg) post-surgery. As previously mentioned, EPO modulates NO activity, which, in addition to its anti-apoptotic actions, also plays a key role in cell growth, contractile function and vascular homeostasis (Seddon et al., 2007). Non-specific inhibition of NOS has been shown to increase fibrosis following MI (Silvestre et al., 1999). Whereas adenoviral gene transfer of eNOS, in a rat model of post-MI heart failure, caused a decrease in myocardial fibrosis and reduced oxidative stress (Smith et al., 2005). These studies highlight the beneficial effects of EPO-mediated up-regulation of NO.

Clinical studies investigating the cardiovascular effects of EPO in CKD have provided somewhat conflicting results. Some studies have shown that administering EPO to partially or fully correct the anaemia associated with CKD induces a regression of

LVH (Silberberg et al., 1990, Hayashi et al., 2000). A reduction in LV mass has been associated with improved survival and reduced hospitalisations in uraemic patients (London et al., 2001).

The CREATE trial demonstrated an improvement in general health and physical capacity in CKD patients with a haemoglobin corrected to within the normal range (13-15g/dL) compared with patients with a subnormal haemoglobin (10.5-11.5g/dL). Interestingly however, no differences were observed in the incidence of cardiovascular events between the two groups (Drueke et al., 2006). A second large clinical trial, the CHOIR trial showed that correcting anaemia to a target haemoglobin of 13.5g/dL did not result in an improved quality of life and actually increased the risk of cardiovascular events in CKD patients (Singh et al., 2006). Further large-scale clinical trials are required to elucidate the potential beneficial effects of EPO.

## **1.7 Objectives**

Uraemic cardiomyopathy is associated with anaemia, hypertension and LVH which contribute to heart failure. EPO is widely used in CKD patients to improve haematocrit. Interestingly, recent studies have observed cardioprotective effects of EPO, independent from erythropoiesis. However, little is known regarding the direct impact of EPO on the uraemic heart. Therefore, this study aims to examine

the functional, structural and metabolic changes in uraemic cardiomyopathy and the effects of chronic EPO administration. Specifically, the aims of this study were

- To determine the impact of uraemia on cardiac function *in vitro* and *in vivo*
- To analyse the effect of acute and chronic EPO treatment on cardiac function
- To assess the extent of cardiac metabolic remodelling in uraemia, and the impact of chronic EPO administration
- To identify the extent of myocardial fibrosis in uraemia and the impact of chronic EPO treatment
- To determine the effect of uraemia and chronic EPO administration on *in vitro* myocardial mitochondrial function

## **Chapter 2: Materials and Methods**

## 2.1 Materials

Table 2.1 provides a list of the materials used in this study. Chemicals were all of analaR grade and purchased from BDH (Poole, UK) unless otherwise stated. Surgical materials were purchased from NHS supplies (IVF unit, Hull Royal Infirmary, UK).

Table 2.1: Materials and Suppliers

Suppliers	Materials
Abbott Laboratories, Kent, UK	Isoflurane
Amgen Ltd. Cambridge, UK	Aranesp® (Darbepoetin alfa)
Apollo Scientific Ltd. Stockport, UK	Deuterated water (D <sub>2</sub> O)
Biorad Laboratories, Munich, Germany	Bio-rad Protein Assay
British Oxygen Corporation, Manchester, UK	Oxygen
Cambridge Isotope Laboratory, Andover, USA	[U- <sup>13</sup> C] Sodium Palmitate [1- <sup>13</sup> C] D-Glucose
Proliant Health & Biologicals Iowa, USA	Bovine serum albumin (fatty acid free <0.001%)
Fisher Scientific, Leicester, UK	L-glutamine (BP379-100)
Harvard Apparatus, Edenbridge, UK	Gaseous anaesthetic (Fluovac vacuum pump, Veterinary fluosorber and Ohmeda Fluotec vaporizer)

Intervet UK Ltd. Cambridge, UK	Amphipen
Johnson & Johnson, North Yorks, UK	Ethicon 3-0 (Vicryl braided) Ethicon 3-0 (Blue monofilament) Mersilk 3-5 (Silk braided) Surgicel®
Merial Animal Health, Harlow, UK	Halothane
Millipore, Ireland	0.45µm filter (HA type) 5.0µm filter (SVPP type)
Nestle, UK	Marvel milk powder
Novartis Animal Health, Herts, UK	Thiovet (sodium thiopentone)
Pall Life Sciences, USA	Acrodisc® (0.2µm syringe filter)
Pfizer Ltd. Sandwich, UK	Rimadyl (5% w/v Carprofen)
Roche Diagnostics, Penzberg, Germany	Complete® Protease inhibitor cocktail
Sakura Finetek Zoeterwoude, Netherlands	Tissue-Tek OCT compound
Sigma-Aldrich Company Poole, UK	2,2'-Azino-bis (3-Ethylbenz-Thiazoline-6-Sulphonic Acid) - ABTS Acetyl CoA Amyloglucosidase Bovine serum albumin (BSA) Bromophenol blue CoA Chelex-100 sodium form

Sigma-Aldrich Company Poole, UK (continued)	Dichloroacetic acid Direct Red 80 EGTA Fast Blue RR Salt Glucose oxidase Glycerol HEPES Imidazole Insulin Lactate dehydrogenase Lactate (sodium salt) Leupeptin Malate 2- Mercaptoethanol Octanyl Co-A Palmitic acid (sodium salt) Palmitoyl carnitine Percoll Peroxidase Pyruvate (sodium salt) Sodium Tetrathionate sodium dodecyl sulphate (SDS) Sucrose TRIS
--	---

## 2.2 Methods

All animal procedures conformed to the UK Home Office guidelines on the operation of laboratory animals (Scientific Procedures Act 1986).

### 2.2.1 Induction of Uraemia

Uraemia was induced surgically in male Sprague-Dawley rats (weighing approximately 250g) *via* a one-stage 5/6<sup>th</sup> nephrectomy (modified from Reddy et al., 2007, Raine et al., 1993). Briefly, animals were anaesthetised with 3.5% isoflurane in 3L/min oxygen and Rimadyl administered (4 mg/Kg body weight), by subcutaneous injection, for post-operative pain relief. Throughout the surgical procedure, anaesthesia was maintained using 2.5% isoflurane in 1 L/min oxygen. Depth of anaesthesia was indicated using the pedal withdrawal reflex.

A midline abdominal incision was made and the left kidney exposed and decapsulated. Approximately two-thirds of the kidney was removed. Surgicel® (Johnson & Johnson, UK) was used to stem excessive bleeding and the remnant kidney replaced. Subsequently, the right kidney was located and decapsulated. The renal vessels were ligated using a non-absorbable suture (Mersilk® Johnson & Johnson, UK) and the whole kidney removed. Abdominal musculature was closed using an absorbable suture (Ethicon 3-0 Vicryl braided, Johnson & Johnson, UK). Non-absorbable sutures (Ethicon 3-0 blue monofilament, Johnson & Johnson, UK) were used to close the skin layer.

In control animals, a sham procedure was performed whereby kidneys were solely decapsulated and replaced intact. The incision was closed as described above. To compensate for fluid loss during surgery, sterile isotonic saline (0.9% w/v) was administered into the abdominal cavity prior to closure of the layer.

Rats were maintained for 3, 6, 9 or 12 weeks post-surgery. Animals were housed individually with 12:12hr light:dark cycles. Uraemic animals were pair-fed with sham operated animals, a diet of standard rat chow. Water was available *ad libitum* for both animal groups.

### **2.2.2 Preparation of Krebs-Henseleit (K-H) Buffer**

Hearts were perfused *in vitro* using Krebs-Henseleit (K-H) buffer containing 3% bovine serum albumin (BSA) and the following components (mM); NaCl (118.5), NaHCO<sub>3</sub> (25), KCl (4.8), KH<sub>2</sub>PO<sub>4</sub> (1.2), MgSO<sub>4</sub> (1.2), CaCl<sub>2</sub> (1.25), glucose (5) (unlabelled or 100% 1-<sup>13</sup>C labelled), sodium pyruvate (0.1), sodium lactate (1), sodium palmitate (0.3) (unlabelled or 50% U-<sup>13</sup>C labelled), glutamine (0.5) and 0.1 mU/L insulin. Buffers were freshly prepared using ultra pure water (18MΩ) gassed with 95% O<sub>2</sub> 5% CO<sub>2</sub> and filtered using a 0.45 μm Millipore filter.

### 2.2.3 Preparation of Bovine Serum Albumin (BSA)

300 g BSA, essentially fatty acid free (< 0.001%), was dissolved in 1 L ultra pure water (18 MΩ) containing 118 mM NaCl and 2.5 mM CaCl<sub>2</sub>. Lengths of dialysis tubing were boiled for 10 minutes in 1 mM EDTA containing 2% (w/v) NaHCO<sub>3</sub>. The tubing was then rinsed in ultra pure water, boiled for a further 10 minutes in 1 mM EDTA and rinsed again using ultra pure water. The tubing was cooled and stored at 4°C.

The BSA solution was poured into prepared tubing and dialysed against 20L ultra pure water (18MΩ) containing 118 mM NaCl and 2.5 mM CaCl<sub>2</sub> at 4°C. After 48 h the BSA was separated into 10 equal aliquots (30% concentration) and stored at -20°C until required.

A correction was made to allow for NaCl and CaCl<sub>2</sub> already present in the BSA solution (Equation 1). This value was then deducted from the amount of NaCl and CaCl<sub>2</sub> required in the K-H buffer.

$$\begin{aligned} \text{Mass of compound in BSA (per litre)} \\ = \text{Volume of BSA (L)} \times \text{Molecular Weight} \times \text{Molarity (M)} \end{aligned}$$

Equation 1: Calculation for NaCl and CaCl<sub>2</sub> present in BSA solution

For example, when using BSA with an aliquoted volume of 170 ml, the amount of NaCl present in the BSA =  $0.170 \times 58.44 \times 0.118 = 1.17\text{g}$  (per litre). This value can then be deducted from the amount required in the K-H buffer, for example when making up a litre of buffer (which requires 6.89g NaCl) the calculation would be  $6.89 - 1.17 = 5.72\text{g}$ .

For the addition of palmitate, sodium palmitate (unlabelled or 50% U-<sup>13</sup>C labelled) was dissolved in boiling ultra pure water (18MΩ) and added slowly to the BSA solution. Subsequently, this mixture was added to the filtered K-H buffer and filtered again using a 5.0μm Millipore filter.

#### **2.2.4 Heart Perfusion**

Animals were anaesthetised with an i/p injection of sodium thiopentone (100mg/Kg body weight). Hearts were excised and immediately placed in ice-cold K-H buffer. Hearts were cannulated *via* the aorta and perfused in a modified isovolumic Langendorff mode (Sample et al., 2006) using BSA K-H buffer gassed with 95% O<sub>2</sub> 5% CO<sub>2</sub> and maintained at 37°C throughout (Figure 2.1).

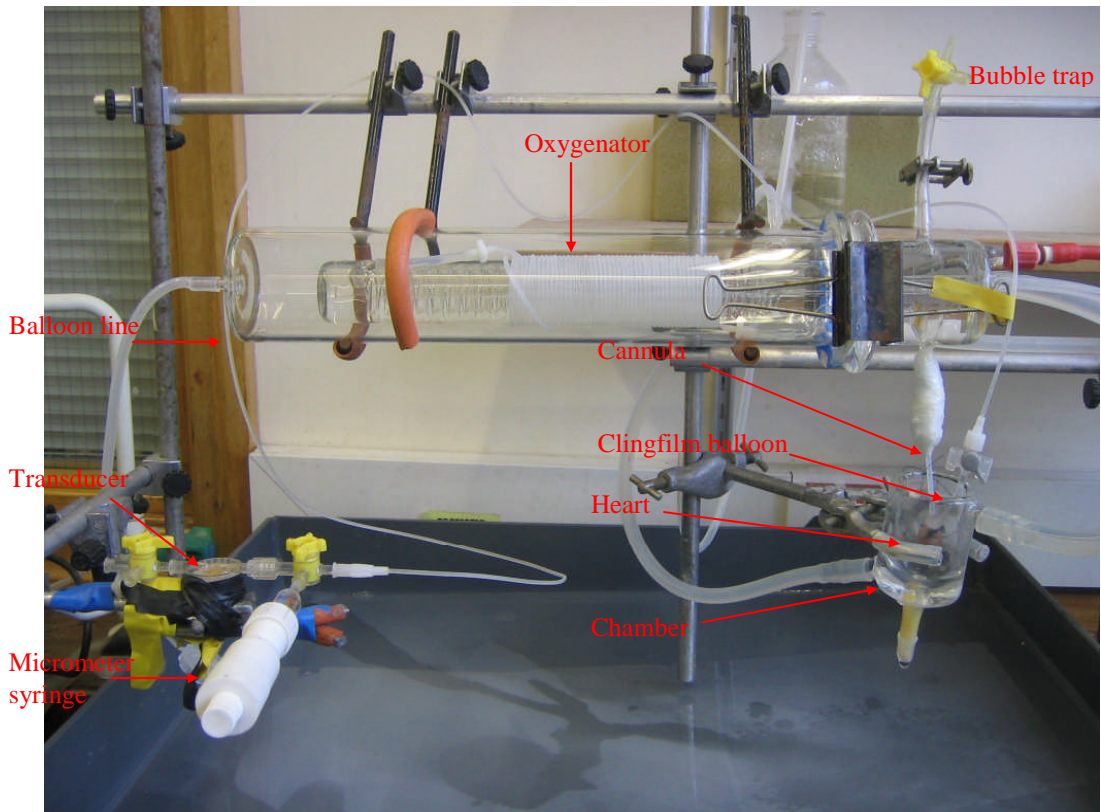


Figure 2.1: Isovolumic Langendorff perfusion apparatus

The apex of the left ventricle was pierced using a 21G needle, passed through the mitral valve, to prevent accumulation of fluid. A balloon made of cling-film, connected to a physiological pressure transducer (SensNor, Horten, Norway) *via* a fluid filled line, was inserted into the left ventricle, *via* the mitral valve, to monitor contractile function continuously (Figures 2.1 and 2.2). The balloon volume was adjusted using a micrometer syringe (Gilmont Instruments, Barrington USA) until a left ventricular diastolic pressure (DP) of approximately 5-7 mmHg was attained (Pabla and Curtis, 1996)

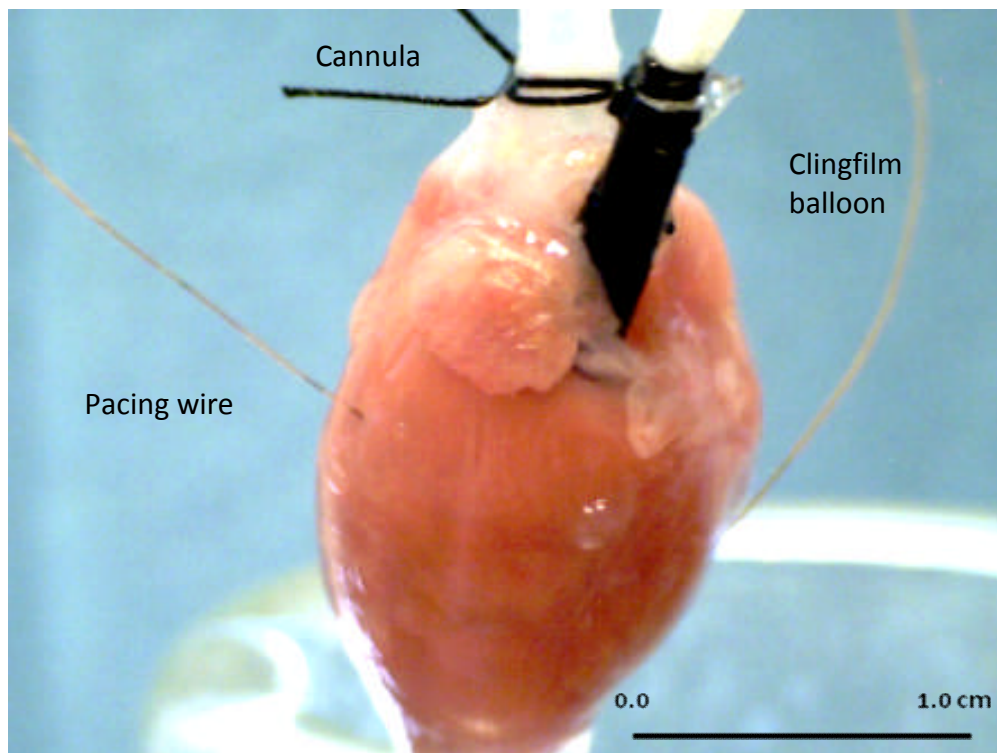


Figure 2.2: Isolated perfused rat heart

#### 2.2.4.1 Pacing

Prior to the insertion of the balloon, the atrioventricular (AV) node was crushed and copper wires were inserted into the heart using 25G needles (Figure 2.2). Wires were connected to the PowerLab stimulator output, which delivered a 1 msec pacing pulse. The pacing voltage was set between 400 mV- 1500 mV and hearts were paced at 300 bpm.

#### **2.2.4.2 *In Vitro* Cardiac Function**

Cardiac function was recorded *via* a bridge amplifier and PowerLab (4/30) using the software, Chart 5.5, and the additional 'blood pressure module' (ADInstruments, Hastings, UK). Heart rate (HR), systolic (SP) and diastolic pressures (DP) were continuously recorded throughout the perfusion. Left ventricular developed pressure (LVDP) was calculated by subtracting diastolic from systolic pressure (Figure 2.3) and rate pressure product (RPP), a measure of cardiac work, was calculated using Equation 2.

$$RPP = HR \times LVDP$$

Equation 2: Calculation for determining RPP

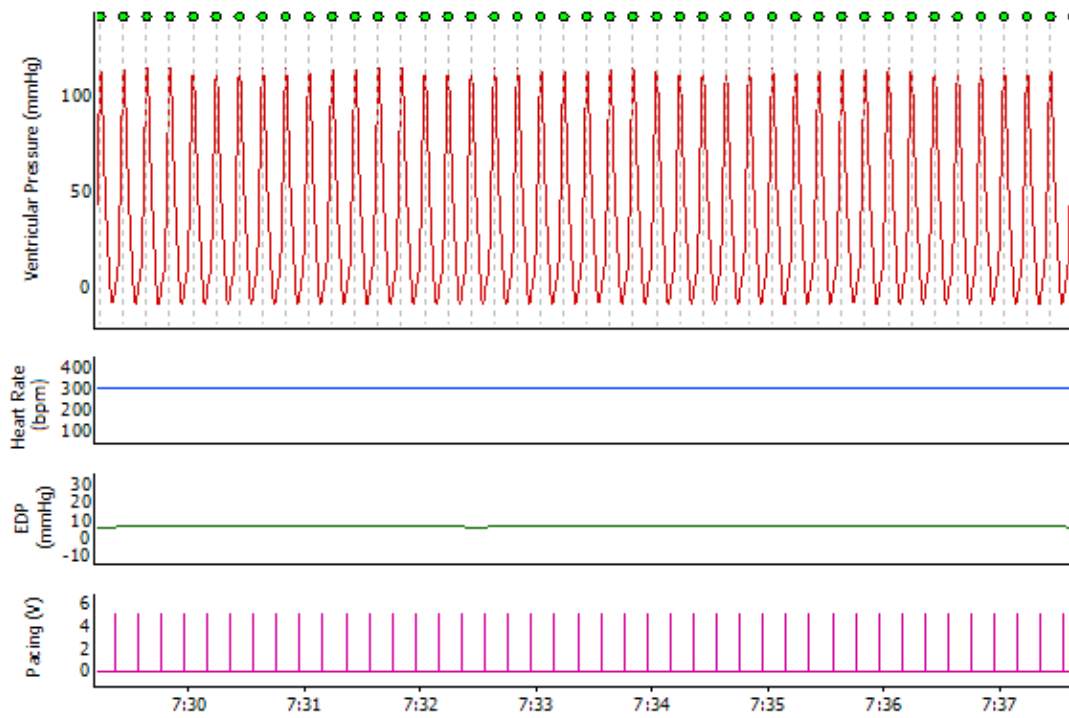


Figure 2.3a: Recording of cardiac function

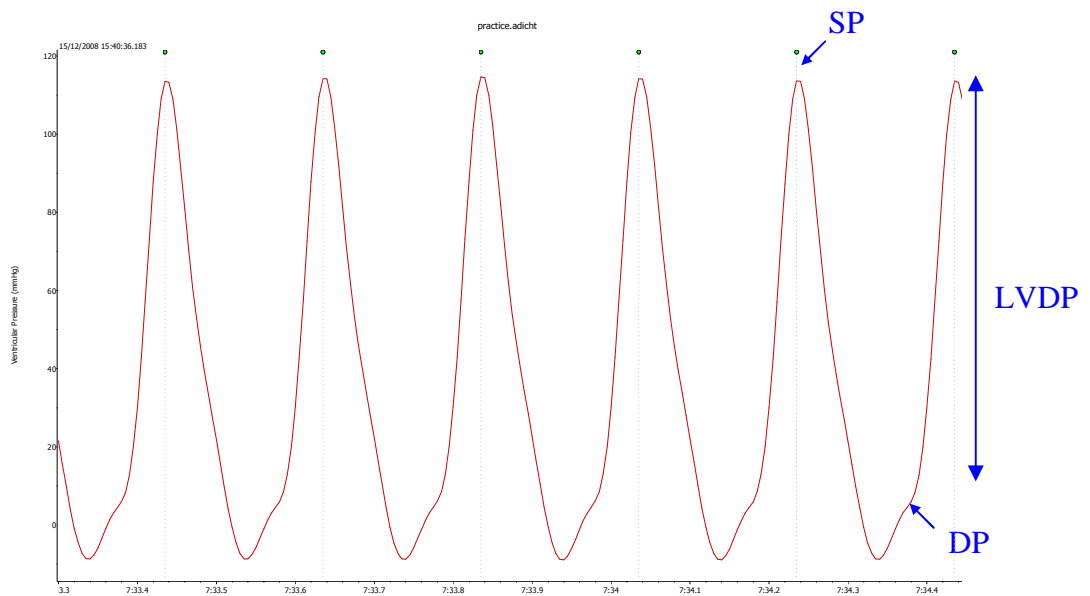


Figure 2.3b: Enlarged view of cardiac function  
(SP systolic pressure; DP diastolic pressure; LVDP left ventricular developed pressure)

To determine the rate of cardiac contractility,  $dP/dt_{\max}$  and  $dP/dt_{\min}$  were derived and recorded throughout the perfusion (Figure 2.4).

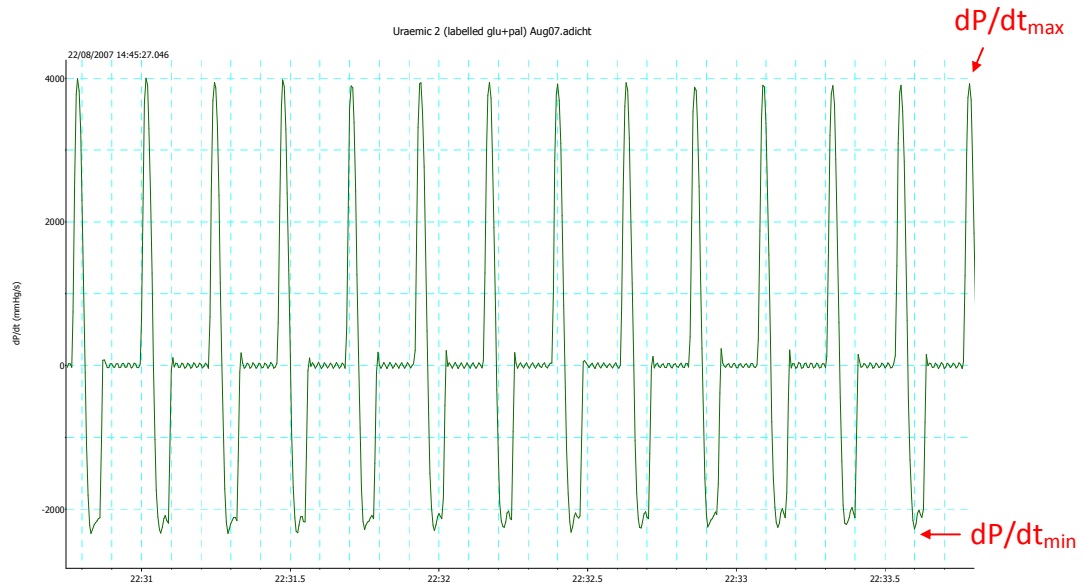


Figure 2.4: Recording of cardiac contractility

### 2.2.4.3 Oxygen Consumption ( $MVO_2$ )

To calculate the  $MVO_2$  of perfused hearts, perfusate and effluent samples were taken at 15 minute intervals throughout the perfusion. The  $pO_2$  content was measured using an ABL77 blood gas analyser (Radiometer Ltd. West Sussex, UK). Oxygen consumption ( $\mu\text{moles/g wet weight/min}$ ) was calculated using Equation 3 (Neely et al., 1967).

$$MVO_2 = \frac{\left( \frac{(pO_2 \text{ perfusate} - pO_2 \text{ effluent (mmHg)})}{760 \text{ mmHg}} \right) \times 0.199^1 \times \text{flow rate (ml/min)}}{\text{wet heart weight (g)}}$$

Equation 3: Calculation for Oxygen Consumption  
(<sup>1</sup>O<sub>2</sub> solubility at 37°C)

Cardiac efficiency (work performed per unit O<sub>2</sub> consumed) was calculated from RPP divided by MVO<sub>2</sub>.

$$\% \text{ lung water} = \left( \frac{(\text{wet lung weight} - \text{dry lung weight})}{\text{wet lung weight}} \right) \times 100$$

Equation 4: Calculation for determining % lung water

As a marker of cardiac failure, lungs were weighed and dried to determine the percentage of water (Equation 4). At the end of the perfusion protocol, atria were removed and ventricular tissue freeze clamped using Wollenberger tongs immersed in liquid nitrogen. Heart tissue was stored at -80°C until required.

#### **2.2.4.4 Indices of Hypertrophy**

At the time of sacrifice, body weight (BW), wet heart weight (HW) and tibia length were recorded. HW: BW and HW: tibia length were calculated to determine the degree of cardiac hypertrophy in uraemic animals (Yin et al., 1982).

#### **2.2.4.5 Haematocrit and Serum Analysis**

Immediately after excision of the heart, 1 ml of blood was taken from the chest cavity into a heparinised syringe for determination of haematocrit using a blood gas analyser (ABL77 Radiometer, UK). The remaining blood was taken from the chest cavity and centrifuged at 4000 g for 10 minutes at 4°C. Serum was removed and stored at -20°C. Serum urea and creatinine were analysed at Clinical Biochemistry, Hull Royal Infirmary, Hull and East Yorkshire NHS trust.

#### **2.2.5 <sup>13</sup>C NMR Spectroscopy**

##### **2.2.5.1 Perchloric Acid (PCA) Tissue Extraction**

Frozen ventricles were ground to a fine powder under liquid nitrogen using a mortar and pestle. Approximately 1 g powdered ventricular tissue was added to 6% PCA at a ratio of 1:5 (w/v) (Seymour et al., 1990). The suspension was left on ice for 10 minutes. Samples were centrifuged at 3000g for 10 minutes at 4°C and the supernatant adjusted to pH 6.5 using 6 M KOH. Samples were centrifuged and the

neutralised supernatant removed, frozen in liquid nitrogen and lyophilised for 48 h in a freeze dryer (Modulyo, BOC Edwards, UK).

#### **2.2.5.2 Preparation of NMR samples**

A phosphate buffer containing 50 mM  $\text{KH}_2\text{PO}_4$  (pH 6.5) was prepared and lyophilised for 48 h using a freeze dryer. The buffer was reconstituted using deuterium oxide ( $\text{D}_2\text{O}$ ).

The lyophilised tissue extract was reconstituted with 0.95 ml deuterated phosphate buffer. A small spatula of a chelating resin (chelex 100-sodium form, Sigma, Poole, UK) was added to remove paramagnetic ions. Following this, the sample was filtered into a 5 mm NMR tube through a 0.2  $\mu\text{m}$  syringe filter (Acrodisc® Pall Life Sciences, USA).

#### **2.2.5.3 Acquisition of $^{13}\text{C}$ Spectra**

High-resolution  $^1\text{H}$  decoupled (WALTZ 16 decoupling)  $^{13}\text{C}$  NMR spectra were collected at 500 MHz using an 11.7 Tesla ultra-shielded superconducting vertical wide bore Bruker magnet (Bruker, Coventry, UK) and 5 mm broadband probe, interfaced with a Bruker spectrometer. Free induction decays (FIDs) were acquired over 36000 scans with a  $90^\circ$  pulse (9.95  $\mu\text{s}$  pulse duration and 1 s interpulse delay) and fourier transformed spectra were analysed using Bruker Topspin (1.3) software.

#### 2.2.5.4 $^{13}\text{C}$ Labelling Profiles

One- $^{13}\text{C}$  labelled glucose and U- $^{13}\text{C}$  labelled palmitate generate [2- $^{13}\text{C}$ ] and [1, 2- $^{13}\text{C}$ ] labelled acetyl-CoA, respectively. When acetyl-CoA enters the TCA cycle, the  $^{13}\text{C}$  labels appear within TCA cycle intermediates, however these intermediates are in insufficient quantities to be detected by NMR analysis. However,  $\alpha$ -ketoglutarate is in rapid exchange with glutamate, which *is* present in sufficient quantities to detect the  $^{13}\text{C}$  label (Chance et al., 1983).

When [2- $^{13}\text{C}$ ] labelled acetyl-CoA (from 1- $^{13}\text{C}$  glucose) enters the TCA cycle and combines with oxaloacetate, the label appears on the C4 of  $\alpha$ -ketoglutarate and subsequently the C4 of glutamate. As the labelled  $\alpha$ -ketoglutarate is further metabolised in the TCA cycle, the label is scrambled randomly to either the C2 or C3 position of fumarate, and thus the C2 or C3 in oxaloacetate. On the next turn of the TCA cycle, the oxaloacetate (labelled in either the C2 or C3 position from the previous round) then combines with another 2- $^{13}\text{C}$  labelled acetyl-CoA, giving rise to glutamate labelled in either the C3 and C4 or C2 and C4 position. With successive turns of the TCA cycle, the label is transferred to the C2, C3 and C4 positions of glutamate (Figure 2.5a).

[U- $^{13}\text{C}$ ] labelled palmitate produces [1, 2  $^{13}\text{C}$ ] labelled acetyl-CoA which enters the TCA cycle, producing glutamate labelled in the C4 and C5 position. As described above, scrambling of the label occurs as  $\alpha$ -ketoglutarate continues through the TCA cycle producing oxaloacetate labelled in either C4 and C3, or C2 and C1 position.

With successive turns of the TCA cycle, the label appears in C5, C4 and C3 or C5, C4, C2 and C1 of glutamate (Figure 2.5b).

When hearts are perfused with both 1-<sup>13</sup>C glucose and U-<sup>13</sup>C palmitate, 9 peaks are observed in the C2 and C4 region and 5 peaks are seen in the C3 region of the glutamate spectra (Figure 2.6).

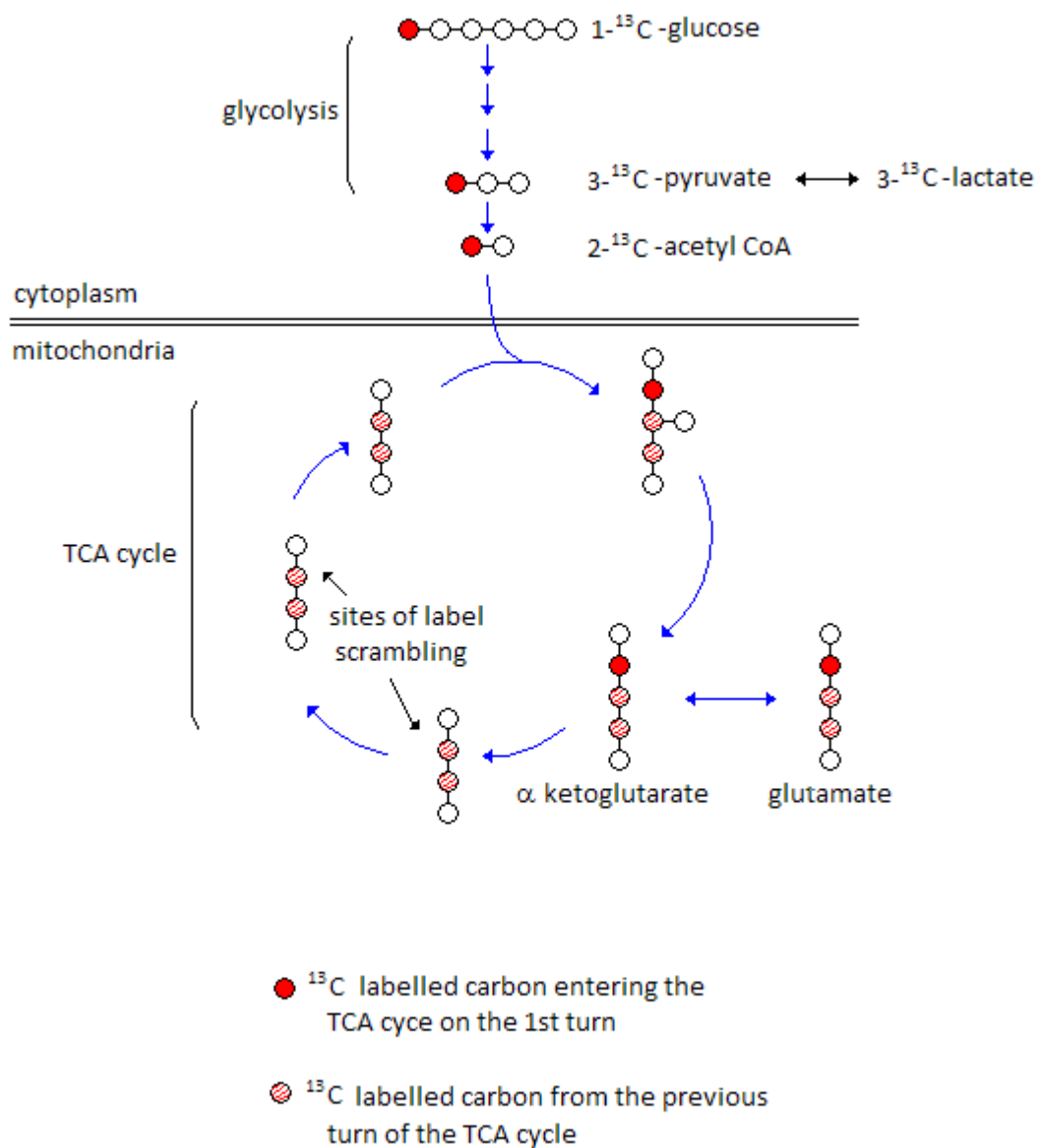
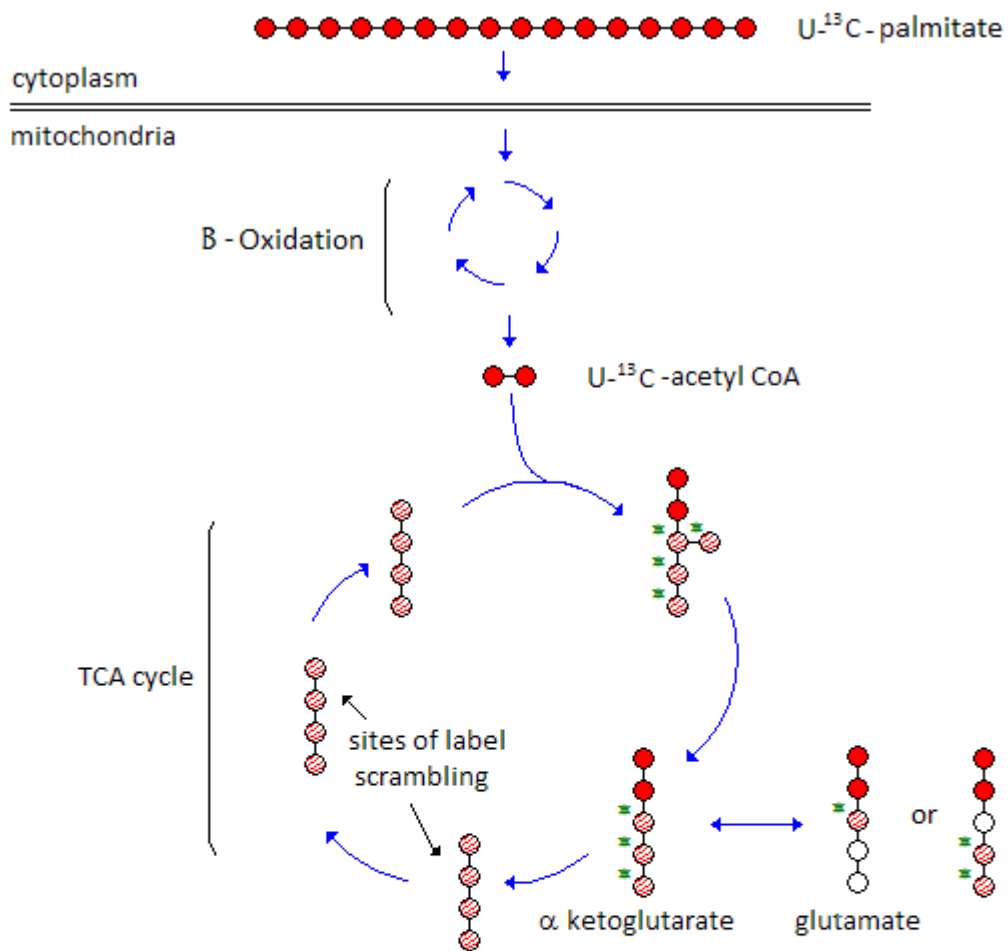


Figure 2.5a: Profile following 1-<sup>13</sup>C glucose  
(adapted from Seymour 2003)



- $^{13}\text{C}$  labelled carbon entering the TCA cycle on the 1st turn
- ◌  $^{13}\text{C}$  labelled carbon from the previous turn of the TCA cycle
- ◌ Half levels of  $^{13}\text{C}$  enrichment as a result of label scrambling

Figure 2.5b: Profile following  $U\text{-}^{13}\text{C}$  palmitate  
(adapted from Seymour 2003)

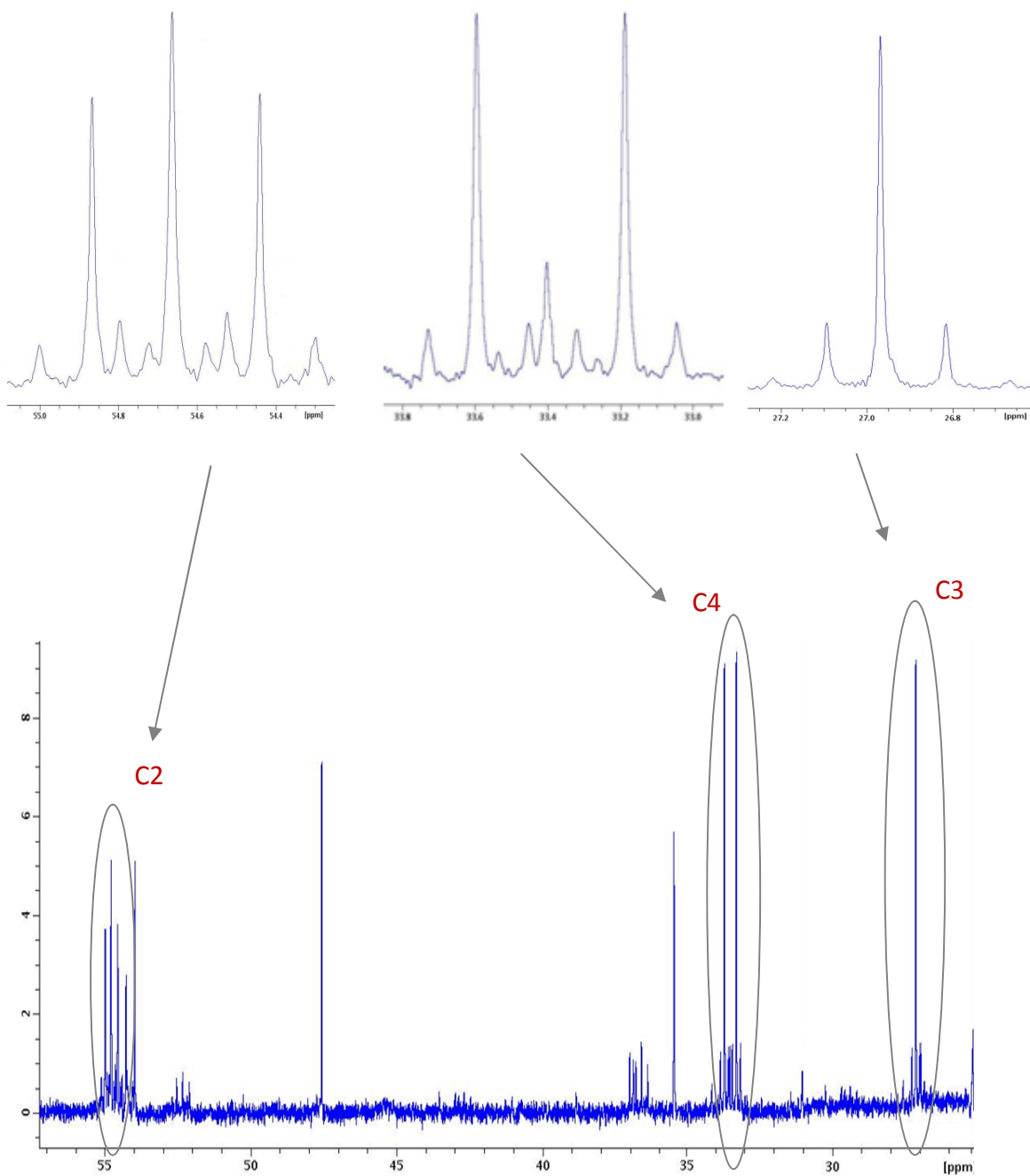


Figure 2.6:  $^{13}\text{C}$  NMR spectra showing expansion of resonances of glutamate

The isotopomers of glutamate were analysed using the TCAcalc program, kindly provided by Dr Mark Jeffrey (University of Texas, USA). The peak intensities of C2, C3 and C4 resonances of glutamate and the ratio of the integrated areas under C3 and C4 resonances (Figure 2.6) were determined, and the contribution of exogenous  $^{13}\text{C}$ -labelled substrates to acetyl-CoA entering the TCA cycle and thus the relative contributions of exogenous  $^{13}\text{C}$  labelled substrates to oxidative metabolism calculated.

The relative fractional enrichments of acetyl-CoA can be defined as follows.

- $F_{C_0}$  is the fraction of acetyl-CoA which is generated from unlabelled substrates.
- $F_{C_1}$  is the fraction of acetyl-CoA with the  $^{13}\text{C}$  label appearing on the first (carbonyl) carbon.
- $F_{C_2}$  is the fraction with the  $^{13}\text{C}$  label appearing on the methyl carbon (2<sup>nd</sup> carbon) of acetyl-CoA (e.g. when using 1- $^{13}\text{C}$  glucose)
- $F_{C_3}$  is the fraction of acetyl-CoA that has a  $^{13}\text{C}$  label in both C1 and C2 of acetyl-CoA (e.g. when using U $^{13}\text{C}$ -palmitate).

By definition  $F_{C_0} + F_{C_1} + F_{C_2} + F_{C_3} = 1$ .

TCAcalc is based on the following assumptions (Malloy et al., 1988, Malloy et al., 1990)

- All carbon enters the TCA cycle *via* acetyl-CoA or through anaplerosis (that is carbon entering the TCA cycle from sources other than acetyl-CoA), which is assumed to be 0.1.

- The TCA cycle is in a steady state
- $\alpha$ -ketoglutarate and glutamate are in constant rapid exchange
- Scrambling of the label occurs randomly at fumarate
- The natural abundance of  $^{13}\text{C}$  does not influence the labelling pattern

Every glucose molecule produces two molecules of acetyl-CoA and therefore the relative contribution obtained must be multiplied by two. Similarly, the relative contribution obtained for palmitate must also be multiplied by two because only 50% [ $\text{U-}^{13}\text{C}$ ] labelled palmitate was used for perfusions

## **2.2.6 Biochemical Assays**

### **2.2.6.1 Pyruvate Dehydrogenase (PDH) Assay**

PDH was assayed using the method of Seymour and Chatham, 1997. To determine the active fraction of PDH (PDHa), the in situ state of the enzyme was maintained by inclusion of specific inhibitors of PDH phosphatase ( $\text{KH}_2\text{PO}_4$  and KF) and PDH kinase (ADP and DCA). To extract total PDH (PDHt), the enzyme was converted into the active form by stimulating PDH phosphatase and inhibiting PDH kinase.

Approximately 200 mg ground ventricular tissue was extracted in the appropriate homogenisation buffer (1:5 w/v) (Table 2.2) and homogenised at maximum speed using an Ultra Turrax T25 homogeniser (IKA<sup>®</sup> Labortechnik, Germany) for 30 s. The

sample was rapidly frozen in liquid nitrogen, thawed and homogenised for a further 30 s. The freeze-thaw cycle was repeated, totalling 3 × 30 s homogenisations. Subsequently, samples were centrifuged at 13,000 g for 7 min at 4°C, and the supernatant assayed.

Table 2.2: Components of PDHt and PDHa homogenisation buffers

Active PDH homogenisation buffer (pH 7)	Total PDH homogenisation buffer (pH 7)
25 mM HEPES	75 mM HEPES
25 mM KH <sub>2</sub> PO <sub>4</sub>	5 mM DCA
25 mM KF	5 mM MgCl <sub>2</sub>
1 mM DCA	1 mM ADP
3 mM EDTA	1 mM DTT
1 mM ADP	0.05 mM Leupeptin
1 mM DTT	1% (v/v) Triton-X
0.05 mM Leupeptin	
1% (v/v) Triton-X	

PDH activity was assayed spectrophotometrically by monitoring the rate of NADH formation. The reaction buffer contained (in mM unless otherwise stated) 50 HEPES, 1 MgCl<sub>2</sub>, 0.08 EDTA, 1 DTT and 4 μM Rotenone (pH7.2).

The reaction buffer (0.75 ml), along with 50 μl of the following (mM) 1.67 NAD, 0.1 CoA, 0.2 TPP, and 16.7 lactate, were added to a cuvette. Five micro-litres LDH (to give a final concentration of 2 U) was added and the mixture incubated at 30°C for 5 minutes. Twenty micro-litres of total extract or 100 μl of the active extract were added and the change in absorbance determined at 340 nm over 3 min. PDH activity was calculated using Equation 5 and an extinction coefficient of 6.22 mM<sup>-1</sup>cm<sup>-1</sup>.

To ensure there were no variations in the extraction procedure, citrate synthase activity was determined in total and active extracts using the reaction buffer as described in Section 2.2.6.2.

$$\left( \frac{\text{Abs change/min}}{\text{Extinction Coefficient}} \right) \times \left( \frac{\text{Total cuvette volume (ml)}}{\text{Vol of supernatant}} \right) \times \left( \frac{\text{Homog. buffer vol (ml)}}{\text{weight of tissue (g)}} \right) \times \text{Dilution}$$

Equation 5: Calculation of enzyme concentration

### **2.2.6.2 Citrate Synthase (CS) Assay**

CS activity was determined spectrophotometrically by following the reduction of 5,5 dithio-bis-2-nitrobenzoic acid (DTNB) (Morgan-Hughes et al., 1977). Briefly, 15 mg ground ventricular tissue was homogenised at full speed ( $2 \times 5$  seconds) using an Ultra Turrax homogeniser (details in Section 2.2.6.1) in 1 ml extraction buffer (100 mM imidazole, 1 mM EGTA 10 mM  $\text{MgCl}_2$ , pH 7.2). Triton X-100 (1% v/v) was added and the mixture was left on ice for 1 h. Samples were then centrifuged at 2000 g for 10 min at 4°C. Twenty micro-litres of the resultant supernatant (diluted 1 in 2) was added to 1.98ml reaction buffer containing 50 mM Tris (pH 8.1), 0.2 mM DTNB, 0.1 mM acetyl CoA, 0.5 mM oxaloacetate and 0.05% v/v Triton X-100. The absorbance was measured at 412 nm over 3 min. Citrate synthase activity was calculated using an extinction coefficient of  $13.6 \text{ mM}^{-1}\text{cm}^{-1}$  (Equation 5).

### **2.2.6.3 Medium chain Acyl-CoA dehydrogenase (MCAD) Assay**

#### **2.2.6.3.1 Preparation of Ferricene Salt**

Ferricenium hexafluorophosphate was synthesised by adding 0.5 g ferrocene to 10 ml concentrated  $\text{H}_2\text{SO}_4$  (Lehman et al., 1990). After 1 h, the solution was diluted to 150 ml using ultra pure water and filtered under pressure. 5 ml saturated hexafluorophosphate monohydrate ( $\text{NaPF}_6$ ) was added and the mixture left on ice for 30 min before filtering again. Prior to use, the ferricenium salt ( $\text{FC}^+\text{PF}_6^-$ ) was dissolved in 10 mM HCl and centrifuged at 3000 g for 10 min at 4°C (Lehman et al.,

1990). The supernatant was collected and the absorbance measured at 300 nm. The concentration was then calculated using an extinction coefficient of  $4.3 \text{ mM}^{-1}\text{cm}^{-1}$ .

#### **2.2.6.3.2 MCAD Assay**

Frozen ventricular tissue (50 mg) was homogenised in 1 ml ice-cold buffer (50 mM  $\text{KH}_2\text{PO}_4$ , 1 mM EDTA, 2 mM  $\text{MgCl}_2$  pH 7.2) at full speed for 30 seconds using an Ultra Turrax homogeniser (details in section 2.2.6.1). Samples were centrifuged at 3000 g for 10 minutes at  $4^\circ\text{C}$ . Twenty micro-litres supernatant was added to 900ml reaction buffer containing 100 mM  $\text{KH}_2\text{PO}_4$ , 1 mM EDTA, 0.5 mM sodium tetrathionate and 200  $\mu\text{M}$  ferricenium hexafluorophosphate (pH 7.2). To initiate the reaction, 50  $\mu\text{M}$  octanoyl-CoA was added and the absorbance measured over 3 min using a wavelength of 300 nm. MCAD activity was calculated using Equation 5 and an extinction coefficient of  $4.3 \text{ mM}^{-1}\text{cm}^{-1}$ .

### **2.2.7 *In Vitro* Mitochondrial Function**

#### **2.2.7.1 Mitochondrial Isolation**

Mitochondria were isolated using the method of Halestrap, 1987. Hearts were rapidly removed, weighed, and the atria trimmed. Ventricles were gently agitated in ice-cold buffer (1:10 w/v) containing (in mM) 300 sucrose, 2 EGTA, 10 Tris (pH 7.4) and homogenised at low speed (8000 rpm) for 10 s using an Ultra Turrax T25 homogeniser (IKA® Labortechnik). The volume was made up to 20 ml using the

isolation buffer containing 5 mg/ml BSA. The suspension was centrifuged at 2000 g for 2 min at 4°C using a Sorvall RC-5B refrigerated centrifuge (DuPont Instruments, UK). The supernatant was removed and retained. The pellet was re-suspended in 20 ml isolation buffer with BSA (5 mg/ml), homogenised again (8000 rpm) and centrifuged. The two supernatants were combined and centrifuged at 11,000 g for 5 min at 4°C. The resultant pellet was re-suspended in 2 ml isolation buffer with 19% v/v percol and centrifuged at 14,500 g for 20 min at 4°C. The pellet was washed in isolation buffer and re-suspended in the respiratory activity buffer, which comprised (in mM) 125 KCl, 20 MOPS, 10 Tris, 0.5 EGTA, 2.5 KH<sub>2</sub>PO<sub>4</sub> and 2.5 MgCl<sub>2</sub> (pH 7.2) to achieve a final protein concentration of 0.4 mg protein/ml, determined using the Biorad assay.

#### **2.2.7.2 Mitochondrial Respiration**

Mitochondrial respiration was determined by measurement of oxygen consumption using a digital oxygen recorder (Digital Model-10 Rank Brothers, Cambridge, UK), connected to a Chart 5.5 recording system (ADInstruments, Hastings, UK). For the calibration, sodium dithionite was added to set the oxygen baseline to zero.

Mitochondrial extract (2 ml) was added to a Clark-type oxygen electrode chamber maintained at 25°C, and allowed to equilibrate for 5 min. State 2 respiratory activities were measured in the presence of the NADH linked (complex I) substrates glutamate (5 mM) + malate (1 mM), FADH<sub>2</sub> linked (complex II) substrates succinate (5 mM) + rotenone (1 µM) (to inhibit electron transport to and from complex I) or

palmitoyl carnitine (20  $\mu\text{M}$ ) + malate (2 mM), which, when oxidised, produces both NADH and  $\text{FADH}_2$ .

The transition to state 3 respiration was stimulated by the addition of ADP (0.2 mM) and state 4 respiration reached with exhaustion of ADP. The ratio of state 3: state 4 respiration, known as the respiratory control index (RCI) indicates the coupling between respiration and phosphorylation. ADP:O ratio was calculated from the amount of  $\text{O}_2$  consumed by phosphorylation of 0.2 mM ADP assuming the concentration of oxygen in an air saturated solution (at 25°C) to be 0.237 micromoles molecular oxygen per ml (Figure 2.7).

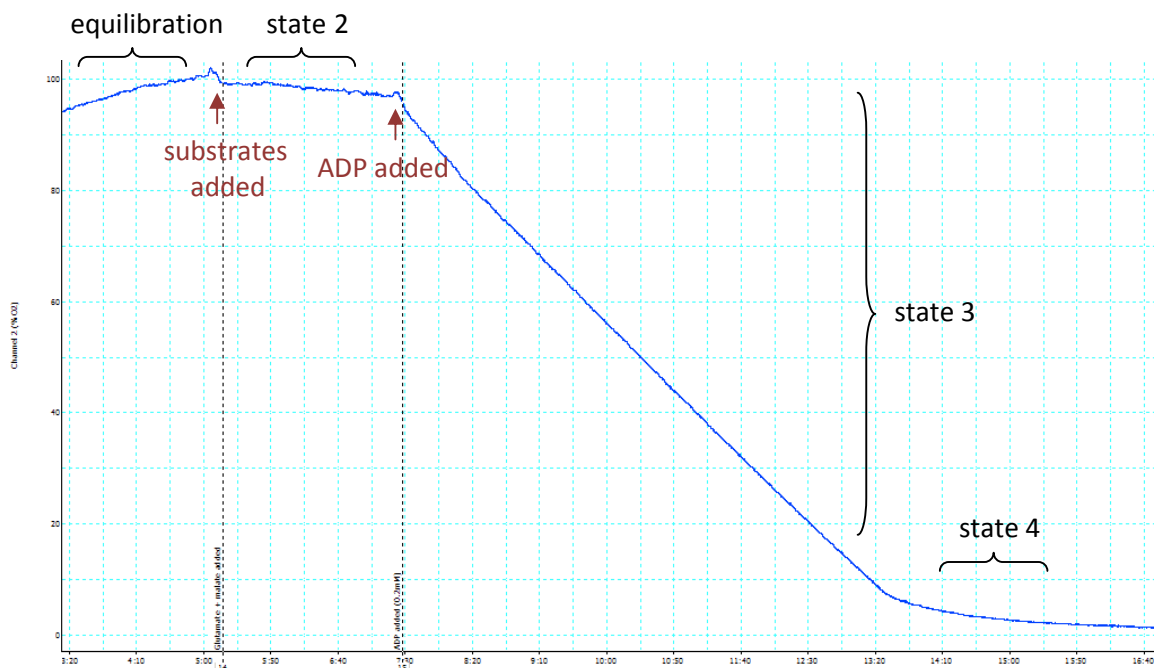


Figure 2.7: Recording showing oxygen consumption of isolated mitochondria

### **2.2.8 Western Blotting**

Western blotting was used to determine the protein expression of PPAR $\alpha$ , CD36 and actin in control and uraemic ventricular tissue.

I would like to thank Mrs Kathleen Bulmer for her assistance with the Western Blotting

#### **2.2.8.1 Preparation of Samples**

Ground ventricular tissue (200 mg) was homogenised (2  $\times$  5 seconds at full speed) using an Ultra Turrax homogeniser (details in section 2.2.6.1) in 1 ml extraction buffer containing 50 mM Tris (pH 7.4), 1% w/v SDS, and complete protease inhibitor cocktail<sup>®</sup> (Roche Diagnostics, Penzberg, Germany). Samples were centrifuged at 12,100 g using a microcentrifuge (MicroCL 17R, Thermo Scientific, UK) for 10 minutes at 4°C and the supernatant collected. Protein concentration was determined using the BioRad assay and samples were diluted in the extraction buffer to achieve a protein concentration of 10  $\mu$ g/ $\mu$ l. An equal volume of SDS-PAGE buffer (45 mM TRIS pH 7.4, 10% glycerol, 1% SDS, 2.5% 2-Mercaptoethanol blue and Bromophenol Blue) was added to achieve a final protein concentration of 5  $\mu$ g/ $\mu$ l. Tubes were placed in boiling water for 3 min, cooled, and stored at -20°C until required.

### **2.2.8.2 SDS- Page**

Proteins were separated using sodium dodecyl sulphate polyacrylamide gel electrophoresis (SDS-Page). Fifty micro-grams of protein was separated using a 3% stacking gel and 10% running gel and transferred to a nitrocellulose membrane for 2 hours at 4°C, using a mini-transblot cell (BioRad laboratories, UK).

Following transfer, membranes were blocked for 1 h in the appropriate blocking buffer (Table 2.3) to decrease non-specific protein binding. Membranes were washed in 0.25% TBS-Tween 3 times for 10 min and exposed to the primary antibody overnight at 4°C (Table 2.3). After another 3 washes in TBS-Tween, membranes were exposed to the secondary antibody for a further 2 h at room temperature (Table 2.3).

### **2.2.8.3 Visualisation and Quantification**

To visualise protein bands, membranes were exposed onto Kodak Biomax Light films (Sigma-Aldrich, UK) using enhanced chemiluminescence (ECL) reagents (Amersham, Uppsala, Sweden). Films were scanned and bands quantified using scanning densitometry and ImageJ<sup>®</sup> software.

Table 2.3: Antibody dilutions and suppliers

			<b>Supplier</b>	<b>Dilution</b>	<b>Dilutant</b>	<b>Blocking Buffer</b>
<b>PPAR<math>\alpha</math></b>	Primary Antibody	Rabbit polyclonal	Santa Cruz, USA	1:1000	0.25% TBS-Tween with 1% milk powder	0.25% TBS-Tween with 5% milk powder
	Secondary Antibody	Donkey Anti-Rabbit (HRP conjugated)	As above	1:4000	As above	As above
<b>CD36</b>	Primary Antibody	Rabbit polyclonal	Abcam, Cambridge, UK	1:6000	As above	As above
	Secondary Antibody	Goat Anti- Rabbit (HRP conjugated)	Santa Cruz, USA	1:8000	As above	As above
<b>Actin</b>	Primary Antibody	Rabbit monoclonal	New England Biolabs	1:1000	0.1% TBS-Tween with 5% BSA	0.1% TBS-Tween with 5% milk powder
	Secondary Antibody	Anti- Rabbit (HRP conjugated)	Santa Cruz, USA	1:2000	As above	As above

### **2.3 Statistical Analysis**

Results are expressed as mean  $\pm$ SEM. Statistical significance was determined using an unpaired *t* test (for single mean comparisons) or two-way ANOVA, for comparisons between all groups at all time points (using the Scheffe post-hoc test). Pearson's analysis was used to determine the significance of bivariate correlations. Statistical analysis was performed using SPSS software (16.0) and level of significance was set at  $p < 0.05$ .

## **Chapter 3: Characterisation of Experimental Uraemia**

### **3.1 Introduction**

Cardiac complications account for approximately 50% of deaths in patients with CKD (USRDS 1998). However, the exact reasons behind the elevated risk remain unclear. Interestingly, the relative importance of arteriosclerotic disease is diminished and those of LVH, heart failure and sudden cardiac death are increased in patients with CKD (Foley et al., 2003). Kidney dysfunction in uraemic patients is evident by high serum creatinine levels and declining glomerular filtration rate (GFR) (Beddhu et al., 2003). In addition, uraemia is characterised by anaemia and hypertension, which contribute to phenotypic cardiac alterations including LVH, myocardial fibrosis and a reduction in capillary density.

#### **3.1.1 Experimental Models of CKD**

To understand the complex relationship between the heart and kidney, and to reduce the high impact of cardiovascular complications on the mortality associated with CKD, a robust and reliable experimental animal model is required. A number of experimental models have been developed employing different strategies of renal mass reduction or renal ischaemia to produce phenotypic alterations with a clinical similarity to those observed in CKD patients (Hewitson et al., 2009).

The  $5/6^{\text{th}}$  nephrectomy model is a surgical procedure whereby the right kidney and subsequently  $2/3^{\text{rds}}$  of the left kidney are removed. Previous studies from this laboratory (Raine et al., 1993, Reddy et al., 2007, Aksentijevic et al., 2009) have shown that this model produces significant kidney dysfunction as evidenced by a 2-fold rise in serum creatinine and urea as early as 3 weeks post-surgery, which increases as the duration of uraemia is extended. Uraemic animals also show severe anaemia and an increase in systolic blood pressure.

A reduction in functional kidney mass can also be achieved using the remnant kidney model (Mishina and Watanabe, 2008). In this experimental model, ligation of three of the four branches of the left renal artery leads to infarct of approximately two-thirds of the kidney. Subsequently, a total nephrectomy is performed on the right kidney. Like the  $5/6^{\text{th}}$  nephrectomy model, an increase in blood pressure and a rise in serum creatinine and urea are observed in addition to cardiac alterations including LVH.

A model frequently used to induce CKD in mice is the surgically induced renal injury (SIRI) model (Gagnon and Gallimore, 1988). In this model, up to 70% of the right kidney is damaged by cauterisation followed by a total left nephrectomy 2 weeks later. Anaemia and a doubling in serum creatinine is observed in addition to cardiac hypertrophy (Siedlecki et al., 2009).

The two-kidney, one-clip (2K1C) model is an experimental model of hypertension-induced CKD, first described in dogs by Goldblatt and colleagues in 1934 (Goldblatt, 1934). This model has since been used to study hypertension and CKD in other animals including mice (Wiesel et al., 1997), pigs (Lerman et al., 1999) and rats (Leenen and de Jong, 1971). In this model, the left renal artery is partially constricted by placing a clip over the renal vessels, whereas the right kidney remains unclipped. Blood pressure is markedly increased due to the secretion of renin from the clipped kidney, which causes the excretion of sodium and water (pressure natriuresis) in the unclipped kidney. This results in a net fluid loss and therefore promotes persistent stimulation of renin secretion (Helle et al., 2009). Variations of the 2K1C model include the two-kidney, two-clip (2K2C) model where both kidneys are clipped (Helle et al., 2009), and the one-kidney, one-clip (1K1C) model where the left kidney is clipped and the right kidney is removed (Wiesel et al., 1997). In these models, unlike the 2K1C model, the elevation in blood pressure is not due to an increase in renin activity because the stenosed kidneys cannot undergo pressure natriuresis, thus the effective blood volume remains low thereby inhibiting renin secretion. Rather, the hypertension in these models is due to sodium retention and volume expansion. Cardiac alterations in the 2K1C, 1K1C, and 2K2C models include LVH, fibrosis and diastolic dysfunction (Signolet et al., 2008).

### 3.1.2 Erythropoietin (EPO) Treatment

Anaemia is a frequently observed characteristic in experimental models as well as in patients with CKD (as described in Chapter 1). Interestingly, it has been shown that haemoglobin level is an independent predictor of LVH in patients with mild to moderate renal insufficiency (Levin et al., 1999), suggesting that anaemia may be a key player in the development of cardiac hypertrophy and thus cardiac complications in CKD.

During CKD, the EPO producing peritubular fibroblast cells in the kidney become damaged, resulting in a reduction in EPO secretion and subsequent anaemia (Caro et al., 1979, Eschbach et al., 2002). Clinical studies have shown that administering EPO to partially or fully correct the anaemia associated with CKD induces a regression of LVH (Silberberg et al., 1990, Hayashi et al., 2000). A reduction in LV mass has been associated with improved survival and reduced hospitalisations in uraemic patients (London et al., 2001). Interestingly, recent cardiac studies have shown that EPO has direct cardioprotective actions, independent from its haematopoietic effects, including decreasing apoptosis (Tramontano et al., 2003), promoting neovascularisation (van der Meer et al., 2005) and reducing oxidative stress (Li et al., 2006). Thus, the decreased EPO production during CKD may render uraemic hearts more susceptible to injury.

The combination of anaemia, oxidative stress and renal fibrosis during CKD contribute to progressive tubular damage. EPO not only improves haematocrit, but also has anti-apoptotic and antioxidant effects (as described in chapter 1). Therefore, it is feasible that EPO administration may slow the progression of kidney failure in CKD patients. A retrospective study found a delay in the progression of renal dysfunction (determined by creatinine clearance) and a prolonged time to the onset of dialysis therapy in pre-dialysis patients receiving EPO, however the mechanisms remain unknown (Jungers et al., 2001). In support of this, Kuriyama *et al.* (1997) showed improved survival rates in EPO treated CKD patients compared with untreated patients (Kuriyama et al., 1997). Conversely, many studies have shown that EPO treatment has little impact on the rate of renal failure progression (Lim et al., 1990, Savica et al., 1995, The US Recombinant Human Erythropoietin Predialysis Study Group 1991).

Clinical trials investigating the cardiovascular effects of EPO during CKD have provided somewhat conflicting results. Surprisingly, two large clinical trials, the CREATE and the CHOIR trial showed either no change, or increased risk of cardiovascular events in CKD patients with EPO administration (Drueke et al., 2006, Singh et al., 2006). EPO is associated with hypertension and elevated risk of thrombotic events (Lee et al., 2007). It is therefore feasible that, in certain disease states, the negative effects of EPO may abrogate the cardioprotection. Further trials are necessary to fully clarify the impact of EPO during CKD.

### 3.1.3 Objectives

- To assess the extent and progression of uraemia in  $5/6$  nephrectomised rats
- To determine the extent of LVH in uraemic animals, and the impact of EPO treatment on LVH
- To investigate the impact of EPO treatment on the haematocrit and degree of uraemia
- To examine the combined impact of uraemia and EPO treatment on blood pressure *in vivo*

## **3.2 Materials and Methods**

### **3.2.1 Induction of Uraemia**

Uraemia was surgically induced in male Sprague-Dawley rats as described in Section

2.2.1. Animals were studied at 3, 6, 9 and 12 weeks post-surgery.

### **3.2.2 Erythropoietin (EPO) Treatment**

Two weeks prior to sacrifice, animals were divided into four experimental groups

- Control animals + saline (- EPO)
- Uraemic animals + saline (- EPO)
- Control animals + EPO
- Uraemic animals + EPO

EPO (Aranesp® Amgen, Cambridge, UK) was administered subcutaneously (s/c) twice a week for two weeks at a dose of 30 µg/Kg (equivalent to approximately 3000 units/Kg) (Figure 3.1). Saline was administered s/c as a control.

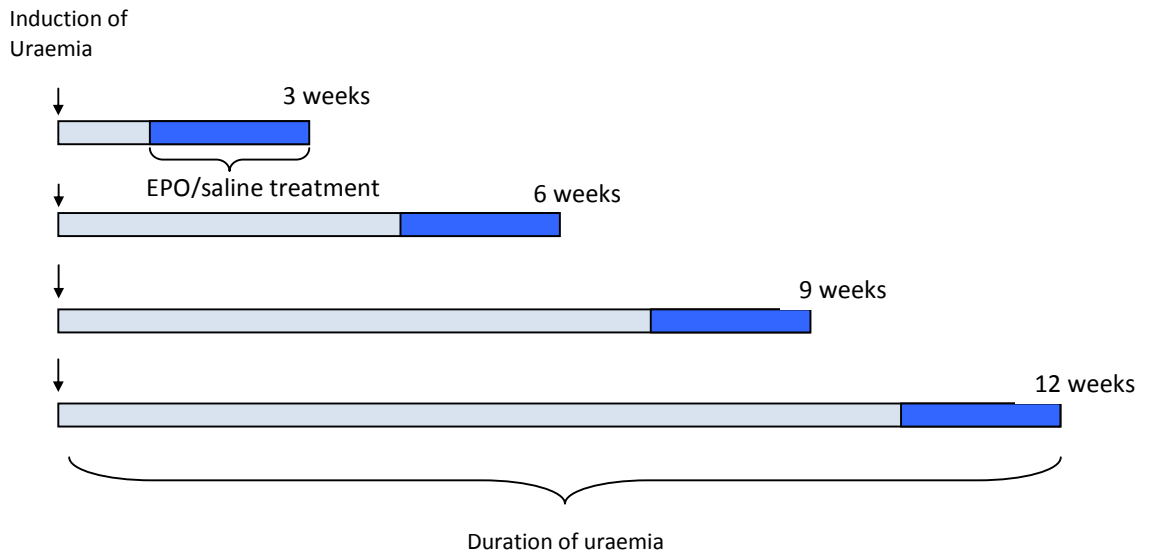


Figure 3.1: Experimental protocol

### 3.2.3 Biochemical Analysis and Determination of LVH

Serum creatinine and urea, and haematocrit levels (from whole blood) were analysed as described in Section 2.2.4.5. The extent of LVH was assessed according to Section 2.2.4.4.

### 3.2.4 *In Vivo* Haemodynamic Analysis

I would like to thank Dr Yong Wang for his assistance with the *in vivo* measurements

Twelve weeks post-surgery, animals were anaesthetised using a mixture of isoflurane (3.5%) and oxygen (3 L/min) and maintained on 2.0% isoflurane in 1 L/min oxygen. The right carotid artery was located and exposed. A suture was tied towards the top of the artery to create a closed circuit to allow pressure transducer measurements. A small incision was made in the artery and a 2.0F microtipped pressure transducer catheter inserted (Millar Instruments, Texas, USA) (Figure 3.2). The catheter was secured in place using a suture.

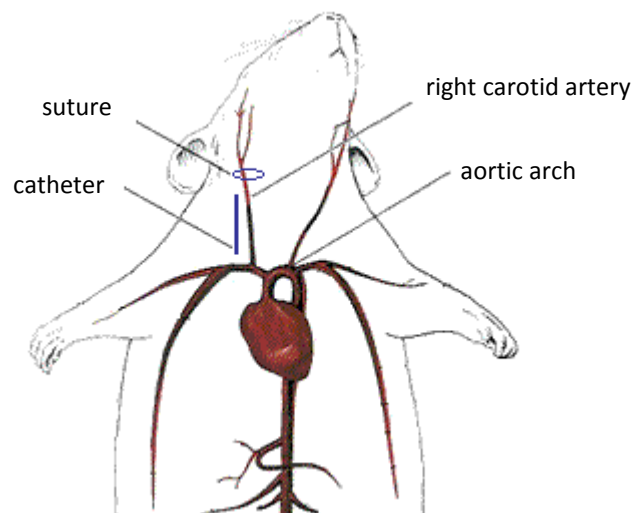


Figure 3.2: Diagram of positioning of catheter

After a short period of stabilisation, carotid artery blood pressure and heart rate were recorded over 10 minutes using Chart 5.5 software and a PowerLab system (4/30) with an additional blood pressure module (AD Instruments, UK). Mean arterial pressure (MAP) was calculated using equation 6 (Wang et al., 2007).

$$MAP = DP + \frac{1}{3} (SP - DP)$$

Equation 6: Calculation of MAP  
DP diastolic pressure; SP systolic pressure

## **3.3 Results**

### **3.3.1 Degree of Uraemia**

#### **Serum Biochemistry**

At 3, 6, 9 and 12 weeks post-induction of uraemia, serum creatinine and urea were significantly increased in uraemic animals compared with controls (Figure 3.3 a and b)

When the duration of uraemia was extended to 12 weeks, the serum creatinine concentration was on average 282% higher and the serum urea concentration 448% higher than controls, indicative of worsening kidney function.

EPO administration (30 µg/Kg twice a week for 2 weeks) had no impact on serum creatinine or urea in either control or uraemic groups at 3, 6, 9 and 12 weeks post-surgery (Figure 3.3 a and b), suggesting that EPO had no effect on the rate of progression of renal dysfunction.

The serum biochemistry results highlighted 5/6<sup>th</sup> nephrectomy generated appropriate kidney dysfunction beginning at least 3 weeks post-surgery.

Figure 3.3a: Serum creatinine concentration

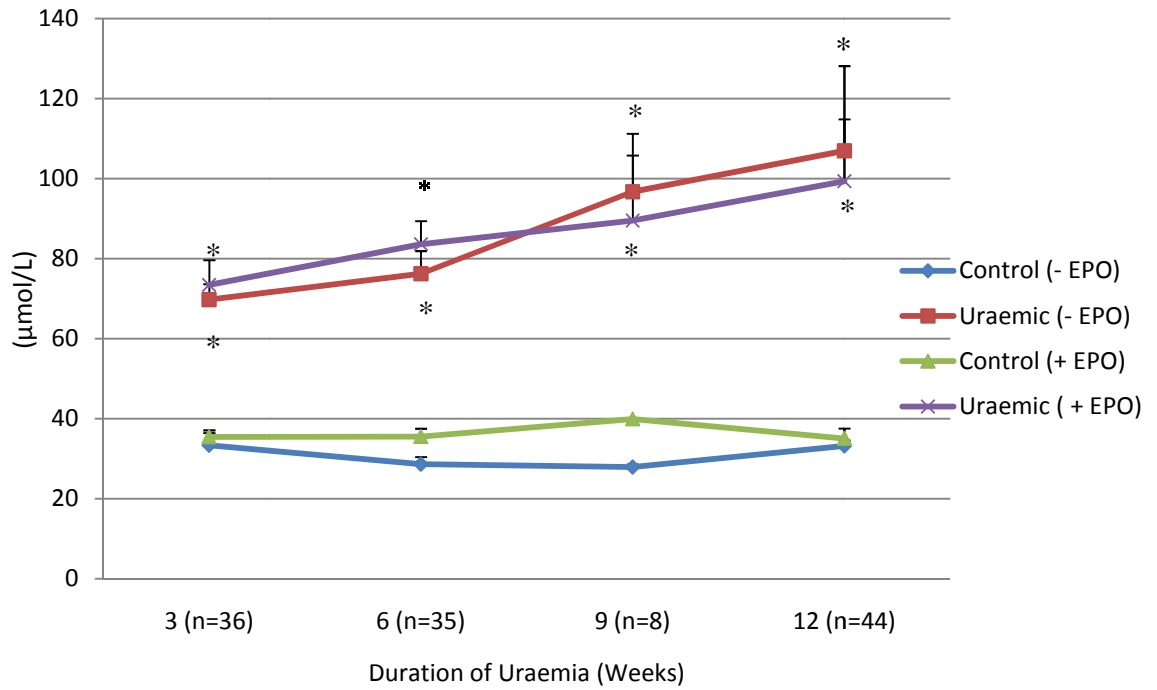


Figure 3.3b: Serum urea concentration

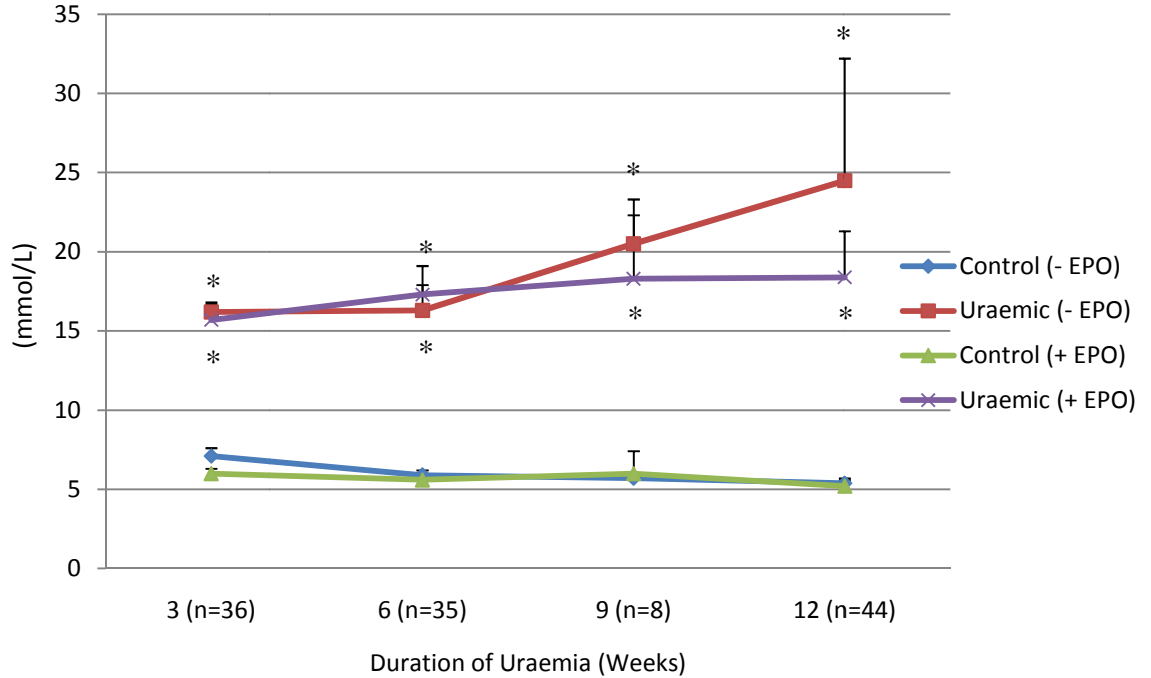


Figure 3.3: Serum biochemistry

(\*  $p < 0.05$  vs. respective control)

## Haematocrit

Table 3.1 and Figure 3.4 show the haematocrit levels for 3, 6, 9 and 12 week control and uraemic animals. Uraemic animals exhibited a reduced haematocrit compared with controls, highlighting development of anaemia. The degree of anaemia did not alter during the progression of uraemia.

EPO treatment resulted in a significant improvement in haematocrit in both uraemic and control animals. At 3, 6, 9 and 12 weeks (with EPO treatment), haematocrit in uraemic animals was comparable with controls.

Table 3.1: Haematocrit (%)

	3 Week		6 Week		9 Week		12 Week	
	Control (n=16)	Uraemic (n=18)	Control (n=14)	Uraemic (n=13)	Control (n=4)	Uraemic (n=4)	Control (n=34)	Uraemic (n=28)
<b>- EPO</b>	38 ±2	32 ±2*	38 ±1	33 ±1*	40 ±2	31 ±0*	42 ±1	33 ±1*
<b>+ EPO</b>	58 ±1*	56 ±2 <sup>‡</sup>	59 ±2*	59 ±2 <sup>‡</sup>	56 ±5*	54 ±5 <sup>‡</sup>	61 ±1*	62 ±1 <sup>‡</sup>

\*  $p < 0.05$  vs. control (- EPO); <sup>‡</sup>  $p < 0.05$  vs. uraemic (- EPO)

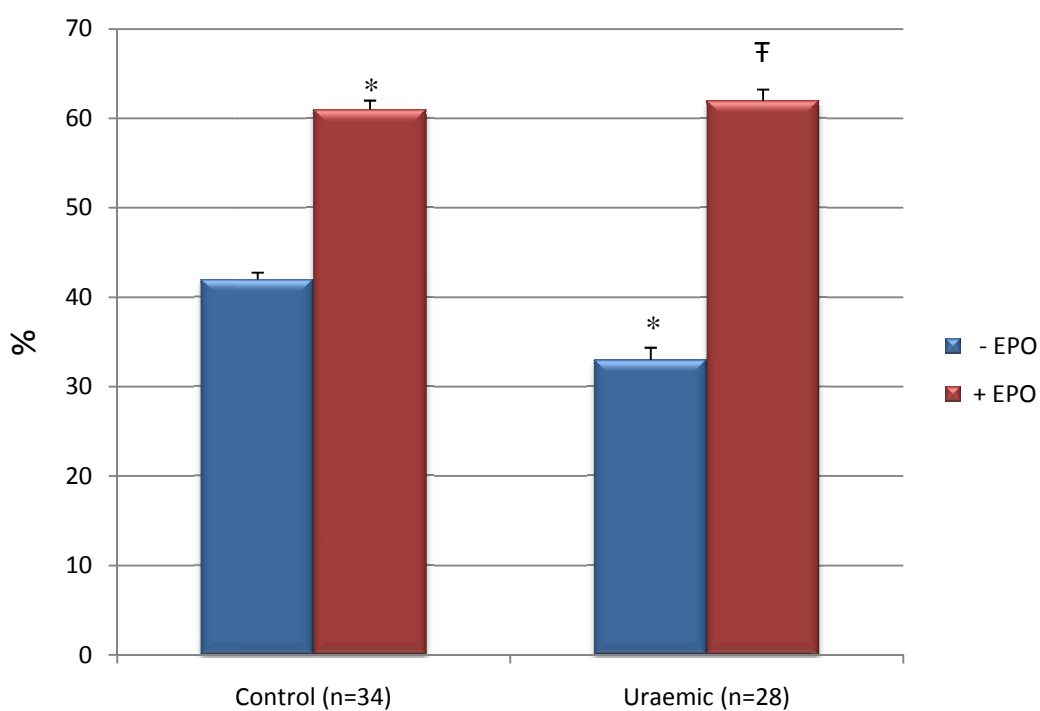


Figure 3.4: Haematocrit 12 weeks post-induction of uraemia

\*  $p < 0.05$  vs. control (- EPO); <sup>‡</sup>  $p < 0.05$  vs. uraemic (- EPO)

## Spleen Weight

Figure 3.5 shows the spleen weights of uraemic and control animals at 3, 6, 9 and 12 weeks uraemia.

In untreated animals, spleen weight was the same in control and uraemic rats. Two weeks of EPO treatment resulted in a significant increase in spleen weight which was comparable for control and uraemic animals (Figure 3.5). In EPO treated uraemic animals, spleen weight was increased 172%, 125%, 129% and 89% at 3, 6, 9 and 12 weeks respectively, relative to the untreated uraemic group. The mean spleen weight was  $0.84 \pm 0.03$  g in untreated vs.  $1.77 \pm 0.06$  g ( $p < 0.05$ ) in EPO treated animals.

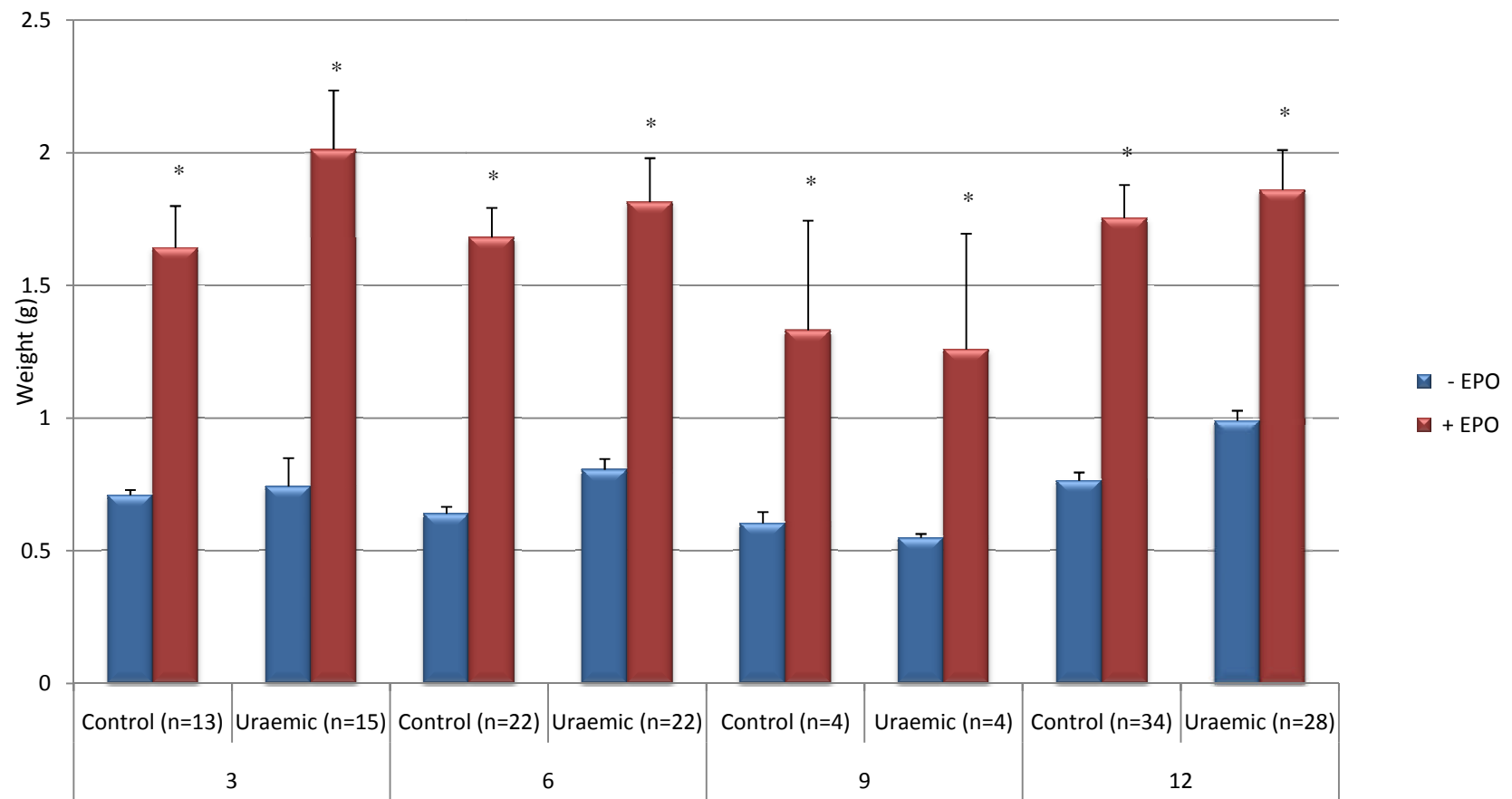


Figure 3.5: Spleen weight at 3, 6, 9 and 12 weeks uremia  
 (\* $p < 0.05$  vs. untreated group)

## Left Kidney Weights

During nephrectomy, approximately two-thirds of the left kidney was removed in uraemic animals. However, at the time of sacrifice the left remnant kidney weights in uraemic animals were similar to control animals, suggesting hypertrophy of the remnant kidney (Table 3.2). EPO had little impact on kidney weights in control or uraemic animals (Table 3.2).

Table 3.2: Left kidney weights

	3 Week		6 Week		9 Week		12 Week	
	Control (n=16)	Uraemic (n=19)	Control (n=22)	Uraemic (n=22)	Control (n=4)	Uraemic (n=4)	Control (n=34)	Uraemic (n=28)
<b>- EPO</b>	1.7 ±0.1	1.5 ±0.1	1.5 ±0.1	1.6 ±0.1	1.3 ±0.1	1.2 ±0.1	1.5 ±0.1	1.7 ±0.1
<b>+ EPO</b>	1.4 ±0.1	1.6 ±0.1	1.5 ±0.1	1.5 ±0.1	1.5 ±0.01	1.5 ±0.2	1.5 ±0.04	1.8 ±0.1

## **Water Content of the Lungs**

At all durations of uraemia, the percentage water content of the lungs was comparable between control and uraemic animals (Figure 3.6).

EPO administration had little impact on the percentage of water within the lungs in control and uraemic animals at 3, 6, 9 and 12 weeks uraemia (Figure 3.6).

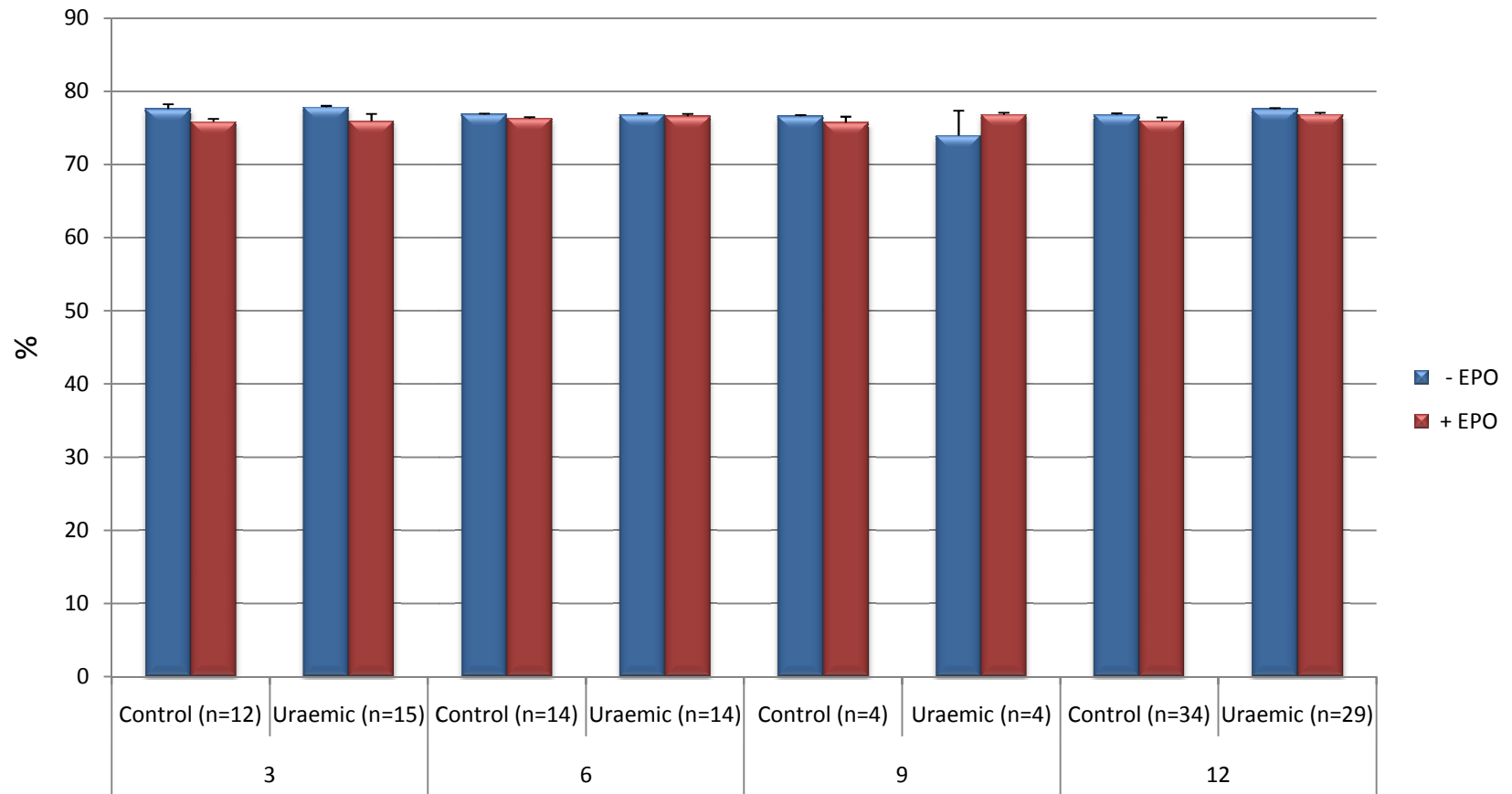


Figure 3.6: Water content of lungs

### **3.3.2 *In Vivo* Blood Pressure**

At 12 weeks, uraemic animals had a significant increase in systolic blood pressure (SP) and mean arterial blood pressure (MAP) compared with control animals (Figure 3.7), but similar heart rate and systolic and diastolic durations (Table 3.3).

Administration of EPO had no significant effect on the blood pressure of uraemic or control animals (Figure 3.7).

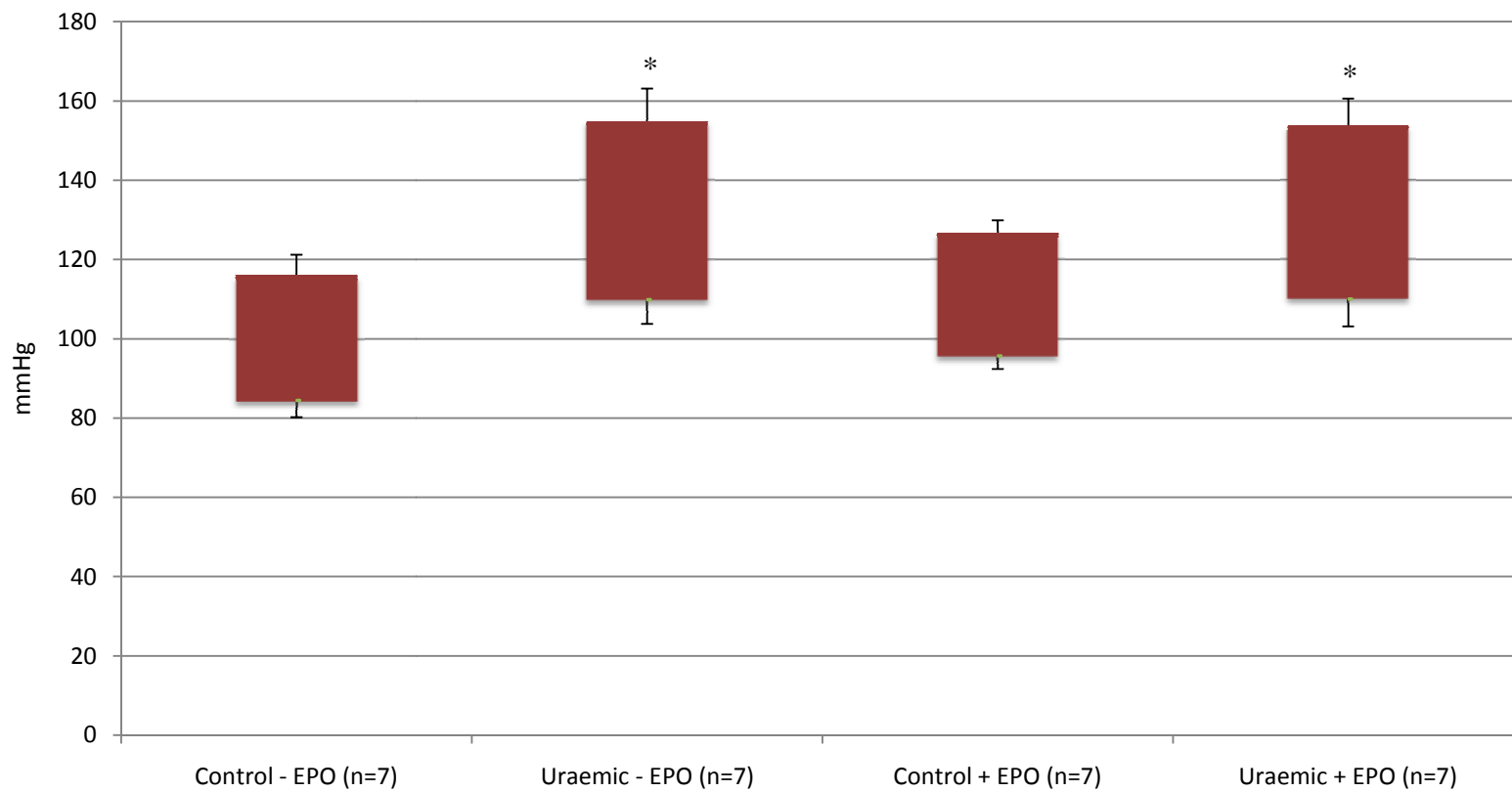


Figure 3.7: Systolic and diastolic blood pressures at 12 weeks post-induction of uraemia  
(\* $p < 0.05$  vs. respective control)

Table 3.3: *In vivo* blood pressure at 12 weeks post-induction of uraemia

		Max Pressure (mmHg)	Mean Arterial Pressure (mmHg)	EDP (mmHg)	Systolic Duration (s)	Diastolic Duration (s)	Cycle Duration (s)	Heart Rate (BPM)
Control (n=7)	- EPO	116.0 ±5.3	94.9 ±4.5	84.4 ±4.2	0.072 ±0.001	0.113 ±0.006	0.185 ±0.007	327 ±11
Uraemic (n=7)	- EPO	155.0 ±8.2*	124.9 ±6.7*	109.8 ±6.0	0.072 ±0.002	0.108 ±0.006	0.180 ±0.008	338 ±15
Control (n=7)	+ EPO	126.8 ±3.2	106 ±3.2	95.6 ±3.2	0.074 ±0.002	0.118 ±0.004	0.191 ±0.005	315 ±8
Uraemic (n=7)	+ EPO	153.7 ±6.9*	124.6 ±6.7	110.1 ±6.9	0.075 ±0.002	0.105 ±0.005	0.180 ±0.004	335 ±8

\*  $p < 0.05$  vs. respective control

### 3.3.3 Indices of LVH

At 3 weeks uraemia (in absence/presence of EPO), there was no significant difference in body weight and also no LVH, as evidenced by HW: BW and HW: tibia length, compared with control animals (Table 3.4a). However, by 6 weeks, uraemic animals showed a significant increase in HW: BW despite no change in body weight (Table 3.4b). EPO had no impact on LVH.

At 9 weeks uraemia, no increase was observed in HW: BW or HW: tibia length (without EPO treatment). However, this is likely due to the small sample size in this group (Table 3.4c).

At 12 weeks, the body weights were comparable between control and uraemic animals. Wet heart weight, HW: BW and HW: tibia length were significantly increased in uraemic animals compared with controls (Table 3.4d and Figures 3.8 a and b). Furthermore, HW: tibia length correlated with haematocrit (Figure 3.9  $p < 0.05$ ) and also serum creatinine (Figure 3.10  $p < 0.05$ ), suggesting exacerbated LVH with worsening kidney function. A positive correlation was also observed between systolic blood pressure and HW: BW (Figure 3.11  $p = 0.05$ ).

Interestingly, the increase in HW: BW and HW: tibia length was lessened following EPO treatment (Table 3.4d and Figures 3.8 a and b). HW: tibia length was increased by 21% in uraemic animals. However, after EPO administration, HW: tibia length

was reduced by 10% in uraemic animals. This suggests that 2 weeks of EPO treatment induces a regression of LVH in uraemic animals.

Table 3.3.4a: Indices of LVH at 3 weeks post-induction of uraemia

	Body Weight (g)		Wet Heart Weight (g)		HW: Tibia length (g/cm)		HW: Body Weight (x10 <sup>3</sup> )	
	Control (n=16)	Uraemic (n=19)	Control (n=16)	Uraemic (n=19)	Control (n=16)	Uraemic (n=19)	Control (n=16)	Uraemic (n=19)
<b>- EPO</b>	406.7 ±6.5	362.1 ±15.6	1.64 ±0.07	1.66 ±0.08	0.40 ± 0.02	0.41 ±0.02	4.04 ±0.18	4.61 ±0.20
<b>+ EPO</b>	356.0 ±9.5	339.3 ±8.8	1.64 ±0.07	1.66 ±0.09	0.41 ±0.02	0.41 ±0.02	4.63 ±0.23	4.88 ±0.22

Table 3.3.4b: Indices of LVH at 6 weeks post-induction of uraemia

	Body Weight (g)		Wet Heart Weight (g)		HW: Tibia length (g/cm)		HW: Body Weight (x10 <sup>3</sup> )	
	Control (n=16)	Uraemic (n=16)	Control (n=16)	Uraemic (n=16)	Control (n=16)	Uraemic (n=16)	Control (n=16)	Uraemic (n=16)
<b>- EPO</b>	432.0 1±0.6	401.1 ±10.9	1.57 ±0.04	1.73 ±0.02	0.36 ±0.01	0.41 ±0.02	3.65 ±0.12	4.31 ±0.11*
<b>+ EPO</b>	416.9 ±13.0	386.1 ±5.0	1.41 ±0.04	1.56 ±0.11	0.33 ±0.01	0.37 ±0.01	3.41 ±0.13	4.04 ±0.24*

(\*p<0.05 vs. respective control)

Table 3.3.4c: Indices of LVH at 9 weeks post-induction of uraemia

	Body Weight (g)		Wet Heart Weight (g)		HW: Tibia length (g/cm)		HW: Body Weight (x10 <sup>3</sup> )	
	Control (n=4)	Uraemic (n=4)	Control (n=4)	Uraemic (n=4)	Control (n=4)	Uraemic (n=4)	Control (n=4)	Uraemic (n=4)
<b>- EPO</b>	387.5 ±22.5	327.5 ±42.5	1.26 ±0.01	1.34 ±0.07	0.30 ±0.001	0.33 ±0.02	3.25 ±0.05	4.20 ±0.75
<b>+ EPO</b>	425.0 ±0.0	355.0 ±10.0	1.32 ±0.002	1.29 ±0.07	0.31 ±0.01	0.31 ±0.02	3.09 ±0.01	3.64 ±0.08

Table 3.3.4d: Indices of LVH at 12 weeks post-induction of uraemia

	Body Weight (g)		Wet Heart Weight (g)		HW: Tibia length (g/cm)		HW: Body Weight (x10 <sup>3</sup> )	
	Control (n=59)	Uraemic (n=50)	Control (n=59)	Uraemic (n=50)	Control (n=59)	Uraemic (n=50)	Control (n=59)	Uraemic (n=50)
<b>- EPO</b>	530.3 ±9.1	513.6 ±13.4	1.73 ±0.04	2.11 ±0.06*	0.39 ±0.01	0.47 ±0.01*	3.27 ±0.07	4.15 ±0.12*
<b>+ EPO</b>	516.0 ±7.7	502.3 ±14.4	1.70 ±0.04	1.91 ±0.07*	0.38 ±0.01	0.42 ±0.01 <sup>†</sup>	3.30 ±0.07	3.84 ±0.14*

(\*p<0.05 vs. respective control †p<0.05 vs. untreated group)

Figure 3.8a

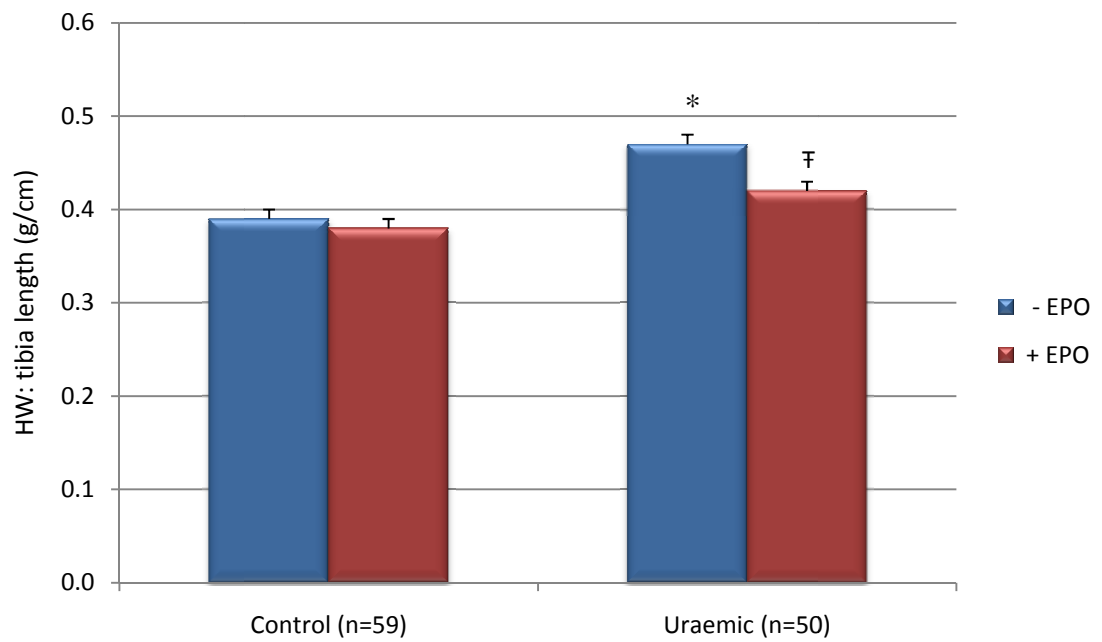


Figure 3.8b

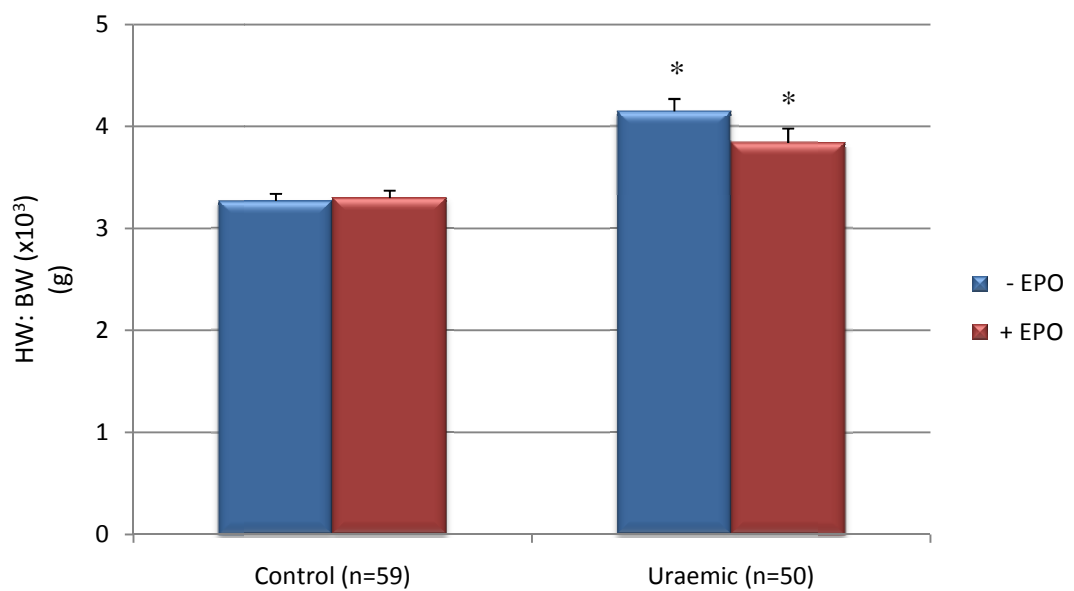


Figure 3.8: Indices of LVH at 12 weeks post-induction of uraemia  
(\* $p < 0.05$  vs. respective control  $\nabla p < 0.05$  vs. untreated group)

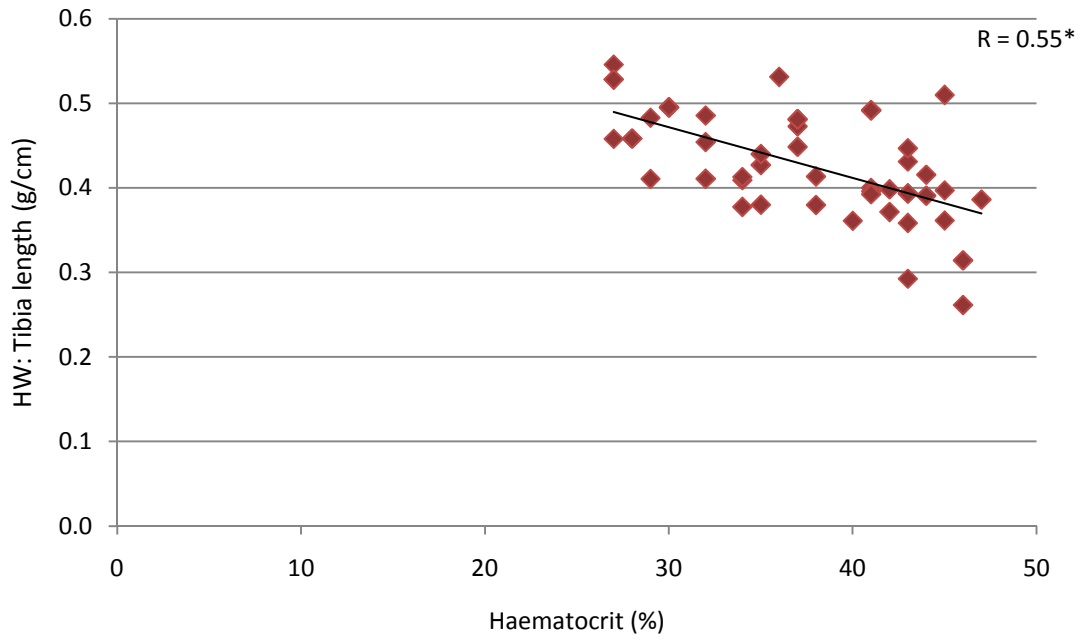


Figure 3.9: Correlation between haematocrit and extent of LVH (\* $p < 0.05$ )

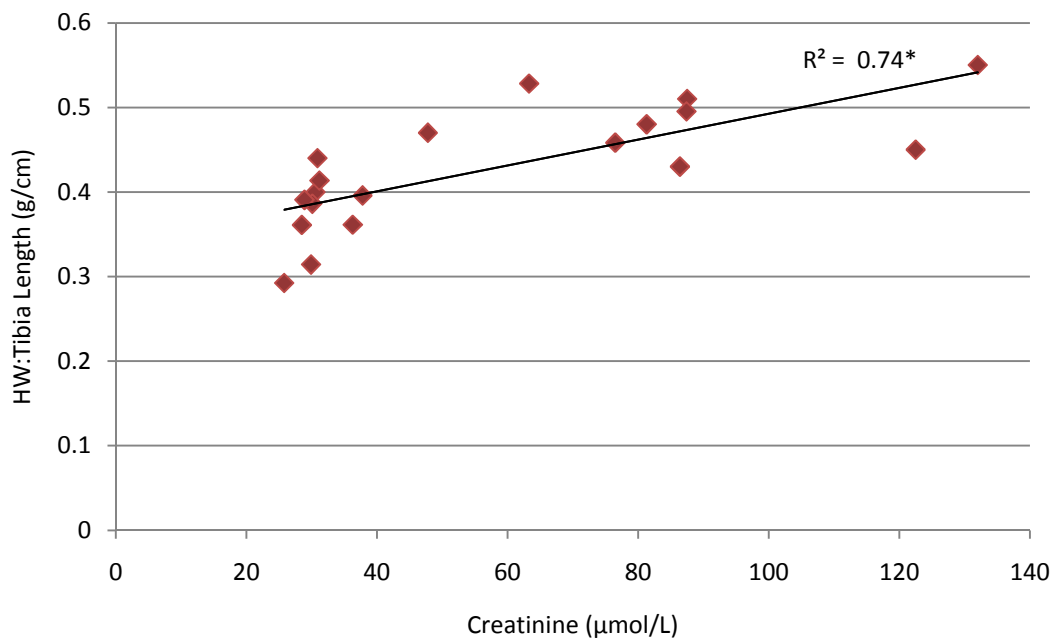


Figure 3.10: Correlation between serum creatinine and extent of LVH (\* $p < 0.05$ )

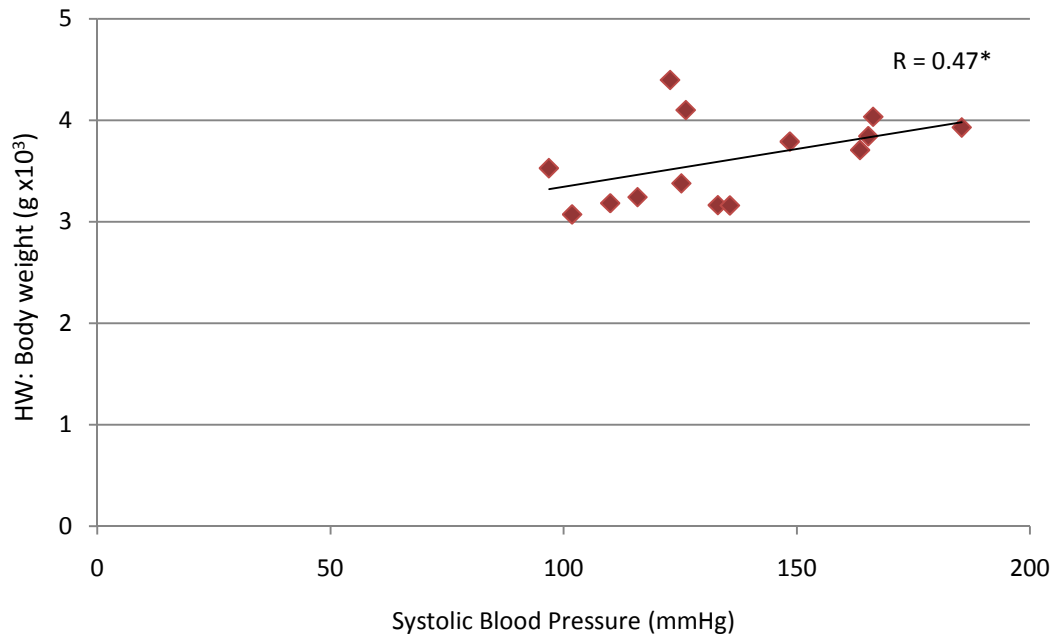


Figure 3.11: Correlation between SP and extent of LVH (\* $p=0.05$ )

## 3.4 Discussion

### 3.4.1 Experimental Model of CKD

Surgical induction of uraemia using the 5/6 nephrectomy model produced marked kidney dysfunction as evidenced by the increased serum creatinine and serum urea and development of anaemia (Figures 3.3 a and b). This is in keeping with previous results from this laboratory (Reddy et al., 2007, Aksentijevic et al., 2009), and others (Dikow et al., 2004). Progressive renal damage leads to the retention of creatinine and urea, thus elevated serum levels. In addition, reduced secretion of EPO from the damaged kidney during CKD results in anaemia (Caro et al., 1979, Eschbach et al., 2002).

EPO, which improves haematocrit, also has anti-apoptotic and antioxidant effects and therefore it is feasible that EPO administration may slow the progression of renal failure (Toba et al., 2009, Moon et al., 2003a). Here however, serum creatinine and urea (which are crude measures of actual renal function) were comparable in untreated and treated uraemic animals, suggesting that EPO had little impact on the progression of renal failure in this model. This is consistent with clinical observations showing that EPO does not limit CKD progression (Lim et al., 1990, The US Recombinant Human Predialysis Study Group 1991, Savica et al., 1995). Furthermore, the EPO-associated rise in blood pressure may actually contribute to glomerular injury and worsening kidney function, however, this was not observed in the present study (Lee et al., 2007, Garcia et al., 1988, Lafferty et

al., 1991). Conversely, a number of clinical studies have shown that, in pre-dialysis patients, the progression of renal failure (determined by creatinine clearance) was slowed, and the time to onset of dialysis therapy prolonged with EPO treatment (Jungers et al., 2001, Kuriyama et al., 1997).

In this study, uraemic animals had a decreased haematocrit with 3 weeks of uraemia (Table 3.1). The anaemia observed may be in part due to decreased EPO production from the damaged kidney, paralleling findings from uraemic patients (Caro et al., 1979). Indeed, anaemia is present in 60-80% of patients with end stage renal disease (ESRD) and low erythropoietin levels correlate with a reduction in haematocrit (Hsu, 2002, Obrador et al., 2001). EPO resistance also occurs in CKD patients, as a consequence of high circulating levels of inflammatory cytokines, including TNF $\alpha$  and IL-6, potentially contributing to worsening anaemia (Goicoechea et al., 1998, Costa et al., 2008). Low haematocrit levels are associated with an increased risk of hospitalisation in CKD patients, and improving haematocrit decreases risk (Xia et al., 1999, Anand et al., 2005). In this study, administration of EPO improved haematocrit in control and uraemic animals at all stages. EPO corrects anaemia by raising erythrocyte production and inhibiting apoptosis of erythrocyte precursors, thereby increasing the number of circulating red blood cells (Fisher, 2003). Coincident with the rise in haematocrit was the increased spleen weight, observed in EPO treated animals (Figure 3.5).

The percentage water content within the lungs was comparable between uraemic and control animals (with and without EPO treatment) at 3, 6, 9 and 12 weeks

uraemia (Figure 3.6). This suggests that although LVH was observed at 6 and 12 weeks, uraemic hearts were in a compensatory phase but not failing. In contrast, experimental models of post-MI heart failure have observed large increases in lung water content, suggesting cardiac failure (Saito et al., 2002). In this regard, EPO treatment has been shown to improve cardiac function and delay the onset of heart failure in a murine model of post-MI heart failure (Li et al., 2006). Interestingly, a number of clinical trials in heart failure patients have shown that EPO is safe and well tolerated and is associated with improved exercise capacity and ejection fraction (Mancini et al., 2003, Silverberg et al., 2001).

### **3.4.2 Blood Pressure**

Blood pressure was determined *in vivo* using an arterial catheter; however, as anaesthesia depresses heart rate and blood pressure, comparisons were not possible with readings obtained from the conscious animal. Non-invasive techniques, such as the tail-cuff method, have also been used for determining blood pressure, which allows repeated measurements to be made without affecting physiological parameters of the animal. However, limitations of this method involve variations of blood pressure due to the restraint of the conscious animal leading to increases in systolic blood pressure and heart rate (Kurtz et al., 2005).

At 12 weeks, uraemic animals had a markedly elevated systolic blood pressure compared with control animals (Figure 3.7 and Table 3.3). Similar findings have been found in previous experimental studies of CKD (Tsujiura et al., 2008,

Kennedy et al., 2003), and are comparable to the raised blood pressures observed in patients with renal insufficiency (Parfrey and Foley, 1999). Hypertension in this model is present from 3 weeks post-induction of uraemia (Reddy et al., 2007).

The reasons behind the elevated blood pressure during CKD remain incompletely understood. Activation of the renin-angiotensin-aldosterone system (RAAS) is considered a key contributor. Indeed, a major impact on the mortality associated with CKD has been achieved through treatment with angiotensin converting enzyme inhibitors (ACEi) and angiotensin receptor blockers (ARB's) (Maschio et al., 1996). Angiotensin II acts directly on vascular smooth muscles cells as a potent vasoconstrictor, but also has mitogenic effects (Rosenkranz, 2004). Angiotensin II also regulates renal sodium and water absorption *via* release of aldosterone. Furthermore, angiotensin II affects cardiac contractility and heart rate through activation of the sympathetic nervous system. Interestingly, a number of studies have shown administration of ACEi and/or ARB's during uraemia diminished renal fibrosis and improved proteinuria (Ikoma et al., 1991, Jaimes et al., 1998). Moreover, several large multicentre trials have proposed renoprotective effects of ACEi independent of their antihypertensive actions (Heart Outcomes Prevention Evaluation Study Investigators 2000, PROGRESS trial 2001). Although a rise in blood pressure was observed in uraemic animals here, other researchers have shown that activation of RAAS is less pronounced in this model compared with other experimental models of CKD which reduce functional renal mass *via* ligation of renal arteries (Kobori et al., 2007).

EPO administration did not significantly increase blood pressure in this study. However, clinically, EPO-associated hypertension occurs in approximately one third of CKD patients (Lee et al., 2007, Shimada et al., 2003, Faulds and Sorkin, 1989). EPO is thought to increase blood pressure due to the expansion of blood volume and increased blood viscosity (Miyashita et al., 2004). In addition, EPO has been shown to raise blood pressure directly and independent of its haematopoietic effects (Shimada et al., 2003). Heidenreich *et al.* (1991) demonstrated direct vasoconstrictive effects of EPO on isolated renal and mesenteric vessels *in vitro* (Heidenreich et al., 1991). Furthermore, EPO promotes release of renin and angiotensin II (Eggena et al., 1991, Brier et al., 1993), and the EPO-associated rise in blood pressure was prevented by inhibition of the RAAS system and endothelin-1 (ET-1) blockade, highlighting a potential role for these systems (Miyashita et al., 2004).

### **3.4.3 LVH**

Cardiac hypertrophy was observed from 6 weeks post-surgery, increasing at 12 weeks in uraemic animals (Figure 3.8 and Table 3.4). HW: BW and HW: tibia length were used to assess LVH in this study. HW: BW can be used to indicate LVH except when body weight is inconsistent such as in aging, and then hypertrophy may be overestimated. Thus, HW: tibia length becomes a better marker of LVH (Yin et al., 1982).

The development of LVH during CKD is complex and incompletely understood. However, the association and persistence of haemodynamic factors, including increased afterload (hypertension and aortic stiffening) and increased preload (anaemia and hypervolaemia) in addition to metabolic and endocrine abnormalities clearly play a role (London, 2003).

Clinical and experimental studies have shown that administration of antihypertensive agents (such as ACEi) during CKD leads to a decrease in blood pressure correlating with regression of LVH (Zoccali et al., 2004, Harnett and Parfrey, 1994). Conversely, some experimental studies have shown that LVH persists despite the normalisation of blood pressure (Rambausek et al., 1993). Furthermore, LVH was observed in a mouse model of CKD without the corresponding increase in blood pressure suggesting that development of LVH during uraemia can be partly dissociated from the impact of hypertension alone (Siedlecki et al., 2009).

Anaemia can also contribute to the development of LVH, independent of blood pressure changes. A combination of decreased blood viscosity and increased flow due to low tissue oxygenation cause an increase in demand and cardiac output (London and Parfrey, 1997). Here, EPO improved anaemia and induced a partial regression of LVH in uraemic animals at 12 weeks post-induction of uraemia. Consistent with these findings, experimental (Amann et al., 2000) and clinical studies (Silberberg et al., 1990) have demonstrated that EPO treatment is associated with a reduction in LVH during CKD. However, controversy exists over

the degree of anaemia correction, with some studies finding that partial, rather than full correction of haematocrit is associated with LVH regression (Silberberg et al., 1990, Cannella et al., 1991, Hayashi et al., 2000).

#### **3.4.4 EPO Treatment**

In the present study, darbepoietin alfa (Aranesp® Amgen, Cambridge, UK) was used, a synthetic analogue of human recombinant erythropoietin (rhEPO). Darbepoietin alfa is a novel erythropoiesis stimulating protein (NESP) with a higher molecular weight, causing a three-fold longer half-life than that of rhEPO. This consequently reduces the frequency of injections (Egrie and Browne, 2001, Macdougall et al., 1999). Injections were given subcutaneously which results in a slower absorption; this also allows for less frequent injections and reduces the injected volume compared with IV administration (Halstenson et al., 1991). The dose of EPO employed in this study (30 µg/Kg) was comparable with those used in other experimental studies (Gao et al., 2007). The amount of EPO needed to achieve a cardioprotective effect was originally thought to be much greater than that required to normalise haematocrit. Gao *et al.* (2007) found that EPO provided a dose-dependent cardioprotective effect with 30 µg/Kg being the optimal dose to reduce infarct size and improve cardiac function post ischaemia/reperfusion (Gao et al., 2007). However, a recent study by Lipsic *et al.* (2008) found that a low-dose of EPO could provide cardioprotection in rat hearts without increasing haematocrit (Lipsic et al., 2008).

### **3.4.5 Conclusions**

In this model, kidney dysfunction was evident from 3 weeks post-induction of uraemia, with no evidence initially of cardiac hypertrophy. When the duration of uraemia was prolonged to 12 weeks, animals showed anaemia, marked hypertension and LVH. Administration of EPO improved haematocrit and lessened cardiac hypertrophy in uraemic animals suggesting a possible beneficial effect of EPO in this model of CKD.

## **Chapter 4: *In Vitro* Cardiac Function and Metabolism**

## 4.1 Introduction

LVH is frequently observed in CKD patients (Foley et al., 1995). Although initially beneficial in terms of reducing wall tension and preserving function, the hypertrophied heart is accompanied by a plethora of intracellular changes, which produce a pathophysiological phenotype, leading ultimately to heart failure (Levy et al., 1990). One such change is remodelling of metabolism involving a switch in substrate preference away from fatty acid oxidation (FAO) towards glucose utilisation, which may contribute to the cardiac dysfunction observed in uraemic patients (Chapter 1) (Barger and Kelly, 1999, Osorio et al., 2002, Sambandam et al., 2002).

### 4.1.1 Determination of *In Vitro* Cardiac Function

The assessment of cardiac function *in vitro* has allowed researchers to study the isolated heart in a variety of experimental models, including LVH and uraemic cardiomyopathy. A number of perfusion systems have been developed including the isovolumic Langendorff and the working-heart preparations, which allow the simultaneous measurement of cardiac function and oxygen consumption (Ross, 1972).

The Langendorff preparation was first described by Oscar Langendorff in 1895 and has since been developed and modified by a number of researchers (Opie, 1965, Bleehen and Fisher, 1954). In this perfusion method, the aorta is cannulated and

the heart retrogradely perfused. The perfusion medium is prevented from entering the heart by the aortic valve, and thus travels through the coronary arteries under hydrostatic pressure. This method has been used for well over a century and remains a standard technique for assessing *in vitro* cardiac function and metabolism. The Langendorff preparation is frequently used as it is technically easier and requires less complex equipment than other perfusion methods (Ross, 1972). However, the ventricle undergoes little or no filling and thus no external work is performed. This was overcome by the introduction of the left-sided working-heart preparation first described by Neely and Morgan (1967). In this method, the left atrium is also cannulated, and after a brief period of retrograde perfusion, the flow is reversed and the perfusion medium enters the left ventricle and is ejected out of the cannulated aorta (Neely et al., 1967). Interestingly, it has been shown that although the Langendorff perfused heart undergoes no external work (i.e. the emptying and filling of the ventricles), this has little impact on metabolism and function when compared with working-heart preparations.

#### **4.1.2. Metabolic Remodelling**

LVH is present in up to 75% of CKD patients (Foley et al., 1995). Cardiomyocytes hypertrophy in response to haemodynamic overload, which helps reduce wall tension and preserve systolic function (Grossman, 1980). Although the early stages of LVH are physiologically beneficial, many of the adaptations become limited and thus maladaptive, initiating the transition to cardiac dysfunction and failure (Levy et al., 1990, Seymour, 2003b). In response to pathophysiological stimuli, the

hypertrophied heart is not simply an enlarged heart. Instead, LVH is accompanied by a number of intracellular changes. One such change is the altered profile of substrate utilisation, known as metabolic remodelling.

In the healthy adult heart, most of the ATP is derived from fatty acid oxidation, with a smaller contribution from glucose and lactate. Experimental models of volume-overload (el Alaoui-Talibi et al., 1992) and pressure-overload (Allard et al., 1994, Akki et al., 2008) cardiac hypertrophy have shown a switch in substrate usage from fatty acids, towards glucose utilisation (Barger and Kelly, 1999, Osorio et al., 2002, Sambandam et al., 2002). The change in substrate preference is consistent with a re-expression of the foetal phenotype and may initially represent a beneficial adaptation in LVH. Indeed, if fatty acid oxidation is reduced, then glucose oxidation would increase *via* the Randle cycle, which could potentially improve coupling between glycolysis and glucose oxidation therefore decreasing the glycolytic production of lactate and protons. Moreover, ATP production from glucose is more oxygen efficient than from fatty acids, owing to more oxygen atoms already present on the glucose molecule, therefore the shift towards glucose utilisation may be important to reduce oxygen consumption and sustain function during LVH (Taegtmeyer, 1986).

In the longer term however, this remodelling may result in complications including energy depletion (Leone et al., 1999, Seymour and Chatham, 1997), thereby initiating the transition to heart failure.

Little research has been undertaken to determine the profile of myocardial substrate utilisation in uraemia. However, given that LVH is frequently observed in experimental models of CKD and in the clinical scenario, it is feasible that the metabolic remodelling associated with LVH also occurs in the uraemic heart and may eventually contribute to cardiac dysfunction and failure. Furthermore, experimental models of CKD have a decrease in the myocardial phosphocreatine (PCr)/ATP ratio suggesting that the uraemic heart is depleted of energy reserves, potentially reflecting altered myocardial energy metabolism (Raine et al., 1993).

#### **4.1.3 Objectives**

In this chapter, *in vitro* cardiac function and the extent of metabolic remodelling were assessed in experimental uraemia. The impact of EPO therapy was also examined in the experimental model. Specifically the aims of this chapter were

- To determine the profile of substrate utilisation in uraemic and control hearts using  $^{13}\text{C}$  NMR
- To examine the impact of chronic EPO administration on cardiac metabolism
- To determine the effect of uraemia and chronic EPO treatment on the activities of key mitochondrial metabolic enzymes
- To assess the impact of acute and chronic EPO administration on *in vitro* cardiac function and efficiency using the Langendorff perfusion method in uraemic and control hearts

- To identify the effects of increasing cardiac workload on untreated and EPO treated uraemic and control hearts

## 4.2 Materials and Methods

### 4.2.1 Effects of Acute EPO Administration

To determine the effect of acute EPO administration on *in vitro* cardiac function, control hearts from male Sprague-Dawley rats (weighing approximately 400 g) were perfused with K-H buffer (as described in Section 2.2.4) containing EPO at the following concentrations 0.006 µg/ml, 0.03 µg/ml and 0.06 µg/ml (equivalent to 1, 5 and 10 U/ml respectively) (Figure 4.1a). Oxygen consumption and cardiac efficiency were calculated as described in Section 2.2.4.3.

### 4.2.2 Effects of Uraemia and Chronic EPO Administration

Uraemia was induced surgically in male Sprague-Dawley rats and animals maintained for up to 12 weeks post-surgery with respective sham operated rats as a control (details provided in Section 2.2.1).

Animals were divided into 4 experimental groups

- Control animals + saline (- EPO)
- Uraemic animals + saline (- EPO)
- Control animals + EPO
- Uraemic animals + EPO

EPO (30 µg/Kg) or equal volumes of saline were administered by subcutaneous injection twice a week for 2 weeks prior to experiments (Section 3.3.2).

Hearts were isolated from the 4 groups of rats and perfused according to the protocol given in Figure 4.1b (details of perfusion provided in Section 2.2.4). To determine the effect of increasing cardiac work, hearts were initially perfused using buffer containing 1.25 mM [Ca<sup>2+</sup>], which was increased to 2.5 mM [Ca<sup>2+</sup>]. To investigate myocardial metabolism, K-H buffer was switched to an identical buffer containing <sup>13</sup>C labelled substrates (Figure 4.1b) and substrate utilisation determined using <sup>13</sup>C NMR (as described in Section 2.2.5).

#### **4.2.3 Mitochondrial Enzyme Activity**

Pyruvate Dehydrogenase (PDH), Citrate Synthase (CS) and Medium-Chain Acyl-CoA Dehydrogenase (MCAD) activities were determined as described in Sections 2.2.6.1, 2.2.6.2 and 2.2.6.3, respectively.

Figure 4.1a: Protocol for acute EPO administration

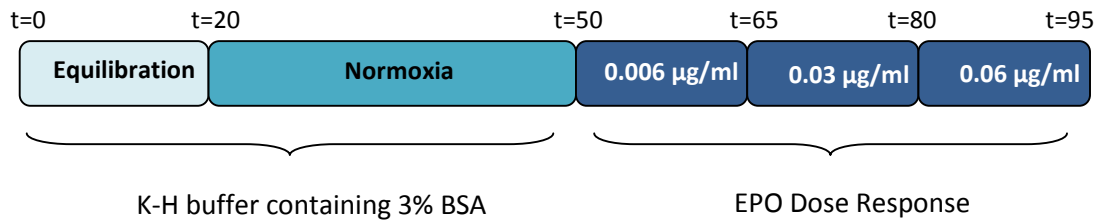


Figure 4.1b: Protocol for chronic EPO treatment

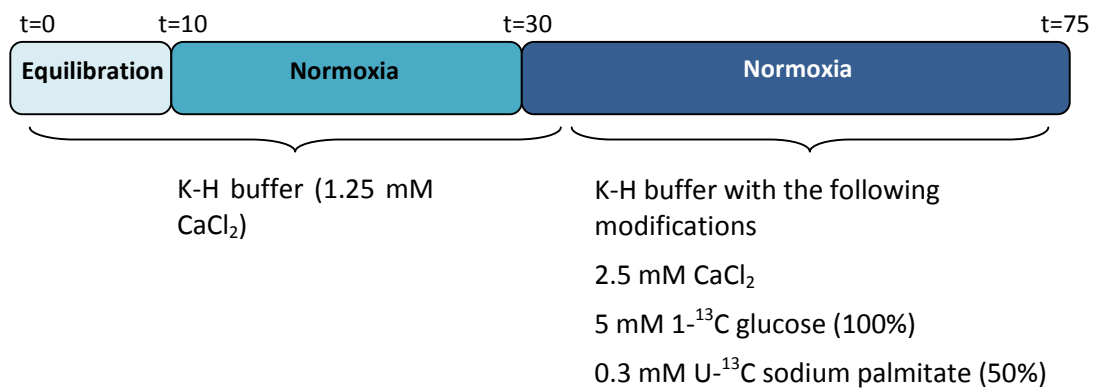


Figure 4.1: Perfusion Protocols

## 4.3 Results

### 4.3.1 Effect of Acute EPO Administration

*In vitro* myocardial function and efficiency were not significantly altered following acute EPO administration regardless of the EPO concentration used (Table 4.1).

Table 4.1: Effects of acute EPO administration

EPO ( $\mu\text{g/ml}$ )	LVDP (mmHg)	RPP $\times 10^3$ (mmHg/bpm)	MVO <sub>2</sub> ( $\mu\text{mol/g}$ wet heart weight/ min)	Cardiac Efficiency $\times 10^3$ (mmHg/ $\mu\text{mol/g}$ wet heart weight)
<b>0</b> (n=4)	128 $\pm$ 17.3	32.2 $\pm$ 5.5	0.87 $\pm$ 0.1	43.0 $\pm$ 3.0
<b>0.006</b> (n=4)	115 $\pm$ 19.5	31.8 $\pm$ 3.0	0.87 $\pm$ 0.1	40.5 $\pm$ 4.5
<b>0.03</b> (n=4)	110 $\pm$ 17.6	30.5 $\pm$ 4.3	0.89 $\pm$ 0.2	39.1 $\pm$ 4.5
<b>0.06</b> (n=4)	115 $\pm$ 17.1	30.4 $\pm$ 5.9	0.86 $\pm$ 0.1	38.5 $\pm$ 4.0

### 4.3.2 Effects of Uraemia and Chronic EPO Administration

#### Three Week

At 3 weeks uraemia, LVDP, RPP and cardiac contractility ( $dP/dt_{\max/\min}$ ) were comparable to control hearts and unaffected by chronic EPO administration (Table 4.2 and Figure 4.2). Consequently, there were no significant differences in oxygen consumption ( $MVO_2$ ) or cardiac efficiency between untreated and EPO treated control and uraemic hearts (Figures 4.3 and 4.4).

Table 4.2: *In Vitro* cardiac function at 3 weeks uraemia

		Systolic Pressure (mmHg)	LVDP (mmHg)	$(dP/dt)_{\max}$ (mmHg/s)	$(dP/dt)_{\min}$ (mmHg/s)
Control (n=6)	- EPO	172 ±20	170 ±19	8143 ±571	-5273 ±242
Uraemic (n=7)	- EPO	188 ±17	186 ±17	7549 ±406	-4683 ±391
Control (n=10)	+ EPO	199 ±16	199 ±15	7329 ±517	-4131 ±216
Uraemic (n=11)	+ EPO	213 ±21	212 ±20	7834 ±678	-4339 ±347

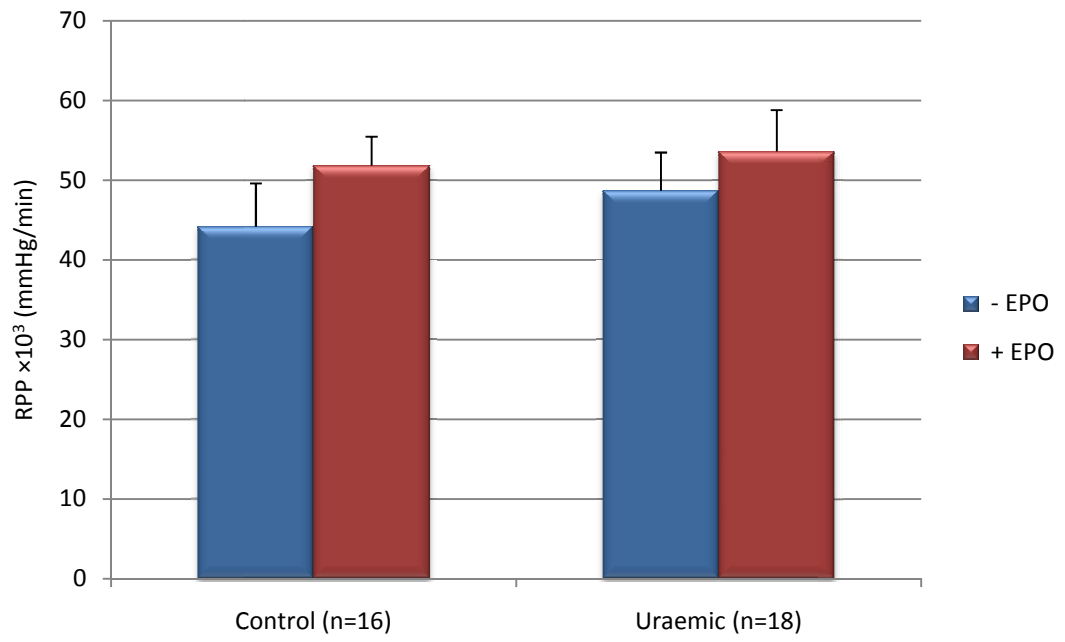


Figure 4.2: Rate pressure product at 3 weeks post-induction of uraemia

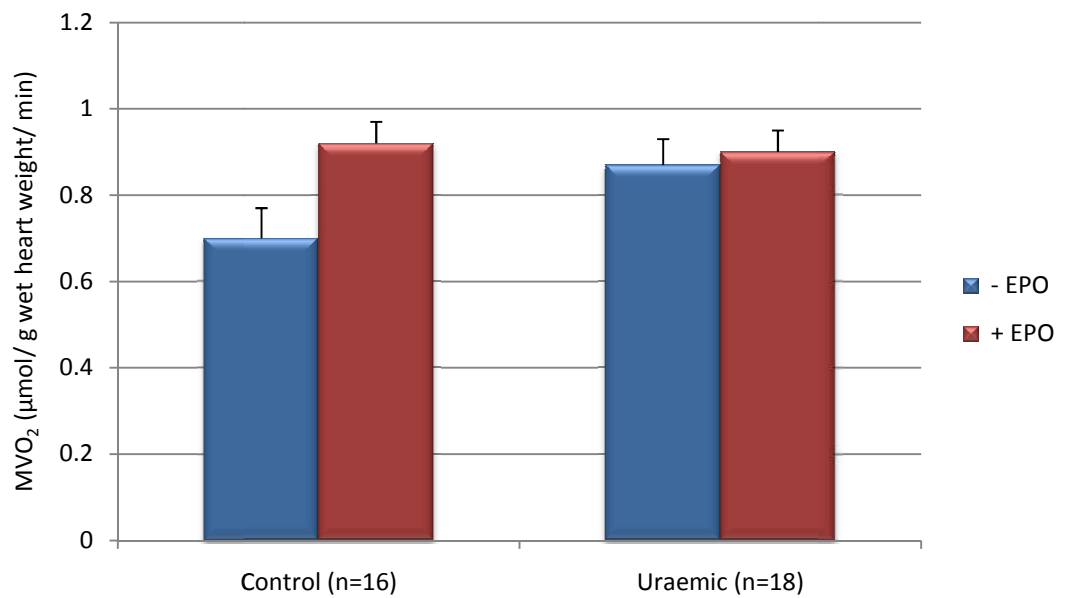


Figure 4.3: MVO<sub>2</sub> at 3 weeks post-induction of uraemia

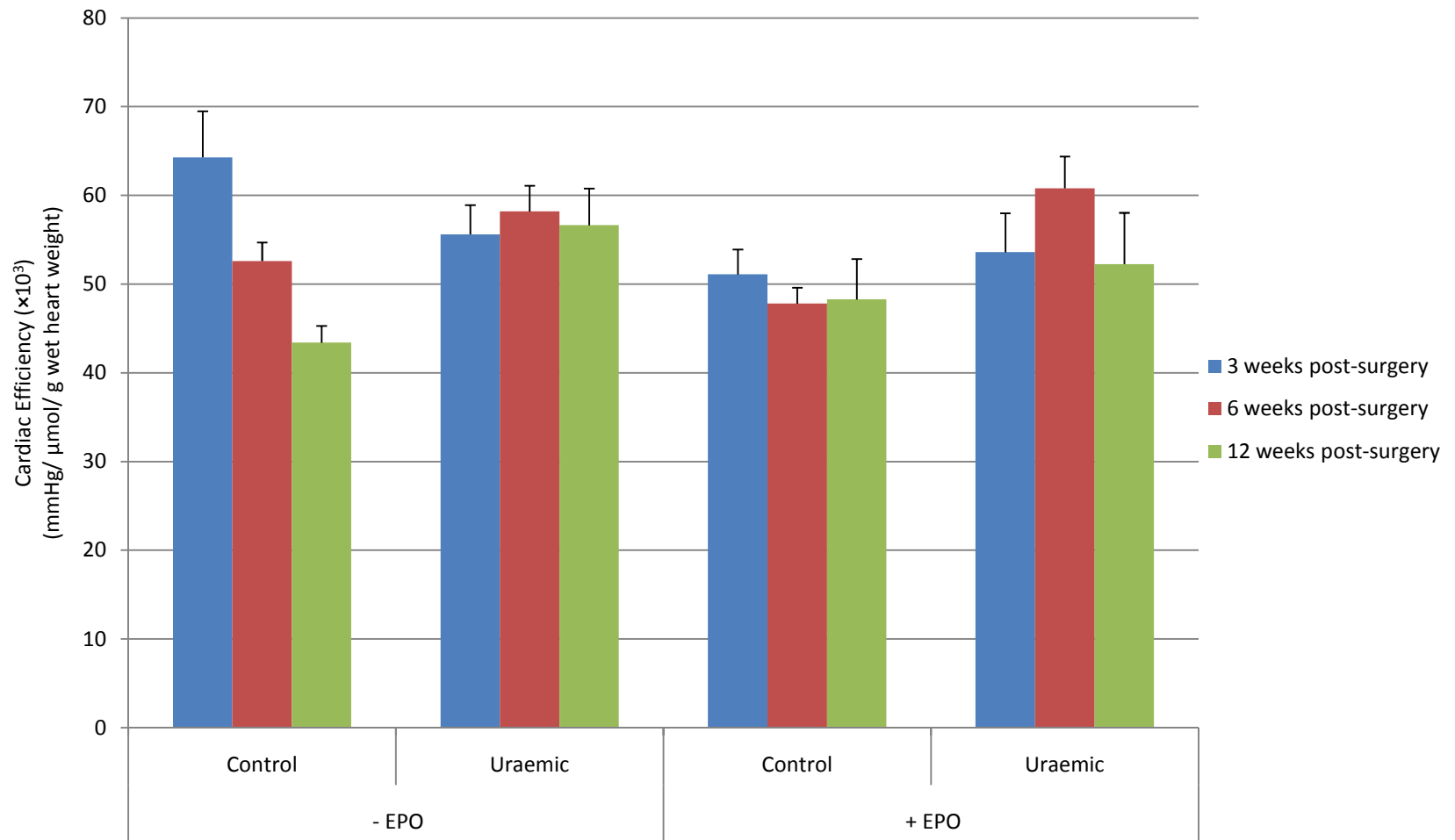


Figure 4.4: Cardiac efficiency in uraemia

## Six Week

At 6 weeks uraemia, hearts perfused with 1.25 mM calcium showed little differences in function,  $MVO_2$  or cardiac efficiency compared with controls, and were unaffected by chronic EPO administration (Table 4.3).

Increasing buffer  $[Ca^{2+}]$  from 1.25 mM to 2.5 mM, resulted in a marked increase in LVDP and RPP (Table 4.3 and Figure 4.5), however, RPP and cardiac efficiency remained comparable between control and uraemic hearts (Figures 4.4, 4.5 and 4.6).

Table 4.3: *In Vitro* cardiac function at 6 weeks uraemia

<b>1.25mM calcium</b>					
		<b>Systolic Pressure (mmHg)</b>	<b>LVDP (mmHg)</b>	<b>(dP/dt)<sub>max</sub> (mmHg/s)</b>	<b>(dP/dt)<sub>min</sub> (mmHg/s)</b>
<b>Control (n=5)</b>	- EPO	125 ±11	123 ±11	4822 ±347	-2629 ±199
<b>Uraemic (n=5)</b>	- EPO	119 ±10	118 ±11	4515 ±362	-2435 ±182
<b>Control (n=5)</b>	+ EPO	137 ±9	137 ±8.9	5101 ±262	-2816 ±174
<b>Uraemic (n=7)</b>	+ EPO	137 ±11	136 ±10	5024 ±349	-2823 ±150

<b>2.5mM calcium</b>					
		<b>Systolic Pressure (mmHg)</b>	<b>LVDP (mmHg)</b>	<b>(dP/dt)<sub>max</sub> (mmHg/s)</b>	<b>(dP/dt)<sub>min</sub> (mmHg/s)</b>
<b>Control (n=5)</b>	- EPO	176 ±11	174 ±11	6976 ±352	-3879 ±247
<b>Uraemic (n=5)</b>	- EPO	171 ±12	171 ±12	6817 ±403	-3924 ±272
<b>Control (n=5)</b>	+ EPO	186 ±13	184 ±13	7084 ±536	-4019 ±212
<b>Uraemic (n=7)</b>	+ EPO	198 ±14	198 ±14	7430 ±474	-4566 ±218

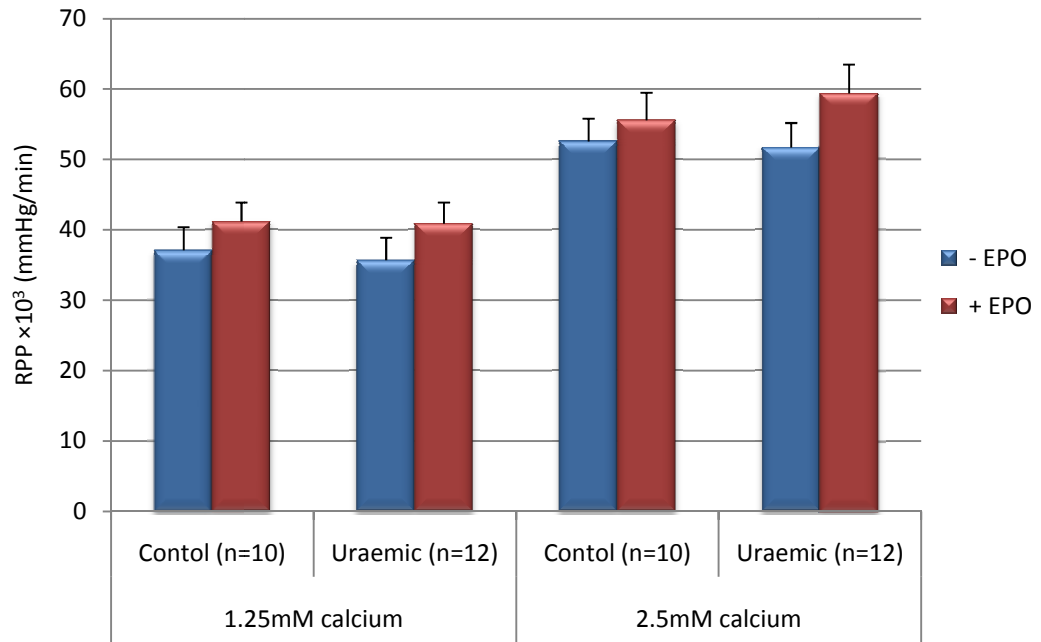


Figure 4.5: Rate pressure product at 6 weeks post-induction of uraemia

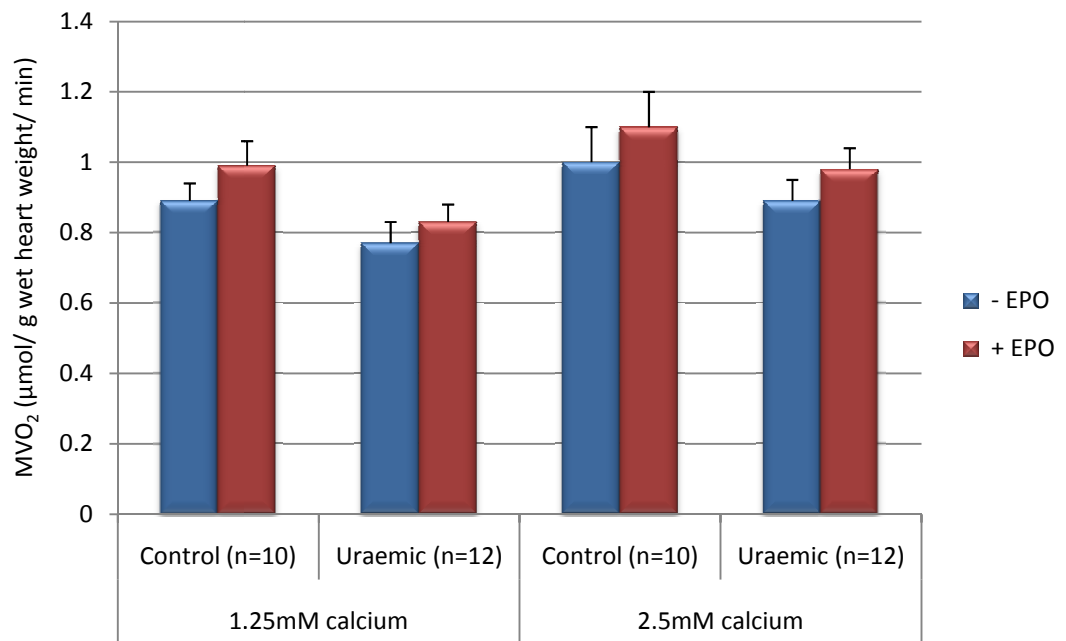


Figure 4.6: MVO<sub>2</sub> at 6 weeks post-induction of uraemia

## Twelve Week

Twelve weeks of uraemia did not modify LV developed pressures, contractility or efficiency when perfused using K-H buffer containing 1.25 mM  $[Ca^{2+}]$ , and were unaffected by chronic EPO treatment (Table 4.4 and Figure 4.7).

When hearts were perfused using 2.5 mM  $[Ca^{2+}]$ , LVDP and RPP significantly increased compared with hearts perfused using 1.25 mM  $[Ca^{2+}]$ . Contractility (as evidenced by  $dP/dt_{\max/\min}$ ) was the same in control and uraemic hearts (Table 4.4). Furthermore,  $MVO_2$  and cardiac efficiency were unchanged in uraemic compared with control hearts (Figures 4.4 and 4.8).

Table 4.4: *In Vitro* cardiac function at 12 weeks uraemia

1.25mM calcium					
		Systolic Pressure (mmHg)	LVDP (mmHg)	(dP/dt) <sub>max</sub> (mmHg/s)	(dP/dt) <sub>min</sub> (mmHg/s)
Control (n=8)	- EPO	105 ±3	102 ±3	3756 ±260	-2169 ±175
Uraemic (n=7)	- EPO	122 ±11	119 ±11	4243 ±355	-2424 ±189
Control (n=8)	+ EPO	105 ±7	105 ±7	3990 ±183	-2211 ±136
Uraemic (n=6)	+ EPO	117 ±11	117 ±11	4378 ±253	-2452 ±203

2.5mM calcium					
		Systolic Pressure (mmHg)	LVDP (mmHg)	(dP/dt) <sub>max</sub> (mmHg/s)	(dP/dt) <sub>min</sub> (mmHg/s)
Control (n=8)	- EPO	136 ±6	135 ±5	5275 ±244	-2995 ±169
Uraemic (n=7)	- EPO	160 ±11	156 ±10	5808 ±252	-3467 ±129
Control (n=8)	+ EPO	140 ±9	139 ±9	5382 ±236	-3101 ±139
Uraemic (n=6)	+ EPO	163 ±11	162 ±11	6279 ±318	-3808 ±224

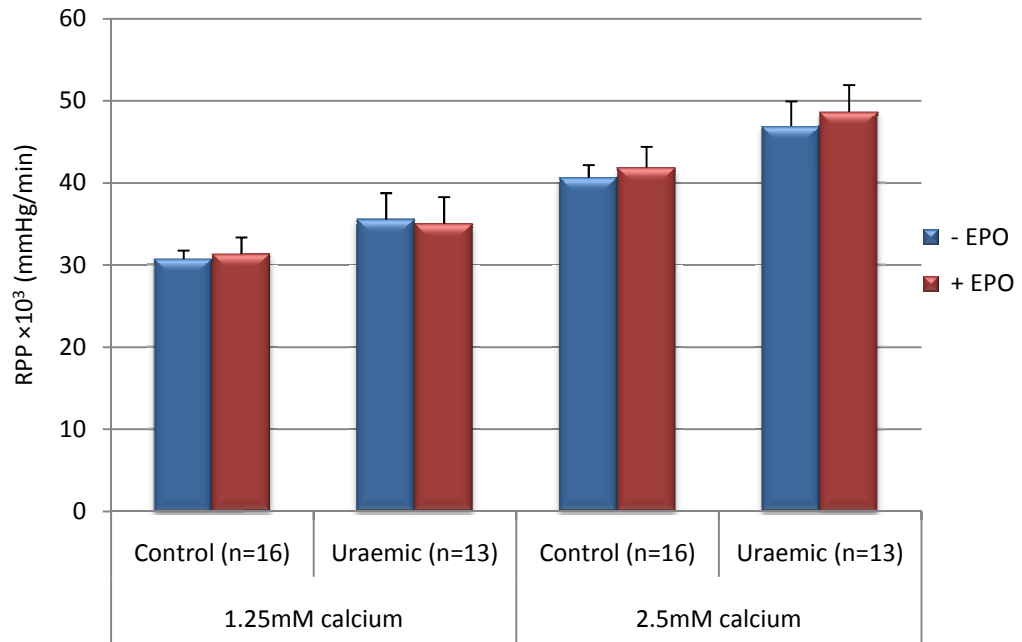


Figure 4.7: Rate pressure product at 12 weeks post-induction of uraemia

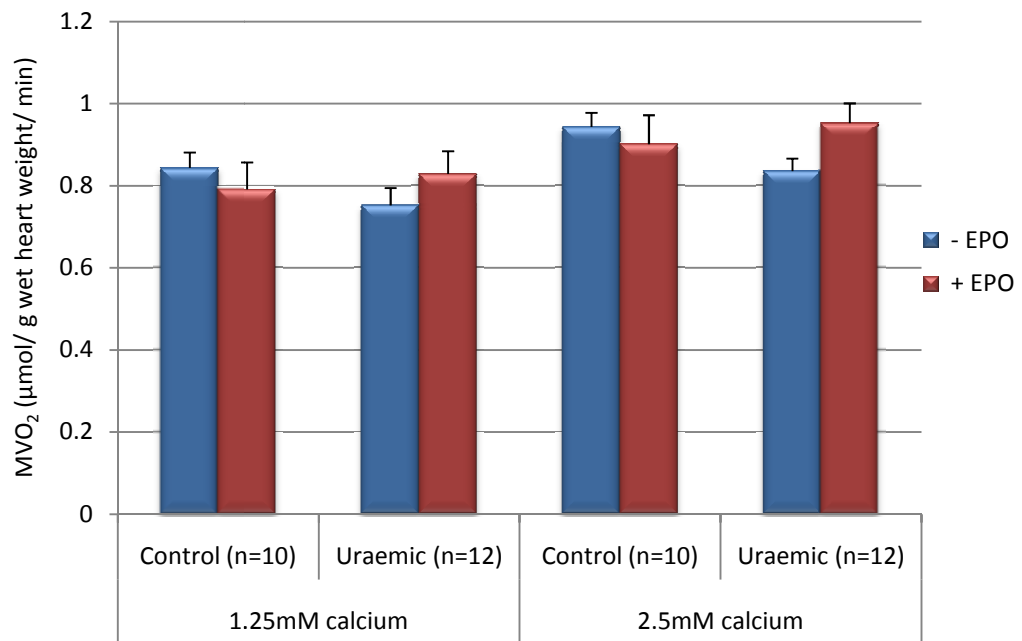


Figure 4.8: MVO<sub>2</sub> at 12 weeks post-induction of uraemia

### 4.3.3 Cardiac Metabolism

The relative contributions of substrates to oxidative metabolism were assessed at 3, 6 and 12 weeks post-induction of uraemia (data given in Figures 4.9 a-c).

By 3 weeks, the contributions of palmitate and glucose to oxidative metabolism were unchanged in all 4 groups (Figure 4.9a). At 6 weeks, there was a reduction in the contribution of palmitate to oxidative metabolism in uraemic hearts compared with controls ( $27.5 \pm 1.9\%$  vs.  $20.0 \pm 1.5\%$   $p < 0.05$ ), consistent with the onset of LVH (see results from Section 3.3.3). Accordingly, there was an increase in glucose and unlabelled substrate utilisation in uraemic compared with control hearts (Figure 4.9b).

At 12 weeks, there were no significant differences in the contribution of substrates to oxidative metabolism between any of the groups (Figure 4.9c).

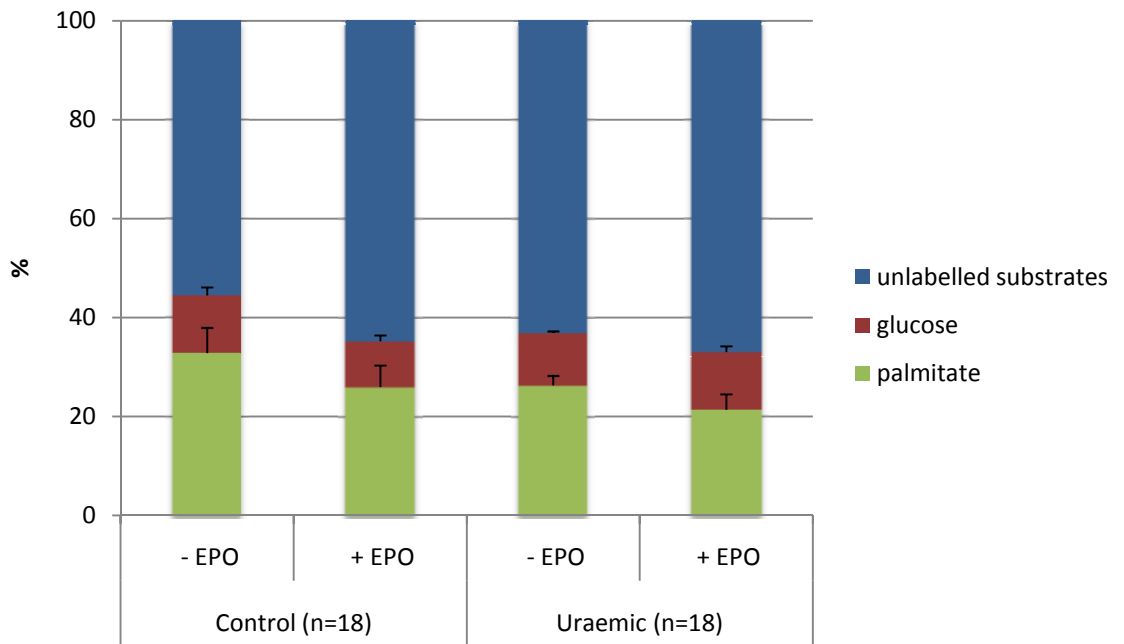


Figure 4.9a: Contribution of <sup>13</sup>C labelled substrates to oxidative metabolism at 3 weeks uraemia

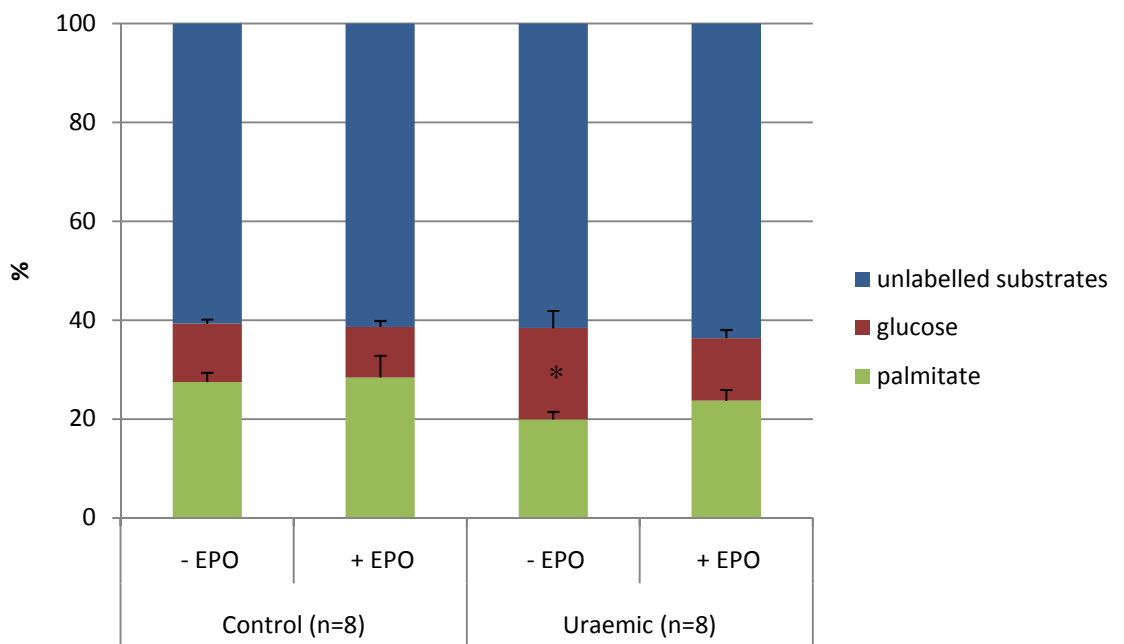


Figure 4.9b: Contribution of <sup>13</sup>C labelled substrates to oxidative metabolism at 6 weeks uraemia

\*  $p < 0.05$  vs. respective control

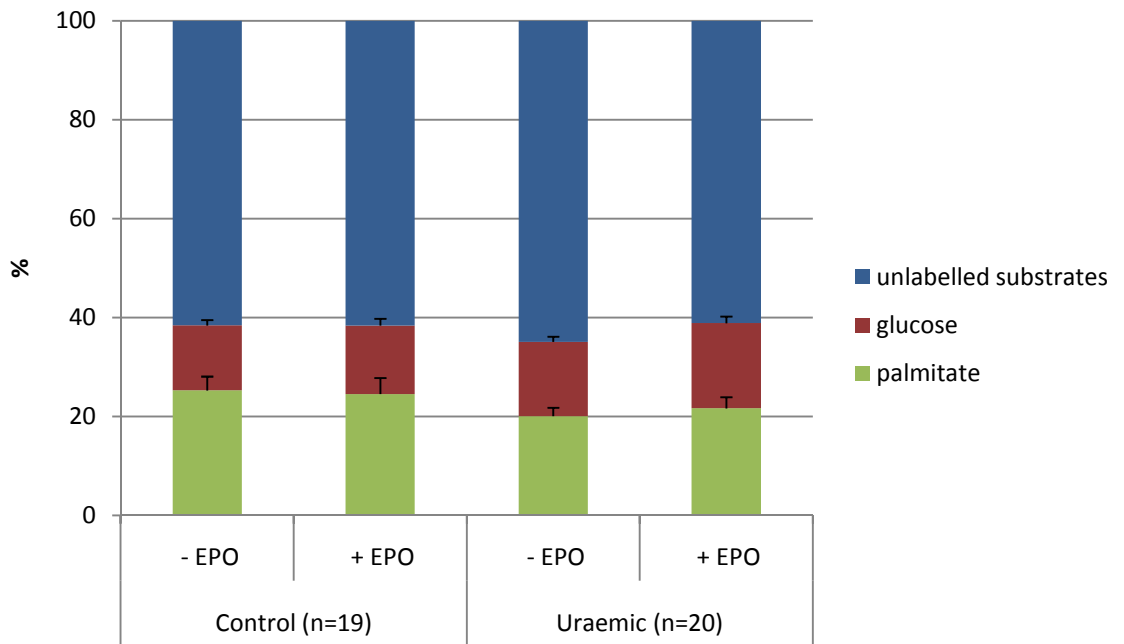


Figure 4.9c: Contribution of  $^{13}\text{C}$  labelled substrates to oxidative metabolism at 12 weeks uraemia

#### 4.3.4 Mitochondrial Enzyme Activities

At 3 and 12 weeks, MCAD activity was similar in uraemic and control hearts irrespective of EPO treatment (Figures 4.10 and 4.11).

PDH activity at 12 weeks post-induction of uraemia is given in Figure 12 (a and b). Total PDH was unaltered in all 4 groups (data not shown). The amount of PDH in the active form (Figure 4.12a) was also unchanged resulting in comparable PDHa/PDHi ratios (Figure 4.12b).

Cardiac CS activity was similar between control and uraemic animals at both 6 and 12 weeks post-induction of uraemia (Table 4.5).

Table 4.5: CS activity at 6 and 12 weeks post-induction of uraemia

	6 week		12 week	
	Control (n=8)	Uraemic (n=8)	Control (n=9)	Uraemic (n=9)
- EPO	73.5 ±1.8	75.1 ±8.5	95.0 ±9.6	96.5 ±6.4
+ EPO	77.0 ±4.6	83.1 ±6.9	94.5 ±5	87.1 ±5.6

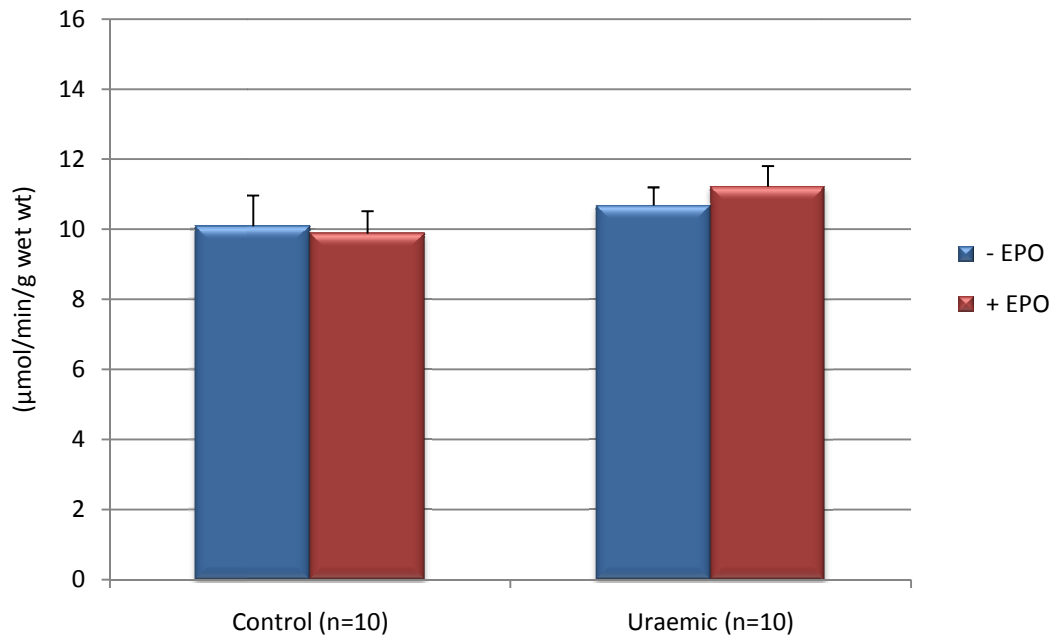


Figure 4.10: MCAD activity at 3 weeks post-induction of uraemia

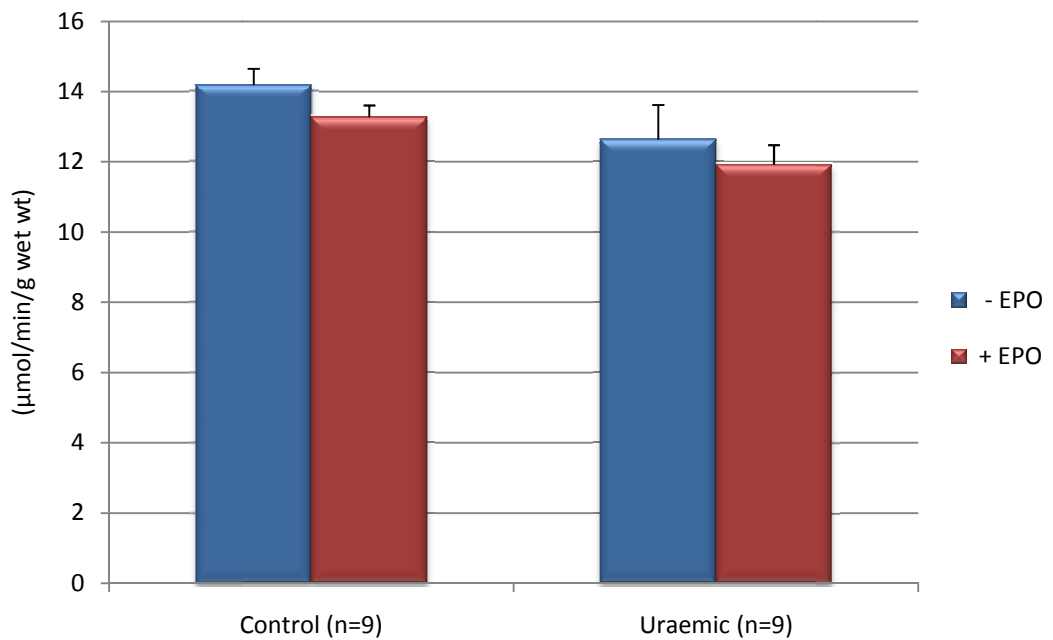


Figure 4.11: MCAD activity at 12 weeks post-induction of uraemia

Figure 4.12a: Active PDH

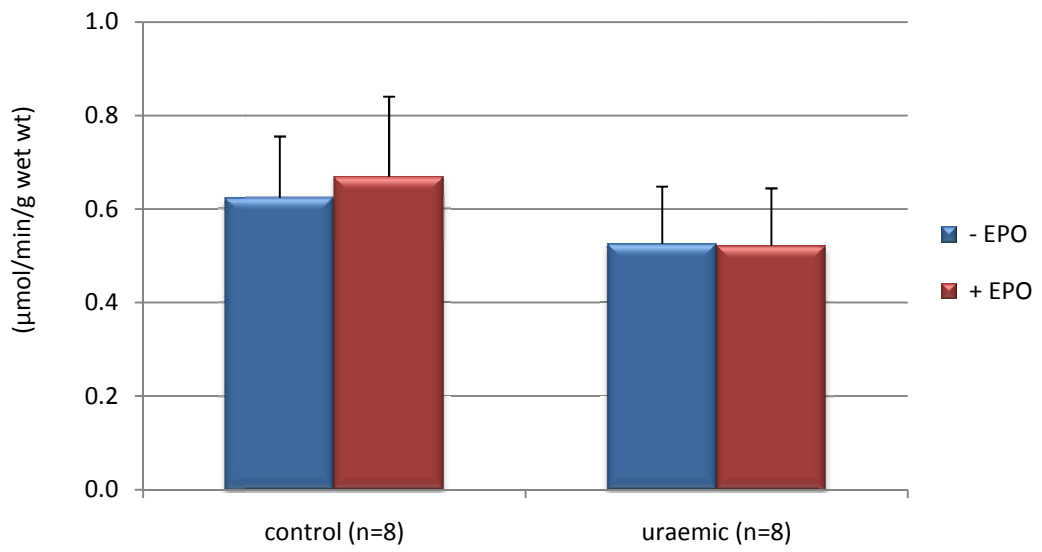


Figure 4.12b: PDHa:PDHt

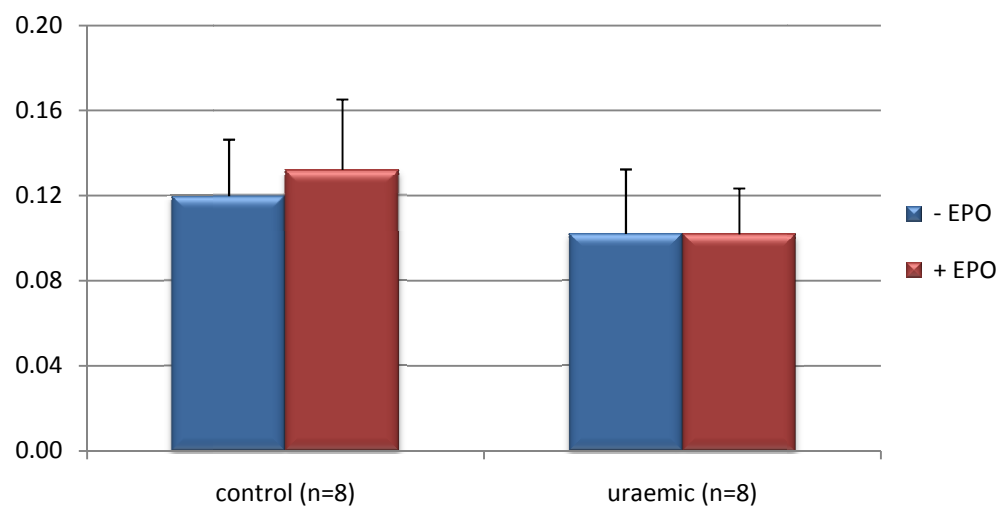


Figure 4.12: PDH activity at 12 weeks post-induction of uraemia

## 4.4 Discussion

EPO perfusion had little impact on *in vitro* cardiac function or efficiency in control hearts. Uraemic rat hearts demonstrated preserved *in vitro* cardiac function, consistent with a compensatory phase of LVH, which was unchanged following chronic EPO administration. At 6 weeks post-induction of uraemia, contribution of palmitate to myocardial oxidative metabolism was decreased compared with control hearts, which parallels observations from studies using the hypertrophied heart.

### 4.4.1 Effects of Acute EPO Administration

Acute EPO administration had little impact on cardiac function in control hearts irrespective of the dose (Table 4.1). This is consistent with previous studies, using similar EPO doses, which showed that, under baseline conditions, EPO had no effect on cardiac function in isolated perfused hearts (Wright et al., 2004). In contrast, Piuhola *et al.* (2008) observed a dose-dependent increase in ventricular developed pressure with acute EPO administration (1-3 U/ml) in the perfused rat heart (Piuhola et al., 2008). EPO has been shown to exert an acute cardioprotective effect after a period of ischaemia, by reducing apoptotic cell death and improving function during reperfusion (Wright et al., 2004). Bullard *et al* (2005) demonstrated that the protective effect of EPO during ischaemia/reperfusion was abolished in the presence of the P13K inhibitors wortmannin and LY294002 and the ERK 1/2 inhibitor U0126, suggesting that the beneficial action of acute EPO treatment is

mediated *via* activation of the RISK (Reperfusion Injury Salvage Kinase) pathway (Bullard et al., 2005).

Acutely administered EPO mediates a number of signalling pathways which can potentially directly modify myocardial function. In rats with renal failure, and in post-hypoxic mice, erythropoietin treatment improved cardiac contractility *via* modulation of Na<sup>+</sup>/K<sup>+</sup> ATPase (Sterin-Borda et al., 2003, Wald et al., 1995). This suggests that EPO may act as a positive inotrope to improve function, however, this was not observed in the present study. EPO may also mediate contractility and acute cardiac function through its effects on intracellular calcium handling. EPO-EPOR interaction leads to phosphorylation of phospholipase C  $\gamma$ -1 (PLC  $\gamma$ -1), which translocates and binds to EPOR. This, in turn, results in the hydrolysis of phosphatidylinositol 4,5 bisphosphate (PIP<sub>2</sub>) forming inositol 1,4,5-triphosphate (IP<sub>3</sub>), and consequently liberates Ca<sup>2+</sup> from intracellular stores, altering force of contraction (Marrero et al., 1998). In support of the involvement of EPO in calcium handling, a number of studies have shown increased intracellular [Ca<sup>2+</sup>] with EPO treatment (Vaziri et al., 1996, Vaziri et al., 1995, Neusser et al., 1993).

#### **4.4.2 Effects of Uraemia and Chronic EPO Administration**

At 3 weeks uraemia, there was little change in cardiac function or efficiency between the four groups, in keeping with previous findings in the laboratory (Reddy et al., 2007) (Table 4.2, Figures 4.2-4.4). At 6 and 12 weeks post-induction of uraemia, no differences in function or efficiency were observed when hearts were

perfused with 1.25 mM  $[Ca^{2+}]$ . When the buffer calcium concentration was increased to 2.5 mM, LVDP and RPP increased proportionally in all groups (Tables 4.3-4 and Figures 4.4-8). Raising the calcium concentration increases calcium influx into the cardiomyocyte, thereby increasing the force of contraction and contractile demand (Gwathmey et al., 2007).

At both 6 and 12 weeks, no significant differences were observed in RPP or dP/dt (max and min) in uraemic hearts compared with respective controls (Table 4.4). Uraemia is associated with hypertension (Section 3.3.2), which may result in a rise in ventricular developed pressure in order to exceed the pressure in the artery, thus maintaining cardiac output, however, this was not observed in the present study. These results are consistent with the view that 12 weeks of uraemia corresponds to a compensatory phase of LVH. With progression of uraemia and sustained insult (such as prolonged pressure or volume overload), the heart may not compensate, thus contractility and LVDP fall and cardiac dysfunction and failure would ensue.

In contrast to the findings from this study, Raine *et al.* (1993) used a working heart preparation to show impaired cardiac function at 4 weeks post-induction of uraemia. However, in addition to the different perfusion methods used, Raine *et al.* induced renal dysfunction *via* a two-stage 5/6<sup>th</sup> nephrectomy and could therefore have produced a more severe model of uraemia than in this study (Raine et al., 1993). Clinical studies also suggest that impairment of cardiac function occurs early in the progression of renal failure (Parfrey et al., 1996, Pehrsson et al., 1984). However, it is difficult to extrapolate results from clinical studies to the

experimental setting, due to the existence of comorbidities, such as diabetes, which are frequently present in CKD patients. McMahon *et al.* (2002) demonstrated impaired relaxation (evidenced by prolonged calcium transients) in isolated cardiomyocytes from uraemic hearts in the presence of 4 mM  $[Ca^{2+}]$  (McMahon *et al.*, 2002). Thus, a combination of uraemia with additional stresses such as elevated  $[Ca^{2+}]$  or increased pacing may unmask dysfunction in uraemic hearts.

#### **4.4.3 Myocardial Metabolism**

In this study, at 3 weeks uraemia, no change in myocardial metabolism was observed. However, by 6 weeks, the contribution of palmitate to oxidative metabolism decreased in uraemic hearts with a corresponding rise in contributions from glucose and unlabelled substrates.

The decrease in palmitate utilisation may result in decreased  $MVO_2$  thus sustaining cardiac function in uraemic hearts as glucose utilisation is more oxygen-efficient than fatty acid oxidation. For one mole of oxygen consumed, glucose yields 6.3 moles of ATP, compared with fatty acids which produce only 5.7 moles of ATP from the same amount of oxygen (Taegtmeyer, 1986).

Few studies have investigated the metabolic profile of the uraemic heart. Reddy *et al.* (2007) showed little alterations in substrate utilisation at 3 or 6 weeks uraemia when hearts were perfused using 1.25 mM calcium. In this study, at 6 and 12 weeks, uraemic animals demonstrated marked LVH compared with controls, and

the altered profile of substrate oxidation is consistent with findings from models of both pressure (Allard et al., 1994, Sambandam et al., 2002, Akki et al., 2008) and volume overload hypertrophy (el Alaoui-Talibi et al., 1992). Experimental models of LVH have shown the metabolic remodelling to reflect a re-expression of the foetal gene programme. After birth, the up-regulation of fatty acid oxidation (FAO) parallels mitochondrial development and an increased expression of the regulatory transcription factor PPAR $\alpha$ .

During hypertrophy, expression of myocardial PPAR $\alpha$  is reduced, coinciding with a reduction in the expression of FAO enzymes including carnitine palmitoyl transferase 1 (CPT1) and MCAD (Barger et al., 2000). Interestingly, in this study, MCAD activity was not significantly altered during uraemia despite the decrease in FAO.

Recent experimental studies have shown that in addition to decreased PPAR $\alpha$  expression, the expression of PGC1 $\alpha$  is also down-regulated and may contribute to diminished FAO in chronic heart failure (Garnier et al., 2003). Interestingly, PGC-1 $\alpha$  mRNA is decreased when Akt is over expressed (Cook et al., 2002) and, given that uraemia is associated with high levels of angiotensin II, which activate the Akt pathway, this may reduce PGC-1 and thus account for decreased FAO in this model (Perlman et al., 2004). Supporting the role of angiotensin II in metabolic remodelling, prolonged exposure of cultured adult rat cardiomyocytes to angiotensin II directly reduced palmitate oxidation. Interestingly, this metabolic adaptation was blocked by inhibition of TNF $\alpha$  (Pellieux et al., 2009). Moreover, in a

separate study, Pellieux *et al.* (2006) observed decreased mRNA expression of key proteins involved in  $\beta$ -oxidation in the myocardium of mice over-expressing angiotensinogen, a precursor for angiotensin II. However, a reduction in FAO was only observed after the onset of heart failure, highlighting that in this particular model, the decline in palmitate oxidation was a consequence, rather than a cause of heart failure (Pellieux *et al.*, 2006).

EPO treatment is associated with RAAS activation and elevated angiotensin II levels, potentially contributing to a rise in blood pressure (Brier *et al.*, 1993, Eggena *et al.*, 1991). It is therefore feasible that EPO may further reduce FAO *via* its effect on angiotensin II. However, this was not observed in the present study.

It remains unclear whether metabolic remodelling characteristic of LVH is a beneficial adaptation to sustain function or the trigger for the onset of heart failure. As previously mentioned, glucose utilisation is more oxygen efficient compared with fatty acids for ATP production (Taegtmeyer, 1986). Moreover, increasing glucose oxidation can improve coupling between glycolysis and glucose oxidation therefore reducing lactate and proton ( $H^+$ ) accumulation. This notion has been supported by a number of studies whereby increasing glucose oxidation (either directly, or indirectly *via* FAO reduction) improves function (McCormack *et al.*, 1996). Furthermore, Young *et al.* (2001) demonstrated that inappropriate reactivation of PPAR $\alpha$  and increased FAO exacerbated dysfunction during cardiac hypertrophy (Young *et al.*, 2001a). This suggests that the switch to glucose

oxidation may be essential for sustaining cardiac function in pathophysiological LVH.

In contrast, experimental models of heart failure have demonstrated improved cardiac function with increased PPAR $\alpha$  activation (Brigadeau et al., 2007, Labinsky et al., 2007). This implies that the reduction in FAO in heart failure may contribute to dysfunction. Indeed, reduced oxidation of lipids and accumulation of lipid intermediates may result in lipotoxicity. Furthermore, inhibition of PDH by fatty acyl components (as described in Chapter 1) limits the entry of glucose in to the TCA cycle. This may render the uraemic heart energy starved. However, the portion of PDH in the active form in this study was not decreased in uraemic hearts. Increasing the duration or severity of uraemia may result in inhibition of PDH and thus may render the uraemic heart 'inflexible' to up-regulate glucose oxidation resulting in energy starvation. Indeed, diminished energy stores (indicated by reduced PCr/ATP ratio), have been observed in an experimental model of uraemia (Raine et al., 1993). Moreover, clinical studies have shown a progressive decline in PCr/ATP ratio in CKD patients with increased duration on peritoneal dialysis (Ogimoto et al., 2003).

#### **4.4.4 Conclusion**

In conclusion, despite LVH and systemic hypertension being prominent features at both 6 and 12 weeks uraemia, *in vitro* cardiac function was preserved, highlighting a compensatory phase of hypertrophy. Palmitate utilisation was decreased at 6

weeks in uraemic hearts consistent with the metabolic remodelling observed in models of LVH. This remodelling may initially be a beneficial adaption to sustain function, however, in the longer term may be a precursor for the transition from compensatory LVH into dysfunction and heart failure.

## **Chapter 5: *In Vivo* Cardiac Function and Fibrosis**

## **5.1 Introduction**

The uraemic heart is characterised by phenotypic alterations including LVH. Initially, an increase in cardiomyocyte size normalises wall tension and allows maintenance of cardiac function (Grossman, 1980). However, persistent elevations in wall stress will eventually exceed the hearts ability to compensate and cardiac failure will ensue (Levy et al., 1990). Coupled with increased cell size is the expansion of extracellular matrix (ECM). As pathophysiological LVH progresses, a disproportionate accumulation of collagen occurs, known as cardiac fibrosis, which contributes to dysfunction and may serve as a contributing mechanism to the onset of heart failure.

### **5.1.1 Cardiac Fibrosis**

Myocardial ECM, comprised primarily of collagen, provides a dense structural network which is vital for structural integrity and force transmission (Weber et al., 1994). An increased amount of collagen within the heart is characteristic of many disease states including LVH (Gao et al., 2005), hypertension (Zhai et al., 2008) and uraemic cardiomyopathy (Amann and Ritz, 1996).

There are two major types of cardiac fibrosis, reparative and reactive. Reparative (or replacement) fibrosis involves increased deposition of collagen to replace necrotic cells and exists as microscopic scarring. Reactive fibrosis is the accumulation of collagen either around vessels (perivascular fibrosis) or diffusely between cardiomyocytes (interstitial fibrosis) (Weber, 1989).

The development of fibrosis is under the control of a number of factors including transforming growth factor  $\beta$  (TGF- $\beta$ ) and angiotensin II, the up-regulation of which are associated with the onset of fibrosis (Weber and Janicki, 1989, Kuwahara et al., 2002). Furthermore, decreased collagen breakdown may also play a role in the development of cardiac fibrosis. Collagen degradation is mediated by the enzymes collagenase and matrix metalloproteinases (MMPs). In the spontaneously hypertensive rat (SHR), cardiac fibrosis was accompanied by decreased collagenase activity contributing to accumulation of collagen and diminished collagen breakdown (Varo et al., 2000). Interestingly, in cultured adult rat cardiac fibroblasts, angiotensin II inhibited collagenase activity, which may be important as elevated angiotensin II is characteristic of CKD, and thus may be a factor in the accumulation of collagen within the uraemic heart (Brilla et al., 1994).

In addition to the increased quantity of collagen, alterations in the relative proportions of type I and type III collagens play an important role in the development of ventricular stiffness. Type I collagen typically forms thick fibres (average diameter 75 nm) and is associated with high tensile strength. Conversely,

type III collagen generally forms thinner strands (average diameter 45 nm) which provide elasticity (de Souza, 2002). Experimental studies have confirmed increased cardiac stiffness with a raised collagen type I/type III ratio (Yamada et al., 2009). An increase in collagen type I relative to type III has been observed in patients with chronic heart failure (Bishop et al., 1990) and dilated cardiomyopathy (Marijjanowski et al., 1995). Furthermore, observations from the uraemic heart also show elevated quantities of type I collagen (Rabkin et al., 2008).

As well as the increased amount of collagen and change in the relative proportions of collagen types, increased cross-linking of collagen fibres contributes to reduced ventricular compliance. Jalil *et al.* (1989) identified increased cross-linking forming a dense network of fibrillar collagen in the pressure-overloaded rat heart (Jalil et al., 1989). Furthermore, in the spontaneously hypertensive rat (SHR), the improvement in myocardial stiffness with hydralazine therapy was associated only with improved collagen solubility whereas the total collagen amount and collagen type I/type III remained unchanged (Norton et al., 1997).

Animal models of CKD (Amann and Ritz, 1996, Kalk et al., 2007, Mall et al., 1988) and post-mortem studies (Mall et al., 1990) have revealed extensive cardiac fibrosis in uraemia. Experimental studies using the 5/6<sup>th</sup> nephrectomy model have identified enhanced activation and proliferation of cardiac interstitial fibroblasts in uraemia (Mall et al., 1988, Amann and Ritz, 1997, Amann et al., 1994). Interestingly, fibrosis has been shown to occur in experimental uraemia despite normalisation of blood pressure and LVH (Piotrkowski et al., 2009, Mall et al., 1988).

The presence of myocardial fibrosis has functional consequences including ventricular arrhythmias and reduced ventricular compliance (Saito et al., 2007, Varnava et al., 2001). Moreover, the deposition of collagen fibres between capillaries and myocytes increases the oxygen diffusion distance and contributes to oxygen starvation, enhancing the susceptibility of the uraemic heart to ischaemic injury. Importantly, an increase in collagen within the myocardium impedes relaxation of the ventricles leading to diastolic dysfunction, which is frequently observed in patients with renal insufficiency (Otsuka et al., 2009).

#### **5.1.2 *In Vivo* Cardiac Function**

Many studies use *in vitro* methods, including perfused heart preparations (Chapter 4), to assess dysfunction in experimental models. However, *in vivo* methods of monitoring cardiac function have the advantage of determining function under the conditions of hormonal and haemodynamic influences as part of the cardiovascular system. Echocardiography is the most widely used non-invasive method for evaluating left ventricular function (including left ventricular shape and size) in patients (Mohrman and Heller, 2006). However, recording and interpreting echocardiographs require extensive training and therefore reliability and quality of results are operator dependent. In addition, many of the functional parameters are derived from calculations based on simplified assumptions, which may introduce

error. MRI (magnetic resonance imaging) overcomes many of these drawbacks (Guttman et al., 1997), however MRI is a complex and expensive technique, and cannot be used on critically ill patients so therefore it is not currently used as a routine diagnostic tool in clinical practice. Using an arterial catheter, inserted into the left ventricle allows accurate measurement of cardiac function *in vivo*. This highly invasive terminal technique is frequently used for determining cardiac function in small animals for research purposes.

### **5.1.3 Objectives**

In this chapter, the combined impact of uraemia and chronic EPO treatment on cardiac function was assessed, in addition to the extent of fibrosis in uraemic heart. Specifically, the aims of this chapter were

- To determine the impact of uraemia and EPO administration on cardiac function *in vivo*
- To identify the extent of myocardial fibrosis in uraemic hearts and the impact of chronic EPO treatment on collagen deposition

## 5.2 Methods

### 5.2.1 Induction of Uraemia and EPO treatment

Uraemia was induced surgically in male Sprague-Dawley rats (details provided in Section 2.2.1). Animals were divided into 4 experimental groups; EPO was administered as described in Section 3.3.2.

- Control animals + saline (- EPO)
- Uraemic animals + saline (- EPO)
- Control animals + EPO
- Uraemic animals + EPO

### 5.2.2 Determination of *In Vivo* Cardiac Function

At 12 weeks post-induction of uraemia, cardiac function was determined *in vivo* using an arterial Millar catheter as described in Section 3.2.5 (Wang et al., 2007). After measurement of blood pressure in the right carotid artery, the catheter was advanced through the aortic arch and into the left ventricle. Successful entry into the ventricle was confirmed by a drop in end diastolic pressure (DP) (Figure 5.1).

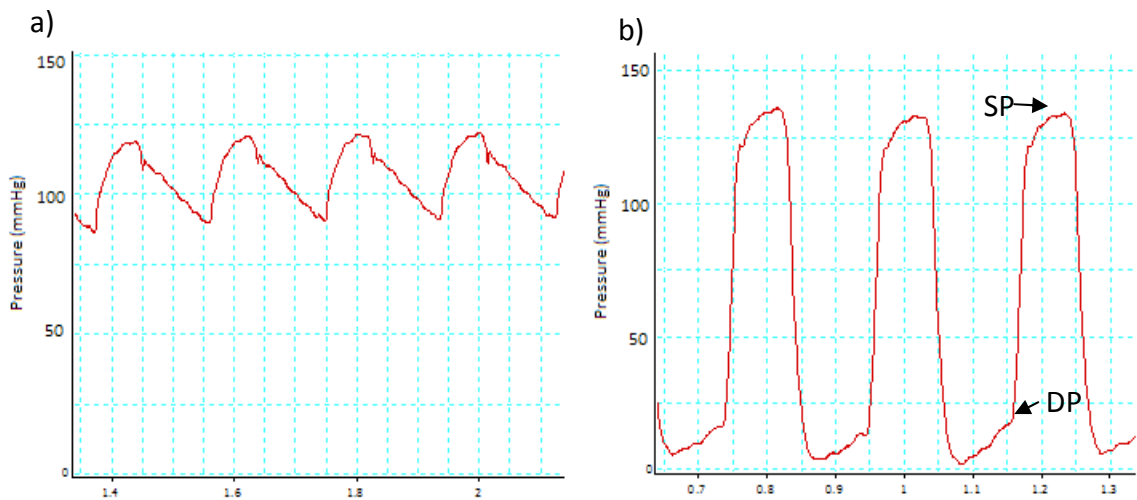


Figure 5.1: Recording of *in vivo* a) arterial blood pressure and b) left ventricular pressure of an anaesthetised rat

RPP was calculated from the product of  $HR \times LVDP$  (as a measure of cardiac work) as detailed in Section 2.2.4.2.

### 5.2.3 Histology of Uraemic Hearts

Twelve weeks post-induction of uraemia, hearts were removed from the 4 groups of animals, rinsed in K-HB buffer and mounted onto a cork platform using Tissue-Tek OCT® compound (Williams et al, 1999). The whole heart was transferred into pre-cooled 2-methyl-butane and placed in liquid nitrogen prior to storage at  $-20^{\circ}\text{C}$ .

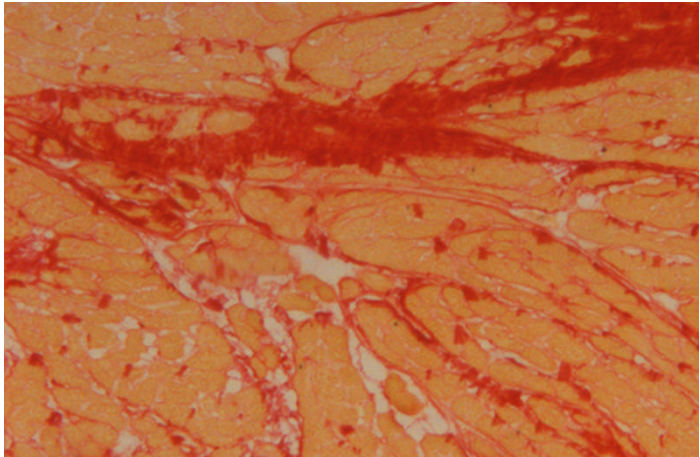
Five 12 µm thick sections were taken from the mid-papillary region of each heart, using a cryostat microtome (Microm HM 505 E Cryostat, Thermo Scientific, Walldorf, Germany) and stained for structure using haematoxylin and eosin (H & E) stain. Briefly, sections were fixed using formal saline and stained with Delafield's haematoxylin for 5 minutes, prior to rinsing under running water for 10 minutes. Sections were dehydrated using a series of ascending ethanol dilutions, and subsequently stained using eosin for 1 minute, before clearing in HistoClear and mounting in Depex.

Collagen was examined using a picro-sirius red stain. Picro-sirius red stains fibrotic areas red and Fast Blue stains healthy tissue yellow (Williams et al., 1999). Sections were fixed (as above), rinsed in distilled water and stained using Fast Blue (prepared in magnesium borate buffer). Subsequently, sections were placed in saturated picric acid for 5 minutes prior to staining with 0.1% (w/v) picro-sirius red for 10 minutes. Sections were rinsed in picric alcohol, dehydrated, cleared and mounted (as above).

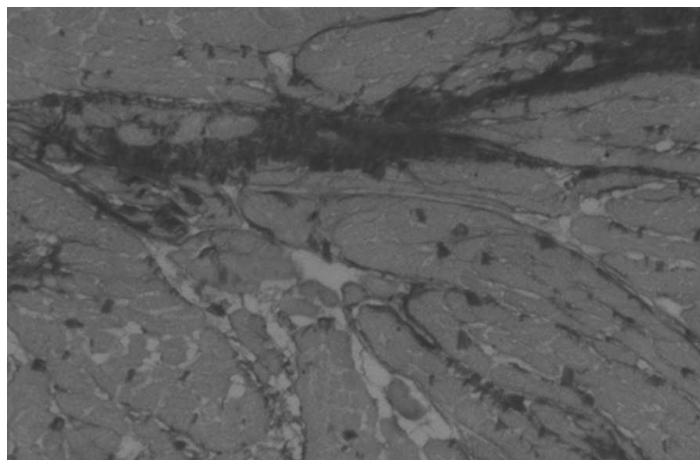
Fifteen fields per section were selected and captured using a light microscope (Leica labor lux5, Leica Microsystems, Milton Keynes, UK) and colour camera (CoolSNAP-Pro, Meyer Instruments, Inc, Texas, UK). Myocardial collagen content was quantified by a blinded observer using ImageJ software. Images were initially converted to an 8-bit black and white image, where collagen appeared black. The

black regions were detected and analysed by adjusting the threshold to ensure only collagen areas were included (Figure 5.2). The collagen amount was expressed as a percentage of the total area examined.

Step 1



Step 2



Step 3

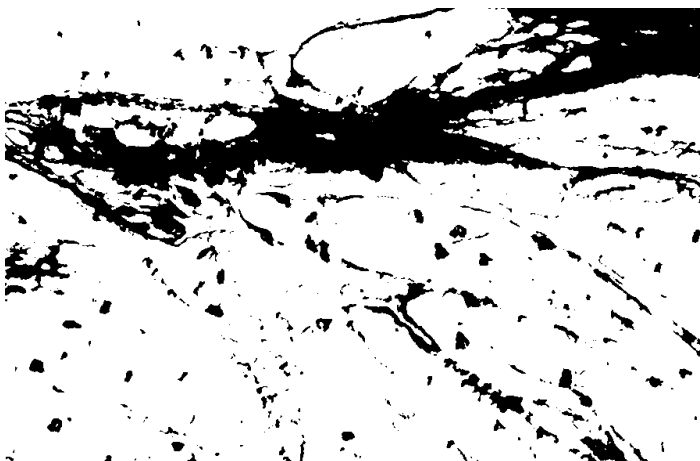


Figure 5.2: Sequence of collagen quantification. Picro-sirius red staining of collagen in ventricular sections (Magnification  $\times 6.3$ )

(Images were converted to an 8-bit black and white image and black regions quantified using ImageJ software)

## 5.3 Results

### 5.3.1 *In Vivo* Cardiac Function

Table 5.1 shows the *in vivo* cardiac function in uraemic and control animals (in the absence and presence of EPO treatment). The ventricular systolic pressures were significantly elevated in uraemic hearts. Heart rate was unchanged and thus cardiac RPP higher in uraemic animals (Table 5.1). Furthermore, in control animals, EPO treatment resulted in a rise in ventricular systolic pressure relative to untreated control hearts, an effect not seen in uraemic hearts.

$dP/dt_{\max}$  and  $dP/dt_{\min}$  (Figure 5.3) were markedly higher in uraemic groups compared with controls. Chronic EPO treatment had no impact on contractility in control or uraemic hearts.

Table 5.1: *In vivo* cardiac function at 12 weeks post-induction of uraemia

		Max Pressure (mmHg)	EDP (mmHg)	LVDP (mmHg)	RPP $\times 10^3$ (mmHg.min <sup>-1</sup> )	Systolic Duration (s)	Diastolic Duration (s)
Control (n=7)	- EPO	121 $\pm$ 5	12 $\pm$ 1	110 $\pm$ 5	35 $\pm$ 2	0.09 $\pm$ 0.001	0.10 $\pm$ 0.01
Uraemic (n=6)	- EPO	158 $\pm$ 6*	13 $\pm$ 2	145 $\pm$ 6*	49 $\pm$ 4*	0.09 $\pm$ 0.003	0.10 $\pm$ 0.01
Control (n=7)	+ EPO	135 $\pm$ 3 <sup>†</sup>	13 $\pm$ 1	122 $\pm$ 3 <sup>†</sup>	40 $\pm$ 2	0.09 $\pm$ 0.001	0.10 $\pm$ 0.01
Uraemic (n=7)	+ EPO	154 $\pm$ 6*	11 $\pm$ 1	143 $\pm$ 6*	48 $\pm$ 3	0.09 $\pm$ 0.002	0.09 $\pm$ 0.01

\* $p < 0.05$  vs. respective control<sup>†</sup>  $p < 0.05$  vs. untreated control

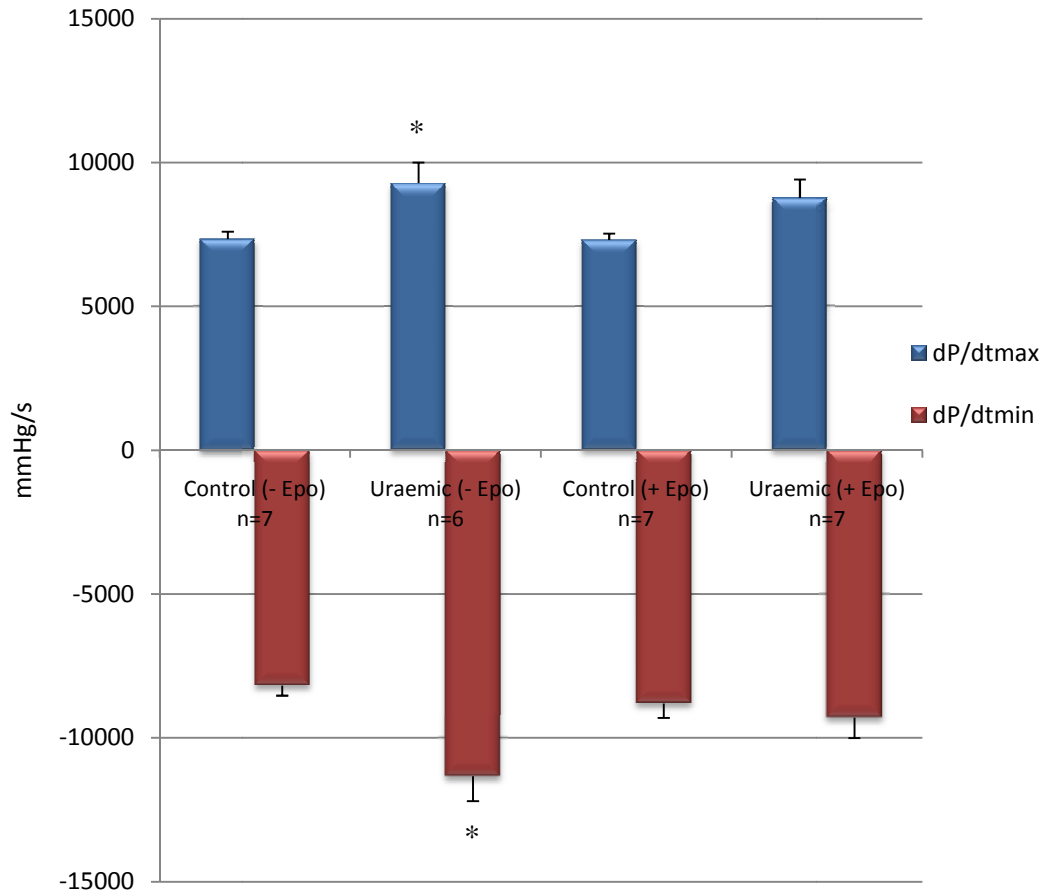


Figure 5.3: *In vivo* cardiac contractility at 12 weeks post-induction of uraemia (\* $p < 0.05$  vs. respective control)

### 5.3.2 Cardiac Fibrosis

Figure 5.4 shows sections stained with picro-sirius red from the 4 groups of hearts. The area of fibrosis was quantified (fibrotic area expressed as a percentage of the total area) and results are given in Figure 5.5. Untreated and EPO treated uraemic hearts exhibited increased fibrosis compared with controls. Chronic EPO administration did not affect the quantity of fibrosis in either control or uraemic hearts.

The types of fibrosis observed in uraemic hearts are provided in Figure 5.6. Reparative, reactive perivascular (fibrosis around vessels), and reactive interstitial fibrosis were observed in uraemic sections. Fibrosis in uraemic hearts appeared to be predominantly reparative in nature, whereas in control animals, no reparative fibrosis was observed.

Cardiac sections were also stained with haematoxylin and eosin, which revealed little structural change between control and uraemic hearts (Figure 5.7).

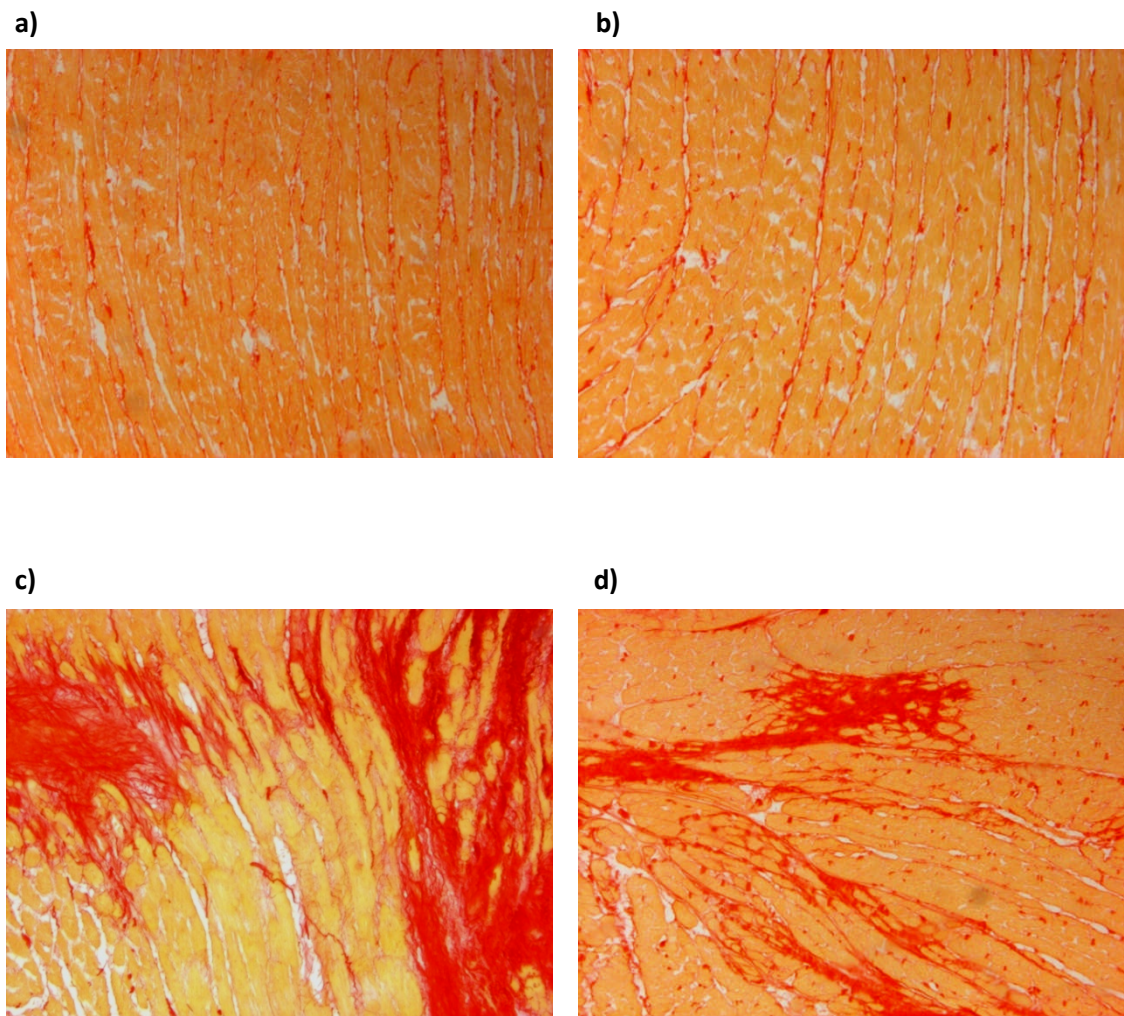


Figure 5.4: Cardiac tissue stained using picro-sirius red from a) control hearts (n=6), b) EPO treated control hearts (n=8), (c) uraemic hearts (n=6), (d) EPO treated uraemic hearts (n=7) Magnification  $\times 6.3$

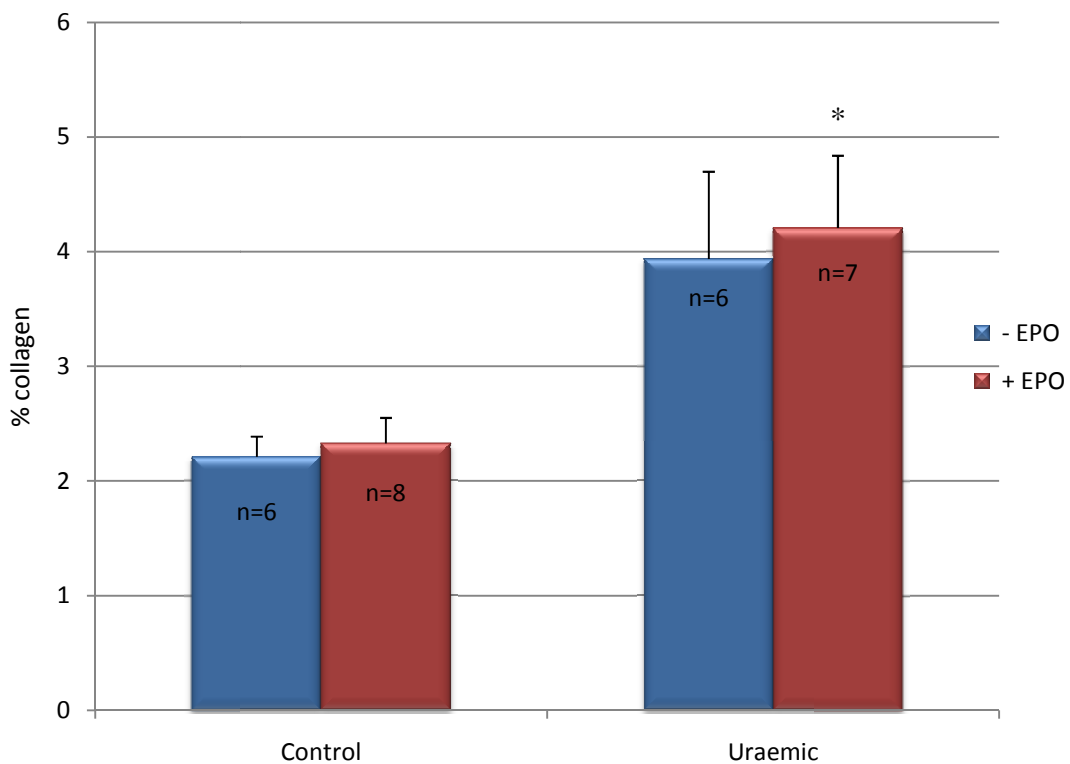
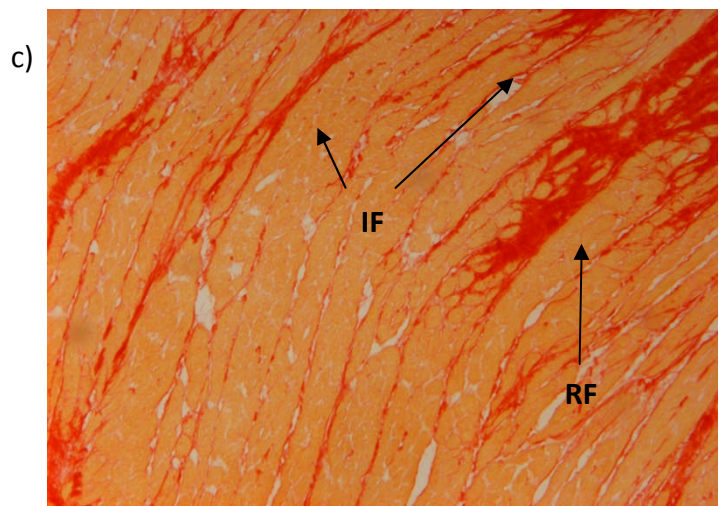
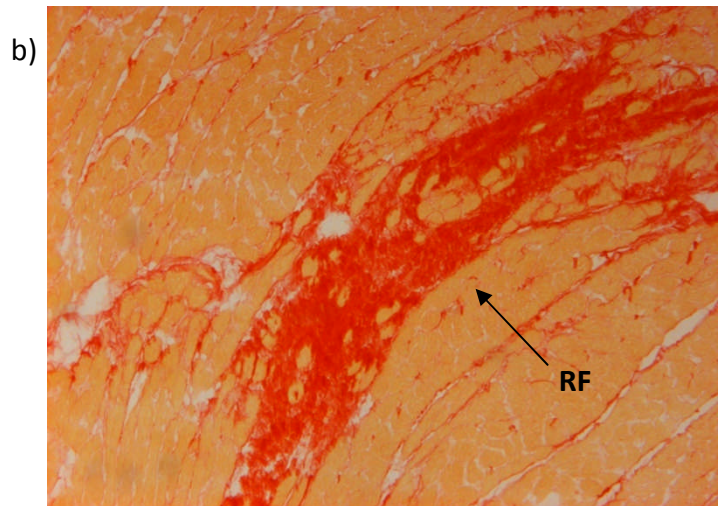
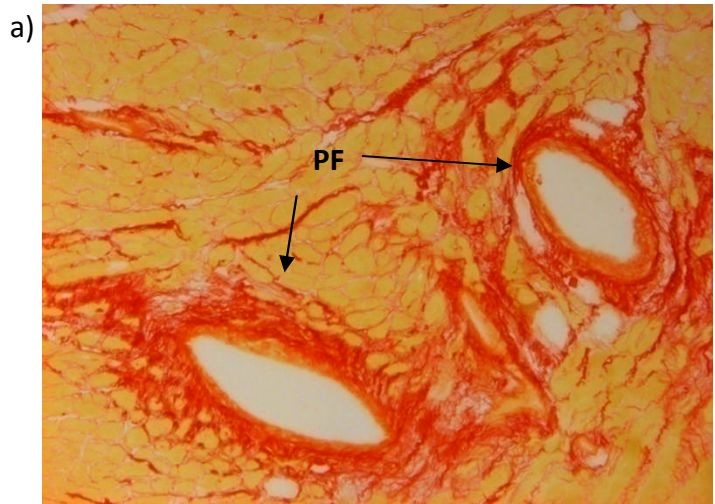


Figure 5.5: Quantification of cardiac fibrosis at 12 weeks uraemia  
(Figures indicate the area of fibrosis expressed as a percentage of the total area)

\* $p < 0.05$  vs. respective control

Figure 5.6: Sections from  
uraemic hearts showing  
types of fibrosis  
Magnification  $\times 6.3$

PF perivascular fibrosis;  
RF reparative fibrosis; IF  
interstitial reactive fibrosis



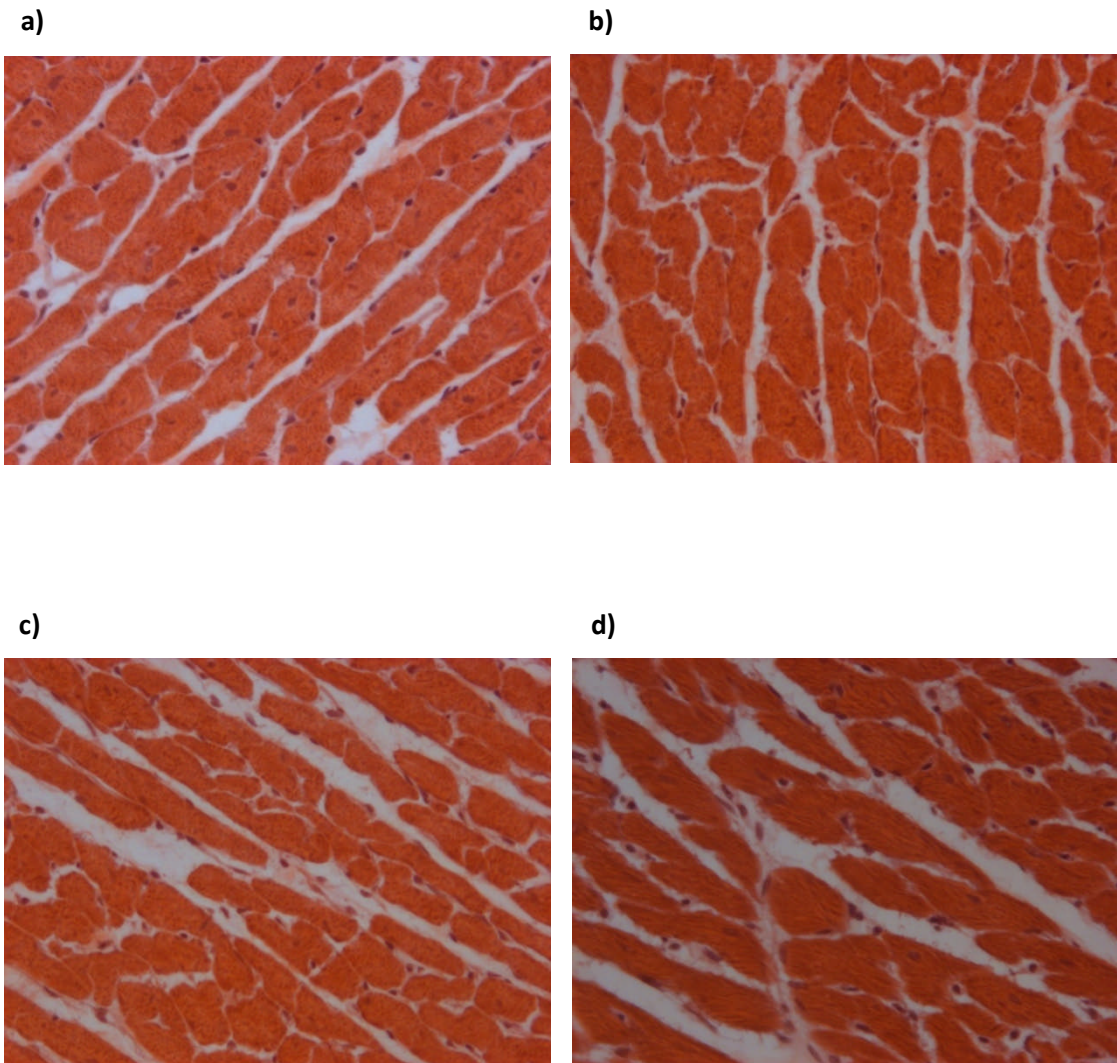


Figure 5.7: Cardiac tissue stained using Haematoxylin and Eosin from a) control hearts (n=6), (b) EPO treated control hearts (n=8), (c) uraemic hearts (n=6), (d) EPO treated uraemic hearts (n=7)

Magnification ×25

## 5.4 Discussion

Uraemic hearts were characterised by increased fibrosis, which was unaffected by EPO administration. *In vivo* assessment of cardiac function revealed a degree of hyperfunction in uraemic animals, consistent with the compensatory phase of LVH. These *in vivo* functional measurements parallel those observed in the *in vitro* assessment in the perfused uraemic heart (Section 4.3.2).

### 5.4.1 *In Vivo* Cardiac Function

At 12 weeks, untreated and EPO treated uraemic animals had significantly elevated LVDP and RPP. This is consistent with the hyperfunction observed in isolated perfused hearts (Chapter 4) and is indicative of a compensatory phase of LVH. In another study, assessment of *in vivo* cardiac function using a pressure-volume Millar catheter, revealed improved systolic function in uraemic mice at 4, 6 and 8 weeks post-induction of uraemia (Kennedy et al., 2008). However, active and passive relaxation times were prolonged in uraemic animals, highlighting diastolic dysfunction (Kennedy et al., 2008). Other studies have observed impaired *in vitro* cardiac function from 4 weeks uraemia (Raine et al., 1993). However, differing severities of uraemia may impact on the observed cardiac phenotypic changes, which may account for the difference in functional results obtained between experimental studies. In CKD patients, cardiac dysfunction is also observed at early

stages of uraemia (Pehrsson et al., 1984). However it is difficult to compare the results obtained in this study to those observed in the clinical setting, due to confounding coexisting conditions such as diabetes.

EPO treatment had no significant impact on *in vivo* cardiac function in uraemia. In controls, EPO increased LVDP and cardiac contractility, in keeping with the observed increase in blood pressure (Section 3.3.2). In this study, dysfunction was not evident in uraemic hearts, therefore the protective role of EPO (in terms of cardiac function) during uraemia could not be established. In non-uraemic models of cardiac dysfunction, the role of EPO as a cardioprotectant has been confirmed (Moon et al., 2005, Moon et al., 2003a, Shi et al., 2004, Wright et al., 2004). Administration of EPO improved ejection fraction, ameliorated apoptosis and reduced ventricular dysfunction after induction of MI in rats (Bullard and Yellon, 2005, Parsa et al., 2003). Interestingly, van der Meer *et al.* (2004) showed that EPO treatment improved cardiac function in a rat model of post-MI heart failure even when administered 3 weeks after coronary artery ligation. In support of these findings, Li *et al* (2006) demonstrated that EPO treatment starting 6 weeks after induction of MI, reduced fibrosis and improved cardiac function in a murine model of chronic post-MI heart failure.

### 5.4.2 Cardiac Fibrosis

Uraemic animals exhibited increased cardiac fibrosis compared with controls, consistent with findings from other experimental studies of CKD, hypertension and LVH (Mall et al., 1988, Zhai et al., 2008, Siedlecki et al., 2009, Varnava et al., 2000). Cardiac fibrosis decreases ventricular compliance and impairs ventricular relaxation. Indeed, left ventricular diastolic dysfunction is highly prevalent in haemodialysis patients and can be detected in early stage CKD patients (Otsuka et al., 2009). Interestingly, cardiac fibrosis in this study was not associated with impaired function. Other experimental studies have shown that cardiac fibrosis was associated with impaired relaxation and diastolic dysfunction despite preserved LVDP and contractility (Merx et al., 2005). Using a pressure-volume catheter to measure end-systolic and end-diastolic volume would have provided a more comprehensive method for evaluating diastolic function and relaxation (Stekelenburg-de Vos et al., 2005).

In addition to the deleterious effects of fibrosis on relaxation and ventricular compliance, collagen has high electrical resistance. Deposition of collagen around myocytes may thus cause a delay in the dissipation of the action potential, resulting in ventricular arrhythmias (Saito et al., 2007). The deposition of collagen fibres between capillaries and myocytes also leads to an increase in the oxygen diffusion distance and contributes to oxygen starvation, enhancing the susceptibility of the

uraemic heart to ischaemic injury (Dikow et al., 2004). In support of this, clinical studies show that CKD patients have an increased risk of death following an acute myocardial infarction, which correlates to the degree of renal dysfunction (Shlipak et al., 2002, Wright et al., 2002).

Myocardial fibrosis can be divided into two main types, reparative and reactive. In this study, both types of fibrosis were observed, with the majority predominantly reparative in nature (Figure 5.6). In the uraemic heart, the increase in reparative fibrosis may be to replace necrotic cells. Indeed, increased myocyte 'drop-out' has been found in experimental uraemia most likely as a result of apoptosis or necrosis (Amann et al., 2003). As uraemia progresses, it is feasible that interstitial collagen increased accompanied by increased cross-linking forming a dense mesh of collagen fibres contributing to impaired diastolic dysfunction.

In addition to experimental models, cardiac fibrosis has been observed in CKD patients using the late gadolinium enhancement (LGE) method (Mark et al., 2006). Gadolinium is an extra-cellular fluid tracer compound that can be detected using magnetic resonance imaging; with expansion of ECM, gadolinium concentration increases demonstrating myocardial fibrosis (Moon et al., 2003b). In addition, cardiac fibrosis has also been confirmed in CKD patients at post-mortem (Mall et al., 1990).

The development of fibrosis during CKD is complex and incompletely understood. Chronic overload, either by pressure or volume, may play a pivotal role. Interestingly, in uraemic patients, cardiac fibrosis was significantly more pronounced than in patients with diabetes or primary hypertension (Mall et al., 1990). Furthermore, experimental studies have also shown that myocardial fibrosis occurring during CKD is partly independent of blood pressure and LVH, suggesting a specific pathophysiological cardiac alteration to uraemic cardiomyopathy (Mall et al., 1990, Amann et al., 1998b).

Transforming growth factor- $\beta$  (TGF $\beta$ ) is a pleiotropic cytokine which can act as a growth factor in the development of LVH and fibrosis (Koleganova et al., 2009a). TGF $\beta$  promotes expression of ECM genes and also inhibits expression of ECM degrading genes (Li et al., 2009a, Roberts et al., 1992). Transgenic mice over-expressing TGF $\beta$  had significantly increased cardiac interstitial fibrosis compared with wild-type animals (Rosenkranz et al., 2002). Furthermore, in mice subjected to transverse aortic constriction, a time dependent increase in TGF $\beta$  was observed from 4 weeks post-surgery, correlating with the progressive rise in cardiac fibrosis (Li et al., 2009a). TGF $\beta$  signalling is modulated by a class of proteins known as Smads. Smad7 has an inhibitory effect on TGF $\beta$  signalling. Interestingly, a reduction in Smad7 within the heart exacerbates fibrosis following myocardial infarction. Furthermore, over-expression of Smad7 results in diminished collagen I and III expression (Wang et al., 2002).

CKD is associated with raised levels of angiotensin II which, in addition to its effect on hypertension, has direct cellular actions including promoting cardiac fibrosis *via* activation of TGF $\beta$  (Rosenkranz et al., 2002). Administration of ACE inhibitors and ARBs reduce cardiac fibrosis in experimental uraemia and in CKD patients (Tachikawa et al., 2003, Kurosawa et al., 2002). Interestingly, a sub-antihypertensive dose of the ACE inhibitor, enalapril, improved fibrosis in the SHR heart, highlighting a blood pressure independent effect of angiotensin II (Piotrkowski et al., 2009). Furthermore, Angiotensin [1-7], known to counteract the effects of angiotensin II, reduced TGF $\beta$  expression and cardiac interstitial fibrosis in the 5/6 nephrectomised mouse (Li et al., 2009b). Experimental studies have shown angiotensin II- mediated up-regulation of TGF $\beta$  to involve the ERK 1/2 pathway (Gao et al., 2009). Indeed, treating isolated cardiac fibroblasts with the ERK inhibitor, PD98059, blocked the angiotensin II induced increase in TGF $\beta$  and reduced collagen I expression (Gao et al., 2009). In the mammalian myocardium, two angiotensin II receptors exist, AT1 and AT2 (Unger et al., 1996). The AT1 receptor is involved in the development of fibrosis and inflammation whereas AT2 activation results in apoptosis. Gao *et al.* (2009) showed that AT1 blockade prevented the angiotensin II induced increase in TGF $\beta$  and collagen I expression in cardiac fibroblasts, whereas AT2 blockade had no effect.

Experimental studies have shown that development of fibrosis is also associated with low vitamin D levels and secondary hyperparathyroidism, which are frequent complications in CKD (Smogorzewski et al., 1993). Subtotally nephrectomised rats

did not develop cardiac fibrosis after removal of the parathyroid gland. Interestingly, administering parathyroid hormone (PTH) to uraemic rats after parathyroidectomy resulted in the development of cardiac fibrosis (Amann et al., 1994). Furthermore, studies in experimental uraemia demonstrated a reduction in PTH when treated with the active vitamin D compound, calcitriol, and this was associated with a reduction in fibrosis (Koleganova et al., 2009b). Calcimimetic agents, which decrease PTH by activating  $\text{Ca}^{2+}$  receptors, also reduced cardiac fibrosis in experimental uraemia (Ogata et al., 2003). In parallel with these observations, clinical studies have demonstrated improved survival in CKD patients following administration of the active vitamin D analogue paricalcitol (Teng et al., 2003). However, in contrast, Repo *et al.* (2007) showed that lowering of PTH with paricalcitol not only did not prevent cardiac fibrosis but actually worsened it in uraemic hearts (Repo et al., 2007). Thus, the situation remains unclear.

#### **5.4.2.1 The Impact of EPO on Cardiac Fibrosis**

In this study, EPO treatment had little effect on cardiac fibrosis in uraemia. However, in experimental models of post- MI heart failure, EPO treatment reduced interstitial fibrosis in non-infarcted regions and decreased collagen I and III mRNA expression, which was associated with decreased expression of TGF $\beta$  (Nishiya et al., 2006, Li et al., 2006). In an experimental model of diabetic kidney damage (db/db mouse), TGF $\beta$  expression was reduced when mice were treated with a continuous

EPO receptor activator (CERA) (Shushakova et al., 2009). Furthermore, in cultured neonatal rat cardiomyocytes, EPO treatment attenuated the rise in TGF $\beta$  in angiotensin II-induced hypertrophy (Wen et al., 2009).

EPO administration is associated with increased Stat 3 activation within the myocardium (Li et al., 2006). Mice with cardiomyocyte specific Stat 3 deletion exhibit significantly greater cardiac fibrosis (Jacoby et al., 2003). It is therefore feasible that EPO mediated Stat 3 activation contributes to a reduction in cardiac fibrosis observed in some animal models. Indeed, in an experimental model of iron deficiency anaemia, the fibrosis observed at 20 weeks was accompanied by decreased EPO levels and significantly reduced Stat 3 phosphorylation (Naito et al., 2009). In contrast, Chan *et al.* (2007) showed that EPO prevents collagen degradation *via* reduction in MMP expression leading to improved function post ischaemia/ reperfusion by preserving the structural integrity of the myocardium (Chan et al., 2007).

#### **5.4.3 Conclusion**

At 12 weeks, uraemic animals exhibit LVH, cardiac fibrosis and preserved cardiac function. As uraemia progresses further, it is feasible that a pathophysiological phenotype will ensue, including accelerated interstitial fibrosis alongside a

reduction in capillary density thereby contributing to decompensation and heart failure.

## **Chapter 6: Mitochondrial Function and Protein Expression**

## 6.1 Introduction

The uraemic heart is characterised by a depleted energy reserve (Ogimoto et al., 2003, Raine et al., 1993) and metabolic remodelling (chapter 4), which contribute to heart failure (Ingwall and Weiss, 2004). Mitochondria are pivotal in providing the heart with energy, in the form of ATP. Furthermore, mitochondria play a key role in the initiation of apoptosis, *via* the intrinsic pathway and release of cytochrome *c* (section 1.6.2.1), thereby controlling a tight balance between life (i.e. energy production) and cell death (Gustafsson and Gottlieb, 2008).

### 6.1.1 Electron Transport Chain (ETC)

Acetyl-CoA, a product of pyruvate oxidation and  $\beta$ -oxidation, enters the TCA cycle generating NADH and FADH<sub>2</sub>, which, in a series of oxidation-reduction reactions, transfer electrons (e<sup>-</sup>) through a chain of inner mitochondrial membrane enzyme complexes known as the ETC (Figure 6.1). NADH and FADH<sub>2</sub> donate electrons to complex I (NADH dehydrogenase) and complex II (succinate dehydrogenase) of the ETC respectively. Electrons are then carried to complex III (cytochrome bc<sub>1</sub> complex) using the mobile electron transporter coenzyme Q (or ubiquinone), and then to complex IV (cytochrome *c* oxidase) using a second mobile electron carrier, cytochrome *c* (Lesnefsky et al., 2001). At complex IV, 2 electrons, along with 2 hydrogen ions combine with the final electron acceptor, oxygen, forming water.

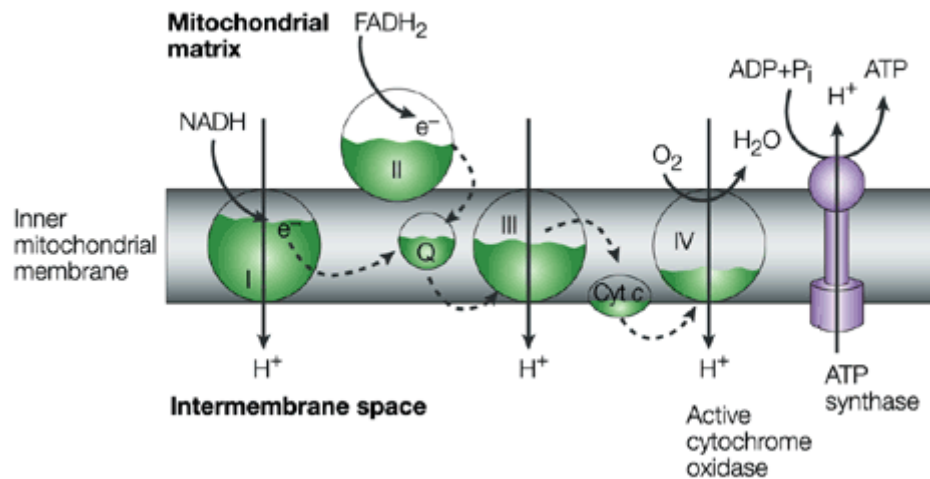


Figure 6.1: Schematic representation of the electron transport chain (ETC)

(NADH, nicotinamideadenine dinucleotide (reduced); FADH<sub>2</sub>, flavin-adenine dinucleotide (reduced); Q, coenzyme Q; Cyt c, cytochrome c)

(adapted from Moncada and Erusalimsky, 2002)

At complex I, III and IV of the ETC, the transfer of electrons is coupled with the movement of hydrogen ions (H<sup>+</sup>) or protons, from the matrix side to the cytosolic side of the inner mitochondrial membrane (Figure 6.1). The energy potential from the proton gradient, known as the protonmotive force ( $\Delta p$ ) is used by ATP synthase (F<sub>1</sub>F<sub>0</sub> ATP synthase) to drive ATP synthesis from ADP and inorganic phosphate (Pi), coupled to proton flux toward the mitochondrial matrix. Chemiosmotic theory is essential to explain the coupling between ETC and ATP synthesis (Equation 7) (Mitchell, 1961).

$$\Delta p = \Delta\varphi - 2.3 \left( \frac{RT}{F} \right) \Delta pH$$

Equation 7: Protonmotive Force (Mitchell, 1961)

( $\Delta\varphi$  membrane potential; R gas constant; T absolute temperature; F Faradays constant)

### 6.1.2 Reactive Oxygen Species (ROS) Production

ROS are free radicals with an unpaired electron in their outermost shell. They are highly reactive and damaging to DNA, lipids and proteins. The primary source of ROS formation is the mitochondrial ETC as a result of electron leakage, predominantly from complex I and complex III (Ambrosio et al., 1993). The major mitochondrial-produced ROS is the superoxide anion ( $O_2^{\cdot-}$ ), formed by the partial reduction of oxygen. Under normal conditions, up to 1-5% of consumed oxygen forms superoxide, which can be scavenged by a number of enzymes, including manganese superoxide dismutase (MnSOD), which converts superoxide to hydrogen peroxide ( $H_2O_2$ ) and then to water (Giulivi et al., 1995).

Uncoupled or impaired mitochondrial function and altered ETC complex activities increase the production of ROS, exceeding the antioxidant defence capacity. Mitochondria are producers of, and targets of, ROS-induced damage. ROS can initiate apoptosis by mediating the opening of non-specific mitochondrial

membrane pores, including MPTP (Section 1.6.2.1), thereby collapsing the membrane potential, resulting in further ROS formation from the ETC (Kowaltowski et al., 2001). This positive feedback mechanism is known as ROS-induced ROS-release (RIRR) (Zorov et al., 2000) (Figure 6.2).

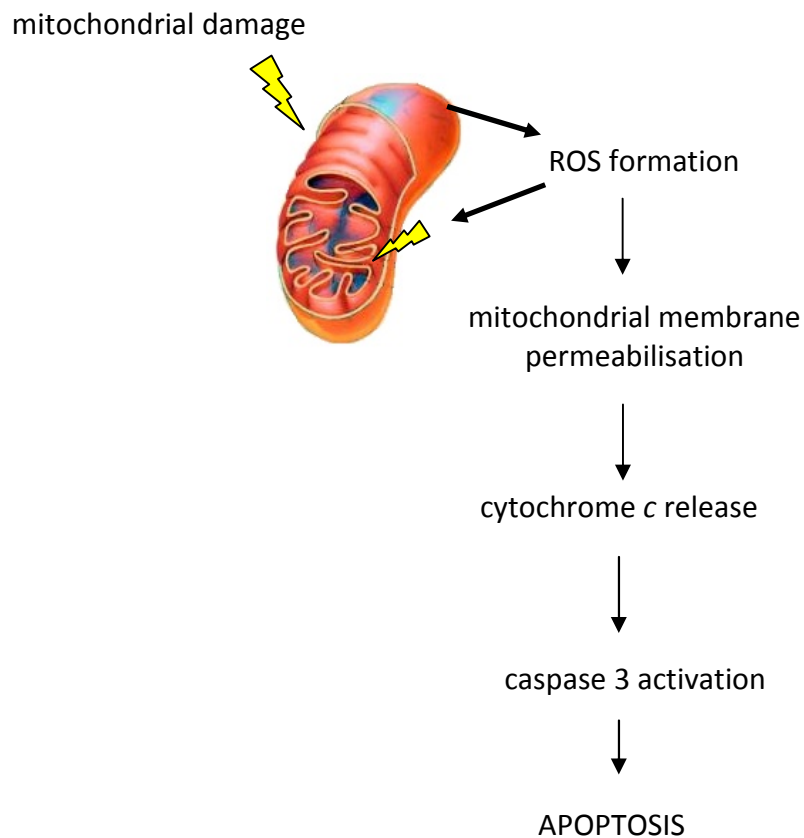


Figure 6.2: Mitochondrial ROS generation and induction of apoptosis

### 6.1.3 Mitochondrial Function in Uraemia

Few studies have investigated cardiac mitochondrial function in uraemia. Using a genomic approach, Granata *et al.* (2009) observed alterations in a number of genes involved in mitochondrial respiration in CKD patients compared with healthy controls. Furthermore, alterations in the expression of genes encoding mitochondrial ETC proteins have been observed in the spontaneously hypertensive rat (SHR) heart (Piotrkowski *et al.*, 2009). Mitochondrial function has also been examined in models of LVH and heart failure. As LVH is present in up to 75% of haemodialysis patients, parallels could be drawn from these studies on the hypertrophied heart (Foley *et al.*, 1995). Experimental hypertrophic cardiomyopathy (HCM) was associated with a decrease in state 3 respiration along with reductions in complex I and IV activities (Lucas *et al.*, 2003). Interestingly, studies on the failing heart have shown both unchanged (Rennison *et al.* 2009) and decreased (Rosca *et al.*, 2009) mitochondrial function. Heather *et al.* (2009) observed reduced mitochondrial respiration rates in the failing heart only when the ejection fraction was markedly reduced ( $\leq 45\%$ ), whereas in hearts exhibiting mild functional impairment, mitochondrial function was preserved.

Alterations in myocardial mitochondrial function during uraemia may compromise ATP production and increase ROS formation leading to apoptotic cell death. In support of this, enhanced ROS generation has been observed in patients with CKD and haemodialysis patients (Dounousi *et al.*, 2006, Granata *et al.*, 2009, Morena *et al.*, 2005). Furthermore, cardiomyocyte apoptosis was exacerbated in rats following

5/6 nephrectomy (Rodriguez-Ayala et al., 2006). Importantly, in addition to reduced mitochondrial respiration and ROS formation, ATP synthesis may also be compromised by altered expression of key proteins involved in substrate metabolism. PPAR $\alpha$  is the primary transcription factor responsible for the regulation of fatty acid metabolism, controlling the expression of proteins including MCAD and CD36. Down-regulation of these proteins may be responsible for the decrease in fatty acid oxidation observed during uraemia, and thus contribute to energy starvation.

#### **6.1.4 Objectives**

In this chapter, the combined impact of uraemia and chronic EPO administration on *in vitro* mitochondrial function was assessed. Specific aims were

- To determine the impact of uraemia and chronic EPO treatment on cellular respiration in isolated cardiac mitochondria.
- To examine the expression of PPAR $\alpha$  and CD36 proteins in untreated and EPO treated control and uraemic ventricular tissue

## 6.2 Methods

### 6.2.1 Mitochondrial Respiration

Uraemia was induced surgically in male Sprague-Dawley rats via a one-stage 5/6<sup>th</sup> nephrectomy (section 2.2.1). Animals were divided into 4 experimental groups

- Control animals + saline (- EPO)
- Uraemic animals + saline (- EPO)
- Control animals + EPO
- Uraemic animals + EPO

EPO was administered twice a week for 2 weeks prior to experiments at a dose of 30 µg/Kg (section 3.3.2).

Cardiac mitochondria were isolated from the 4 groups of rats at 9 and 12 weeks post-induction of uraemia, and ADP-stimulated respiration determined using a Clark-type electrode, as described in Section 2.2.7.

A Clark-type electrode consists of a silver anode and platinum cathode connected *via* an electrolyte solution (KCl). The sample chamber is separated from the electrode compartment by a Teflon membrane, which prevents the electrolyte solution mixing with the sample (Figure 6.3). When a constant polarising voltage (0.6 V) is held between the two electrodes, the platinum electrode becomes

negative relative to the silver electrode. Oxygen diffuses through the membrane from the sample chamber and is reduced to water at the cathode. The reduction of oxygen generates a current which is directly proportional to the oxygen concentration. The current can then be amplified and converted to a digital signal for analysis (Robinson, 2001).

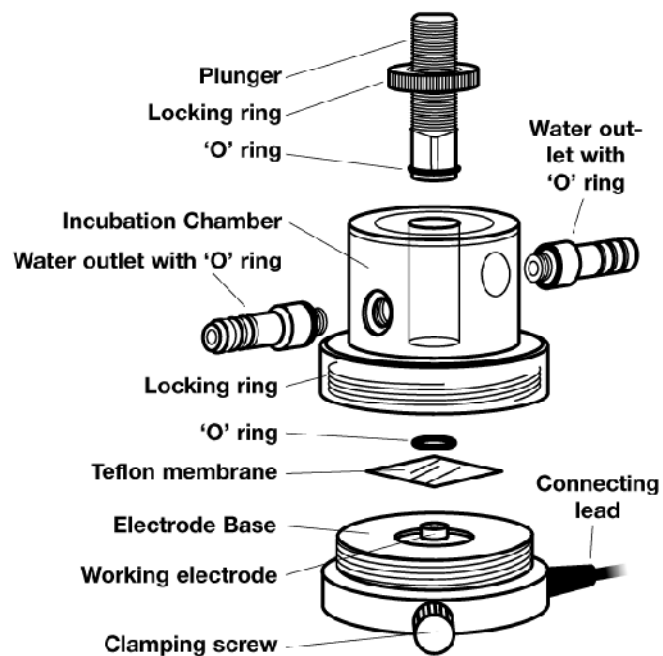


Figure 6.3: Clark- type electrode

(from Rank Brothers manual [www.rankbrothers.co.uk/download/digioxy.pdf](http://www.rankbrothers.co.uk/download/digioxy.pdf))

Oxygen consumption of mitochondrial preparations (0.4 mg protein/ ml), was determined in the presence of the following substrates

- glutamate (5 mM) and malate (1 mM) (Complex I)
- palmitoyl carnitine (20  $\mu$ M) and malate (2 mM)
- succinate (5 mM) and rotenone (1  $\mu$ M) (Complex II)

ADP (0.2 mM) was added to stimulate state 3 respiration. State 4 respiration was monitored after exhaustion of ADP.

### **6.2.2 Protein Expression**

PAGE (PolyAcrylamide Gel Electrophoresis), using a 3% stacking gel and 10% running gel, and western blotting, was used to determine protein expression of PPAR $\alpha$ , CD36 and Actin (as a control), in 12 week untreated and EPO treated control and uraemic ventricular tissue (section 2.2.8). The optimum antibody dilutions and suppliers are given in Table 2.3.

I would like to thank Mrs Kathleen Bulmer for her assistance with the Western Blotting

## 6.3 Results

### 6.3.1 Mitochondrial Respiration

Mitochondria were isolated from 9 and 12 week untreated and EPO treated control and uraemic hearts. At both stages of uraemia, the mitochondrial protein yield was comparable between all 4 groups, suggesting that the mitochondrial content was not altered by 9 or 12 weeks uraemia (Table 6.1).

At 9 weeks uraemia, mitochondrial respiration rates were determined in the presence of complex I substrates, glutamate and malate (representative traces given in Figure 6.4) and complex II substrates, succinate and rotenone.

To confirm state 3 (ADP-stimulated) respiration in the presence of glutamate and malate, rotenone (a specific complex I inhibitor) was added which significantly reduced oxygen consumption (Figure 6.5). When rotenone was added in the presence of succinate, respiration was not inhibited as succinate drives the electron transport chain through complex II, by-passing complex I.

Table 6.1: Myocardial mitochondrial protein yields at 12 weeks uraemia

	Protein concentration mg/ml	
	Control (n=4)	Uraemic (n=4/5)
- EPO	5.63 ±0.69	4.65 ±0.44
+ EPO	5.11 ±0.27	5.04 ±0.74

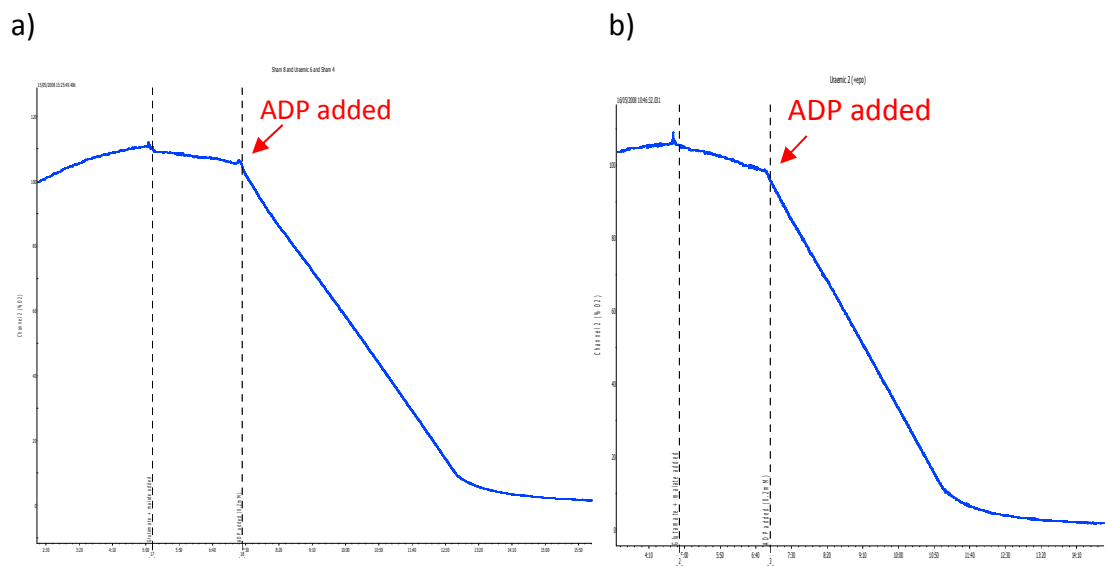


Figure 6.4: Myocardial mitochondrial respiration using complex I substrates

Representative traces from a) untreated uraemic hearts and b) EPO treated uraemic hearts

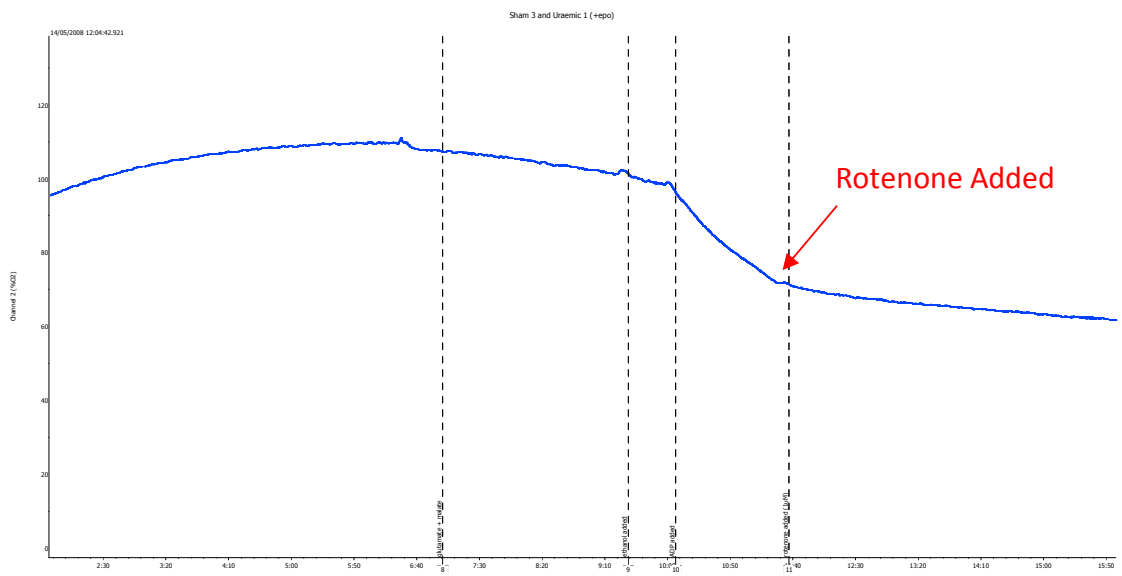


Figure 6.5: State 3 respiration in the presence of rotenone

After 9 weeks uraemia, the rates of state 3 and 4 respiration was comparable between all 4 groups in the presence of complex I and complex II substrates (Table 6.2 a and b). Similarly, the ADP:O ratio was similar in all groups.

Table 6.2: Mitochondrial respiration at 9 weeks post-induction of uraemia

a) Complex I substrates (glutamate and malate)

		<b>State 3 Respiration</b> (nmol /min/ mg protein)	<b>State 4 Respiration</b> (nmol /min/ mg protein)	<b>Respiratory Control Index (RCI)</b>	<b>ADP:O</b>
<b>Control (n=2)</b>	- EPO	170.2 ±40.4	32.8 ±18.4	7.2 ±3.1	0.50 ±0.03
<b>Uraemic (n=2)</b>	- EPO	140.3 ±38.1	24.9 ±17.6	9.2 ±5.0	0.47 ±0.02
<b>Control (n=2)</b>	+ EPO	204.6 ±22.0	39.6 ±7.7	5.3 ±0.5	0.53 ±0.03
<b>Uraemic (n=2)</b>	+ EPO	194.3 ±44.6	50.5 ±15.3	3.9 ±0.3	0.53 ±0.01

b) Complex II substrates (succinate + rotenone)

		<b>State 3 Respiration</b> (nmol /min/ mg protein)	<b>State 4 Respiration</b> (nmol /min/ mg protein)	<b>Respiratory Control Index (RCI)</b>	<b>ADP:O</b>
<b>Control (n=2)</b>	- EPO	187.1 ±7.1	26.2 ±16.8	12.4 ±8.2	0.54 ±0.02
<b>Uraemic (n=2)</b>	- EPO	149.2 ±20.4	23.4 ±15.0	9.9 ±5.4	0.52 ±0.05
<b>Control (n=2)</b>	+ EPO	203.1 ±12.2	44.7 ±7.5	4.6 ±0.5	0.54 ±0.04
<b>Uraemic (n=2)</b>	+ EPO	229.1 ±99.3	32.9 ±6.5	6.9 ±2.0	0.54 ±0.02

By 12 weeks uraemia, no differences were observed in the rates of mitochondrial respiration or the ADP:O ratio in all 4 groups (Table 6.3 a, b and c and Figure 6.6)

Table 6.3: Mitochondrial respiration at 12 weeks post-induction of uraemia

a) Complex I substrates (glutamate and malate)

		<b>State 3 Respiration</b> (nmol /min/ mg protein)	<b>State 4 Respiration</b> (nmol /min/ mg protein)	<b>Respiratory Control Index (RCI)</b>	<b>ADP:O</b>
<b>Control (n=3)</b>	- EPO	127.7 ±12.0	25.2 ±1.9	5.9 ±1.1	0.46 ±0.06
<b>Uraemic (n=4)</b>	- EPO	122.5 ±2.7	21.7 ±8.4	15.0 ±6.7	0.46 ±0.02
<b>Control (n=5)</b>	+ EPO	128.2 ±11.1	25.4 ±6.4	7.6 ±2.9	0.48 ±0.01
<b>Uraemic (n=3)</b>	+ EPO	125.7 ±15.0	30.8 ±2.6	4.2 ±0.8	0.48 ±0.04

b) Complex II substrates (succinate + rotenone)

		<b>State 3 Respiration</b> (nmol /min/ mg protein)	<b>State 4 Respiration</b> (nmol /min/ mg protein)	<b>Respiratory Control Index (RCI)</b>	<b>ADP:O</b>
<b>Control (n=3)</b>	- EPO	178.6 ±38.4	22.8 ±9.8	13.8 ±7.9	0.50 ±0.02
<b>Uraemic (n=3)</b>	- EPO	191.8 ±21.4	35.4 ±6.5	6.1 ±1.7	0.52 ±0.02
<b>Control (n=5)</b>	+ EPO	154.7 ±22.7	22.2 ±3.1	7.8 ±1.9	0.48 ±0.02
<b>Uraemic (n=3)</b>	+ EPO	111.2 ±2.9	20.0 ±2.9	5.8 ±1.6	0.52 ±0.02

c) Palmitoyl carnitine + malate

		<b>State 3 Respiration</b> (nmol /min/ mg protein)	<b>State 4 Respiration</b> (nmol /min/ mg protein)	<b>Respiratory Control Index (RCI)</b>	<b>ADP:O</b>
<b>Control (n=2)</b>	- EPO	146.7 ±38.1	17.8 ±12.2	14.2 ±5.7	0.50 ±0.02
<b>Uraemic (n=2)</b>	- EPO	104.7 ±7.0	10.4 ±5.0	13.9 ±6.5	0.48 ±0.01
<b>Control (n=1)</b>	+ EPO	111.3	10	12.2	0.46
<b>Uraemic (n=1)</b>	+ EPO	110.6	9.9	11.3	0.46

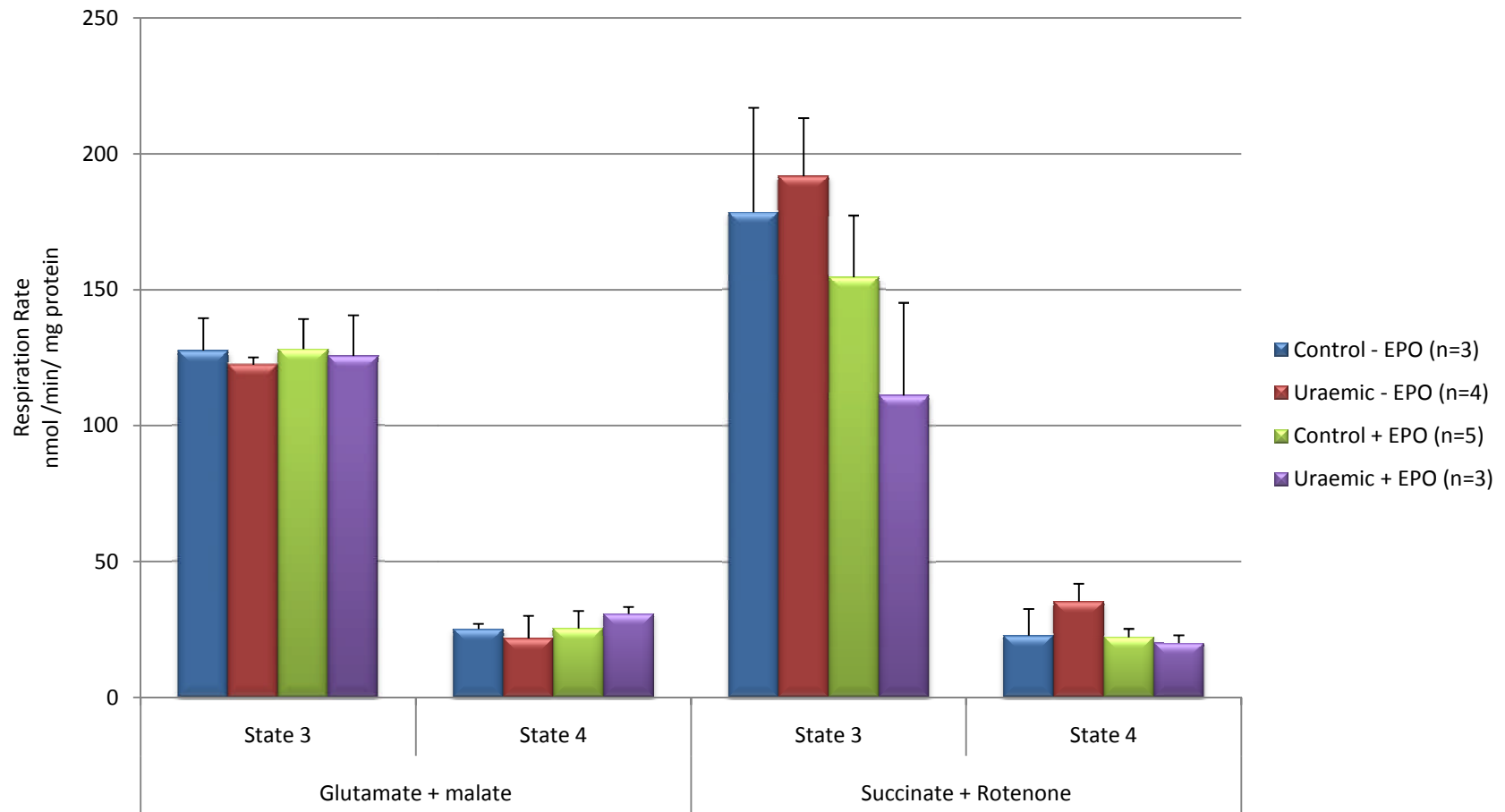


Figure 6.6: Myocardial respiration rates using complex I substrates at 12 weeks uraemia

### **6.3.2 Metabolic Protein Expression**

PPAR $\alpha$  and CD36 protein expression were determined in ventricular tissue and normalised to actin.

At 12 weeks uraemia, PPAR $\alpha$  and CD36 expression did not significantly differ in untreated and EPO treated control and uraemic hearts (Figures 6.7 and 6.8).

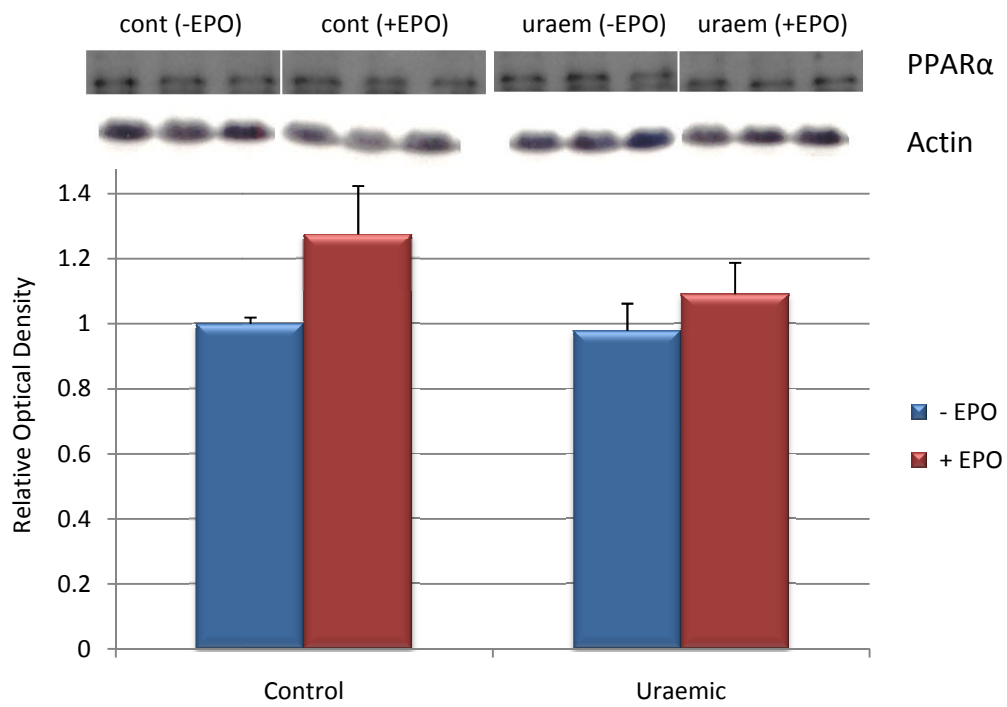


Figure 6.7: Cardiac PPAR $\alpha$  protein expression at 12 weeks uraemia (n=3)

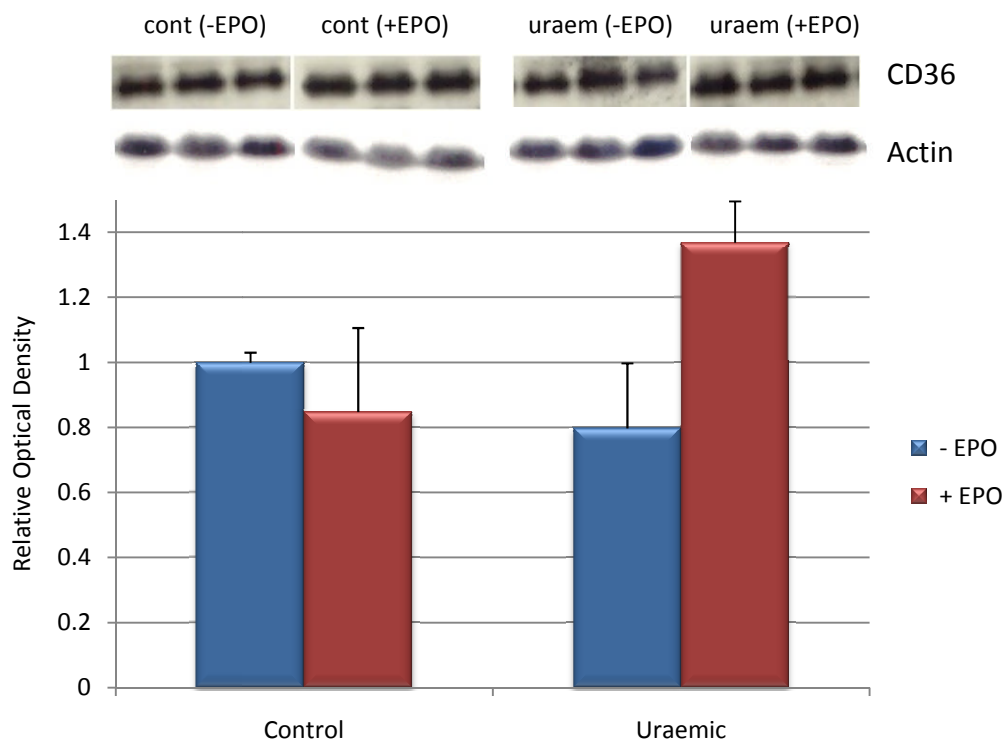


Figure 6.8: Cardiac CD36 protein expression at 12 weeks uraemia (n=3)

## 6.4 Discussion

Mitochondrial respiration rates were similar in control and uraemic hearts at 9 and 12 weeks post-induction of uraemia and were unaffected by chronic EPO treatment. This highlights unchanged efficiency under *in vitro* conditions. These results are consistent with observations from the perfused heart showing unchanged efficiency in uraemic animals. Expression of key proteins controlling fatty acid metabolism were unchanged by uraemia or chronic EPO administration.

### 6.4.1 Mitochondrial Respiration

At 9 and 12 weeks uraemia, myocardial mitochondrial respiration was unaltered in control and uraemic hearts, consistent with a compensatory phase of LVH. Furthermore, uraemia was not associated with a reduction in mitochondrial density as evidenced by unaltered mitochondrial yields and comparable citrate synthase activities (Section 4.3.4). State 3 and state 4 respiration rates, observed here, are comparable with previous studies in cardiac mitochondria (Lucas et al., 2003).

Little work has been undertaken with regards to the impact of experimental uraemia on myocardial mitochondrial respiration. In a recent study, DNA analysis on peripheral blood mononuclear cells revealed differences in 44 genes involved in mitochondrial respiration in CKD patients. Specifically, a 65% reduction in complex IV activity (determined by following the rate of ferrocytochrome *c* oxidation) was

observed in uraemic and haemodialysis patients compared with healthy controls (Granata et al., 2009). Whether these alterations also occur in myocardial mitochondria during CKD has yet to be determined.

Alterations in ETC complex activities and impaired myocardial mitochondrial function during uraemia would lead to elevated ROS production, potentially exceeding the antioxidant capacity of the heart, resulting in oxidative stress. At high levels, ROS initiates necrosis *via* membrane lipid peroxidation; at low levels, ROS can induce apoptosis (Lennon et al., 1991). Indeed, antioxidant therapy effectively reduced apoptosis in cultured cells (Kelso et al., 2001). Furthermore, down-regulation of the antioxidant defence system is associated with increased apoptosis (Fujii et al., 2006).

The exact mechanisms behind ROS-induced apoptosis have not been fully elucidated. ROS initiates the release of cytochrome *c* and caspase 3 activation, possibly *via* modulation of mitochondrial membrane permeability (MPT) (Higuchi et al., 1998). The impact of ROS on MPT has been mainly ascribed to the effects on the MPT pore (MPTP) (Zorov et al., 2000). MPTP is a non-specific mitochondrial membrane pore, which, when open, allows the free movement of ions and solutes (<1500 daltons) into the mitochondria causing swelling and rupture of the outer mitochondrial membrane resulting in release of pro-apoptotic factors including cytochrome *c*. Cytochrome *c* is a potent activator of the caspase cascade, leading to apoptotic cell death. Indeed, blocking MPTP with agents such as cyclosporin A and bongkreic acid prevents apoptosis (Zamzami et al., 1996).

The structure of MPTP remains in debate (Grimm and Brdiczka, 2007, Halestrap, 2009). It was originally thought to consist of three principal components, the adenine nucleotide translocator (ANT), the voltage-dependent anion channel (VDAC), and cyclophilin D (CycD). However, using knockout animal models, it has recently been shown that ANT is more likely a regulatory component (Kokoszka et al., 2004). Interestingly, in CycD knockout mice, the loss of membrane potential with H<sub>2</sub>O<sub>2</sub> was abolished, suggesting that CycD may be the site for ROS-induced MPTP opening (Baines et al., 2005).

ROS production is also a characteristic of heart failure, possibly as a result of impaired mitochondrial respiration and/or structural abnormalities (Ide et al., 1999, Ide et al., 2001, Sharov et al., 2000). In experimental heart failure induced by aortic constriction, myocardial mitochondrial respiration was significantly impaired as evidenced by decreased state 3 respiration rates (Bugger et al., 2009). Moreover, reduced complex III and IV activities have been observed in patients with congestive heart failure (Buchwald et al., 1990, Jarreta et al., 2000). In contrast, in the post-MI failing rat heart, mitochondrial respiration rates were not impaired (O'Shea et al., 2009). Furthermore, Wistar rats with heart failure induced by coronary artery ligation, showed no alterations in state 3 respiration when using glutamate or succinate. However, with palmitoyl carnitine as a substrate, state 3 respiration was elevated in mitochondria from failing rat hearts compared with controls (Rennison et al., 2008). Interestingly, this effect was only seen in the subsarcolemmal (SSM) population not in interfibrillar mitochondria (IFM).

Separating the two populations of mitochondria in this study may have unmasked subtle differences in respiratory activities between control and uraemic hearts.

Conflicting results have also been found with regard to mitochondrial function in LVH. In a mouse model of hypertrophic cardiomyopathy (genetically induced by mutating cardiac troponin T), mitochondrial respiration was preserved (Lucas et al., 2003). However, mice with hypertrophic cardiomyopathy induced by the myosin heavy chain gene mutation, demonstrated impaired state 3 respiration compared with wild-type animals (Lucas et al., 2003).

It is feasible that during compensated hypertrophy, mitochondrial function is preserved. With cardiac dysfunction and transition to heart failure, mitochondrial respiration may become compromised. In support of this, Heather *et al.* (2009) observed no differences in state 3 or state 4 respiration rates in failing hearts with an ejection fraction >45%. Interestingly, with severe functional deterioration post-MI (ejection fraction  $\leq$ 45%) mitochondrial function was compromised (Heather et al., 2009). These studies suggest that mitochondrial dysfunction might be a consequence, rather than a cause of impaired cardiac function, which is consistent with the results from this study. With progression of uraemia and deteriorating cardiac function, mitochondrial function may potentially become compromised.

ADP:O ratios were similar in all 4 groups and unchanged at 9 or 12 weeks uraemia, although values were substantially lower than those observed in previous studies (Heather et al., 2009, O'Shea et al., 2009).

The ADP:O ratio is essentially mediated by the coupling of electron transport to ATP synthesis. Uncoupling of oxygen consumption with ATP synthesis frequently increases state 4 respiration, i.e. ADP-independent respiration. State 4 respiration was not raised in this study, suggesting well coupled mitochondria. The addition of uncouplers such as 2,4-Dinitrophenol (2,4-DNP) and carbonyl cyanide-p-trifluoromethoxyphenylhydrazone (FCCP), to the mitochondrial preparation could confirm the degree of uncoupling; well coupled mitochondria would exhibit a rapid burst of oxygen consumption, greater than that observed during state 3 respiration.

Uncouplers prevent the link between electron transfer and ATP synthesis without affecting electron transport itself. Protons are carried across the mitochondrial membrane by uncouplers thus dissipating the proton gradient. The degree of uncoupling within mitochondria can be mediated *via* expression of uncoupling proteins (UCPs). The predominant form of UCP within the heart is UCP3. In transgenic mice over expressing UCP3, state 4 respiration was significantly increased along with markedly higher oxygen consumption in skeletal muscle (Clapham et al., 2000). Interestingly, elevated plasma free fatty acid concentrations have been shown to correlate with UCP expression (Murray et al., 2004). In particular, cardiac UCP3 levels are augmented by free fatty acids in a PPAR $\alpha$  dependent manner (Young et al., 2001b). Free fatty acids are increased in patients with CKD and could potentially contribute to raised mitochondrial UCP expression resulting in uncoupling (Gadegbeku et al., 2004). However, in this study, a similar degree of uncoupling was observed between control and uraemic cardiac mitochondria *in vitro*. In response to challenges such as increased free fatty acids,

it is feasible that mitochondria from uraemic hearts may become uncoupled resulting in compromised mitochondrial function and ROS generation leading to apoptosis.

#### **6.4.2 Metabolic Protein Expression**

Twelve weeks uraemia had little effect on PPAR $\alpha$  protein expression (Figure 6.7) despite the observed decrease in fatty acid oxidation. Only few studies have assessed PPAR $\alpha$  in the uraemic heart. Mori *et al.* (2007) observed a 44% reduction in liver PPAR $\alpha$  mRNA at 10 weeks post-induction of uraemia (Mori et al., 2007). In the hypertrophied heart, experimental studies have observed unchanged (Duda et al., 2007) and decreased (Akki et al., 2008) PPAR $\alpha$  mRNA. Importantly, mRNA levels may not always reflect protein expression due to post-transcriptional modification. Furthermore, changes in protein levels may not necessarily relate to altered activity. The activity of PPAR $\alpha$  is modulated by the heterodimeric receptor RXR, and the co-factor PGC-1 $\alpha$ , each of which may affect the expression of mRNAs (Vega et al., 2000). Interestingly, in an experimental model of chronic heart failure, PGC-1 $\alpha$  was down-regulated (Garnier et al., 2003). Decreased PGC-1 $\alpha$  reduces the transcription of FAO related proteins, and may account for the diminished palmitate oxidation observed in this model.

CD36 expression was reduced in untreated uraemic hearts compared with respective controls (Figure 6.8). In an experimental model of angiotensin II-induced hypertension, CD36 mRNA expression was significantly decreased (Yamashita et al.,

2008). Given that uraemia is associated with hypertension and elevated angiotensin II, it is feasible that this could account for the reduction in CD36 protein expression observed in this model. Conversely, in a rat model of hypertrophic cardiomyopathy, cardiac CD36 expression was significantly up-regulated compared with hearts from wild-type animals (Luedde et al., 2009). However, the decrease in CD36 may be a direct result of enhanced angiotensin II rather than hypertrophy per se.

#### **6.4.2.1 Impact of EPO on Protein Expression**

Chronic EPO administration did not significantly impact on the protein expression of PPAR $\alpha$  or CD36 (Figure 6.8). There has been little research into the effect of EPO on key metabolic protein expression. PPAR $\alpha$ , which regulates CD36 expression, can be modified post-transcriptionally *via* the ERK/ MAPK pathways, leading to reduced activity without alterations in expression (Barger et al., 2000). Thus, activation of these pathways may decrease PPAR $\alpha$  activity, in turn resulting in decreased expression of PPAR $\alpha$ -regulated proteins including CD36 (Barger et al., 2000). Interestingly, EPO has been shown to activate the ERK and MAPK pathways in the reperfused heart, as part of the reperfusion injury salvage kinase pathway (RISK) (Bullard et al., 2005, Chan et al., 2007, Rafiee et al., 2005). Therefore, could potentially reduce PPAR $\alpha$  activity and decrease the expression of proteins which PPAR $\alpha$  regulates including CD36. Furthermore, a number of experimental studies have shown EPO to activate the Akt pathway (Bahlmann et al., 2004, Li et al., 2006). Cook *et al.* (2002) observed a decrease in PGC1 $\alpha$  mRNA in mice over expressing Akt.

It is therefore feasible that EPO may decrease CD36 by reducing PGC1 $\alpha$  therefore decreasing PPAR $\alpha$  activity, however this was not observed in this study.

### **6.4.3 Conclusion**

PPAR $\alpha$  and CD35 protein expression were unchanged in uraemic hearts. Despite LVH and fibrosis observed by 12 weeks uraemia, mitochondrial function was not compromised during uraemia. It is feasible that with prolonged uraemia and increased challenges to the heart, mitochondrial dysfunction will ensue, leading to ROS production, apoptosis and instigating the transition to heart failure.

## **Chapter 7: Discussion and Future Work**

## **7.1 Discussion**

Surgical induction of uraemia *via* a single 5/6<sup>th</sup> nephrectomy resulted in elevated serum creatinine and anaemia from 3 weeks post-surgery. By 12 weeks uraemia, animals exhibited worsening kidney function, anaemia, hypertension and cardiac hypertrophy, characteristic features of CKD. At this stage of uraemia, there was no evidence of cardiac or mitochondrial dysfunction suggesting a compensatory phase of LVH.

### **7.1.1 Extent of Kidney Dysfunction**

In this study, kidney function was assessed by analysing serum creatinine concentration. Unfortunately, serum creatinine is also affected by other factors including muscle mass. As uraemia progresses, some animals lose muscle mass, which may falsely lower serum creatinine resulting in underestimated kidney dysfunction (Lindeman, 1993). In CKD patients, determining glomerular filtration rate (GFR) provides a more accurate measure of kidney function, and is frequently estimated using the MDRD (modification of diet in renal disease) equation, which takes into consideration a number of variables in addition to serum creatinine including age, sex and race (Levey et al., 1999). In rats, collecting urine over a 24 h period would allow estimation of GFR by measurement of creatinine clearance (Perrone et al., 1992). Furthermore, urine could also be analysed for other markers of kidney dysfunction including microalbuminuria.

The extent of kidney damage in this model of uraemia was moderate, with mild renal fibrosis, which parallels early stages of CKD (Figure 7.1). This allowed the cardiac alterations in uraemia to be investigated prior to onset of cardiac dysfunction. Such cardiac changes may be responsible for the onset of heart failure and thus potentially provide useful therapeutic targets or diagnostic markers. Inducing uraemia *via* surgical resection of the upper and lower kidney poles would have created more severe kidney damage consistent with end stage renal disease (ESRD). Furthermore, infarcting the kidney by ligating the renal vessels would have also produced more advanced renal dysfunction, however, the degree of damage is less consistent (Liu et al., 2003). Producing a more severe model of kidney disease may have induced pathophysiological cardiac changes resulting in impaired cardiac function, and would have therefore allowed the cardioprotective nature of EPO (in terms of improving function) to be further assessed.

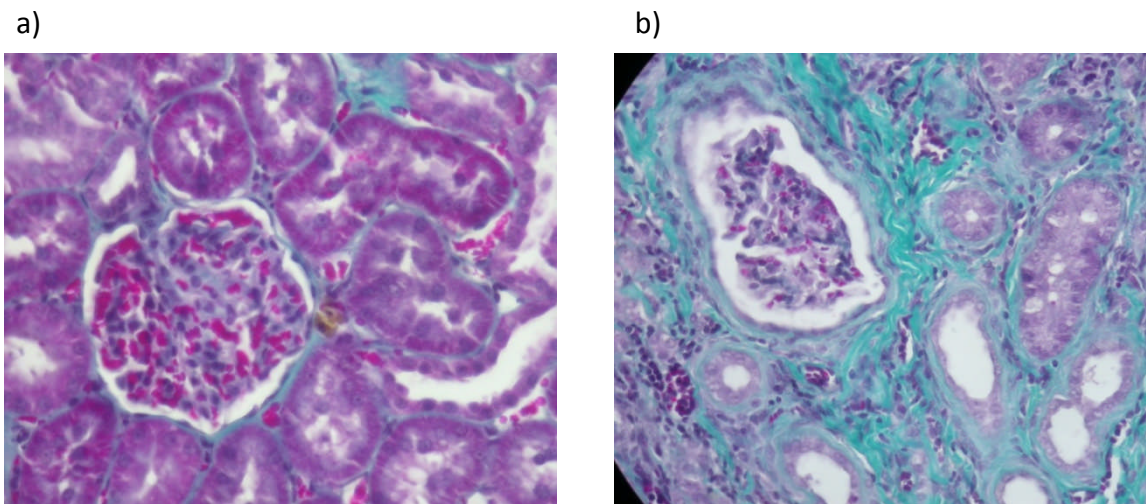


Figure 7.1: Kidney sections stained using Masson's trichrome stain  
from a) control and b) uraemic remnant kidney  
(Pictures kindly provided by Dr Chee Kay Cheung)  
×40 magnification

### 7.1.2 EPO Treatment

Chronic EPO administration did not impact on the progression of renal dysfunction. However, it improved haematocrit and induced partial regression of hypertrophy in uraemic animals despite continued hypertension.

Approximately, 90% of haemodialysis patients in the UK receive EPO (Richardson et al., 2007), which improves anaemia and increases quality of life. However, the direct cellular impact of EPO in uraemic cardiomyopathy is incompletely understood. Acute and chronic EPO administration improve cardiac function and delay the onset of heart failure in a number of experimental models (Li et al., 2006, van der Meer et al., 2005). Interestingly however, clinical trials have provided conflicting results regarding the efficacy of EPO in the uraemic heart and the future of EPO as a cardioprotectant remains uncertain (Hayat, 2009, Pfeffer et al., 2009). EPO has adverse effects including hypertension, the most frequent complication associated with EPO therapy (Lee et al., 2007). Moreover, EPO increases production and reactivity of platelets, thereby raising the risk of cardiovascular events (Stohlawetz et al., 2000). Although EPO does improve quality of life for CKD patients by treating anaemia, it is feasible that any direct beneficial effects on the heart are cancelled out by the complications associated with EPO treatment resulting in no improvement in survival rates in CKD patients.

EPO has been shown to be cardioprotective in animal models of heart failure (Li et al., 2006, van der Meer et al., 2005, Westenbrink et al., 2007). However, effects of EPO on the heart could be related to elevated erythropoiesis and consequently, increased oxygen delivery to the myocardium. In this regard, in experimental uraemia, it is difficult to dissociate direct cardiac effects of chronic EPO administration from the improvement in haematocrit. Specifically, the EPO-induced regression of LVH could result from the amelioration of anaemia, or the EPO-mediated activation of anti-hypertrophic signalling pathways, or a combination of

both. Recent studies using low-dose EPO treatment have shown cardioprotection post-MI without a rise in haematocrit (Lipsic et al., 2008). Furthermore, carbamylated erythropoietin (CEPO), which does not stimulate erythropoiesis, maintains its cardioprotective properties despite no change in haematocrit (Fiordaliso et al., 2005, Moon et al., 2006). Administration of EPO without the rise in haematocrit would allow the dissociation of direct cardiac actions from the anti-anaemic effects in uraemic cardiomyopathy.

## **7.2 Future Work**

By 12 weeks uraemia, hearts exhibited LVH with preserved function. It is feasible that, although cardiac function is not compromised at this stage of uraemia, with increased stresses to the heart, dysfunction may ensue. Indeed, recent studies from this laboratory have shown that post-ischæmia, uraemic hearts have a poorer recovery during reperfusion (Figure 7.2). This is consistent with the findings of Dikow *et al.* (2004), showing reduced ischaemic tolerance post-MI. Moreover, the death rate following acute MI is much higher in CKD patients compared with the normal population (Shlipak et al., 2002). Even mild renal insufficiency was associated with an increased risk of death following MI, and risk increases with worsening renal function (Wright et al., 2002).

During ischaemia/reperfusion, the addition of insulin in the perfusion medium is known to be cardioprotective, reducing cell death and improving cardiac function *via* activation of the RISK pathway (Jonassen et al., 2000). Uraemia is characterised by insulin resistance (DeFronzo et al., 1981). Indeed, studies from this laboratory have demonstrated that insulin had little impact on the recovery of function in uraemic hearts during reperfusion (Figure 7.2). It would be interesting to examine the impact of EPO in uraemic hearts during ischaemia/reperfusion. EPO, like insulin, has been shown to improve function post-ischaemia (Bullard et al., 2005, Cai and Semenza, 2004). However, it is unknown whether EPO has the same protective effects during ischaemia/reperfusion in uraemic hearts. It is feasible that since EPO may exert its effects through the same pathway as insulin (*via* activation of the RISK pathway), the effects of EPO in ischaemia/reperfusion may also be blunted in the same way as insulin protection is lost.

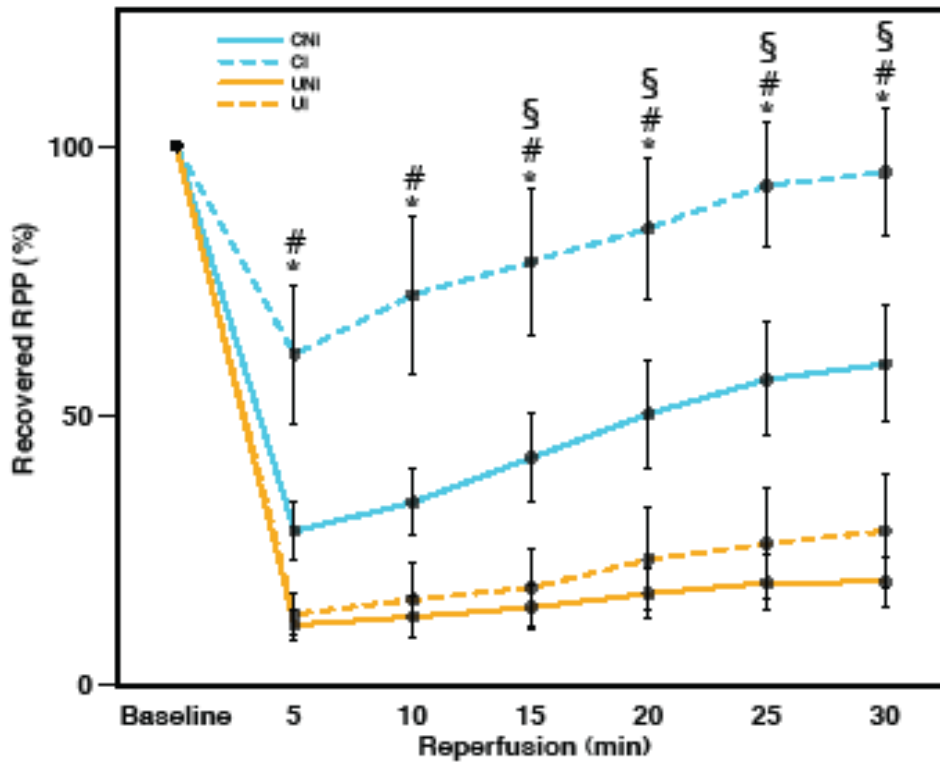


Figure 7.2: Recovery of rate pressure product (RPP) during reperfusion

CNI Control no insulin; CI Control with insulin; UNI Uraemic no insulin;  
 UI Uraemic with insulin  
 (all groups n=5)

§  $p < 0.05$  vs. control no insulin #  $p < 0.05$  vs. uraemic with insulin \*  $p < 0.05$  vs. uraemic no insulin

Hearts may also be stressed *in vitro* by increasing cardiac work, which can be achieved by pacing hearts at a higher rate or raising the buffer calcium concentration. In support of this, McMahon *et al.* (2002) observed impaired relaxation of isolated uraemic cardiomyocytes only in the presence of 4 mM calcium.

*In vivo*, following induction of uraemia, hearts could be subjected to MI, by ligating the coronary artery. Again, this may expose differences in the functional capacity between uraemic and control hearts. Furthermore, it would be interesting, if uraemic hearts did exhibit impaired function during increased challenges, if this could be improved with EPO treatment.

In this model of uraemia, metabolic remodelling was observed at 6 and 12 weeks consistent with the onset of LVH. Interestingly, PPAR $\alpha$  expression, which, in models of LVH, is typically down-regulated, was unchanged (Lehman et al., 2000). PPAR $\alpha$  is regulated by the co-factor PGC1 $\alpha$  (Finck and Kelly, 2006). In experimental models of heart failure, expression of PGC1 $\alpha$  is diminished, which may account for the observed reduction in fatty acid oxidation (Garnier et al., 2003). PGC1 $\alpha$  also plays a key role in mitochondrial biogenesis. Indeed, in PGC1 $\alpha$ -/- mice, expression of genes involved in FAO, electron transport chain and oxidative phosphorylation are decreased, along with a reduction in mitochondrial density (Lehman et al., 2008). It would be interesting to determine expression of PGC1 $\alpha$  in the uraemic heart. It is feasible that decreased PGC1 $\alpha$  may account for the change in substrate use from fatty acids to glucose and although *in vitro* mitochondrial function was preserved at this stage, with progression of uraemia, the reduction in PGC1 $\alpha$  may eventually lead to compromised mitochondrial function, impaired ATP synthesis and ROS production, thereby initiating the onset of heart failure.

The switch in substrate usage may represent a beneficial adaptation to sustain function in LVH given that glucose is more oxygen efficient than fatty acids (van Bilsen et al., 2009). It would therefore be interesting to prevent this remodelling during uraemia and determine the impact this has on cardiac function. Young *et al.* (2001) found that preventing the decrease in fatty acid oxidation by reactivating PPAR $\alpha$  worsened cardiac function in LVH, an affect which may also occur in the uraemic heart.

## Publications

### Papers

- AKKI, A., SMITH, K. & SEYMOUR, A.M. 2008 Compensated hypertrophy is characterised by a decline in palmitate oxidation. *Mol Cell Biochem*, 311, 215-24
- SEMPLE, D., SMITH, K., BHANDARI, S. & SEYMOUR, A.M. 2010. Uraemic cardiomyopathy and insulin resistance: A critical role for Akt? *J Am Soc Nephrol* (in press)
- SMITH, K., SEMPLE, D., AKSENTIJEVIC, D., BHANDARI, S & SEYMOUR, A.M. 2010a. Functional and metabolic adaptation in uraemic cardiomyopathy. *Frontiers in Bioscience* (accepted)
- SMITH, K., SEMPLE, D., BHANDARI, S & SEYMOUR, A.M. 2009. Cellular basis of uraemic cardiomyopathy: a role for erythropoietin? *Eur J Heart Fail*, 11, 732-8
- SMITH, K., WANG, Y., WALTHER, T., BHANDARI, S., & SEYMOUR, A.M. 2010b. The impact of erythropoietin on *in vivo* cardiac function and fibrosis in experimental uraemia (in preparation)

### Published Abstracts

- SMITH, K., BHANDARI, S & SEYMOUR, A.M. 2009 Erythropoietin induces regression of hypertrophy in experimental uraemic cardiomyopathy *Eur J Heart Fail*, 8
- AKSENTIJEVIC, D., LEE, K.Y., SMITH, K., BHANDARI, S & SEYMOUR, A.M. 2007. Altered expression of myocardial Ca<sup>2+</sup> handling proteins in experimental uraemia *J Mol Cell Cardio* 42, S139-140

## References

1991. Double-blind, placebo-controlled study of the therapeutic use of recombinant human erythropoietin for anemia associated with chronic renal failure in predialysis patients. The US Recombinant Human Erythropoietin Predialysis Study Group. *Am J Kidney Dis*, 18, 50-9.
1998. Causes of death. United States Renal Data System. *Am J Kidney Dis*, 32, S81-8.
2000. Effects of ramipril on cardiovascular and microvascular outcomes in people with diabetes mellitus: results of the HOPE study and MICRO-HOPE substudy. Heart Outcomes Prevention Evaluation Study Investigators. *Lancet*, 355, 253-9.
2001. Randomised trial of a perindopril-based blood-pressure-lowering regimen among 6,105 individuals with previous stroke or transient ischaemic attack. *Lancet*, 358, 1033-41.
- AKKI, A., SMITH, K. & SEYMOUR, A. M. 2008. Compensated cardiac hypertrophy is characterised by a decline in palmitate oxidation. *Mol Cell Biochem*, 311, 215-24.
- AKSENTIJEVIC, D., BHANDARI, S. & SEYMOUR, A. M. 2009. Insulin resistance and altered glucose transporter 4 expression in experimental uremia. *Kidney Int*, 75, 711-8.
- ALLARD, M. F., SCHONEKESS, B. O., HENNING, S. L., ENGLISH, D. R. & LOPASCHUK, G. D. 1994. Contribution of oxidative metabolism and glycolysis to ATP production in hypertrophied hearts. *Am J Physiol*, 267, H742-50.
- AMANN, K., BREITBACH, M., RITZ, E. & MALL, G. 1998a. Myocyte/capillary mismatch in the heart of uremic patients. *J Am Soc Nephrol*, 9, 1018-22.
- AMANN, K., BUZELLO, M., SIMONAVICIENE, A., MILTENBERGER-MILTENYI, G., KOCH, A., NABOKOV, A., GROSS, M. L., GLESS, B., MALL, G. & RITZ, E. 2000. Capillary/myocyte mismatch in the heart in renal failure--a role for erythropoietin? *Nephrol Dial Transplant*, 15, 964-9.
- AMANN, K., KRONENBERG, G., GEHLEN, F., WESSELS, S., ORTH, S., MUNTER, K., EHMKE, H., MALL, G. & RITZ, E. 1998b. Cardiac remodelling in experimental renal failure--an immunohistochemical study. *Nephrol Dial Transplant*, 13, 1958-66.
- AMANN, K., NEIMEIER, K. A., SCHWARZ, U., TORNIG, J., MATTHIAS, S., ORTH, S. R., MALL, G. & RITZ, E. 1997. Rats with moderate renal failure show capillary deficit in heart but not skeletal muscle. *Am J Kidney Dis*, 30, 382-8.
- AMANN, K. & RITZ, E. 1996. Reduced cardiac ischaemia tolerance in uraemia - what is the role of structural abnormalities of the heart? *Nephrol Dial Transplant*, 11, 1238-41.
- AMANN, K. & RITZ, E. 1997. Cardiac disease in chronic uremia: pathophysiology. *Adv Ren Replace Ther*, 4, 212-24.
- AMANN, K., RITZ, E., WIEST, G., KLAUS, G. & MALL, G. 1994. A role of parathyroid hormone for the activation of cardiac fibroblasts in uremia. *J Am Soc Nephrol*, 4, 1814-9.

- AMANN, K., TYRALLA, K., GROSS, M. L., SCHWARZ, U., TORNIG, J., HAAS, C. S., RITZ, E. & MALL, G. 2003. Cardiomyocyte loss in experimental renal failure: prevention by ramipril. *Kidney Int*, 63, 1708-13.
- AMANN, K., WIEST, G., ZIMMER, G., GRETZ, N., RITZ, E. & MALL, G. 1992. Reduced capillary density in the myocardium of uremic rats--a stereological study. *Kidney Int*, 42, 1079-85.
- AMBROSIO, G., ZWEIER, J. L., DUILIO, C., KUPPUSAMY, P., SANTORO, G., ELIA, P. P., TRITTO, I., CIRILLO, P., CONDORELLI, M., CHIARIELLO, M. & ET AL. 1993. Evidence that mitochondrial respiration is a source of potentially toxic oxygen free radicals in intact rabbit hearts subjected to ischemia and reflow. *J Biol Chem*, 268, 18532-41.
- AMMARGUELLAT, F., GOGUSEV, J. & DRUEKE, T. B. 1996. Direct effect of erythropoietin on rat vascular smooth-muscle cell via a putative erythropoietin receptor. *Nephrol Dial Transplant*, 11, 687-92.
- ANAGNOSTOU, A., LIU, Z., STEINER, M., CHIN, K., LEE, E. S., KESSIMIAN, N. & NOGUCHI, C. T. 1994. Erythropoietin receptor mRNA expression in human endothelial cells. *Proc Natl Acad Sci U S A*, 91, 3974-8.
- ANAND, I. S., KUSKOWSKI, M. A., RECTOR, T. S., FLOREA, V. G., GLAZER, R. D., HESTER, A., CHIANG, Y. T., AKNAY, N., MAGGIONI, A. P., OPASICH, C., LATINI, R. & COHN, J. N. 2005. Anemia and change in hemoglobin over time related to mortality and morbidity in patients with chronic heart failure: results from Val-HeFT. *Circulation*, 112, 1121-7.
- ANVERSA, P., KAJSTURA, J. & OLIVETTI, G. 1996. Myocyte death in heart failure. *Curr Opin Cardiol*, 11, 245-51.
- BAHLMANN, F. H., SONG, R., BOEHM, S. M., MENGEL, M., VON WASIELEWSKI, R., LINDSCHAU, C., KIRSCH, T., DE GROOT, K., LAUDELEY, R., NIEMCZYK, E., GULER, F., MENNE, J., HALLER, H. & FLISER, D. 2004. Low-dose therapy with the long-acting erythropoietin analogue darbepoetin alpha persistently activates endothelial Akt and attenuates progressive organ failure. *Circulation*, 110, 1006-12.
- BAINES, C. P., KAISER, R. A., PURCELL, N. H., BLAIR, N. S., OSINSKA, H., HAMBLETON, M. A., BRUNSKILL, E. W., SAYEN, M. R., GOTTLIEB, R. A., DORN, G. W., ROBBINS, J. & MOLKENTIN, J. D. 2005. Loss of cyclophilin D reveals a critical role for mitochondrial permeability transition in cell death. *Nature*, 434, 658-662.
- BARGER, P. M., BRANDT, J. M., LEONE, T. C., WEINHEIMER, C. J. & KELLY, D. P. 2000. Deactivation of peroxisome proliferator-activated receptor-alpha during cardiac hypertrophic growth. *J Clin Invest*, 105, 1723-30.
- BARGER, P. M. & KELLY, D. P. 1999. Fatty acid utilization in the hypertrophied and failing heart: molecular regulatory mechanisms. *Am J Med Sci*, 318, 36-42.
- BARGER, P. M. & KELLY, D. P. 2000. PPAR signaling in the control of cardiac energy metabolism. *Trends Cardiovasc Med*, 10, 238-45.
- BEDDHU, S., SAMORE, M. H., ROBERTS, M. S., STODDARD, G. J., PAPPAS, L. M. & CHEUNG, A. K. 2003. Creatinine production, nutrition, and glomerular filtration rate estimation. *J Am Soc Nephrol*, 14, 1000-5.
- BEN-DOR, I., HARDY, B., FUCHS, S., KAGANOVSKY, E., KADMON, E., SAGIE, A., COLEMAN, R., MANSUR, M., POLITI, B., FRASER, A., HARELL, D., OKON, E.,

- BATTLER, A. & HAIM, M. 2007. Repeated low-dose of erythropoietin is associated with improved left ventricular function in rat acute myocardial infarction model. *Cardiovasc Drugs Ther*, 21, 339-46.
- BERNAUDIN, M., BELLAIL, A., MARTI, H. H., YVON, A., VIVIEN, D., DUCHATELLE, I., MACKENZIE, E. T. & PETIT, E. 2000. Neurons and astrocytes express EPO mRNA: oxygen-sensing mechanisms that involve the redox-state of the brain. *Glia*, 30, 271-8.
- BERS, D. M. 2002. Cardiac excitation-contraction coupling. *Nature*, 415, 198-205.
- BERS, D. M., DESPA, S. & BOSSUYT, J. 2006. Regulation of Ca<sup>2+</sup> and Na<sup>+</sup> in normal and failing cardiac myocytes. *Ann N Y Acad Sci*, 1080, 165-77.
- BISHOP, J. E., GREENBAUM, R., GIBSON, D. G., YACOUB, M. & LAURENT, G. J. 1990. Enhanced deposition of predominantly type I collagen in myocardial disease. *J Mol Cell Cardiol*, 22, 1157-65.
- BLEEHEN, N. M. & FISHER, R. B. 1954. The action of insulin in the isolated rat heart. *J Physiol*, 123, 260-76.
- BORUTAITE, V. & BROWN, G. C. 2003. Mitochondria in apoptosis of ischemic heart. *FEBS Lett*, 541, 1-5.
- BRIER, M. E., BUNKE, C. M., LATHON, P. V. & ARONOFF, G. R. 1993. Erythropoietin-induced antinatriuresis mediated by angiotensin II in perfused kidneys. *J Am Soc Nephrol*, 3, 1583-90.
- BRIGADEAU, F., GELE, P., WIBAUX, M., MARQUIE, C., MARTIN-NIZARD, F., TORPIER, G., FRUCHART, J. C., STAELS, B., DURIEZ, P. & LACROIX, D. 2007. The PPARalpha activator fenofibrate slows down the progression of the left ventricular dysfunction in porcine tachycardia-induced cardiomyopathy. *J Cardiovasc Pharmacol*, 49, 408-15.
- BRILLA, C. G., ZHOU, G., MATSUBARA, L. & WEBER, K. T. 1994. Collagen metabolism in cultured adult rat cardiac fibroblasts: response to angiotensin II and aldosterone. *J Mol Cell Cardiol*, 26, 809-20.
- BRINES, M., GRASSO, G., FIORDALISO, F., SFACTERIA, A., GHEZZI, P., FRATELLI, M., LATINI, R., XIE, Q. W., SMART, J., SU-RICK, C. J., POBRE, E., DIAZ, D., GOMEZ, D., HAND, C., COLEMAN, T. & CERAMI, A. 2004. Erythropoietin mediates tissue protection through an erythropoietin and common beta-subunit heteroreceptor. *Proc Natl Acad Sci U S A*, 101, 14907-12.
- BRINES, M. L., GHEZZI, P., KEENAN, S., AGNELLO, D., DE LANEROLLE, N. C., CERAMI, C., ITRI, L. M. & CERAMI, A. 2000. Erythropoietin crosses the blood-brain barrier to protect against experimental brain injury. *Proc Natl Acad Sci U S A*, 97, 10526-31.
- BUCHWALD, A., TILL, H., UNTERBERG, C., OBERSCHMIDT, R., FIGULLA, H. R. & WIEGAND, V. 1990. Alterations of the mitochondrial respiratory chain in human dilated cardiomyopathy. *Eur Heart J*, 11, 509-16.
- BUGGER, H., SCHWARZER, M., CHEN, D., SCHREPPER, A., AMORIM, P. A., SCHOEPE, M., NGUYEN, T. D., MOHR, F. W., KHALIMONCHUK, O., WEIMER, B. C. & DOENST, T. 2009. Proteomic remodelling of mitochondrial oxidative pathways in pressure overload-induced heart failure. *Cardiovasc Res*.
- BULLARD, A. J., GOVEWALLA, P. & YELLON, D. M. 2005. Erythropoietin protects the myocardium against reperfusion injury in vitro and in vivo. *Basic Res Cardiol*, 100, 397-403.

- BULLARD, A. J. & YELLON, D. M. 2005. Chronic erythropoietin treatment limits infarct-size in the myocardium in vitro. *Cardiovasc Drugs Ther*, 19, 333-6.
- BURGER, D., LEI, M., GEOGHEGAN-MORPHET, N., LU, X., XENOCOSTAS, A. & FENG, Q. 2006. Erythropoietin protects cardiomyocytes from apoptosis via up-regulation of endothelial nitric oxide synthase. *Cardiovasc Res*, 72, 51-9.
- CAI, Z. & SEMENZA, G. L. 2004. Phosphatidylinositol-3-kinase signaling is required for erythropoietin-mediated acute protection against myocardial ischemia/reperfusion injury. *Circulation*, 109, 2050-3.
- CALVILLO, L., LATINI, R., KAJSTURA, J., LERI, A., ANVERSA, P., GHEZZI, P., SALIO, M., CERAMI, A. & BRINES, M. 2003. Recombinant human erythropoietin protects the myocardium from ischemia-reperfusion injury and promotes beneficial remodeling. *Proc Natl Acad Sci U S A*, 100, 4802-6.
- CANNELLA, G., LA CANNA, G., SANDRINI, M., GAGGIOTTI, M., NORDIO, G., MOVILLI, E., MOMBELLONI, S., VISIOLI, O. & MAIORCA, R. 1991. Reversal of left ventricular hypertrophy following recombinant human erythropoietin treatment of anaemic dialysed uraemic patients. *Nephrol Dial Transplant*, 6, 31-7.
- CARO, J., BROWN, S., MILLER, O., MURRAY, T. & ERSLEV, A. J. 1979. Erythropoietin levels in uremic nephric and anephric patients. *J Lab Clin Med*, 93, 449-58.
- CHAN, C. Y., CHEN, Y. S., LEE, H. H., HUANG, H. S., LAI, Y. L., CHEN, C. F. & MA, M. C. 2007. Erythropoietin protects post-ischemic hearts by preventing extracellular matrix degradation: role of Jak2-ERK pathway. *Life Sci*, 81, 717-23.
- CHANCE, E. M., SEEHOLZER, S. H., KOBAYASHI, K. & WILLIAMSON, J. R. 1983. Mathematical analysis of isotope labeling in the citric acid cycle with applications to <sup>13</sup>C NMR studies in perfused rat hearts. *J Biol Chem*, 258, 13785-94.
- CHENG, W., KAJSTURA, J., NITAHARA, J. A., LI, B., REISS, K., LIU, Y., CLARK, W. A., KRAJEWSKI, S., REED, J. C., OLIVETTI, G. & ANVERSA, P. 1996. Programmed myocyte cell death affects the viable myocardium after infarction in rats. *Exp Cell Res*, 226, 316-27.
- CHURCH, R. L., PFEIFFER, S. E. & TANZER, M. L. 1971. Collagen biosynthesis: synthesis and secretion of a high molecular weight collagen precursor (procollagen). *Proc Natl Acad Sci U S A*, 68, 2638-42.
- CLAPHAM, J. C., ARCH, J. R., CHAPMAN, H., HAYNES, A., LISTER, C., MOORE, G. B., PIERCY, V., CARTER, S. A., LEHNER, I., SMITH, S. A., BEELEY, L. J., GODDEN, R. J., HERRITY, N., SKEHEL, M., CHANGANI, K. K., HOCKINGS, P. D., REID, D. G., SQUIRES, S. M., HATCHER, J., TRAIL, B., LATCHAM, J., RASTAN, S., HARPER, A. J., CADENAS, S., BUCKINGHAM, J. A., BRAND, M. D. & ABUIN, A. 2000. Mice overexpressing human uncoupling protein-3 in skeletal muscle are hyperphagic and lean. *Nature*, 406, 415-8.
- COOK, S. A., MATSUI, T., LI, L. & ROSENZWEIG, A. 2002. Transcriptional effects of chronic Akt activation in the heart. *J Biol Chem*, 277, 22528-33.
- COSTA, E., ROCHA, S., ROCHA-PEREIRA, P., NASCIMENTO, H., CASTRO, E., MIRANDA, V., FARIA MDO, S., LOUREIRO, A., QUINTANILHA, A., BELO, L. & SANTOS-SILVA, A. 2008. Neutrophil activation and resistance to recombinant human erythropoietin therapy in hemodialysis patients. *Am J Nephrol*, 28, 935-40.

- CROW, M. T., MANI, K., NAM, Y. J. & KITSIS, R. N. 2004. The mitochondrial death pathway and cardiac myocyte apoptosis. *Circ Res*, 95, 957-70.
- D'USCIO, L. V., SMITH, L. A., SANTHANAM, A. V., RICHARDSON, D., NATH, K. A. & KATUSIC, Z. S. 2007. Essential role of endothelial nitric oxide synthase in vascular effects of erythropoietin. *Hypertension*, 49, 1142-8.
- DE SOUZA, R. R. 2002. Aging of myocardial collagen. *Biogerontology*, 3, 325-35.
- DEFRONZO, R. A., ALVESTRAND, A., SMITH, D., HENDLER, R., HENDLER, E. & WAHREN, J. 1981. Insulin resistance in uremia. *J Clin Invest*, 67, 563-8.
- DEPPING, R., KAWAKAMI, K., OCKER, H., WAGNER, J. M., HERINGLAKE, M., NOETZOLD, A., SIEVERS, H. H. & WAGNER, K. F. 2005. Expression of the erythropoietin receptor in human heart. *J Thorac Cardiovasc Surg*, 130, 877-8.
- DIGICAYLIOGLU, M. & LIPTON, S. A. 2001. Erythropoietin-mediated neuroprotection involves cross-talk between Jak2 and NF-kappaB signalling cascades. *Nature*, 412, 641-7.
- DIKOW, R., KIHM, L. P., ZEIER, M., KAPITZA, J., TORNIG, J., AMANN, K., TIEFENBACHER, C. & RITZ, E. 2004. Increased infarct size in uremic rats: reduced ischemia tolerance? *J Am Soc Nephrol*, 15, 1530-6.
- DOUNOUDI, E., PAPAVALIOU, E., MAKEDOU, A., IOANNOU, K., KATOPODIS, K. P., TSELEPIS, A., SIAMOPOULOS, K. C. & TSAKIRIS, D. 2006. Oxidative stress is progressively enhanced with advancing stages of CKD. *Am J Kidney Dis*, 48, 752-60.
- DRUEKE, T. B., LOCATELLI, F., CLYNE, N., ECKARDT, K. U., MACDOUGALL, I. C., TSAKIRIS, D., BURGER, H. U. & SCHERHAG, A. 2006. Normalization of hemoglobin level in patients with chronic kidney disease and anemia. *N Engl J Med*, 355, 2071-84.
- DUDA, M. K., O'SHEA, K. M., LEI, B., BARROWS, B. R., AZIMZADEH, A. M., MCELFRISH, T. E., HOIT, B. D., KOP, W. J. & STANLEY, W. C. 2007. Dietary supplementation with omega-3 PUFA increases adiponectin and attenuates ventricular remodeling and dysfunction with pressure overload. *Cardiovasc Res*, 76, 303-10.
- EGGENA, P., WILLSEY, P., JAMGOTCHIAN, N., TRUCKENBROD, L., HU, M. S., BARRETT, J. D., EGGENA, M. P., CLEGG, K., NAKHOUL, F. & LEE, D. B. 1991. Influence of recombinant human erythropoietin on blood pressure and tissue renin-angiotensin systems. *Am J Physiol*, 261, E642-6.
- EGRIE, J. C. & BROWNE, J. K. 2001. Development and characterization of novel erythropoiesis stimulating protein (NESP). *Nephrol Dial Transplant*, 16 Suppl 3, 3-13.
- EHRENREICH, H., HASSELBLATT, M., DEMBOWSKI, C., CEPEK, L., LEWCZUK, P., STIEFEL, M., RUSTENBECK, H. H., BREITER, N., JACOB, S., KNERLICH, F., BOHN, M., POSER, W., RUTHER, E., KOCHEN, M., GEFELLER, O., GLEITER, C., WESSEL, T. C., DE RYCK, M., ITRI, L., PRANGE, H., CERAMI, A., BRINES, M. & SIREN, A. L. 2002. Erythropoietin therapy for acute stroke is both safe and beneficial. *Mol Med*, 8, 495-505.
- EL ALAOUI-TALIBI, Z., LANDORMY, S., LOIREAU, A. & MORAVEC, J. 1992. Fatty acid oxidation and mechanical performance of volume-overloaded rat hearts. *Am J Physiol*, 262, H1068-74.

- ESCHBACH, J. W., VARMA, A. & STIVELMAN, J. C. 2002. Is it time for a paradigm shift? Is erythropoietin deficiency still the main cause of renal anaemia? *Nephrol Dial Transplant*, 17 Suppl 5, 2-7.
- FABIATO, A. & FABIATO, F. 1979. Calcium and cardiac excitation-contraction coupling. *Annu Rev Physiol*, 41, 473-84.
- FAULDS, D. & SORKIN, E. M. 1989. Epoetin (recombinant human erythropoietin). A review of its pharmacodynamic and pharmacokinetic properties and therapeutic potential in anaemia and the stimulation of erythropoiesis. *Drugs*, 38, 863-99.
- FELDMAN, A. M., WEINBERG, E. O., RAY, P. E. & LORELL, B. H. 1993. Selective changes in cardiac gene expression during compensated hypertrophy and the transition to cardiac decompensation in rats with chronic aortic banding. *Circ Res*, 73, 184-92.
- FINCK, B. N. & KELLY, D. P. 2002. Peroxisome proliferator-activated receptor alpha (PPARalpha) signaling in the gene regulatory control of energy metabolism in the normal and diseased heart. *J Mol Cell Cardiol*, 34, 1249-57.
- FINCK, B. N. & KELLY, D. P. 2006. PGC-1 coactivators: inducible regulators of energy metabolism in health and disease. *J Clin Invest*, 116, 615-22.
- FIORDALISO, F., CHIMENTI, S., STASZEWSKY, L., BAI, A., CARLO, E., CUCCOVILLO, I., DONI, M., MENGOZZI, M., TONELLI, R., GHEZZI, P., COLEMAN, T., BRINES, M., CERAMI, A. & LATINI, R. 2005. A nonerythropoietic derivative of erythropoietin protects the myocardium from ischemia-reperfusion injury. *Proc Natl Acad Sci U S A*, 102, 2046-51.
- FISHER, J. W. 2003. Erythropoietin: physiology and pharmacology update. *Exp Biol Med (Maywood)*, 228, 1-14.
- FOLEY, R. N., HERZOG, C. A. & COLLINS, A. J. 2003. Smoking and cardiovascular outcomes in dialysis patients: the United States Renal Data System Wave 2 study. *Kidney Int*, 63, 1462-7.
- FOLEY, R. N., PARFREY, P. S., HARNETT, J. D., KENT, G. M., MARTIN, C. J., MURRAY, D. C. & BARRE, P. E. 1995. Clinical and echocardiographic disease in patients starting end-stage renal disease therapy. *Kidney Int*, 47, 186-92.
- FOLEY, R. N., PARFREY, P. S. & SARNAK, M. J. 1998. Clinical epidemiology of cardiovascular disease in chronic renal disease. *Am J Kidney Dis*, 32, S112-9.
- FOO, R. S., MANI, K. & KITSIS, R. N. 2005. Death begets failure in the heart. *J Clin Invest*, 115, 565-71.
- FUJII, H., LI, S. H., SZMITKO, P. E., FEDAK, P. W. & VERMA, S. 2006. C-reactive protein alters antioxidant defenses and promotes apoptosis in endothelial progenitor cells. *Arterioscler Thromb Vasc Biol*, 26, 2476-82.
- GADEGBEKU, C. A., SHRAYYEF, M. Z., LAPORTE, F. B. & EGAN, B. M. 2004. Lipids enhance alpha1-adrenoceptor pressor sensitivity in patients with chronic kidney disease. *Am J Kidney Dis*, 44, 446-54.
- GAGNON, R. F. & GALLIMORE, B. 1988. Characterization of a mouse model of chronic uremia. *Urol Res*, 16, 119-26.
- GAO, E., BOUCHER, M., CHUPRUN, J. K., ZHOU, R. H., ECKHART, A. D. & KOCH, W. J. 2007. Darbepoetin alfa, a long-acting erythropoietin analog, offers novel and delayed cardioprotection for the ischemic heart. *Am J Physiol Heart Circ Physiol*, 293, H60-8.

- GAO, X., HE, X., LUO, B., PENG, L., LIN, J. & ZUO, Z. 2009. Angiotensin II increases collagen I expression via transforming growth factor-beta1 and extracellular signal-regulated kinase in cardiac fibroblasts. *Eur J Pharmacol*, 606, 115-20.
- GAO, X. M., KIRIAZIS, H., MOORE, X. L., FENG, X. H., SHEPPARD, K., DART, A. & DU, X. J. 2005. Regression of pressure overload-induced left ventricular hypertrophy in mice. *Am J Physiol Heart Circ Physiol*, 288, H2702-7.
- GARCIA, D. L., ANDERSON, S., RENNKE, H. G. & BRENNER, B. M. 1988. Anemia lessens and its prevention with recombinant human erythropoietin worsens glomerular injury and hypertension in rats with reduced renal mass. *Proc Natl Acad Sci U S A*, 85, 6142-6.
- GARNIER, A., FORTIN, D., DELOMENIE, C., MOMKEN, I., VEKSLER, V. & VENTURA-CLAPIER, R. 2003. Depressed mitochondrial transcription factors and oxidative capacity in rat failing cardiac and skeletal muscles. *J Physiol*, 551, 491-501.
- GEORGE, J., GOLDSTEIN, E., ABASHIDZE, A., WEXLER, D., HAMED, S., SHMILOVICH, H., DEUTSCH, V., MILLER, H., KEREN, G. & ROTH, A. 2005. Erythropoietin promotes endothelial progenitor cell proliferative and adhesive properties in a PI 3-kinase-dependent manner. *Cardiovasc Res*, 68, 299-306.
- GIULIVI, C., BOVERIS, A. & CADENAS, E. 1995. Hydroxyl radical generation during mitochondrial electron transfer and the formation of 8-hydroxydesoxyguanosine in mitochondrial DNA. *Arch Biochem Biophys*, 316, 909-16.
- GOICOECHEA, M., MARTIN, J., DE SEQUERA, P., QUIROGA, J. A., ORTIZ, A., CARRENO, V. & CARAMELO, C. 1998. Role of cytokines in the response to erythropoietin in hemodialysis patients. *Kidney Int*, 54, 1337-43.
- GOLDBLATT, H. L., J. HANZAL, R. F. SUMMERVILLE, W. W. 1934. Studies on Experimental Hypertension: I. The production of persistent elevation of systolic blood pressure by means of renal ischaemia. *The Journal of Experimental Medicine*, 59, 347-379.
- GRANATA, S., ZAZA, G., SIMONE, S., VILLANI, G., LATORRE, D., PONTRELLI, P., CARELLA, M., SCHENA, F. P., GRANDALIANO, G. & PERTOSA, G. 2009. Mitochondrial dysregulation and oxidative stress in patients with chronic kidney disease. *BMC Genomics*, 10, 388.
- GRIMM, S. & BRDICZKA, D. 2007. The permeability transition pore in cell death. *Apoptosis*, 12, 841-55.
- GROSS, M. L. & RITZ, E. 2008. Hypertrophy and fibrosis in the cardiomyopathy of uremia--beyond coronary heart disease. *Semin Dial*, 21, 308-18.
- GROSSMAN, W. 1980. Cardiac hypertrophy: useful adaptation or pathologic process? *Am J Med*, 69, 576-84.
- GUPTA, S., DAS, B. & SEN, S. 2007. Cardiac hypertrophy: mechanisms and therapeutic opportunities. *Antioxid Redox Signal*, 9, 623-52.
- GUSTAFSSON, A. B. & GOTTLIEB, R. A. 2008. Heart mitochondria: gates of life and death. *Cardiovasc Res*, 77, 334-43.
- GUTTMAN, M. A., ZERHOUNI, E. A. & MCVEIGH, E. R. 1997. Analysis of Cardiac Function from MR Images. *IEEE Comput Graph Appl*, 17, 30-38.

- GWATHMEY, J., DEL MONTE, F. & HAJJAR, R. J. 2007. Abnormalities in Calcium Cycling in Heart Failure. *In: HOSENPUD, J. D. G., B. H. (ed.) Congestive Heart Failure*. Third ed. Philadelphia: Lippincott Williams & Wilkins.
- HALESTRAP, A. P. 1987. The regulation of the oxidation of fatty acids and other substrates in rat heart mitochondria by changes in the matrix volume induced by osmotic strength, valinomycin and Ca<sup>2+</sup>. *Biochem J*, 244, 159-64.
- HALESTRAP, A. P. 2009. What is the mitochondrial permeability transition pore? *J Mol Cell Cardiol*, 46, 821-31.
- HALSTENSON, C. E., MACRES, M., KATZ, S. A., SCHNIEDERS, J. R., WATANABE, M., SOBOTA, J. T. & ABRAHAM, P. A. 1991. Comparative pharmacokinetics and pharmacodynamics of epoetin alfa and epoetin beta. *Clin Pharmacol Ther*, 50, 702-12.
- HANLON, P. R., FU, P., WRIGHT, G. L., STEENBERGEN, C., ARCASOY, M. O. & MURPHY, E. 2005. Mechanisms of erythropoietin-mediated cardioprotection during ischemia-reperfusion injury: role of protein kinase C and phosphatidylinositol 3-kinase signaling. *Faseb J*, 19, 1323-5.
- HARNETT, J. D. & PARFREY, P. S. 1994. Blood pressure control and regression of LV hypertrophy in dialysis patients. *Contrib Nephrol*, 106, 110-3.
- HASENFUSS, G. 1998. Alterations of calcium-regulatory proteins in heart failure. *Cardiovasc Res*, 37, 279-89.
- HASENFUSS, G. & PIESKE, B. 2002. Calcium cycling in congestive heart failure. *J Mol Cell Cardiol*, 34, 951-69.
- HAYASHI, T., SUZUKI, A., SHOJI, T., TOGAWA, M., OKADA, N., TSUBAKIHARA, Y., IMAI, E. & HORI, M. 2000. Cardiovascular effect of normalizing the hematocrit level during erythropoietin therapy in predialysis patients with chronic renal failure. *Am J Kidney Dis*, 35, 250-6.
- HAYAT, M. 2009. Erythropoietin Friend or Foe in Chronic Kidney Disease Anemia: An Analysis of Randomized Controlled Trials, Observational Studies and Meta-analyses. *British Journal of Medical Practitioners*, 2, 12-20.
- HEATHER, L. C., CARR, C. A., STUCKEY, D. J., POPE, S., MORTEN, K. J., CARTER, E. E., EDWARDS, L. M. & CLARKE, K. 2009. Critical role of complex III in the early metabolic changes following myocardial infarction. *Cardiovasc Res*.
- HEIDENREICH, S., RAHN, K. H. & ZIDEK, W. 1991. Direct vasopressor effect of recombinant human erythropoietin on renal resistance vessels. *Kidney Int*, 39, 259-65.
- HELLE, F., HULTSTROM, M., SKOGSTRAND, T., PALM, F. & IVERSEN, B. M. 2009. Angiotensin II-induced contraction is attenuated by nitric oxide in afferent arterioles from the nonclipped kidney in 2K1C. *Am J Physiol Renal Physiol*, 296, F78-86.
- HEWITSON, T. D., ONO, T. & BECKER, G. J. 2009. Small animal models of kidney disease: a review. *Methods Mol Biol*, 466, 41-57.
- HIGUCHI, M., HONDA, T., PROSKE, R. J. & YE, E. T. 1998. Regulation of reactive oxygen species-induced apoptosis and necrosis by caspase 3-like proteases. *Oncogene*, 17, 2753-60.
- HSU, C. Y. 2002. Epidemiology of anemia associated with chronic renal insufficiency. *Curr Opin Nephrol Hypertens*, 11, 337-41.

- HUNTER, G. R. & HARRIS, R. T. 2008. Structure and Function of the Muscular, Neuromuscular, Cardiovascular and Respiratory Systems. In: BAECHLE, T. R. & EARLE, R. W. (eds.) *Essentials of Strength Training and Conditioning*. 3rd ed.: Human Kinetics.
- IDE, T., TSUTSUI, H., HAYASHIDANI, S., KANG, D., SUEMATSU, N., NAKAMURA, K., UTSUMI, H., HAMASAKI, N. & TAKESHITA, A. 2001. Mitochondrial DNA damage and dysfunction associated with oxidative stress in failing hearts after myocardial infarction. *Circ Res*, 88, 529-35.
- IDE, T., TSUTSUI, H., KINUGAWA, S., UTSUMI, H., KANG, D., HATTORI, N., UCHIDA, K., ARIMURA, K., EGASHIRA, K. & TAKESHITA, A. 1999. Mitochondrial electron transport complex I is a potential source of oxygen free radicals in the failing myocardium. *Circ Res*, 85, 357-63.
- IKOMA, M., KAWAMURA, T., KAKINUMA, Y., FOGO, A. & ICHIKAWA, I. 1991. Cause of variable therapeutic efficiency of angiotensin converting enzyme inhibitor on glomerular lesions. *Kidney Int*, 40, 195-202.
- INGWALL, J. S. 2009. Energy metabolism in heart failure and remodelling. *Cardiovasc Res*, 81, 412-9.
- INGWALL, J. S. & WEISS, R. G. 2004. Is the failing heart energy starved? On using chemical energy to support cardiac function. *Circ Res*, 95, 135-45.
- JACOBY, J. J., KALINOWSKI, A., LIU, M. G., ZHANG, S. S., GAO, Q., CHAI, G. X., JI, L., IWAMOTO, Y., LI, E., SCHNEIDER, M., RUSSELL, K. S. & FU, X. Y. 2003. Cardiomyocyte-restricted knockout of STAT3 results in higher sensitivity to inflammation, cardiac fibrosis, and heart failure with advanced age. *Proc Natl Acad Sci U S A*, 100, 12929-34.
- JAIMES, E. A., GALCERAN, J. M. & RAIJ, L. 1998. Angiotensin II induces superoxide anion production by mesangial cells. *Kidney Int*, 54, 775-84.
- JALIL, J. E., DOERING, C. W., JANICKI, J. S., PICK, R., SHROFF, S. G. & WEBER, K. T. 1989. Fibrillar collagen and myocardial stiffness in the intact hypertrophied rat left ventricle. *Circ Res*, 64, 1041-50.
- JAQUET, K., KRAUSE, K., TAWAKOL-KHODAI, M., GEIDEL, S. & KUCK, K. H. 2002. Erythropoietin and VEGF exhibit equal angiogenic potential. *Microvasc Res*, 64, 326-33.
- JARRETA, D., ORUS, J., BARRIENTOS, A., MIRO, O., ROIG, E., HERAS, M., MORAES, C. T., CARDELLACH, F. & CASADEMONT, J. 2000. Mitochondrial function in heart muscle from patients with idiopathic dilated cardiomyopathy. *Cardiovasc Res*, 45, 860-5.
- JI, Y., LI, B., REED, T. D., LORENZ, J. N., KAETZEL, M. A. & DEDMAN, J. R. 2003. Targeted inhibition of Ca<sup>2+</sup>/calmodulin-dependent protein kinase II in cardiac longitudinal sarcoplasmic reticulum results in decreased phospholamban phosphorylation at threonine 17. *J Biol Chem*, 278, 25063-71.
- JONASSEN, A. K., BRAR, B. K., MJOS, O. D., SACK, M. N., LATCHMAN, D. S. & YELLON, D. M. 2000. Insulin administered at reoxygenation exerts a cardioprotective effect in myocytes by a possible anti-apoptotic mechanism. *J Mol Cell Cardiol*, 32, 757-64.
- JOYEUX-FAURE, M., RAMOND, A., BEGUIN, P. C., BELAIDI, E., GODIN-RIBUOT, D. & RIBUOT, C. 2006. Early pharmacological preconditioning by erythropoietin

- mediated by inducible NOS and mitochondrial ATP-dependent potassium channels in the rat heart. *Fundam Clin Pharmacol*, 20, 51-6.
- JUNGERS, P., CHOUKROUN, G., OUALIM, Z., ROBINO, C., NGUYEN, A. T. & MAN, N. K. 2001. Beneficial influence of recombinant human erythropoietin therapy on the rate of progression of chronic renal failure in predialysis patients. *Nephrol Dial Transplant*, 16, 307-12.
- JUNK, A. K., MAMMIS, A., SAVITZ, S. I., SINGH, M., ROTH, S., MALHOTRA, S., ROSENBAUM, P. S., CERAMI, A., BRINES, M. & ROSENBAUM, D. M. 2002. Erythropoietin administration protects retinal neurons from acute ischemia-reperfusion injury. *Proc Natl Acad Sci U S A*, 99, 10659-64.
- KALK, P., EGGERT, B., RELLE, K., GODES, M., HEIDEN, S., SHARKOVSKA, Y., FISCHER, Y., ZIEGLER, D., BIELENBERG, G. W. & HOCHER, B. 2007. The adenosine A1 receptor antagonist SLV320 reduces myocardial fibrosis in rats with 5/6 nephrectomy without affecting blood pressure. *Br J Pharmacol*, 151, 1025-32.
- KELSO, G. F., PORTEOUS, C. M., COULTER, C. V., HUGHES, G., PORTEOUS, W. K., LEDGERWOOD, E. C., SMITH, R. A. & MURPHY, M. P. 2001. Selective targeting of a redox-active ubiquinone to mitochondria within cells: antioxidant and antiapoptotic properties. *J Biol Chem*, 276, 4588-96.
- KENNEDY, D., OMRAN, E., PERIYASAMY, S. M., NADOOR, J., PRIYADARSHI, A., WILLEY, J. C., MALHOTRA, D., XIE, Z. & SHAPIRO, J. I. 2003. Effect of chronic renal failure on cardiac contractile function, calcium cycling, and gene expression of proteins important for calcium homeostasis in the rat. *J Am Soc Nephrol*, 14, 90-7.
- KENNEDY, D. J., ELKAREH, J., SHIDYAK, A., SHAPIRO, A. P., SMAILI, S., MUTGI, K., GUPTA, S., TIAN, J., MORGAN, E., KHOURI, S., COOPER, C. J., PERIYASAMY, S. M., XIE, Z., MALHOTRA, D., FEDOROVA, O. V., BAGROV, A. Y. & SHAPIRO, J. I. 2008. Partial nephrectomy as a model for uremic cardiomyopathy in the mouse. *Am J Physiol Renal Physiol*, 294, F450-4.
- KIM, M. Y., KIM, M. J., YOON, I. S., AHN, J. H., LEE, S. H., BAIK, E. J., MOON, C. H. & JUNG, Y. S. 2006. Diazoxide acts more as a PKC-epsilon activator, and indirectly activates the mitochondrial K(ATP) channel conferring cardioprotection against hypoxic injury. *Br J Pharmacol*, 149, 1059-70.
- KOBORI, H., NANGAKU, M., NAVAR, L. G. & NISHIYAMA, A. 2007. The intrarenal renin-angiotensin system: from physiology to the pathobiology of hypertension and kidney disease. *Pharmacol Rev*, 59, 251-87.
- KOKOSZKA, J. E., WAYMIRE, K. G., LEVY, S. E., SLIGH, J. E., CAI, J., JONES, D. P., MACGREGOR, G. R. & WALLACE, D. C. 2004. The ADP/ATP translocator is not essential for the mitochondrial permeability transition pore. *Nature*, 427, 461-465.
- KOLEGANOVA, N., PIECHA, G., RITZ, E., BEKEREDJIAN, R., SCHIRMACHER, P., SCHMITT, C. P. & GROSS, M. L. 2009a. Interstitial fibrosis and microvascular disease of the heart in uremia: amelioration by a calcimimetic. *Lab Invest*, 89, 520-30.
- KOLEGANOVA, N., PIECHA, G., RITZ, E. & GROSS, M. L. 2009b. Calcitriol ameliorates capillary deficit and fibrosis of the heart in subtotal nephrectomized rats. *Nephrol Dial Transplant*, 24, 778-87.

- KOWALTOWSKI, A. J., CASTILHO, R. F. & VERCESI, A. E. 2001. Mitochondrial permeability transition and oxidative stress. *FEBS Lett*, 495, 12-5.
- KUNAPULI, S., ROSANIO, S. & SCHWARZ, E. R. 2006. "How do cardiomyocytes die?" apoptosis and autophagic cell death in cardiac myocytes. *J Card Fail*, 12, 381-91.
- KURIYAMA, S., TOMONARI, H., YOSHIDA, H., HASHIMOTO, T., KAWAGUCHI, Y. & SAKAI, O. 1997. Reversal of anemia by erythropoietin therapy retards the progression of chronic renal failure, especially in nondiabetic patients. *Nephron*, 77, 176-85.
- KUROSAWA, Y., KATOH, M., DOI, H. & NARITA, H. 2002. Tissue Angiotensin-converting enzyme activity plays an important role in pressure overload-induced cardiac fibrosis in rats. *J Cardiovasc Pharmacol*, 39, 600-9.
- KURTZ, T. W., GRIFFIN, K. A., BIDANI, A. K., DAVISSON, R. L. & HALL, J. E. 2005. Recommendations for blood pressure measurement in humans and experimental animals. Part 2: Blood pressure measurement in experimental animals: a statement for professionals from the subcommittee of professional and public education of the American Heart Association council on high blood pressure research. *Hypertension*, 45, 299-310.
- KUWAHARA, F., KAI, H., TOKUDA, K., KAI, M., TAKESHITA, A., EGASHIRA, K. & IMAIZUMI, T. 2002. Transforming growth factor-beta function blocking prevents myocardial fibrosis and diastolic dysfunction in pressure-overloaded rats. *Circulation*, 106, 130-5.
- LABINSKY, V., BELLOMO, M., CHANDLER, M. P., YOUNG, M. E., LIONETTI, V., QANUD, K., BIGAZZI, F., SAMPIETRO, T., STANLEY, W. C. & RECCHIA, F. A. 2007. Chronic Activation of PPAR{alpha} With Fenofibrate Prevents Alterations in Cardiac Metabolic Phenotype Without Changing The Onset Of Decompensation in Pacing-Induced Heart Failure. *J Pharmacol Exp Ther*.
- LACOMBE, C., DA SILVA, J. L., BRUNEVAL, P., FOURNIER, J. G., WENDLING, F., CASADEVALL, N., CAMILLERI, J. P., BARIETY, J., VARET, B. & TAMBOURIN, P. 1988. Peritubular cells are the site of erythropoietin synthesis in the murine hypoxic kidney. *J Clin Invest*, 81, 620-3.
- LAFFERTY, H. M., GARCIA, D. L., RENNKE, H. G., TROY, J. L., ANDERSON, S. & BRENNER, B. M. 1991. Anemia ameliorates progressive renal injury in experimental DOCA-salt hypertension. *J Am Soc Nephrol*, 1, 1180-5.
- LEE, M. S., LEE, J. S. & LEE, J. Y. 2007. Prevention of erythropoietin-associated hypertension. *Hypertension*, 50, 439-45.
- LEENEN, F. H. & DE JONG, W. 1971. A solid silver clip for induction of predictable levels of renal hypertension in the rat. *J Appl Physiol*, 31, 142-4.
- LEHMAN, J. J., BARGER, P. M., KOVACS, A., SAFFITZ, J. E., MEDEIROS, D. M. & KELLY, D. P. 2000. Peroxisome proliferator-activated receptor gamma coactivator-1 promotes cardiac mitochondrial biogenesis. *J Clin Invest*, 106, 847-56.
- LEHMAN, J. J., BOUDINA, S., BANKE, N. H., SAMBANDAM, N., HAN, X., YOUNG, D. M., LEONE, T. C., GROSS, R. W., LEWANDOWSKI, E. D., ABEL, E. D. & KELLY, D. P. 2008. The transcriptional coactivator PGC-1alpha is essential for maximal and efficient cardiac mitochondrial fatty acid oxidation and lipid homeostasis. *Am J Physiol Heart Circ Physiol*, 295, H185-96.

- LEHMAN, J. J. & KELLY, D. P. 2002. Gene regulatory mechanisms governing energy metabolism during cardiac hypertrophic growth. *Heart Fail Rev*, 7, 175-85.
- LEHMAN, T. C., HALE, D. E., BHALA, A. & THORPE, C. 1990. An acyl-coenzyme A dehydrogenase assay utilizing the ferricenium ion. *Anal Biochem*, 186, 280-4.
- LENNON, S. V., MARTIN, S. J. & COTTER, T. G. 1991. Dose-dependent induction of apoptosis in human tumour cell lines by widely diverging stimuli. *Cell Prolif*, 24, 203-14.
- LEONE, T. C., WEINHEIMER, C. J. & KELLY, D. P. 1999. A critical role for the peroxisome proliferator-activated receptor alpha (PPARalpha) in the cellular fasting response: the PPARalpha-null mouse as a model of fatty acid oxidation disorders. *Proc Natl Acad Sci U S A*, 96, 7473-8.
- LERMAN, L. O., SCHWARTZ, R. S., GRANDE, J. P., SHEEDY, P. F. & ROMERO, J. C. 1999. Noninvasive evaluation of a novel swine model of renal artery stenosis. *J Am Soc Nephrol*, 10, 1455-65.
- LESNEFSKY, E. J., MOGHADDAS, S., TANDLER, B., KERNER, J. & HOPPEL, C. L. 2001. Mitochondrial dysfunction in cardiac disease: ischemia--reperfusion, aging, and heart failure. *J Mol Cell Cardiol*, 33, 1065-89.
- LEVEY, A. S., BOSCH, J. P., LEWIS, J. B., GREENE, T., ROGERS, N. & ROTH, D. 1999. A more accurate method to estimate glomerular filtration rate from serum creatinine: a new prediction equation. Modification of Diet in Renal Disease Study Group. *Ann Intern Med*, 130, 461-70.
- LEVIN, A., THOMPSON, C. R., ETHIER, J., CARLISLE, E. J., TOBE, S., MENDELSSOHN, D., BURGESS, E., JINDAL, K., BARRETT, B., SINGER, J. & DJURDJEV, O. 1999. Left ventricular mass index increase in early renal disease: impact of decline in hemoglobin. *Am J Kidney Dis*, 34, 125-34.
- LEVY, D., GARRISON, R. J., SAVAGE, D. D., KANNEL, W. B. & CASTELLI, W. P. 1990. Prognostic implications of echocardiographically determined left ventricular mass in the Framingham Heart Study. *N Engl J Med*, 322, 1561-6.
- LI, X. M., MA, Y. T., YANG, Y. N., LIU, F., CHEN, B. D., HAN, W., ZHANG, J. F. & XIAO, G. 2009a. Downregulation of survival signaling pathways and increased apoptosis in the transition of pressure overload-induced cardiac Hypertrophy towards to heart failure. *Clin Exp Pharmacol Physiol*.
- LI, Y., TAKEMURA, G., OKADA, H., MIYATA, S., MARUYAMA, R., LI, L., HIGUCHI, M., MINATOGUCHI, S., FUJIWARA, T. & FUJIWARA, H. 2006. Reduction of inflammatory cytokine expression and oxidative damage by erythropoietin in chronic heart failure. *Cardiovasc Res*, 71, 684-94.
- LI, Y., WU, J., HE, Q., SHOU, Z., ZHANG, P., PEN, W., ZHU, Y. & CHEN, J. 2009b. Angiotensin (1-7) prevent heart dysfunction and left ventricular remodeling caused by renal dysfunction in 5/6 nephrectomy mice. *Hypertens Res*, 32, 369-74.
- LIM, V. S., FANGMAN, J., FLANIGAN, M. J., DEGOWIN, R. L. & ABELS, R. T. 1990. Effect of recombinant human erythropoietin on renal function in humans. *Kidney Int*, 37, 131-6.
- LIN, F. K., SUGGS, S., LIN, C. H., BROWNE, J. K., SMALLING, R., EGRIE, J. C., CHEN, K. K., FOX, G. M., MARTIN, F., STABINSKY, Z. & ET AL. 1985. Cloning and

- expression of the human erythropoietin gene. *Proc Natl Acad Sci U S A*, 82, 7580-4.
- LINDEMAN, R. D. 1993. Assessment of renal function in the old. Special considerations. *Clin Lab Med*, 13, 269-77.
- LIPSIC, E., WESTENBRINK, B. D., VAN DER MEER, P., VAN DER HARST, P., VOORS, A. A., VAN VELDHUISEN, D. J., SCHOEMAKER, R. G. & VAN GILST, W. H. 2008. Low-dose erythropoietin improves cardiac function in experimental heart failure without increasing haematocrit. *Eur J Heart Fail*, 10, 22-9.
- LITWIN, S. E., ZHANG, D. & BRIDGE, J. H. 2000. Dyssynchronous Ca(2+) sparks in myocytes from infarcted hearts. *Circ Res*, 87, 1040-7.
- LIU, Z. C., CHOW, K. M. & CHANG, T. M. 2003. Evaluation of two protocols of uremic rat model: partial nephrectomy and infarction. *Ren Fail*, 25, 935-43.
- LONDON, G. M. 2003. Left ventricular hypertrophy: why does it happen? *Nephrol Dial Transplant*, 18 Suppl 8, viii2-6.
- LONDON, G. M., PANNIER, B., GUERIN, A. P., BLACHER, J., MARCHAIS, S. J., DARNE, B., METIVIER, F., ADDA, H. & SAFAR, M. E. 2001. Alterations of left ventricular hypertrophy in and survival of patients receiving hemodialysis: follow-up of an interventional study. *J Am Soc Nephrol*, 12, 2759-67.
- LONDON, G. M. & PARFREY, P. S. 1997. Cardiac disease in chronic uremia: pathogenesis. *Adv Ren Replace Ther*, 4, 194-211.
- LOPASCHUK, G. D. 2002. Metabolic abnormalities in the diabetic heart. *Heart Fail Rev*, 7, 149-59.
- LUCAS, D. T., ARYAL, P., SZWEDA, L. I., KOCH, W. J. & LEINWAND, L. A. 2003. Alterations in mitochondrial function in a mouse model of hypertrophic cardiomyopathy. *Am J Physiol Heart Circ Physiol*, 284, H575-83.
- LUEDDE, M., FLOGEL, U., KNORR, M., GRUNDT, C., HIPPE, H. J., BRORS, B., FRANK, D., HASELMANN, U., ANTONY, C., VOELKERS, M., SCHRADER, J., MOST, P., LEMMER, B., KATUS, H. A. & FREY, N. 2009. Decreased contractility due to energy deprivation in a transgenic rat model of hypertrophic cardiomyopathy. *J Mol Med*, 87, 411-22.
- MACDOUGALL, I. C., GRAY, S. J., ELSTON, O., BREEN, C., JENKINS, B., BROWNE, J. & EGRIE, J. 1999. Pharmacokinetics of novel erythropoiesis stimulating protein compared with epoetin alfa in dialysis patients. *J Am Soc Nephrol*, 10, 2392-5.
- MAIESE, K., LI, F. & CHONG, Z. Z. 2005. New avenues of exploration for erythropoietin. *Jama*, 293, 90-5.
- MALL, G., HUTHER, W., SCHNEIDER, J., LUNDIN, P. & RITZ, E. 1990. Diffuse intermyocardiocytic fibrosis in uraemic patients. *Nephrol Dial Transplant*, 5, 39-44.
- MALL, G., RAMBAUSEK, M., NEUMEISTER, A., KOLLMAR, S., VETTERLEIN, F. & RITZ, E. 1988. Myocardial interstitial fibrosis in experimental uremia--implications for cardiac compliance. *Kidney Int*, 33, 804-11.
- MALLOY, C. R., SHERRY, A. D. & JEFFREY, F. M. 1988. Evaluation of carbon flux and substrate selection through alternate pathways involving the citric acid cycle of the heart by <sup>13</sup>C NMR spectroscopy. *J Biol Chem*, 263, 6964-71.
- MALLOY, C. R., SHERRY, A. D. & JEFFREY, F. M. 1990. Analysis of tricarboxylic acid cycle of the heart using <sup>13</sup>C isotope isomers. *Am J Physiol*, 259, H987-95.

- MANCINI, D. M., KATZ, S. D., LANG, C. C., LAMANCA, J., HUDAIHED, A. & ANDRONE, A. S. 2003. Effect of erythropoietin on exercise capacity in patients with moderate to severe chronic heart failure. *Circulation*, 107, 294-9.
- MARIJANOWSKI, M. M., TEELING, P., MANN, J. & BECKER, A. E. 1995. Dilated cardiomyopathy is associated with an increase in the type I/type III collagen ratio: a quantitative assessment. *J Am Coll Cardiol*, 25, 1263-72.
- MARK, P. B., JOHNSTON, N., GROENNING, B. A., FOSTER, J. E., BLYTH, K. G., MARTIN, T. N., STEEDMAN, T., DARGIE, H. J. & JARDINE, A. G. 2006. Redefinition of uremic cardiomyopathy by contrast-enhanced cardiac magnetic resonance imaging. *Kidney Int*, 69, 1839-45.
- MARON, B. J., OLIVOTTO, I., SPIRITO, P., CASEY, S. A., BELLONE, P., GOHMAN, T. E., GRAHAM, K. J., BURTON, D. A. & CECCHI, F. 2000. Epidemiology of hypertrophic cardiomyopathy-related death: revisited in a large non-referral-based patient population. *Circulation*, 102, 858-64.
- MARRERO, M. B., VENEMA, R. C., MA, H., LING, B. N. & EATON, D. C. 1998. Erythropoietin receptor-operated Ca<sup>2+</sup> channels: activation by phospholipase C-gamma 1. *Kidney Int*, 53, 1259-68.
- MARX, S. O., REIKEN, S., HISAMATSU, Y., JAYARAMAN, T., BURKHOF, D., ROSEMBLIT, N. & MARKS, A. R. 2000. PKA phosphorylation dissociates FKBP12.6 from the calcium release channel (ryanodine receptor): defective regulation in failing hearts. *Cell*, 101, 365-76.
- MASCHIO, G., ALBERTI, D., JANIN, G., LOCATELLI, F., MANN, J. F., MOTOLESE, M., PONTICELLI, C., RITZ, E. & ZUCHELLI, P. 1996. Effect of the angiotensin-converting-enzyme inhibitor benazepril on the progression of chronic renal insufficiency. The Angiotensin-Converting-Enzyme Inhibition in Progressive Renal Insufficiency Study Group. *N Engl J Med*, 334, 939-45.
- MCCORMACK, J. G., BARR, R. L., WOLFF, A. A. & LOPASCHUK, G. D. 1996. Ranolazine stimulates glucose oxidation in normoxic, ischemic, and reperfused ischemic rat hearts. *Circulation*, 93, 135-42.
- MCMAHON, A. C., GREENWALD, S. E., DODD, S. M., HURST, M. J. & RAINE, A. E. 2002. Prolonged calcium transients and myocardial remodelling in early experimental uraemia. *Nephrol Dial Transplant*, 17, 759-64.
- MEERSON, F. Z. 1971. Mechanism of hypertrophy of the heart and experimental prevention of acute cardiac insufficiency. *Br Heart J*, 33, Suppl:100-8.
- MERX, M. W., SCHAFFER, C., WESTENFELD, R., BRANDENBURG, V., HIDAJAT, S., WEBER, C., KETTELER, M. & JAHNEN-DECHENT, W. 2005. Myocardial stiffness, cardiac remodeling, and diastolic dysfunction in calcification-prone fetuin-A-deficient mice. *J Am Soc Nephrol*, 16, 3357-64.
- MISHINA, M. & WATANABE, T. 2008. Development of hypertension and effects of benazepril hydrochloride in a canine remnant kidney model of chronic renal failure. *J Vet Med Sci*, 70, 455-60.
- MITCHELL, P. 1961. Coupling of phosphorylation to electron and hydrogen transfer by a chemi-osmotic type of mechanism. *Nature*, 191, 144-8.
- MIYASHITA, K., TOJO, A., KIMURA, K., GOTO, A., OMATA, M., NISHIYAMA, K. & FUJITA, T. 2004. Blood pressure response to erythropoietin injection in hemodialysis and predialysis patients. *Hypertens Res*, 27, 79-84.

- MOHRMAN, D. E. & HELLER, L. J. 2006. *Cardiovascular Physiology*, McGraw-Hill Professional, 2006.
- MONCADA, S. & ERUSALIMSKY, J. D. 2002. Does nitric oxide modulate mitochondrial energy generation and apoptosis? *Nat Rev Mol Cell Biol*, 3, 214-20.
- MOON, C., KRAWCZYK, M., AHN, D., AHMET, I., PAIK, D., LAKATTA, E. G. & TALAN, M. I. 2003a. Erythropoietin reduces myocardial infarction and left ventricular functional decline after coronary artery ligation in rats. *Proc Natl Acad Sci U S A*, 100, 11612-7.
- MOON, C., KRAWCZYK, M., PAIK, D., COLEMAN, T., BRINES, M., JUHASZOVA, M., SOLLOTT, S. J., LAKATTA, E. G. & TALAN, M. I. 2006. Erythropoietin, modified to not stimulate red blood cell production, retains its cardioprotective properties. *J Pharmacol Exp Ther*, 316, 999-1005.
- MOON, C., KRAWCZYK, M., PAIK, D., LAKATTA, E. G. & TALAN, M. I. 2005. Cardioprotection by recombinant human erythropoietin following acute experimental myocardial infarction: dose response and therapeutic window. *Cardiovasc Drugs Ther*, 19, 243-50.
- MOON, J. C., MCKENNA, W. J., MCCROHON, J. A., ELLIOTT, P. M., SMITH, G. C. & PENNELL, D. J. 2003b. Toward clinical risk assessment in hypertrophic cardiomyopathy with gadolinium cardiovascular magnetic resonance. *J Am Coll Cardiol*, 41, 1561-7.
- MORENA, M., DELBOSC, S., DUPUY, A. M., CANAUD, B. & CRISTOL, J. P. 2005. Overproduction of reactive oxygen species in end-stage renal disease patients: a potential component of hemodialysis-associated inflammation. *Hemodial Int*, 9, 37-46.
- MORGAN-HUGHES, J. A., DARVENIZA, P., KAHN, S. N., LANDON, D. N., SHERRATT, R. M., LAND, J. M. & CLARK, J. B. 1977. A mitochondrial myopathy characterized by a deficiency in reducible cytochrome b. *Brain*, 100, 617-40.
- MORI, Y., HIRANO, T., NAGASHIMA, M., SHIRAIISHI, Y., FUKUI, T. & ADACHI, M. 2007. Decreased peroxisome proliferator-activated receptor alpha gene expression is associated with dyslipidemia in a rat model of chronic renal failure. *Metabolism*, 56, 1714-8.
- MURRAY, A. J., ANDERSON, R. E., WATSON, G. C., RADDA, G. K. & CLARKE, K. 2004. Uncoupling proteins in human heart. *Lancet*, 364, 1786-8.
- NAGATA, S. 1997. Apoptosis by death factor. *Cell*, 88, 355-65.
- NAITO, Y., TSUJINO, T., MATSUMOTO, M., SAKODA, T., OHYANAGI, M. & MASUYAMA, T. 2009. Adaptive response of the heart to long-term anemia induced by iron deficiency. *Am J Physiol Heart Circ Physiol*, 296, H585-93.
- NASCIMBEN, L., INGWALL, J. S., LORELL, B. H., PINZ, I., SCHULTZ, V., TORNHEIM, K. & TIAN, R. 2004. Mechanisms for increased glycolysis in the hypertrophied rat heart. *Hypertension*, 44, 662-7.
- NAZARETH, W., YAFEI, N. & CROMPTON, M. 1991. Inhibition of anoxia-induced injury in heart myocytes by cyclosporin A. *J Mol Cell Cardiol*, 23, 1351-4.
- NEELY, J. R., LIEBERMEISTER, H., BATTERSBY, E. J. & MORGAN, H. E. 1967. Effect of pressure development on oxygen consumption by isolated rat heart. *Am J Physiol*, 212, 804-14.

- NEUBAUER, S. 2007. The failing heart--an engine out of fuel. *N Engl J Med*, 356, 1140-51.
- NEUSSER, M., TEPEL, M. & ZIDEK, W. 1993. Erythropoietin increases cytosolic free calcium concentration in vascular smooth muscle cells. *Cardiovasc Res*, 27, 1233-6.
- NISHIYA, D., OMURA, T., SHIMADA, K., MATSUMOTO, R., KUSUYAMA, T., ENOMOTO, S., IWAO, H., TAKEUCHI, K., YOSHIKAWA, J. & YOSHIYAMA, M. 2006. Effects of erythropoietin on cardiac remodeling after myocardial infarction. *J Pharmacol Sci*, 101, 31-9.
- NORTON, G. R., TSOTETSI, J., TRIFUNOVIC, B., HARTFORD, C., CANDY, G. P. & WOODIWISS, A. J. 1997. Myocardial stiffness is attributed to alterations in cross-linked collagen rather than total collagen or phenotypes in spontaneously hypertensive rats. *Circulation*, 96, 1991-8.
- O'SHEA, K. M., KHAIRALLAH, R. J., SPARAGNA, G. C., XU, W., HECKER, P. A., ROBILLARD-FRAYNE, I., DES ROSIERS, C., KRISTIAN, T., MURPHY, R. C., FISKUM, G. & STANLEY, W. C. 2009. Dietary omega-3 fatty acids alter cardiac mitochondrial phospholipid composition and delay Ca<sup>2+</sup>-induced permeability transition. *J Mol Cell Cardiol*, 47, 819-27.
- OBRADOR, G. T., ROBERTS, T., ST PETER, W. L., FRAZIER, E., PEREIRA, B. J. & COLLINS, A. J. 2001. Trends in anemia at initiation of dialysis in the United States. *Kidney Int*, 60, 1875-84.
- OGATA, H., RITZ, E., ODoni, G., AMANN, K. & ORTH, S. R. 2003. Beneficial effects of calcimimetics on progression of renal failure and cardiovascular risk factors. *J Am Soc Nephrol*, 14, 959-67.
- OGIMOTO, G., SAKURADA, T., IMAMURA, K., KUBOSHIMA, S., MAEBA, T., KIMURA, K. & OWADA, S. 2003. Alteration of energy production by the heart in CRF patients undergoing peritoneal dialysis. *Mol Cell Biochem*, 244, 135-8.
- OHORI, K., MIURA, T., TANNO, M., MIKI, T., SATO, T., ISHIKAWA, S., HORIO, Y. & SHIMAMOTO, K. 2008. Ser9 phosphorylation of mitochondrial GSK-3{beta} is a primary mechanism of cardiomyocyte protection by erythropoietin against oxidant-induced apoptosis. *Am J Physiol Heart Circ Physiol*, 295, H2079-86.
- OLIVETTI, G., ABBI, R., QUAINI, F., KAJSTURA, J., CHENG, W., NITAHARA, J. A., QUAINI, E., DI LORETO, C., BELTRAMI, C. A., KRAJEWSKI, S., REED, J. C. & ANVERSA, P. 1997. Apoptosis in the failing human heart. *N Engl J Med*, 336, 1131-41.
- OPIE, L. H. 1965. Coronary flow rate and perfusion pressure as determinants of mechanical function and oxidative metabolism of isolated perfused rat heart. *J Physiol*, 180, 529-41.
- OSORIO, J. C., STANLEY, W. C., LINKE, A., CASTELLARI, M., DIEP, Q. N., PANCHAL, A. R., HINTZE, T. H., LOPASCHUK, G. D. & RECCHIA, F. A. 2002. Impaired myocardial fatty acid oxidation and reduced protein expression of retinoid X receptor-alpha in pacing-induced heart failure. *Circulation*, 106, 606-12.
- OTSUKA, T., SUZUKI, M., YOSHIKAWA, H. & SUGI, K. 2009. Left ventricular diastolic dysfunction in the early stage of chronic kidney disease. *J Cardiol*, 54, 199-204.

- PABLA, R. & CURTIS, M. J. 1996. Effect of endogenous nitric oxide on cardiac systolic and diastolic function during ischemia and reperfusion in the rat isolated perfused heart. *J Mol Cell Cardiol*, 28, 2111-21.
- PARFREY, P. S. & FOLEY, R. N. 1999. The clinical epidemiology of cardiac disease in chronic renal failure. *J Am Soc Nephrol*, 10, 1606-15.
- PARFREY, P. S., FOLEY, R. N., HARNETT, J. D., KENT, G. M., MURRAY, D. & BARRE, P. E. 1996. Outcome and risk factors of ischemic heart disease in chronic uremia. *Kidney Int*, 49, 1428-34.
- PARSA, C. J., MATSUMOTO, A., KIM, J., RIEL, R. U., PASCAL, L. S., WALTON, G. B., THOMPSON, R. B., PETROFSKI, J. A., ANNEX, B. H., STAMLER, J. S. & KOCH, W. J. 2003. A novel protective effect of erythropoietin in the infarcted heart. *J Clin Invest*, 112, 999-1007.
- PEHRSSON, S. K., JONASSON, R. & LINS, L. E. 1984. Cardiac performance in various stages of renal failure. *Br Heart J*, 52, 667-73.
- PELLIEUX, C., AASUM, E., LARSEN, T. S., MONTESSUIT, C., PAPAGEORGIOU, I., PEDRAZZINI, T. & LERCH, R. 2006. Overexpression of angiotensinogen in the myocardium induces downregulation of the fatty acid oxidation pathway. *J Mol Cell Cardiol*, 41, 459-66.
- PELLIEUX, C., MONTESSUIT, C., PAPAGEORGIOU, I. & LERCH, R. 2009. Angiotensin II downregulates the fatty acid oxidation pathway in adult rat cardiomyocytes via release of tumour necrosis factor-alpha. *Cardiovasc Res*, 82, 341-50.
- PERLMAN, A., LAWSIN, L. M., KOLACHANA, P., SAJI, M., MOORE, J., JR. & RINGEL, M. D. 2004. Angiotensin II regulation of TGF-beta in murine mesangial cells involves both PI3 kinase and MAP kinase. *Ann Clin Lab Sci*, 34, 277-86.
- PERRONE, R. D., MADIAS, N. E. & LEVEY, A. S. 1992. Serum creatinine as an index of renal function: new insights into old concepts. *Clin Chem*, 38, 1933-53.
- PFEFFER, M. A., BURDMANN, E. A., CHEN, C. Y., COOPER, M. E., DE ZEEUW, D., ECKARDT, K. U., FEYZI, J. M., IVANOVICH, P., KEWALRAMANI, R., LEVEY, A. S., LEWIS, E. F., MCGILL, J. B., MCMURRAY, J. J., PARFREY, P., PARVING, H. H., REMUZZI, G., SINGH, A. K., SOLOMON, S. D. & TOTO, R. 2009. A trial of darbepoetin alfa in type 2 diabetes and chronic kidney disease. *N Engl J Med*, 361, 2019-32.
- PIOTRKOWSKI, B., KOCH, O. R., DE CAVANAGH, E. M. & FRAGA, C. G. 2009. Cardiac mitochondrial function and tissue remodelling are improved by a non-antihypertensive dose of enalapril in spontaneously hypertensive rats. *Free Radic Res*, 43, 390-9.
- PIUHOLA, J., KERKELA, R., KEENAN, J. I., HAMPTON, M. B., RICHARDS, A. M. & PEMBERTON, C. J. 2008. Direct cardiac actions of erythropoietin (EPO): effects on cardiac contractility, BNP secretion and ischaemia/reperfusion injury. *Clin Sci (Lond)*, 114, 293-304.
- RABKIN, R., AWWAD, I., CHEN, Y., ASHLEY, E. A., SUN, D., SOOD, S., CLUSIN, W., HEIDENREICH, P., PIECHA, G. & GROSS, M. L. 2008. Low-dose growth hormone is cardioprotective in uremia. *J Am Soc Nephrol*, 19, 1774-83.
- RAFIEE, P., SHI, Y., SU, J., PRITCHARD, K. A., JR., TWEDDELL, J. S. & BAKER, J. E. 2005. Erythropoietin protects the infant heart against ischemia-reperfusion injury by triggering multiple signaling pathways. *Basic Res Cardiol*, 100, 187-97.

- RAINE, A. E., MARGREITER, R., BRUNNER, F. P., EHRICH, J. H., GEERLINGS, W., LANDAIS, P., LOIRAT, C., MALLICK, N. P., SELWOOD, N. H., TUFVESON, G. & ET AL. 1992. Report on management of renal failure in Europe, XXII, 1991. *Nephrol Dial Transplant*, 7 Suppl 2, 7-35.
- RAINE, A. E., SEYMOUR, A. M., ROBERTS, A. F., RADDA, G. K. & LEDINGHAM, J. G. 1993. Impairment of cardiac function and energetics in experimental renal failure. *J Clin Invest*, 92, 2934-40.
- RAMBAUSEK, M., AMANN, K., MALL, G. & RITZ, E. 1993. Structural causes of cardiac dysfunction in uremia. *Ren Fail*, 15, 421-8.
- RAZAVI, H. M., HAMILTON, J. A. & FENG, Q. 2005. Modulation of apoptosis by nitric oxide: implications in myocardial ischemia and heart failure. *Pharmacol Ther*, 106, 147-62.
- REDDY, V., BHANDARI, S. & SEYMOUR, A. M. 2007. Myocardial function, energy provision, and carnitine deficiency in experimental uremia. *J Am Soc Nephrol*, 18, 84-92.
- RENNISON, J. H., MCELFFRESH, T. A., OKERE, I. C., PATEL, H. V., FOSTER, A. B., PATEL, K. K., STOLL, M. S., MINKLER, P. E., FUJIOKA, H., HOIT, B. D., YOUNG, M. E., HOPPEL, C. L. & CHANDLER, M. P. 2008. Enhanced acyl-CoA dehydrogenase activity is associated with improved mitochondrial and contractile function in heart failure. *Cardiovasc Res*, 79, 331-40.
- REPO, J. M., RANTALA, I. S., HONKANEN, T. T., MUSTONEN, J. T., KOOBI, P., TAHVANAINEN, A. M., NIEMELA, O. J., TIKKANEN, I., RYSA, J. M., RUSKOAHO, H. J. & PORSTI, I. H. 2007. Paricalcitol aggravates perivascular fibrosis in rats with renal insufficiency and low calcitriol. *Kidney Int*, 72, 977-84.
- RICARD-BLUM, S. & RUGGIERO, F. 2005. The collagen superfamily: from the extracellular matrix to the cell membrane. *Pathol Biol (Paris)*, 53, 430-42.
- RICHARDSON, D., HODSMAN, A., VAN SCHALKWYK, D., TOMSON, C. & WARWICK, G. 2007. Management of anaemia in haemodialysis and peritoneal dialysis patients (chapter 8). *Nephrol Dial Transplant*, 22 Suppl 7, vii78-104.
- RITZ, E. & MCCLELLAN, W. M. 2004. Overview: increased cardiovascular risk in patients with minor renal dysfunction: an emerging issue with far-reaching consequences. *J Am Soc Nephrol*, 15, 513-6.
- ROBERTS, A. B., MCCUNE, B. K. & SPORN, M. B. 1992. TGF-beta: regulation of extracellular matrix. *Kidney Int*, 41, 557-9.
- ROBINSON, P. K. 2001. Electrochemical techniques. In: WILSON, K. & WALKER, J. (eds.) *Principles and techniques of practical biochemistry*. 5th ed.: Cambridge University Press.
- RODRIGUEZ-AYALA, E., AVILA-DIAZ, M., FOYO-NIEMBRO, E., AMATO, D., RAMIREZ-SAN-JUAN, E. & PANIAGUA, R. 2006. Effect of parathyroidectomy on cardiac fibrosis and apoptosis: possible role of aldosterone. *Nephron Physiol*, 103, p112-8.
- RONCO, C., HOUSE, A. A. & HAAPIO, M. 2008. Cardiorenal syndrome: refining the definition of a complex symbiosis gone wrong. *Intensive Care Med*, 34, 957-62.
- ROSENKRANZ, S. 2004. TGF-beta1 and angiotensin networking in cardiac remodeling. *Cardiovasc Res*, 63, 423-32.

- ROSENKRANZ, S., FLESCHE, M., AMANN, K., HAEUSELER, C., KILTER, H., SEELAND, U., SCHLUTER, K. D. & BOHM, M. 2002. Alterations of beta-adrenergic signaling and cardiac hypertrophy in transgenic mice overexpressing TGF-beta(1). *Am J Physiol Heart Circ Physiol*, 283, H1253-62.
- ROSS, B. D. 1972. *Perfusion Techniques in Biochemistry: A Laboratory Manual in the Use of Isolated Perfused Organs in Biochemical Experimentation*. Oxford University (Clarendon) Press.
- RUI, T., FENG, Q., LEI, M., PENG, T., ZHANG, J., XU, M., ABEL, E. D., XENOCOSTAS, A. & KVIETYS, P. R. 2005. Erythropoietin prevents the acute myocardial inflammatory response induced by ischemia/reperfusion via induction of AP-1. *Cardiovasc Res*, 65, 719-27.
- RUSSELL, R. R., 3RD & TAEGTMEYER, H. 1992. Coenzyme A sequestration in rat hearts oxidizing ketone bodies. *J Clin Invest*, 89, 968-73.
- SAITO, T., HU, F., TAYARA, L., FAHAS, L., SHENNIB, H. & GIAID, A. 2002. Inhibition of NOS II prevents cardiac dysfunction in myocardial infarction and congestive heart failure. *Am J Physiol Heart Circ Physiol*, 283, H339-45.
- SAITO, T., TAMURA, K., UCHIDA, D., SAITO, T., TOGASHI, M., NITTA, T. & SUGISAKI, Y. 2007. Histopathological features of the resected left atrial appendage as predictors of recurrence after surgery for atrial fibrillation in valvular heart disease. *Circ J*, 71, 70-8.
- SALEM, J. E., SAIDEL, G. M., STANLEY, W. C. & CABRERA, M. E. 2002. Mechanistic model of myocardial energy metabolism under normal and ischemic conditions. *Ann Biomed Eng*, 30, 202-16.
- SAMBANDAM, N., LOPASCHUK, G. D., BROWNSEY, R. W. & ALLARD, M. F. 2002. Energy metabolism in the hypertrophied heart. *Heart Fail Rev*, 7, 161-73.
- SAMPLE, J., CLELAND, J. G. & SEYMOUR, A. M. 2006. Metabolic remodeling in the aging heart. *J Mol Cell Cardiol*, 40, 56-63.
- SAVICA, V., COSTANTINO, G., MONARDO, P. & BELLINGHERI, G. 1995. Subcutaneous low doses of recombinant human erythropoietin in predialysis patients do not interfere with the progression of renal failure. *Am J Nephrol*, 15, 10-4.
- SAWYER, S. T. & PENTA, K. 1996. Association of JAK2 and STAT5 with erythropoietin receptors. Role of receptor phosphorylation in erythropoietin signal transduction. *J Biol Chem*, 271, 32430-7.
- SCHWINGER, R. H., MUNCH, G., BOLCK, B., KARCEWSKI, P., KRAUSE, E. G. & ERDMANN, E. 1999. Reduced Ca(2+)-sensitivity of SERCA 2a in failing human myocardium due to reduced serin-16 phospholamban phosphorylation. *J Mol Cell Cardiol*, 31, 479-91.
- SEDDON, M., SHAH, A. M. & CASADEI, B. 2007. Cardiomyocytes as effectors of nitric oxide signalling. *Cardiovasc Res*, 75, 315-26.
- SEMENZA, G. L. 1994. Regulation of erythropoietin production. New insights into molecular mechanisms of oxygen homeostasis. *Hematol Oncol Clin North Am*, 8, 863-84.
- SEYMOUR, A. M. 2003a. Imaging cardiac metabolism in heart failure: the potential of NMR spectroscopy in the era of metabolism revisited. *Heart Lung Circ*, 12, 25-30.

- SEYMOUR, A. M. 2003b. Mitochondrial Function- A limiting factor in heart failure? .  
*In: N.S DHALLA, H. R., A. ANGEL, G.N. PIERCE (ed.) Pathophysiology of Cardiovascular Disease.* Boston: Kluwer Academic Publishers.
- SEYMOUR, A. M. & CHATHAM, J. C. 1997. The effects of hypertrophy and diabetes on cardiac pyruvate dehydrogenase activity. *J Mol Cell Cardiol*, 29, 2771-8.
- SEYMOUR, A. M., ELDAR, H. & RADDI, G. K. 1990. Hyperthyroidism results in increased glycolytic capacity in the rat heart. A <sup>31</sup>P-NMR study. *Biochim Biophys Acta*, 1055, 107-16.
- SHARMA, A. K., DHINGRA, S., KHAPER, N. & SINGAL, P. K. 2007. Activation of apoptotic processes during transition from hypertrophy to heart failure in Guinea pigs. *Am J Physiol Heart Circ Physiol*.
- SHAROV, V. G., TODOR, A. V., SILVERMAN, N., GOLDSTEIN, S. & SABBAH, H. N. 2000. Abnormal mitochondrial respiration in failed human myocardium. *J Mol Cell Cardiol*, 32, 2361-7.
- SHI, Y., RAFIEE, P., SU, J., PRITCHARD, K. A., JR., TWEDDELL, J. S. & BAKER, J. E. 2004. Acute cardioprotective effects of erythropoietin in infant rabbits are mediated by activation of protein kinases and potassium channels. *Basic Res Cardiol*, 99, 173-82.
- SHIMADA, N., SAKA, S., SEKIZUKA, K., TANAKA, A., TAKAHASHI, Y., NAKAMURA, T., EBIHARA, I. & KOIDE, H. 2003. Increased endothelin: nitric oxide ratio is associated with erythropoietin-induced hypertension in hemodialysis patients. *Ren Fail*, 25, 569-78.
- SHLIPAK, M. G., HEIDENREICH, P. A., NOGUCHI, H., CHERTOW, G. M., BROWNER, W. S. & MCCLELLAN, M. B. 2002. Association of renal insufficiency with treatment and outcomes after myocardial infarction in elderly patients. *Ann Intern Med*, 137, 555-62.
- SHUSHAKOVA, N., PARK, J. K., MENNE, J. & FLISER, D. 2009. Chronic erythropoietin treatment affects different molecular pathways of diabetic cardiomyopathy in mouse. *Eur J Clin Invest*, 39, 755-60.
- SIEDLECKI, A. M., JIN, X. & MUSLIN, A. J. 2009. Uremic cardiac hypertrophy is reversed by rapamycin but not by lowering of blood pressure. *Kidney Int*, 75, 800-8.
- SIGNOLET, I. L., BOUSQUET, P. P. & MONASSIER, L. J. 2008. Improvement of cardiac diastolic function by long-term centrally mediated sympathetic inhibition in one-kidney, one-clip hypertensive rabbits. *Am J Hypertens*, 21, 54-60.
- SILBERBERG, J., RACINE, N., BARRE, P. & SNIDERMAN, A. D. 1990. Regression of left ventricular hypertrophy in dialysis patients following correction of anemia with recombinant human erythropoietin. *Can J Cardiol*, 6, 1-4.
- SILBERBERG, J. S., BARRE, P. E., PRICHARD, S. S. & SNIDERMAN, A. D. 1989. Impact of left ventricular hypertrophy on survival in end-stage renal disease. *Kidney Int*, 36, 286-90.
- SILVA, M., BENITO, A., SANZ, C., PROSPER, F., EKHTERAE, D., NUNEZ, G. & FERNANDEZ-LUNA, J. L. 1999. Erythropoietin can induce the expression of bcl-x(L) through Stat5 in erythropoietin-dependent progenitor cell lines. *J Biol Chem*, 274, 22165-9.
- SILVERBERG, D. S., WEXLER, D., SHEPS, D., BLUM, M., KEREN, G., BARUCH, R., SCHWARTZ, D., YACHNIN, T., STEINBRUCH, S., SHAPIRA, I., LANIADO, S. &

- IAINA, A. 2001. The effect of correction of mild anemia in severe, resistant congestive heart failure using subcutaneous erythropoietin and intravenous iron: a randomized controlled study. *J Am Coll Cardiol*, 37, 1775-80.
- SILVESTRE, J. S., HEYMES, C., OUBENAÏSSA, A., ROBERT, V., AUPETIT-FAISANT, B., CARAYON, A., SWYNGHEDAUW, B. & DELCAYRE, C. 1999. Activation of cardiac aldosterone production in rat myocardial infarction: effect of angiotensin II receptor blockade and role in cardiac fibrosis. *Circulation*, 99, 2694-701.
- SINGH, A. K., SZCZECHE, L., TANG, K. L., BARNHART, H., SAPP, S., WOLFSON, M. & REDDAN, D. 2006. Correction of anemia with epoetin alfa in chronic kidney disease. *N Engl J Med*, 355, 2085-98.
- SIVERTSEN, E. A., HYSTAD, M. E., GUTZKOW, K. B., DOSEN, G., SMELAND, E. B., BLOMHOFF, H. K. & MYKLEBUST, J. H. 2006. PI3K/Akt-dependent Epo-induced signalling and target genes in human early erythroid progenitor cells. *Br J Haematol*, 135, 117-28.
- SMITH, K. J., BLEYER, A. J., LITTLE, W. C. & SANE, D. C. 2003. The cardiovascular effects of erythropoietin. *Cardiovasc Res*, 59, 538-48.
- SMITH, R. S., JR., AGATA, J., XIA, C. F., CHAO, L. & CHAO, J. 2005. Human endothelial nitric oxide synthase gene delivery protects against cardiac remodeling and reduces oxidative stress after myocardial infarction. *Life Sci*, 76, 2457-71.
- SMOGORZEWSKI, M., ZAYED, M., ZHANG, Y. B., ROE, J. & MASSRY, S. G. 1993. Parathyroid hormone increases cytosolic calcium concentration in adult rat cardiac myocytes. *Am J Physiol*, 264, H1998-2006.
- SOCOLOVSKY, M., FALLON, A. E., WANG, S., BRUGNARA, C. & LODISH, H. F. 1999. Fetal anemia and apoptosis of red cell progenitors in Stat5a<sup>-/-</sup>5b<sup>-/-</sup> mice: a direct role for Stat5 in Bcl-X(L) induction. *Cell*, 98, 181-91.
- STANLEY, W. C. & CHANDLER, M. P. 2002. Energy metabolism in the normal and failing heart: potential for therapeutic interventions. *Heart Fail Rev*, 7, 115-30.
- STANLEY, W. C., RECCHIA, F. A. & LOPASCHUK, G. D. 2005. Myocardial substrate metabolism in the normal and failing heart. *Physiol Rev*, 85, 1093-129.
- STEKELENBURG-DE VOS, S., STEENDIJK, P., URSEM, N. T., WLADIMIROFF, J. W., DELFOS, R. & POELMANN, R. E. 2005. Systolic and diastolic ventricular function assessed by pressure-volume loops in the stage 21 venous clipped chick embryo. *Pediatr Res*, 57, 16-21.
- STERIN-BORDA, L., BARCELO, A. C. & BOZZINI, C. E. 2003. Erythropoietin improves cardiac contractility in post-hypoxic mice. *Br J Haematol*, 121, 180-6.
- STOHLAWETZ, P. J., DZIRLO, L., HERGOVICH, N., LACKNER, E., MENSIK, C., EICHLER, H. G., KABRNA, E., GEISLER, K. & JILMA, B. 2000. Effects of erythropoietin on platelet reactivity and thrombopoiesis in humans. *Blood*, 95, 2983-9.
- TACHIKAWA, H., KODAMA, M., HUI, L., YOSHIDA, T., HAYASHI, M., ABE, S., KASHIMURA, T., KATO, K., HANAWA, H., WATANABE, K., NAKAZAWA, M. & AIZAWA, Y. 2003. Angiotensin II type 1 receptor blocker, valsartan, prevented cardiac fibrosis in rat cardiomyopathy after autoimmune myocarditis. *J Cardiovasc Pharmacol*, 41 Suppl 1, S105-10.

- TAEGETMEYER, H. 1986. Myocardial Metabolism. *In: PHELPS, M. M., J. SHELBERT, H. (ed.) Position Emission Tomography and Autoradiography: Principles and Applications for the Brain and Heart.* New York Raven Press.
- TENG, M., WOLF, M., LOWRIE, E., OFSTHUN, N., LAZARUS, J. M. & THADHANI, R. 2003. Survival of patients undergoing hemodialysis with paricalcitol or calcitriol therapy. *N Engl J Med*, 349, 446-56.
- TOBA, H., SAWAI, N., MORISHITA, M., MURATA, S., YOSHIDA, M., NAKASHIMA, K., MORITA, Y., KOBARA, M. & NAKATA, T. 2009. Chronic treatment with recombinant human erythropoietin exerts renoprotective effects beyond hematopoiesis in streptozotocin-induced diabetic rat. *Eur J Pharmacol*, 612, 106-14.
- TRAMONTANO, A. F., MUNIYAPPA, R., BLACK, A. D., BLENDEA, M. C., COHEN, I., DENG, L., SOWERS, J. R., CUTAIA, M. V. & EL-SHERIF, N. 2003. Erythropoietin protects cardiac myocytes from hypoxia-induced apoptosis through an Akt-dependent pathway. *Biochem Biophys Res Commun*, 308, 990-4.
- TSUJIMURA, T., NAGAMINE, J., SUGARU, E., NAKAGAWA, T., ONO-KISHINO, M., TOKUNAGA, T., KITO, M., NAGATA, R. & TAJI, M. 2008. Chronic administration of SMP-534 ameliorates renal dysfunction in 5/6 nephrectomized rats. *Nephron Exp Nephrol*, 110, e99-108.
- UM, M. & LODISH, H. F. 2006. Antiapoptotic effects of erythropoietin in differentiated neuroblastoma SH-SY5Y cells require activation of both the STAT5 and AKT signaling pathways. *J Biol Chem*, 281, 5648-56.
- UNGER, T., CHUNG, O., CSIKOS, T., CULMAN, J., GALLINAT, S., GOHLKE, P., HOHLE, S., MEFFERT, S., STOLL, M., STROTH, U. & ZHU, Y. Z. 1996. Angiotensin receptors. *J Hypertens Suppl*, 14, S95-103.
- URAO, N., OKIGAKI, M., YAMADA, H., AADACHI, Y., MATSUNO, K., MATSUI, A., MATSUNAGA, S., TATEISHI, K., NOMURA, T., TAKAHASHI, T., TATSUMI, T. & MATSUBARA, H. 2006. Erythropoietin-mobilized endothelial progenitors enhance reendothelialization via Akt-endothelial nitric oxide synthase activation and prevent neointimal hyperplasia. *Circ Res*, 98, 1405-13.
- VAN BILSEN, M., VAN NIEUWENHOVEN, F. A. & VAN DER VUSSE, G. J. 2009. Metabolic remodelling of the failing heart: beneficial or detrimental? *Cardiovasc Res*, 81, 420-8.
- VAN DER MEER, P., LIPSIC, E., HENNING, R. H., BODDEUS, K., VAN DER VELDEN, J., VOORS, A. A., VAN VELDHUISEN, D. J., VAN GILST, W. H. & SCHOEMAKER, R. G. 2005. Erythropoietin induces neovascularization and improves cardiac function in rats with heart failure after myocardial infarction. *J Am Coll Cardiol*, 46, 125-33.
- VAN DER MEER, P., VOORS, A. A., LIPSIC, E., VAN GILST, W. H. & VAN VELDHUISEN, D. J. 2004. Erythropoietin in cardiovascular diseases. *Eur Heart J*, 25, 285-91.
- VAN DER REST, M. & GARRONE, R. 1991. Collagen family of proteins. *Faseb J*, 5, 2814-23.
- VARNAVA, A. M., ELLIOTT, P. M., MAHON, N., DAVIES, M. J. & MCKENNA, W. J. 2001. Relation between myocyte disarray and outcome in hypertrophic cardiomyopathy. *Am J Cardiol*, 88, 275-9.

- VARNAVA, A. M., ELLIOTT, P. M., SHARMA, S., MCKENNA, W. J. & DAVIES, M. J. 2000. Hypertrophic cardiomyopathy: the interrelation of disarray, fibrosis, and small vessel disease. *Heart*, 84, 476-82.
- VARO, N., IRABURU, M. J., VARELA, M., LOPEZ, B., ETAYO, J. C. & DIEZ, J. 2000. Chronic AT(1) blockade stimulates extracellular collagen type I degradation and reverses myocardial fibrosis in spontaneously hypertensive rats. *Hypertension*, 35, 1197-202.
- VAZIRI, N. D., ZHOU, X. J., NAQVI, F., SMITH, J., OVEISI, F., WANG, Z. Q. & PURDY, R. E. 1996. Role of nitric oxide resistance in erythropoietin-induced hypertension in rats with chronic renal failure. *Am J Physiol*, 271, E113-22.
- VAZIRI, N. D., ZHOU, X. J., SMITH, J., OVEISI, F., BALDWIN, K. & PURDY, R. E. 1995. In vivo and in vitro pressor effects of erythropoietin in rats. *Am J Physiol*, 269, F838-45.
- VEGA, R. B., HUSS, J. M. & KELLY, D. P. 2000. The coactivator PGC-1 cooperates with peroxisome proliferator-activated receptor alpha in transcriptional control of nuclear genes encoding mitochondrial fatty acid oxidation enzymes. *Mol Cell Biol*, 20, 1868-76.
- WALD, M., GUTNISKY, A., BORDA, E. & STERIN-BORDA, L. 1995. Erythropoietin modified the cardiac action of ouabain in chronically anaemic-uraemic rats. *Nephron*, 71, 190-6.
- WANG, B., HAO, J., JONES, S. C., YEE, M. S., ROTH, J. C. & DIXON, I. M. 2002. Decreased Smad 7 expression contributes to cardiac fibrosis in the infarcted rat heart. *Am J Physiol Heart Circ Physiol*, 282, H1685-96.
- WANG, Y., DE WAARD, M. C., STERNER-KOCK, A., STEPAN, H., SCHULTHEISS, H. P., DUNCKER, D. J. & WALTHER, T. 2007. Cardiomyocyte-restricted over-expression of C-type natriuretic peptide prevents cardiac hypertrophy induced by myocardial infarction in mice. *Eur J Heart Fail*, 9, 548-57.
- WEBER, K. T. 1989. Cardiac interstitium in health and disease: the fibrillar collagen network. *J Am Coll Cardiol*, 13, 1637-52.
- WEBER, K. T. & JANICKI, J. S. 1989. Angiotensin and the remodelling of the myocardium. *Br J Clin Pharmacol*, 28 Suppl 2, 141S-149S; discussion 149S-150S.
- WEBER, K. T., JANICKI, J. S., SHROFF, S. G., PICK, R., CHEN, R. M. & BASHEY, R. I. 1988. Collagen remodeling of the pressure-overloaded, hypertrophied nonhuman primate myocardium. *Circ Res*, 62, 757-65.
- WEBER, K. T., SUN, Y., TYAGI, S. C. & CLEUTJENS, J. P. 1994. Collagen network of the myocardium: function, structural remodeling and regulatory mechanisms. *J Mol Cell Cardiol*, 26, 279-92.
- WEN, Y., ZHANG, X. J., MA, Y. X., XU, X. J., HONG, L. F. & LU, Z. H. 2009. Erythropoietin attenuates hypertrophy of neonatal rat cardiac myocytes induced by angiotensin-II in vitro. *Scand J Clin Lab Invest*, 69, 518-25.
- WESTENBRINK, B. D., LIPSIC, E., VAN DER MEER, P., VAN DER HARST, P., OESEBURG, H., DU MARCHIE SARVAAS, G. J., KOSTER, J., VOORS, A. A., VAN VELDHIJSEN, D. J., VAN GILST, W. H. & SCHOEMAKER, R. G. 2007. Erythropoietin improves cardiac function through endothelial progenitor cell and vascular endothelial growth factor mediated neovascularization. *Eur Heart J*.

- WIESEL, P., MAZZOLAI, L., NUSSBERGER, J. & PEDRAZZINI, T. 1997. Two-kidney, one clip and one-kidney, one clip hypertension in mice. *Hypertension*, 29, 1025-30.
- WILLIAMS, P., SIMPSON, H., KYBERD, P., KENWRIGHT, J. & GOLDSPINK, G. 1999. Effect of rate of distraction on loss of range of joint movement, muscle stiffness, and intramuscular connective tissue content during surgical limb-lengthening: a study in the rabbit. *Anat Rec*, 255, 78-83.
- WITTHUHN, B. A., QUELLE, F. W., SILVENNOINEN, O., YI, T., TANG, B., MIURA, O. & IHLE, J. N. 1993. JAK2 associates with the erythropoietin receptor and is tyrosine phosphorylated and activated following stimulation with erythropoietin. *Cell*, 74, 227-36.
- WOJCHOWSKI, D. M., GREGORY, R. C., MILLER, C. P., PANDIT, A. K. & PIRCHER, T. J. 1999. Signal transduction in the erythropoietin receptor system. *Exp Cell Res*, 253, 143-56.
- WRIGHT, G. L., HANLON, P., AMIN, K., STEENBERGEN, C., MURPHY, E. & ARCASOY, M. O. 2004. Erythropoietin receptor expression in adult rat cardiomyocytes is associated with an acute cardioprotective effect for recombinant erythropoietin during ischemia-reperfusion injury. *Faseb J*, 18, 1031-3.
- WRIGHT, R. S., REEDER, G. S., HERZOG, C. A., ALBRIGHT, R. C., WILLIAMS, B. A., DVORAK, D. L., MILLER, W. L., MURPHY, J. G., KOPECKY, S. L. & JAFFE, A. S. 2002. Acute myocardial infarction and renal dysfunction: a high-risk combination. *Ann Intern Med*, 137, 563-70.
- XIA, H., EBBEN, J., MA, J. Z. & COLLINS, A. J. 1999. Hematocrit levels and hospitalization risks in hemodialysis patients. *J Am Soc Nephrol*, 10, 1309-16.
- XU, M., WANG, Y., HIRAI, K., AYUB, A. & ASHRAF, M. 2001. Calcium preconditioning inhibits mitochondrial permeability transition and apoptosis. *Am J Physiol Heart Circ Physiol*, 280, H899-908.
- YAMADA, T., NAGATA, K., CHENG, X. W., OBATA, K., SAKA, M., MIYACHI, M., NARUSE, K., NISHIZAWA, T., NODA, A., IZAWA, H., KUZUYA, M., OKUMURA, K., MUROHARA, T. & YOKOTA, M. 2009. Long-term administration of nifedipine attenuates cardiac remodeling and diastolic heart failure in hypertensive rats. *Eur J Pharmacol*, 615, 163-70.
- YAMASHITA, H., BHARADWAJ, K. G., IKEDA, S., PARK, T. S. & GOLDBERG, I. J. 2008. Cardiac metabolic compensation to hypertension requires lipoprotein lipase. *Am J Physiol Endocrinol Metab*, 295, E705-13.
- YANO, M., IKEDA, Y. & MATSUZAKI, M. 2005. Altered intracellular Ca<sup>2+</sup> handling in heart failure. *J Clin Invest*, 115, 556-64.
- YIN, F. C., SPURGEON, H. A., RAKUSAN, K., WEISFELDT, M. L. & LAKATTA, E. G. 1982. Use of tibial length to quantify cardiac hypertrophy: application in the aging rat. *Am J Physiol*, 243, H941-7.
- YOUNG, M. E., LAWS, F. A., GOODWIN, G. W. & TAEGTMEYER, H. 2001a. Reactivation of peroxisome proliferator-activated receptor alpha is associated with contractile dysfunction in hypertrophied rat heart. *J Biol Chem*, 276, 44390-5.
- YOUNG, M. E., PATIL, S., YING, J., DEPRE, C., AHUJA, H. S., SHIPLEY, G. L., STEPKOWSKI, S. M., DAVIES, P. J. A. & TAEGTMEYER, H. 2001b. Uncoupling

- protein 3 transcription is regulated by peroxisome proliferator-activated receptor {alpha} in the adult rodent heart. *FASEB J.*, 15, 833-845.
- ZAMZAMI, N., SUSIN, S. A., MARCHETTI, P., HIRSCH, T., GOMEZ-MONTERREY, I., CASTEDO, M. & KROEMER, G. 1996. Mitochondrial control of nuclear apoptosis. *J Exp Med*, 183, 1533-44.
- ZHAI, Y., GAO, X., WU, Q., PENG, L., LIN, J. & ZUO, Z. 2008. Fluvastatin decreases cardiac fibrosis possibly through regulation of TGF-beta(1)/Smad 7 expression in the spontaneously hypertensive rats. *Eur J Pharmacol*, 587, 196-203.
- ZOCCALI, C., BENEDETTO, F. A., TRIPEPI, G. & MALLAMACI, F. 2004. Cardiac consequences of hypertension in hemodialysis patients. *Semin Dial*, 17, 299-303.
- ZORATTI, M. & SZABO, I. 1995. The mitochondrial permeability transition. *Biochim Biophys Acta*, 1241, 139-76.
- ZOROV, D. B., FILBURN, C. R., KLOTZ, L. O., ZWEIER, J. L. & SOLLOTT, S. J. 2000. Reactive oxygen species (ROS)-induced ROS release: a new phenomenon accompanying induction of the mitochondrial permeability transition in cardiac myocytes. *J Exp Med*, 192, 1001-14.